

Preparation of Project Technical Reports for the IREC

Team 139 Project Technical Report for the 2022 IREC

Delaney Dymont, Roman Kobets, Zachariah Mears, Stefan Arroyo-Cottier, Zhenbo Bian, Cristian Bicheru, Robert Cai, Jack Christensen, Matthew Gencher, Joel Godard, ABM Hussein, Dawson Kletke, Shirley Kong, Adam Lastovka, Aaron Leszkowiat, Ben Levy, Austin Lew, Gavin Liu, Rio Liu, Jerry Lu, Christopher Sankey, Artem Sotnikov, Kyle Tam, Teresa Tang, Zachary Teper, Kaveeshan Thurairajah, Lana Tomlin, Carol Xu, Francis Yao, Michael Zhou, Nahvid Zolfaghari

University of Waterloo, Waterloo, Ontario, N2L 3G1, Canada

Kraken of the Sky (KotS) is a hybrid rocket developed by Waterloo Rocketry for the 30,000ft apogee, Student Research & Developed (SRAD) hybrid/liquid propulsion system category at the 2022 Intercollegiate Rocket Engineering Competition (IREC). The primary object of the KotS launch campaign is to attain an apogee greater than 26,000 ft and achieve a non-hazardous descent using a new reefed parachute system. The secondary objective is to collect data on the performance of different radiation shielding materials against galactic cosmic rays passing through the payload module during flight. The KotS launch vehicle is powered by the Kismet engine, a nitrous oxide/hydroxyl-terminated polybutadiene SRAD hybrid engine. Engine control is managed by RocketCAN, a modular and extensible avionics system which also includes subsystems for radio communication, GPS tracking and remote recovery arming. All launch operations are conducted using the Remote Launch Control System (RLCS), which provides launch control capabilities from a range of over 3,000 ft.

I.Nomenclature

g	=	gravitational Constant of 9.81 m/s ²
I_{sp}	=	engine specific impulse
ft	=	feet
kg	=	kilograms
m	=	meters
N	=	Newtons
s	=	seconds
Ns	=	total impulse
m/s	=	velocity (also denoted by ft/s)
m/s ²	=	acceleration
cal	=	caliber, 1 body tube diameter

II.Introduction

Waterloo Rocketry is a student engineering design team representing the University of Waterloo from Waterloo, Ontario, Canada. The team will be competing in the 2022 Intercollegiate Rocketry Engineering Competition (IREC) at the Spaceport America Cup (SAC) with the Kraken of the Sky (KotS) rocket, which is entered in the 30,000 ft apogee Student Researched and Developed (SRAD) hybrid/liquid propulsion category.

A. Project Background and Scope

Kraken of the Sky is the third iteration rocket in the Kismet series, following Unexploded Ordnance (UXO), 2018, and Shark of the Sky (SotS), 2019.

The primary mission goal of KotS is to reach an apogee of 26,000 ft \pm 2,000 ft and complete a non-hazardous descent. Both parts of the primary goal are mission critical outcomes of equal importance. The secondary mission goal is to collect data for the scientific payload housed in the rocket, which aims to test the capabilities of different radiation shielding materials against the galactic cosmic rays found in low earth orbit (LEO).

Above all else, the primary objective of the team is to provide students with opportunities to engage in hands-on learning through practical engineering and science challenges. The research, design, manufacturing, and testing that are involved with the creation of KotS are some of the most involved and complex projects the team has ever taken on.

In order to achieve the above goals, there have been projects to redesign almost every component from SotS and optimize them for KotS. Waterloo Rocketry prides itself on making as many components as possible in-house. The structure has been redesigned to use fully SRAD composite parts, making this the first year that the team has developed body tubes completely in-house.

B. Team Structure and Operations

Waterloo Rocketry comprises approximately 50 students studying science, mathematics, and engineering at the University of Waterloo. The active members are all undergraduate students, though the team still consults with its alumni. Team Leads are responsible for overall project management and team direction, including overseeing all technical, administrative, and operational activities necessary to achieve the primary objectives and goals. Subsystem Leads are responsible for managing the main sections of the rocket and ground support equipment (GSE), including avionics, aerostructures, recovery, propulsion, and payload. They supervise the overall timelines, integration, and development of each project in their subsystem. Technical projects are led by Project Leads, who are chosen based on experience, skillset, and interest. Project Leads are responsible for coordinating and managing all aspects related to their projects, leading the design, manufacture, and testing of their projects, and ensuring the successful integration of their project with other vehicle and ground systems. Team members are welcome to work on any projects that interest them, and project sub-teams often have significant overlap and collaboration. The Operations Lead oversees all launch and propulsion testing logistics and procedures. The Safety Captain is responsible for the development and maintenance of safety documentation and procedures; however, safety is the responsibility of every member and is always Waterloo Rocketry's highest priority.

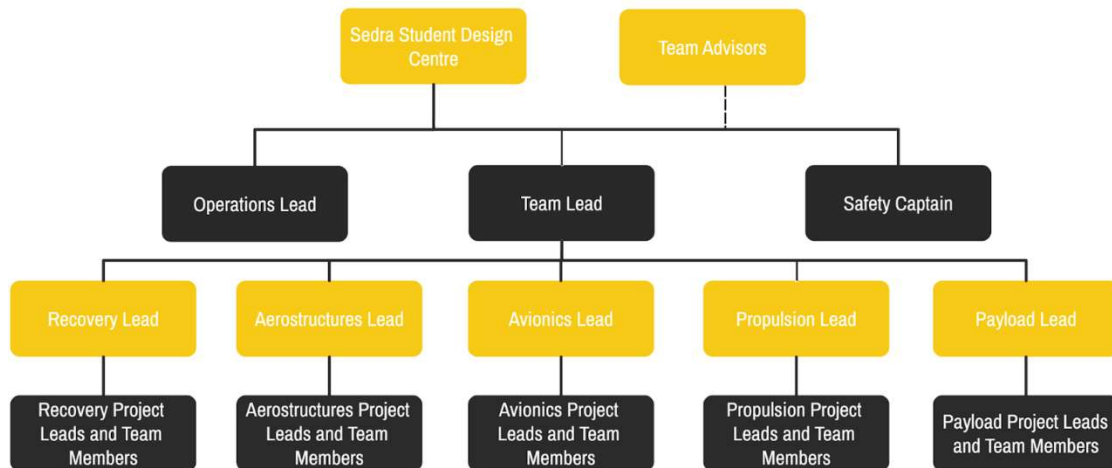


Fig. 1 Waterloo Rocketry organization chart

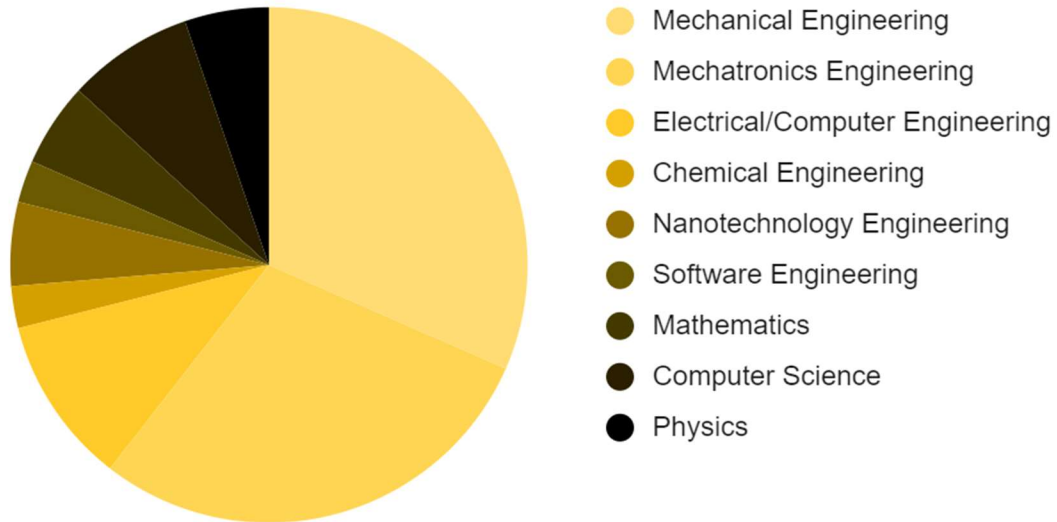


Fig. 2 Breakdown of team structure by program

Waterloo Rocketry’s stakeholders include its academic partners, advisors, sponsors, and members. The team represents the University of Waterloo and owes much to the institutions and resources that the University makes available to student teams. Sponsors are additional stakeholders, as they have provided significant material and financial support essential for the team’s operation. Advisors from within the University and from industry share knowledge and provide insight as Waterloo Rocketry continues to develop more complex and sophisticated systems. Finally, the team’s most important stakeholders are its members. Waterloo Rocketry’s growth and continuity is contingent on its ability to maintain this atmosphere of learning and collaboration while remaining competitive and improving year-to-year. Past and present members dedicate significant time, energy, and resources to achieve the team's objectives, and Waterloo Rocketry owes its continued success to the commitment of its members.

In general, the design strategy of each project will follow the process shown in Fig. 3:

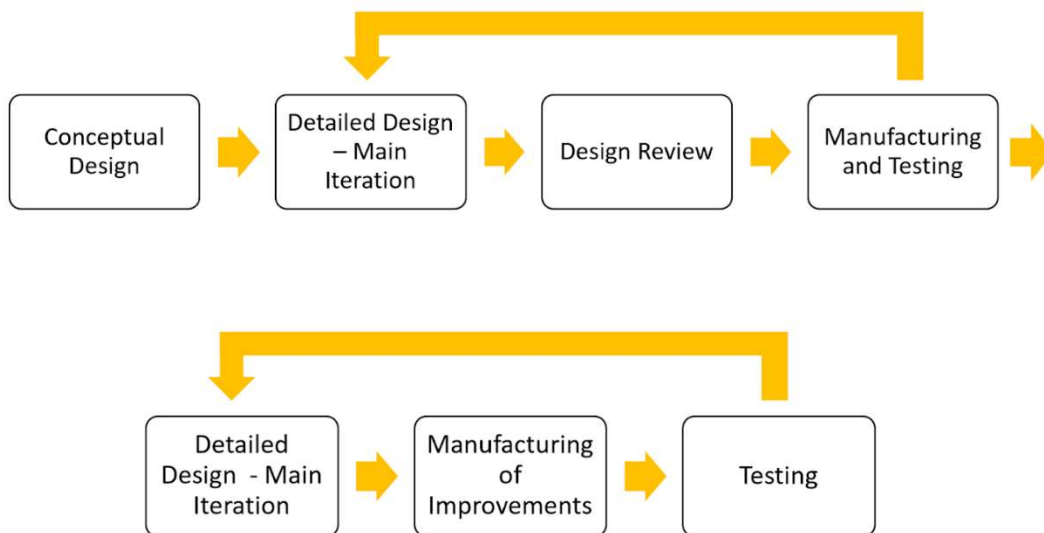


Fig. 3 Project design process

In each phase, integration considerations with all interfacing systems are considered. The team has run regular integration meetings throughout the design cycle in order to address these concerns.

C. Design Goals and Success Criteria

The following table details the overall vehicle requirements of Kraken of the Sky, as well as additional requirements for each subsystem.

Table 1 Kraken of the Sky System Requirements

1.0	Vehicle Requirements
1.1	The rocket shall reach an altitude of 26,000 ft, with an uncertainty of 2,000 ft.
Final verification of this requirement will be performed at the SAC with the rocket’s first launch attempt. Preliminary verification will be accomplished through flight simulation using data from static fire testing.	
1.2	The rocket shall descend safely from apogee and land without significant damage.
Meeting this requirement is the primary responsibility of the recovery system. Recovery system-derived requirements are detailed under section 2.3. Final verification of this requirement will be performed at the SAC with the rocket’s first launch attempt. Derived requirements will be verified through a series of ground tests and wind tunnel tests.	
1.3	The rocket shall maintain a static stability margin between 1.5 and 6.0 cal throughout ascent.
Verification will be accomplished through flight simulation using data from static fire testing.	
2.0	Propulsion System Requirements
2.1	The total impulse of the engine shall not exceed 40,960 Ns.
The Kismet engine must not exceed the total impulse limit of an O-class motor. Verification will be carried out by a full-scale static fire test.	
2.2	The engine shall employ a method by which the amount of oxidizer loaded into the oxidizer tank can be reliably estimated.
The fill sensing system will use a load cell on the launch tower to measure the difference in rocket weight when loading propellant. A temperature sensor will be placed at the exit of the vent valve to determine when the liquid level has reached the dip tube. A propellant loading test using a proxy fluid for nitrous oxide (liquid CO2) will be performed to verify that this system is able to correctly measure the level of oxidizer.	
2.3	The aluminum shell of the combustion chamber shall not exceed a temperature of 250 °C.
This will ensure the combustion chamber is not annealed by the engine burn. Temperatures will be kept low using an ablative G-11 fiberglass liner. Extensive thermal simulations will be conducted as preliminary design validation. Final verification will be carried out by a full-scale static fire test.	
3.0	Recovery System Requirements
3.1	The recovery system shall deploy the main parachute in a reefed state when the rocket reaches apogee.
Verification will be performed through ground testing of the recovery system using a wind tunnel to simulate flight.	

3.2	The recovery system shall trigger the disreefing event when the rocket has descended to an altitude of 1,500 ft above ground level (AGL).
Verification has been performed in a wind tunnel, as outlined in Section 2.3 and Appendix 2.	
3.3	The recovery system shall be capable of being armed remotely.
Ground testing of the remote arming system will take place prior to the launch campaign to verify that the system can be remotely armed and disarmed.	
3.4	A communication failure with the remote arming system shall not prevent the recovery system from being disarmed.
The recovery system will always be capable of being disarmed from outside of the rocket using its internal magnetic switches. Ground testing will be performed on this system to verify the disarming method.	
4.0	Avionics Systems Requirements
4.1	The rocket shall transmit telemetry regarding altitude, velocity, and attitude throughout the flight from ignition to touchdown.
This functionality will be performed by the RocketCAN Live Telemetry Transmitter (LTT) Board as well as the BigRedBee commercial off-the-shelf (COTS) GPS module. Telemetry functionality and range testing will be performed on the ground.	
4.2	The rocket shall log all system commands and sensor data gathered during flight for post-flight analysis and troubleshooting.
This will be the function of the RocketCAN Logger Board. All RocketCAN boards communicate over a shared CANbus, and Logger records and saves every controller area network (CAN) message to an SD card. This SD card can be recovered after the flight. Electrical system integration tests will be performed to ensure the Logger is capable of logging every message when all boards are active and message throughput is high.	
4.3	It shall be possible to replace any avionics board with an identical copy without compromising or negatively affecting the avionics system.
All boards must be trivially replaceable. This ensures that if a component on one board fails in the field during final assembly, it can be replaced with an identical board without issue. RocketCAN is designed with modularity and ease of replacement in mind, and several copies of each board will be assembled and packed to ensure sufficient spares are on hand. All replacement boards will have identical hardware, so no configuration changes will be necessary.	
4.4	All flight electronics shall comply with Appendix B of the IREC DTEG, Safety Critical Wiring Guidelines.
Although the Safety Critical Wiring Guidelines are only explicitly binding on safety critical wiring, it is desirable to ensure all flight wiring is in compliance. This ensures all flight systems are robust and reliable. It also makes pre-flight inspection easier, as all wiring must be held to the same standard. Design considerations and selection of components will be verified for compliance during the electrical design review process. Assembly considerations will be verified for compliance during pre-flight inspection.	
5.0	Aerostructures Requirements

5.1	The rocket fins shall have an aeroelastic flutter threshold velocity higher than the maximum rocket airspeed.
Dimensions of the fin set and fin flutter calculations are available in section 2.2.	
5.2	The airframe shall withstand all bending, compression, and impact loads encountered throughout flight.
Preliminary design validation will use analytical methods of determining loads experienced by the structure. Further validation on manufactured prototypes will be conducted through destructive testing of components.	
5.3	Airframe manufacturing processes shall endeavor to reduce surface roughness in the interest of drag reduction wherever possible.
This will be accomplished through surface finishing techniques such as sanding, polishing, and use of glossy coatings.	
6.0	Payload Requirements
6.1	The payload shall conform to the CubeSat standard with a form factor of 3U.
Compliance will be ensured throughout all design reviews leading up to manufacturing. Final verification will be accomplished via measurement of dimensions and mass.	
6.2	The payload shall be unnecessary for nominal rocket performance - that is, if the payload is replaced with a dead weight of equivalent mass and form factor, all non-payload mission objectives shall still be met.
The payload will perform no flight functions. Although it will be capable of interfacing with the RocketCAN communications bus to provide an additional stream of sensor data, this data will be redundant and not necessary for flight or for post-flight analysis of vehicle trajectory.	
6.3	It shall be possible to test the radiation detectors in the payload before flight.
The specifications of the selected detectors indicate that they are sensitive enough to detect the natural radiation found at ground level. Under the assumption that this is true, functionality tests of the detectors will be performed at ground level.	
7.0	Ground Support Equipment Requirements
7.1	The fill and ignition process shall be operable remotely from a range of at least 2,000 ft.
Verification of the remote fill and ignition systems will take place during static fire testing and Wet Dress Rehearsals. Launch control system range testing will be separately held to verify the operating range of radio communication.	
7.2	An electrical or software failure in the launch control system shall not cause the rocket to enter an unsafe state when personnel are nearby.
All actuators will have power disabled and controls locked out via key switch when any personnel are at the launch pad.	

7.3	There shall be a method of remotely disconnecting the fill system plumbing from the rocket prior to launch.
This system will be remotely actuated using a linear actuator controlled by the launch control system. The fill disconnect system will be tested in launch configuration during the Wet Dress Rehearsal.	
8.0	Operational and Safety Requirements
8.1	Rocket “final assembly” (all assembly steps that can happen only immediately prior to launch) shall take no longer than 3 hours to complete.
This requirement is important to ensure that launch day operations are efficient and can be completed in a timely manner. Verification will take place through assembly rehearsals prior to the launch campaign.	
8.2	A safe perimeter shall be established around test and launch sites prior to fill system pressurization. Only designated test personnel with proper personal protective equipment (PPE) shall be permitted to enter this perimeter while the fill system is in a pressurized state.
Procedural checks will be in place to ensure that the test site or launch pad are clear prior to the start of pressurization.	

III. System Architecture Review

Kraken of the Sky is a hybrid rocket, and an iteration of the UXO series. It has an outer diameter of 6 inches and is 214 inches in length. It has three main modules: the Kismet engine, the payload bay, and the recovery system.

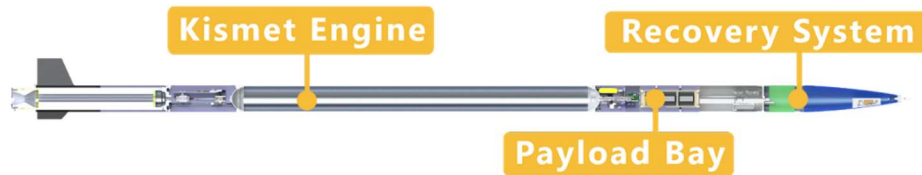


Fig. 4 Sectional view of KotS

A Work Breakdown Structure (WBS) for the Kraken of the Sky project can be seen in Fig. 5. The project is primarily divided into Flight Systems and Ground Systems. Flight Systems are divided into the key subsystems of Airframe, Recovery, Avionics, Payload, and Propulsion, while Ground Systems include both launch systems and testing infrastructure.

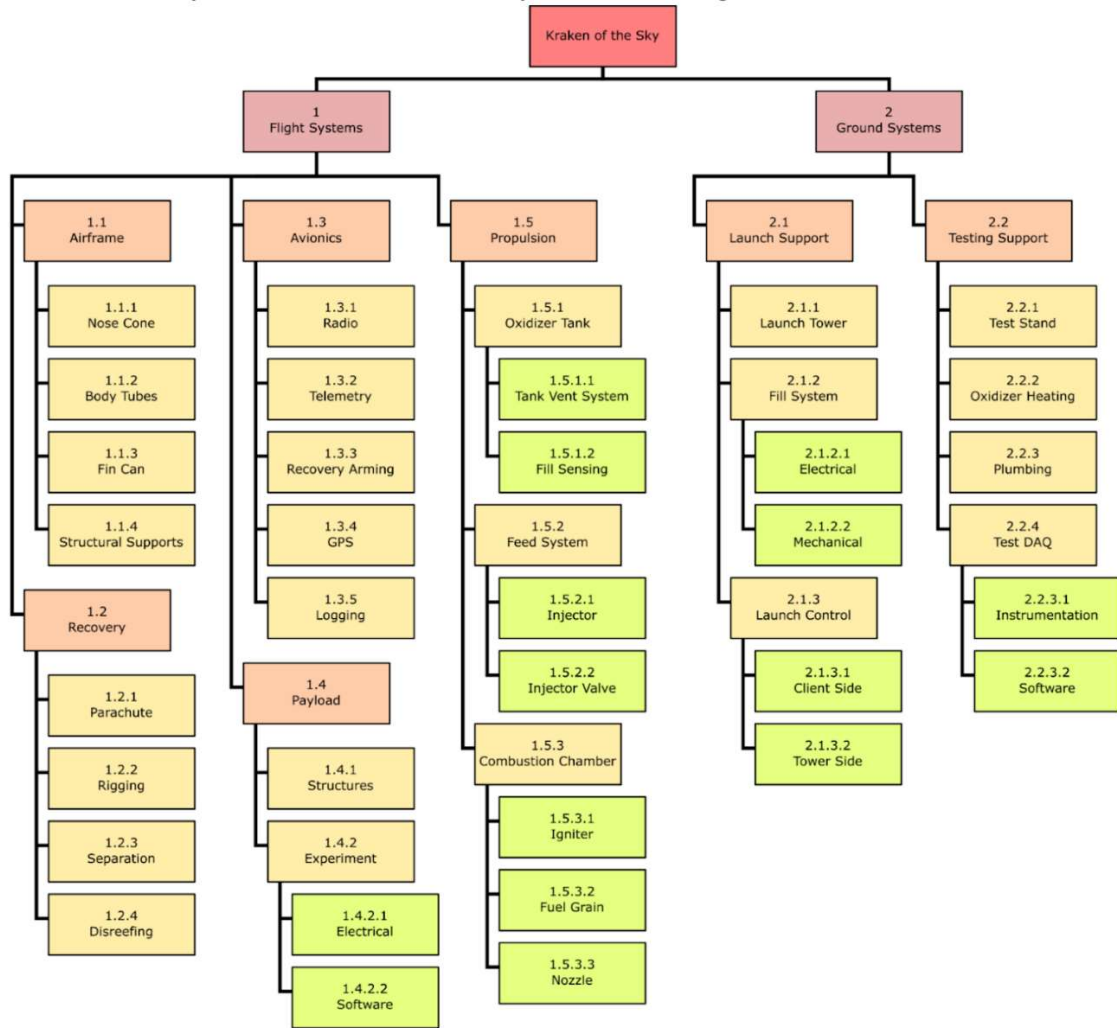


Fig. 5 Work breakdown structure of Kraken of the Sky

A. Propulsion

KotS is powered by an iteration of the Kismet engine, which was first flown on UXO at the 2018 IREC. In order to support efforts to reach 30,000 ft, modifications over the 2019-2022 design cycle primarily focused on increasing total impulse and thrust as well as decreasing the mass of engine components. Kismet is an SRAD hybrid engine using hydroxyl-terminated polybutadiene (HTPB) as the fuel and nitrous oxide (N₂O) as the oxidizer. Fig. 6 shows the section view of the engine and Fig. 7 shows the piping and instrumentation diagram (P&ID).

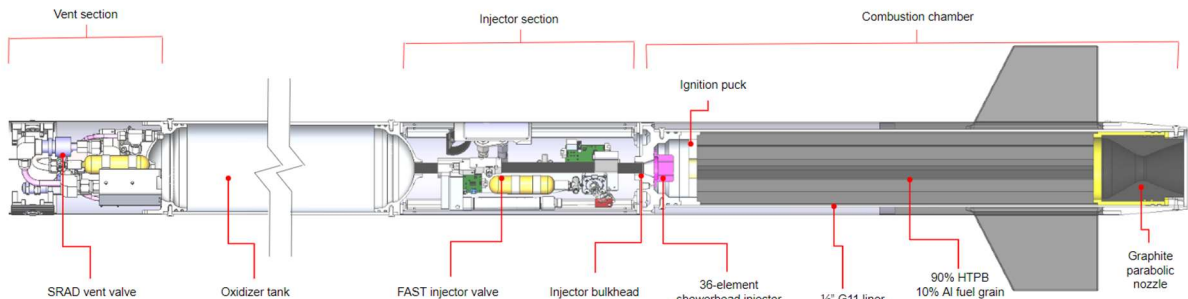


Fig. 6 Sectional view of KotS

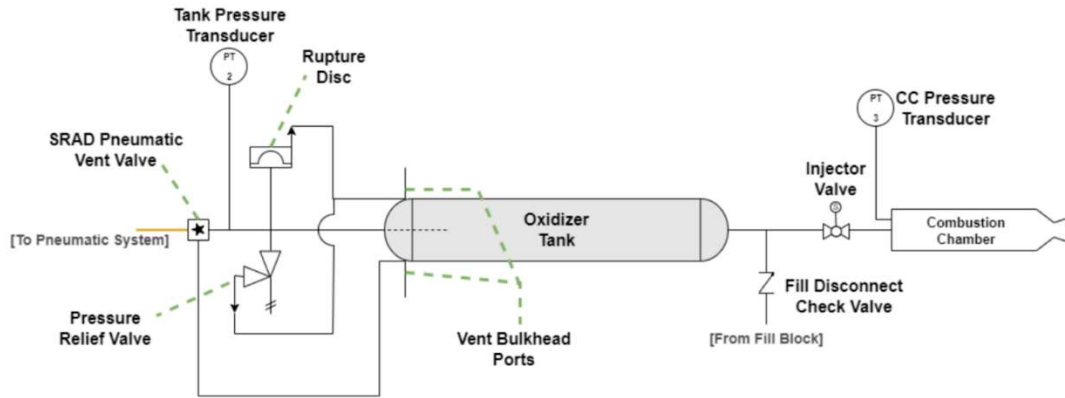


Fig. 7 Kismet P&ID

Differences from the previous iteration include an improved SRAD pneumatically actuated injector valve, a new SRAD pneumatic vent valve, and a new graphite bell nozzle in place of a graphite conical-approximation nozzle. These modifications were implemented to improve system reliability and performance by incorporating lessons learned from the previous competition cycle. Table 2 is an overview of the engine's key performance metrics. Table 3 and Table 4 tabulate engine subsystem parameters and propellant details, respectively.

Table 2 Engine performance parameters

Peak Thrust	1253 lbf
Total impulse	8565 lbf-s
Specific impulse	144 s
Nominal burn duration	13 s
O/F ratio	4.6

Table 3 Engine subsystem parameters

Injector	Type	36-element showerhead
	Hole length	0.984 in
	Hole diameter	0.079 in
	Material	AISI 304 stainless steel
Nozzle	Shape	Thrust-optimized parabolic, 80% equivalent length
	Throat diameter	1.551 in
	Exit diameter	3.397 in
	Inlet diameter	3.881 in
	Expansion ratio	4.8
	Convergent angle	30°
	Expansion inlet angle	25°

	Expansion exit angle	15°
Combustion Chamber	Outer diameter	5.00 in
	Inner diameter	4.75 in
	Chamber pressure	420 psi
Propellant tank	Max operating pressure	1000 psi
	Nominal operating pressure	850 psi
	Firing cutoff pressure	650 psi

Table 4 Propellant parameters

Propellants	Fuel composition	90% HTPB / 10% Al (powder, 200 mesh)
	Fuel mass	12.3 lbs
	Oxidizer composition	100% N2O
	Oxidizer mass	45 lbs
Fuel Grain	Length	26.18 in
	Diameter	4.50 in
	Diameter with G11 liner	4.75 in
	Geometry	6-slot pseudo-finocyl
	Slot width	0.625 in
	Core diameter	1.50 in
	Slot depth	0.724 in

The fuel used in Kismet is a mixture of 90% HTPB and 10% powdered aluminum by mass. The fuel grain has a pseudo-finocyl grain geometry (shown in Fig. 8) achieved through investment casting. Extruded polystyrene is used to create a mold for the port while the fuel is cast inside the liner. The polystyrene is dissolved in acetone after the fuel has solidified. This geometry provides a large surface area for fuel-oxidizer contact, as well as maintaining a relatively similar O/F ratio throughout the burn.



Fig. 8 Cross-section of Kismet fuel grain [1]

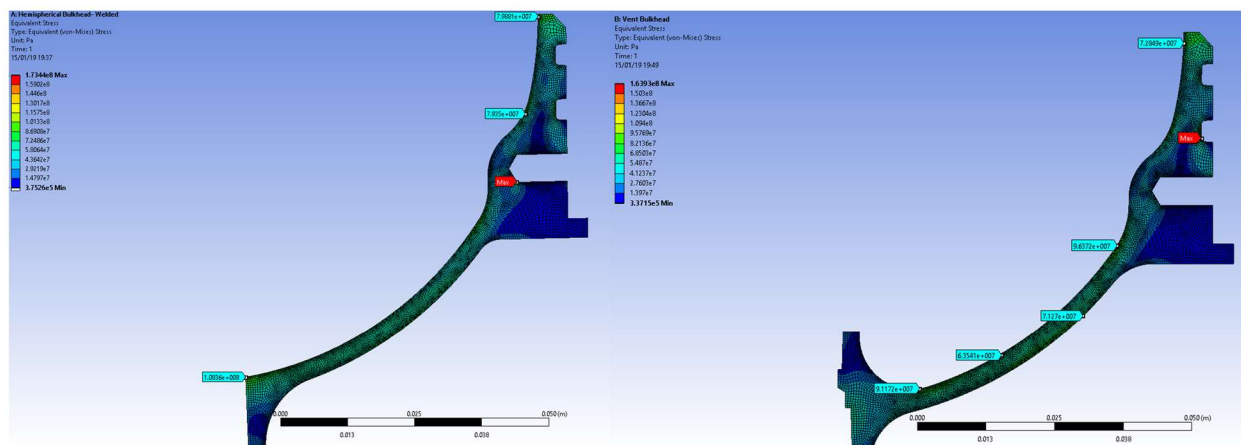
The oxidizer is a saturated liquid-vapor mixture of nitrous oxide. This oxidizer is self-pressurizing, and no additional pressurization device is required; at operating temperatures, N₂O vapour will provide enough pressure to both keep some N₂O in liquid form and eject it out of the tank.

1. Feed System

Oxidizer Tank

The oxidizer tank is a 6" OD, 80" long tank sealed on both ends with removable hemispherical bulkheads. The system is blow-down by utilizing the self-pressurizing properties of nitrous oxide to feed oxidizer into the injector. The oxidizer tank is made of 6061-T6.

The oxidizer tank bulkheads are attached to either side of the tank with a radial bolt pattern using 24 1/4"-28 bolts to attach each bulkhead. The oxidizer tank was designed with a minimum FOS of 2 against yielding for nominal 1000 psi service and is hydrostatically tested to 1500 psi. The bulkhead design is carried over from that used in 2019 SoTS and the detailed discussion of its design can be found in section A. Propulsion Subsystems of Ref. [1]. In summary, the hemispherical design was chosen for mass reduction and improved accessibility to plumbing. Design calculations can be found in Appendix III of Ref. [2]. The design was simulated in Ansys Mechanical to verify the factor of safety of 2.5 for the fill bulkhead and 3.0 for the vent bulkhead, assuming a yield strength of 276 MPa. The results are included in Fig. 9. Fig. 10 shows the finished bulkhead, manufactured with a 3-axis CNC mill.



a) Hemispherical oxidizer tank fill bulkhead

b) Vent bulkhead

Fig. 9 Ansys Mechanical FEA results of hemispherical oxidizer tank fill bulkhead and vent bulkhead



Fig. 10 Hemispherical oxidizer bulkhead [1]

The oxidizer tank utilizes 2 Buna-N o-rings per bulkhead for sealing. Buna-N is generally not recommended for usage with nitrous oxide [3, 4] since it can soak up nitrous oxide and present an ignition hazard with multiple/long-term uses but limiting the material's exposure time is considered a viable risk mitigation strategy [5]. In practice, Buna-N O-rings are replaced after every exposure to nitrous oxide.

Fill System

The fill system has been redesigned to reduce drag by fitting all components within the airframe. The fill system is accessed through a hatch in the oxidizer tank aft skirt. A 1/4" male quick connect fitting is used to connect to ground-side fill plumbing. The quick connect fitting is followed by a 1/4" check valve, after which it is routed to a T-fitting with a tube. The T-fitting is of a SRAD design with two, in-line 1/2" female NPT connections and a perpendicular 1/4" female NPT connection. Together with the bent tube, this T-fitting eliminates an adaptor and allows the plumbing assembly to fit within the airframe.

The T-fitting was machined out of AISI 303 stainless steel. This provides compatibility with N2O and is easier to machine than AISI 304 stainless steel. The fitting was designed to a maximum pressure of 1000 PSI with a safety factor of 2.2. The fitting was hydrostatically tested to 1500 PSI.

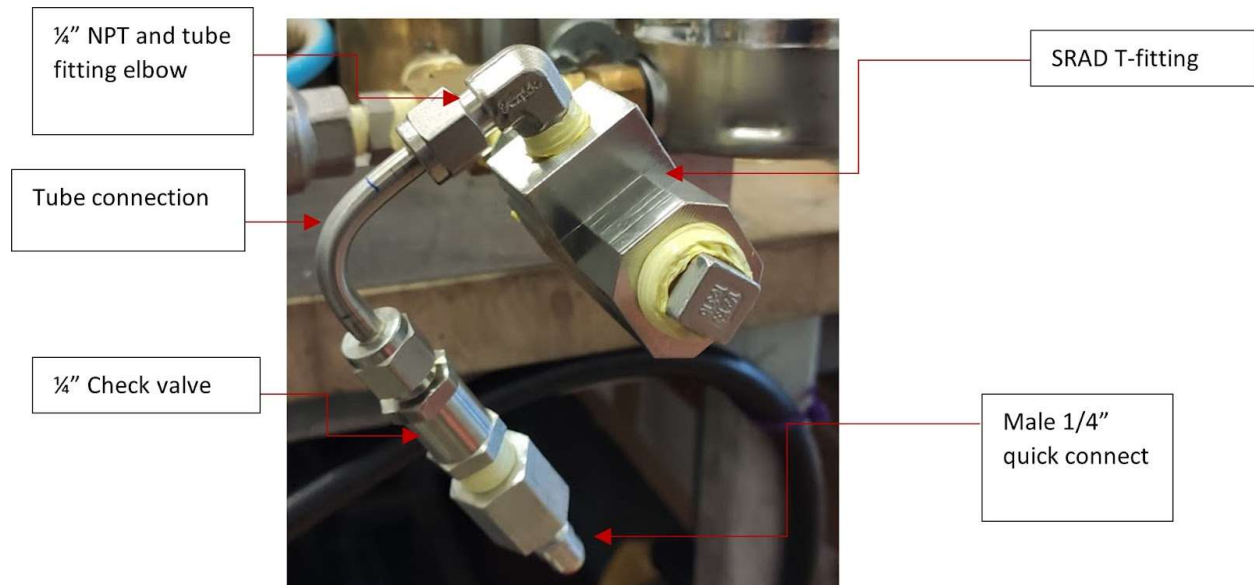


Fig. 11 Fill assembly

Injector Valve

The 2022 iteration of Kismet uses SRAD Fast-Actuation Solenoid oxidizer-Transfer pneumatically-actuated valve (FAST) in place of the gear-actuated injector valve used in 2019. FAST is shown in Fig. 12. FAST actuates a pneumatic cylinder which turns a machined arm to open the ½” NPT Assured Automation ball valve, feeding the oxidizer to the combustion chamber from the oxidizer tank. The ball valve, a Nitra pneumatic cylinder (A12030DP), an SMC 3 port solenoid valve (VKF333-6G-01N), and empty 38 g CO₂ cartridge are mounted to a bent aluminum bracket.

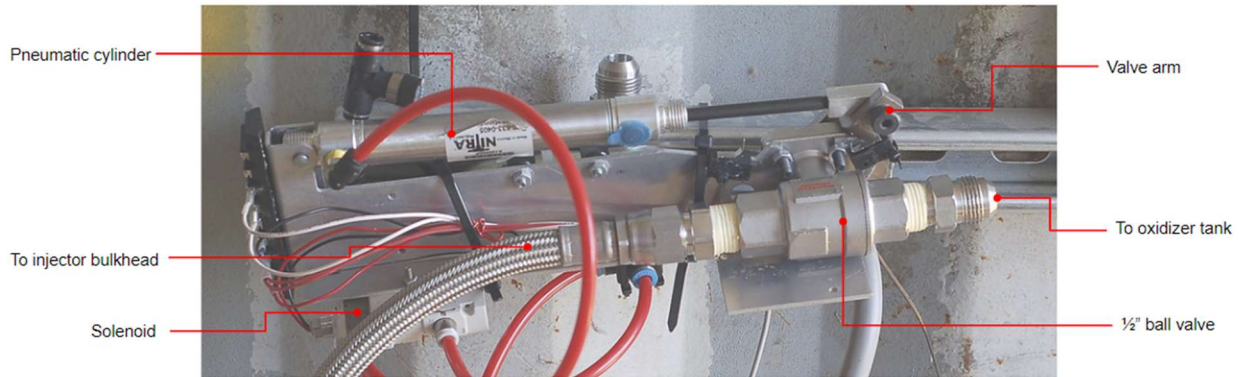


Fig. 12 FAST assembled for static fire testing

Pneumatic actuation is achieved with 90 psi air. The expended 38 g CO₂ cartridge is the onboard air reservoir. The air reservoir is charged via the ground air supply system, accessed through the same oxidizer tank aft skirt hatch as the oxidizer fill system. Limit switches are used to sense the state of FAST. Fig. 13 shows the plumbing & instrumentation of the FAST system.

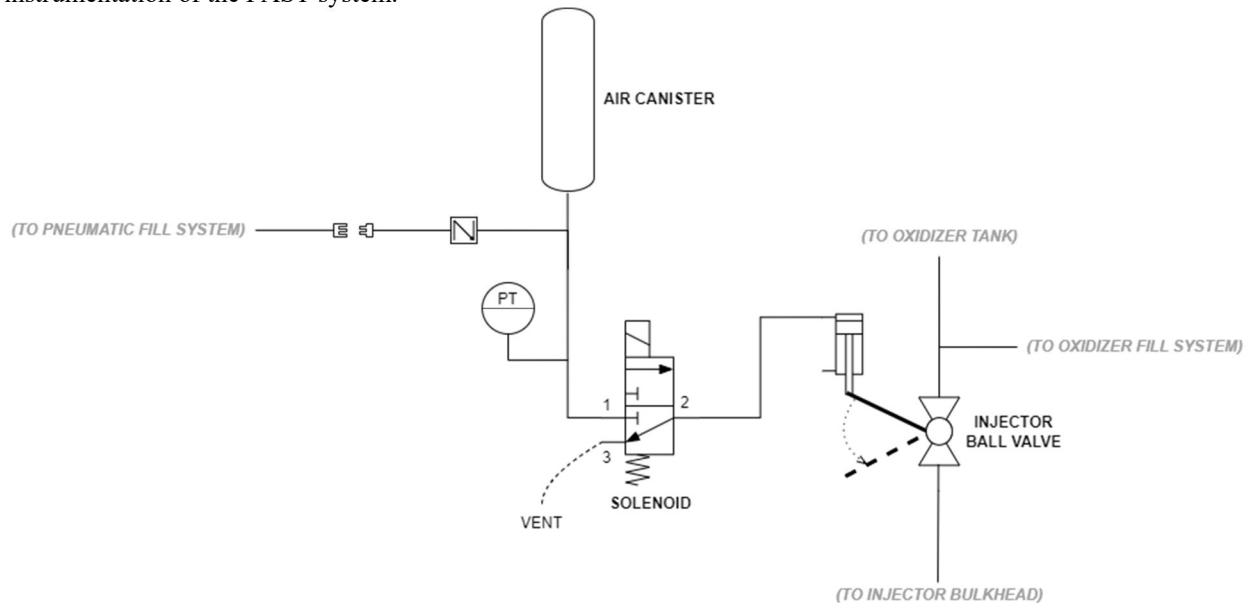


Fig. 13 FAST P&ID

The main advantages of FAST include 1.1 lb of weight savings, faster actuation, and less load on the electrical system (actuation is facilitated through a solenoid valve and not a geared motor). The system has been cold-flowed individually, was test-proven in a static fire conducted in July 2021 and is due for another test in the upcoming static fire of the engine. The system was sized to handle a valve with double the amount of torque. Calculations used for sizing this system are found in Appendix III of Ref. [2].

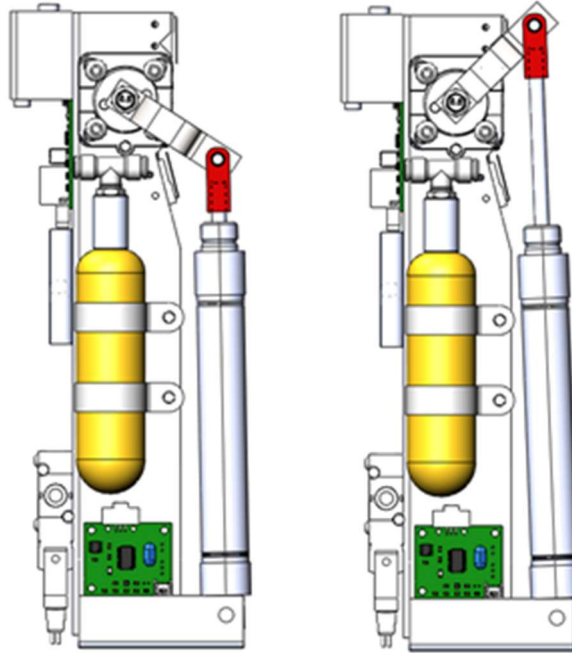


Fig. 14 Diagram of the FAST injector valve operation (pneumatic lines not shown), showing closed (left) and open (right) actuation states.

Part Sanitation for Oxidizer Service

All materials in contact with nitrous oxide are selected for compatibility. Throughout the rocket's plumbing, nitrous oxide comes in contact with stainless steel (valves, instruments), 6061-T6 aluminum (oxidizer tank) and PTFE/Teflon (valve seals, inner tube of braided hoses), all of which are compatible with nitrous oxide. Buna-N is used for O-rings, and while it is not recommended for long-term repeated use with nitrous oxide due to swelling with prolonged contact with the oxidizer, the contact time is not long-term or repeated as the O-rings are expendable with every assembly of the engine and/or launch setup.

All components that are in contact with N₂O are cleaned with a five-step sanitation process:

1. Initial abrasive cleaning
2. Detergent cleaning
3. Solvent cleaning
4. Drying
5. Inspection and clean storage

In mechanical/initial cleaning, all components like valves are disassembled, any large particulates are manually removed from the surface of any components. Contaminants like dirt or sand are scrubbed off in this step. The components are given an initial rinse with water to remove any remaining loose particulates and water-soluble materials. Scrubbing may be used in this step to assist with removing as much undesirable material as possible. Any damaged components (i.e. damaged valve seals) are discarded and replaced accordingly.

Once the initial aqueous cleaning is done, the component undergoes detergent cleaning. If any signs of rust show on the part, it is first immersed in EvapoRust, CLR or similar rust-attacking detergent. Once it is rust-free and re-rinsed, the component is immersed in Simple Green detergent (in an ultrasonic cleaner, with heating, if the material can withstand heat) for 3 minutes, provided the part fits the ultrasonic cleaner. Use of clean sanitized tools (cleaned with this same procedure) to assist with scrubbing etc. is common in this step, and parts like hoses are "sloshed" around to ensure the detergent and the following rinse reach the entire inner surface. Parts that do not fit the ultrasonic cleaner are manually cleaned repeatedly, thoroughly, and conservatively with Simple Green detergent as well, noting to not miss any surface. Once the part is cleaned and has been in contact with detergent for 3-5 minutes, it is rinsed thoroughly at least twice with deionized water. Depending on the state of the part after this step, it can, on its entirety, be repeated as needed.

Once the component is cleaned by detergent and thoroughly rinsed, any metal, slow-to-dry or large components are rinsed with >99% isopropyl alcohol, ensuring contact with the component's entire surface. This is to eliminate any remaining organic contaminants.

The clean components are finally dried with high-pressure high-purity nitrogen gas (>99.98%), to prevent DI water or solvent from remaining in the system and to ensure any crevices are free of liquid (i.e. corners of fittings, inner holes) until fully dry or for a conservatively lengthy period of time.

Finally, the parts are inspected for dryness and debris. A UV inspection light is used to aid visual assessment. Sanitized parts are then sealed from the ends or fully covered in aluminum foil (held by tape if necessary) and stored in sealed, clean particle-free bags to keep them clean until assembled. Parts like valves are kept in assembled form if they are needed soon.

The entire cleaning process is done by trained team members wearing new compatible gloves between steps, avoiding any non-sanitary contact with the components. The components never come in contact with tabletop surfaces; work surfaces are covered with clean sheets of aluminum foil.

The detailed sanitation procedure is discussed in the Assembly, Preflight, and Launch Checklists Appendix of Ref. [1].

2. *Injector*

Kismet v3's injector is a 36-element showerhead type injector identical to that used in the Kismet v2 engine. Compared to Kismet v1, this injector produces a larger oxidizer mass flow, which is necessary given the higher target apogee and system mass. The length of the injector holes was also increased to reduce the risk of catastrophic back-propagation towards the oxidizer tank. The injector design was initially determined with a custom C++ program, using a homogeneous equilibrium model to account for the two-phase flow behavior of N_2O [6]. The required quantity and dimensions of the injector holes were predicted given various inputs (temperature, pressure, desired mass flow, nozzle throat diameter, combustion chamber pressure, and fluid thermochemical properties). However, two-phase flow is notoriously difficult to model accurately, and so cold-flow tests were conducted to fine-tune the design. This involves running pressurized CO_2 through the injector to characterize performance. Since CO_2 exhibits two-phase flow behavior similar to N_2O for the temperatures and pressures in question, it is an excellent analogue for this purpose. Data from cold flow tests was used to adjust the dimensions and number of injector elements until a combination which produced the desired mass flow rate was found. The resulting injector configuration was used successfully in Kismet v2 during many static fire tests as well as a flight and is expected to perform identically for Kismet v3. The pressure drop across the injector is specified at >35%. From an operational perspective, this means that the minimum cutoff pressure for firing the engine is 650 psi (based on a chamber pressure of 420 psi). Below this point, back-propagation through the injector elements is a risk and the fire attempt must be aborted. The injector itself is shown in the figure below.



Fig. 15 36-element showerhead injector installed in injector bulkhead

3. Combustion Chamber

The combustion chamber of the rocket holds the injector bulkhead, the ignition puck, the fuel grain, and the nozzle together. Two Buna-N O-rings and flame-resistant caulking are used to seal the injector bulkhead and nozzle to the combustion chamber. The 5" OD, 1/8" wall thickness 6061-T6 aluminum engine wall is separated from the fuel grain by a 1/8" wall thickness G11 fiberglass tube that lines and protects the chamber walls from the heat of combustion by delaying heat transfer with its low conductivity. The liner choice is a design decision from the 2019 iteration of Kismet.

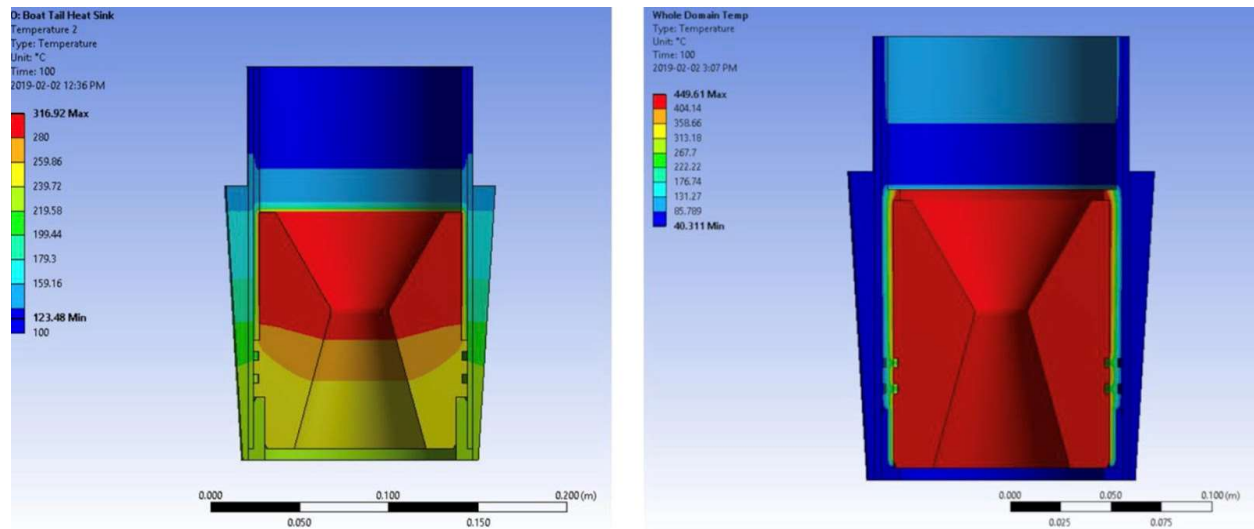


Fig. 16 Heat transfer simulations of the SotS nozzle area with G10 (left) and G11 (right) liner

The chamber is expected to have a maximum pressure of 700 psi. The limiting failure case is tensile hoop failure with FOS 2.6 [1]. The fuel grain, its ablative thermal liner, and the combustion chamber itself (i.e. the aluminum pressure vessel) are identical in design to previous versions of Kismet and have therefore been validated by previous static fire tests.

4. Nozzle

The team's previous engine (Kismet v2, which flew at the 2019 SAC) used a graphite nozzle with a conical divergent section. This type of nozzle is simple to design and manufacture, at the expense of reduced efficiency. Thus, one of the main areas identified for improvement in Kismet v3 was the nozzle. Initially, the task of developing an improved nozzle was undertaken by a group of students as an upper-year course project, but ultimately this design did not prove feasible. Therefore, a second nozzle concept was designed and built, and will be validated in an upcoming static fire.

The first design concept, nicknamed 'Ghost Pepper', was intended to demonstrate an experimental cooling method, in which water would remove heat by undergoing a phase change. In contrast to more typical cooling methods for metal nozzles, such as regenerative or film cooling, no pumps or pressurant would be needed. This simplified the system design and flight integration, as well as saving considerable weight. This project made use of a sponsorship by MSAM (the additive manufacturing laboratory at the University of Waterloo), which made 3D-printed components both financially and technically accessible to the team. Using additive manufacturing techniques allowed for a more efficient thrust-optimized parabola (TOP) geometry for the expansion section, instead of the previous conical approximation. Additive manufacturing can also produce complex internal geometry which would be very difficult to accomplish with conventional techniques. In case of this design, a topologically-optimized internal lattice structure was incorporated into the water reservoir to support the thermal and pressure loads. The material selected was Inconel 625, due to its excellent strength at high temperature, wide availability, and good characterization in literature.



Fig. 17 A cross-sectional render of the design (left) and the actual printed part (right)

The previous graphite nozzle usually became cracked or eroded after a burn, preventing its reuse for fear of affecting the combustion chamber's performance or risking mechanical failure. Thus, a key objective for this design was reusability. Unlike graphite (which is both chemically reactive with the exhaust products as well as physically soft), the Inconel construction of this nozzle would allow it to be used for many burns. Another issue with graphite is poor mechanical performance: the previous nozzle required mechanical support and impact protection, which was provided by the combustion chamber (the liner and boattail more specifically). This added to the overall system weight, and also introduced the risk of annealing the combustion chamber walls due to the high thermal loads and causing mechanical failure due to overpressure. This design would have addressed all of these issues, being substantially lighter (by 1515 g, about 50%), requiring no external mechanical support, and, with a much lower heat flux into the combustion chamber (since it is mostly outside of it), posing less risk of thermally-induced mechanical failure.

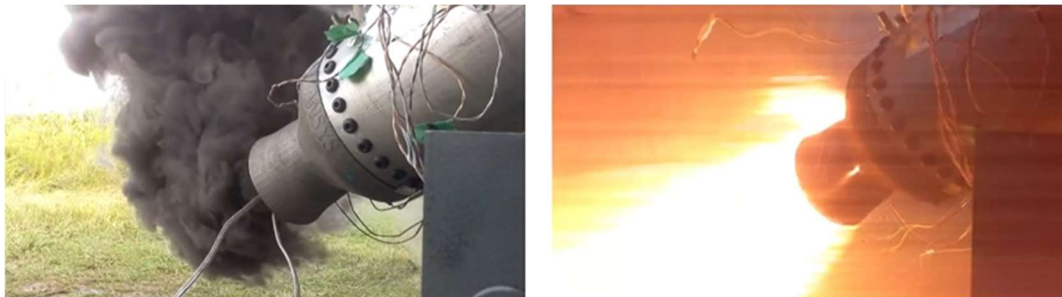


Fig. 18 The nozzle just prior to firing (left); visible burnthrough at the throat (right)

As previously referred to, this design did not perform as expected during static fire testing. The water was vaporized and ejected from the reservoir much faster than predicted, which stopped any meaningful cooling and caused the nozzle to melt. It might have been possible to tune the design to avoid this result if more analysis was performed, but plausible models would be very complex (likely Navier-Stokes coupled with generalized heat transfer and phase change). This was infeasible given the team's resources, and so the decision was made to proceed with a static test fire to acquire data. A more detailed discussion of the design and analysis of this nozzle is outside the scope of this report, since it was not selected for flight. However, detailed documentation is given by [7].

At the end of the printed nozzle project, the need for an upgraded nozzle design persisted. An obvious improvement to the original design would be a more efficient expansion section geometry (instead of a conical profile), but achieving this was not previously feasible, as the team lacked access to a CNC machine on which graphite machining was permissible. However, since the conclusion of the printed nozzle project, the team had gained access to such a machine. Also, by this point in Kismet v3's design cycle, the time available for new projects was short, and so a

project with fewer large unknowns was desirable. For these reasons, the selected nozzle design is essentially the same as that of Kismet v2, with the only difference being a change to a parabolic (TOP) geometry for the expansion section. This made the design and system integration of the new nozzle (nicknamed the ‘bell nozzle’) much simpler, increasing the likelihood of completing the project on time.

The starting point for this design was to determine the profile of the convergent, throat, and divergent sections. Spreadsheet calculations were used together with RPA (Rocket Propulsion Analysis) software to specify the parameters of the nozzle (and thus the engine itself) and generate a profile. Certain key inputs were taken as averages from previous Kismet v2 static fire data. These were the chamber pressure ($P_c = 420$ psi), oxidizer mass flow ($\dot{m}_i = 1.9$ kg/s), and oxidizer fuel/ratio ($O/F = 4.6$). The governing nozzle exit condition was the expansion area ratio ($\epsilon = 4.8$), identical to Kismet v2. Specifying the propellant combination as well as P_c and ϵ allows throat gas velocity and density (v_t and ρ_t , respectively) to be calculated using RPA. These thermochemical values are independent of geometry (excepting ϵ , but an exit pressure or expansion pressure ratio could be used instead). With \dot{m}_i , O/F , v_t and ρ_t known, the throat area A_t was calculated with the following relation [8]:

$$A_t = \dot{m}_i \frac{1+O/F}{v_t \rho_t O/F} \quad (1)$$

The value of A_t allowed the throat diameter ($D_t = 39.3851$ mm) to be calculated. Similarly to the exit condition, the governing nozzle inlet condition was the inlet area ratio ($A_c/A_t = 6.27$ where A_c is the ‘chamber area’, i.e. the nozzle inlet area). With all the numeric inputs defined, only some key choices on geometry remained in order to generate a profile. The contraction angle of the convergent section ($b = 30^\circ$) was also identical to that of Kismet v2. To simplify design and fabrication, a TOP profile based on the ideal bell-shaped expansion section contour was chosen [9]. Values for the relative length ($L_c = 0.8$), initial angle ($T_n = 25^\circ$), and exit angle ($T_e = 15^\circ$) were initially those suggested by Ref.[10], and were iteratively explored to strike a balance between efficiency and mechanical packaging constraints. All of the aforementioned parameters were finally used in RPA to generate the profile, which was incorporated into a CAD model of the nozzle.

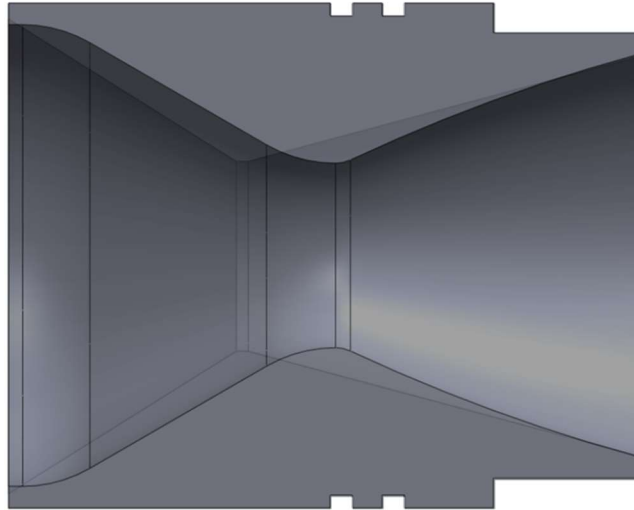


Fig. 19 Cross-sectional comparison of the previous and proposed nozzle profiles

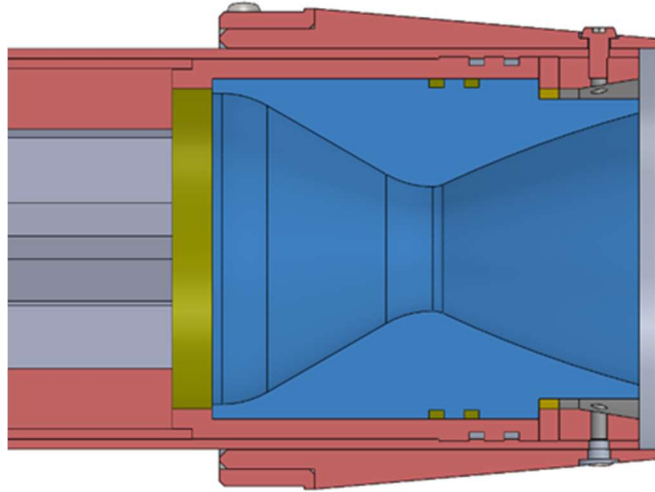


Fig. 20 Cross-section of the aft end of the CC, showing the nozzle and its profile

The theoretical nominal thrust F of this design is given by the following relationship from Ref. [10]

$$F = C_f * P_c * A_t$$

where ($C_f = 1.57744$) is the thrust coefficient for a given nozzle geometry; this value is an output from RPA. The previously-calculated values of P_c and A_t yield a predicted thrust of approximately 1253 lbf, which is consistent with static fire data from earlier iterations of Kismet.

As mentioned in the discussion on the printed nozzle, heat transfer from the nozzle into the CC is a large concern due to the possibility of annealing which could cause a mechanical failure. Even though the mechanical packaging of this new nozzle design is identical to that of Kismet v2, and the heat flux and mass of graphite present are essentially identical, the team still decided to conduct thermal finite-element modeling (FEM) to validate the new design from a thermal perspective. The boundary conditions of the model are the same as those of Ref. [8]. The analysis was conducted with ANSYS Mechanical and was set up as a transient thermal solution, where the heat fluxes specified by the boundary conditions were applied for the duration of the burn. The heat flux from the combustion chamber into the CC wall is difficult to model accurately, being largely governed by ablative heat transfer, so instead it is modeled as a ‘ramp-up’ over a short time period. This assumption, as well as all of the other heat fluxes and boundary conditions, were validated during static fire testing of the Kismet v1 engine and found to be conservative. The mesh setup of the model (with a mesh density focused on the CC wall itself, being the main region of interest) as well as the temperature results predicted for the CC wall are shown below.

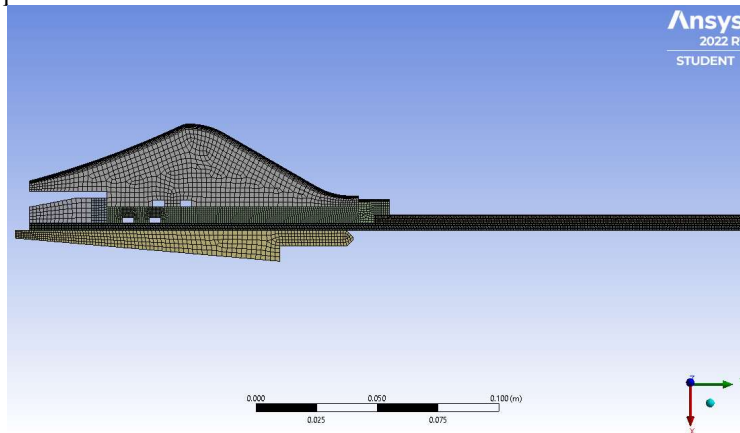


Fig. 21 Mesh setup of the transient thermal model to investigate annealing in the CC

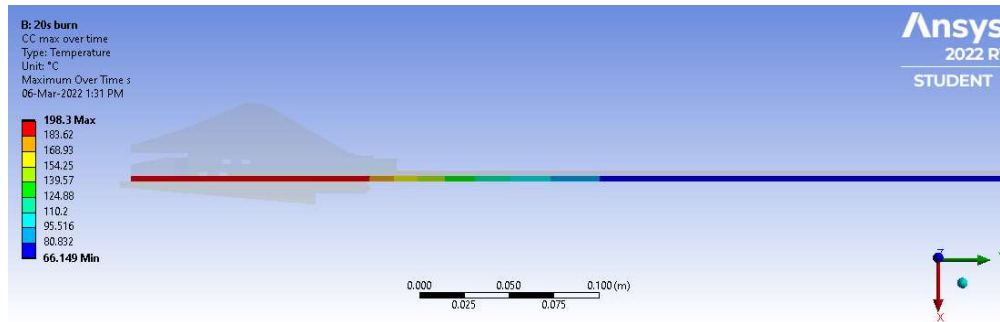


Fig. 22 Temperature plot of the results of the transient thermal model

As shown above, the peak temperature predicted in the CC wall is less than 200 °C, which is within the acceptable value determined by previous static fire testing. This result indicates that annealing caused by excessive thermal loads is not a significant cause for concern. In any case, the accuracy of this model does not pose a safety risk, since hydrostatic testing of the CC is performed before firings to physically validate the integrity of the CC.

While the selected graphite nozzle design does not address all of the issues outlined earlier (it does not offer substantial weight savings, nor reusability), these issues are not egregious and can be improved in future designs. Importantly, the improved geometry of the new nozzle is predicted to increase the theoretical specific impulse (I_{sp}) of the engine by around 1% (compared to an identical conical-expansion nozzle, as calculated by RPA). However, the keyword in the previous statement is ‘theoretical’: this amount of increase is less than the variability seen between static fires with Kismet v2, so it is unclear how much this increased efficiency will translate into a higher flight altitude. The new Kismet v3 nozzle will be static fire tested before the 2022 SAC to validate its functionality as well as gather data to improve future simulations and analysis.



Fig. 23 The as-machined graphite ‘bell’ nozzle

5. Ignition

Engine ignition relies on two separate events: heat application via ignition of a puck of solid rocket fuel, and oxidizer flow initiation through opening of the injector valve. The ignition puck is a toroidal disc composed of 70% potassium nitrate (KNO₃) and 30% epoxy, and sits above the fuel grain at the top of the combustion chamber. The puck is cast with two embedded coils of nichrome wire, which connect to wires that exit the chamber through the nozzle. The puck is ignited when current passes through the nichrome coils, causing them to heat up. Once the puck successfully ignites, the nichrome coils break, and the change in current is displayed by the Remote Launch Control System (RLCS). The operator then sends the signal to open the injector valve, which is performed by RocketCAN. Once the valve opens and oxidizer flow begins, thrust ramp of the engine is immediate.

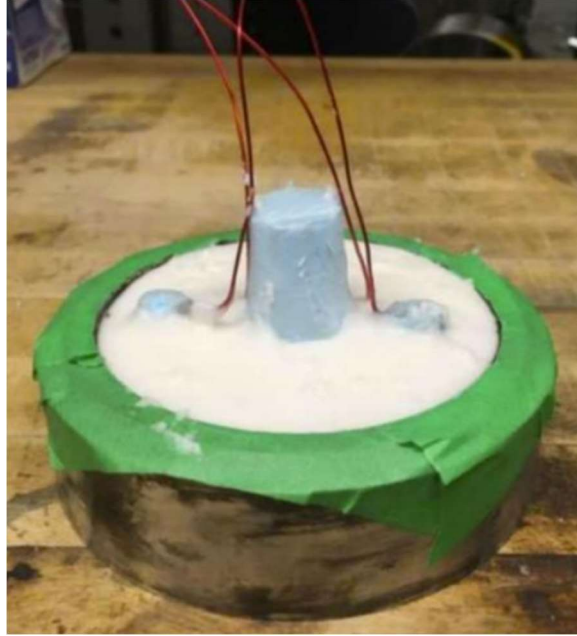


Fig. 24 Cast ignition puck prior to insertion into the combustion chamber

6. Vent Section

The vent section is responsible for controlling the pressure of the oxidizer tank during filling and flight by sealing and venting the ullage volume in a controlled manner. The vent section is physically located above the oxidizer tank and includes the Vent Valve, high pressure oxidizer plumbing, pneumatics control plumbing, electronics, and the airframe section that houses these components. The figure below shows the vent section assembly without the body tube. Hydrostatic testing of the assembly up to 1000 psi will be conducted prior to flight to verify proper sealing at all connections.



Fig. 25 Assembled vent section without body tube

The Vent Valve is integrated into the vent section via high pressure plumbing that routes oxidizer from the oxidizer tank to the outside of the rocket and pneumatics control plumbing that actuates the Vent Valve. Each plumbing system has many components that all need to fit within the compact 6"-diameter of the rocket, so an important consideration for the vent section assembly is the flexibility to adjust the layout and dimensions of the plumbing systems in response to deviations of the actual assembly from its CAD model.

For this reason, as well as for its N₂O compatibility and high reliability, various Swagelok fittings and tubing are used in the high-pressure plumbing to vent oxidizer from the oxidizer tank to the outside of the rocket. The oxidizer would flow through the Vent Valve, a Swagelok 1000psi-rated pressure relief valve, or a ZOOK 1500psi-rated burst disc, with the last two options being fail-safe alternatives in the event that the oxidizer tank pressure exceeds its maximum operating pressure of 1000psi. The high pressure plumbing also connects to a pressure transducer that monitors the oxidizer tank pressure. The figure below summarizes the high pressure plumbing in the vent section.

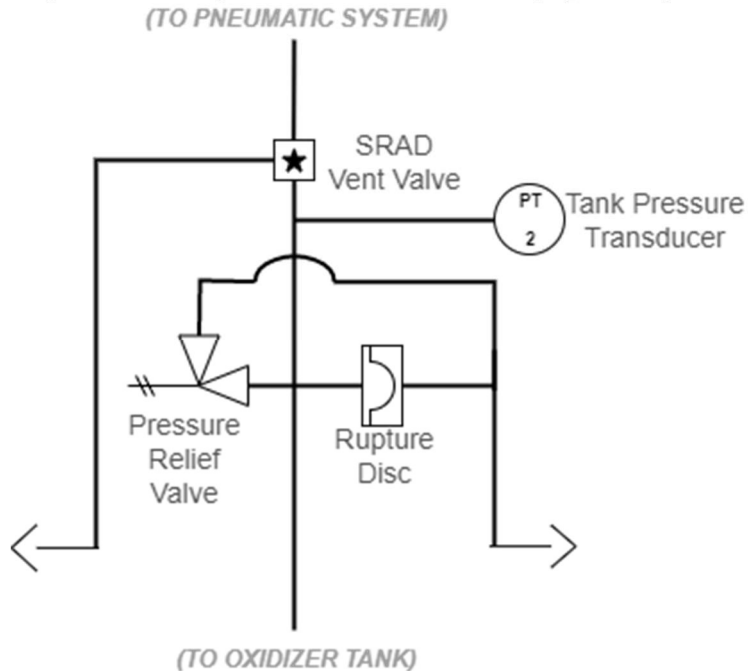


Fig. 26 Overview Diagram of Oxidizer Plumbing in the Vent Section

The pneumatics control plumbing consists of a compressed air canister as a pressure source, a solenoid valve, an actuator circuit board, and a flow control valve. The actuator board controls the solenoid valve to release air into and out of the Vent Valve to actuate its piston. The flow control valve is a manually adjusted valve that regulates the final air flow into the Vent Valve and will be fully opened prior to Vent Valve operation. The P&ID of the pneumatic system is shown in the figure below.

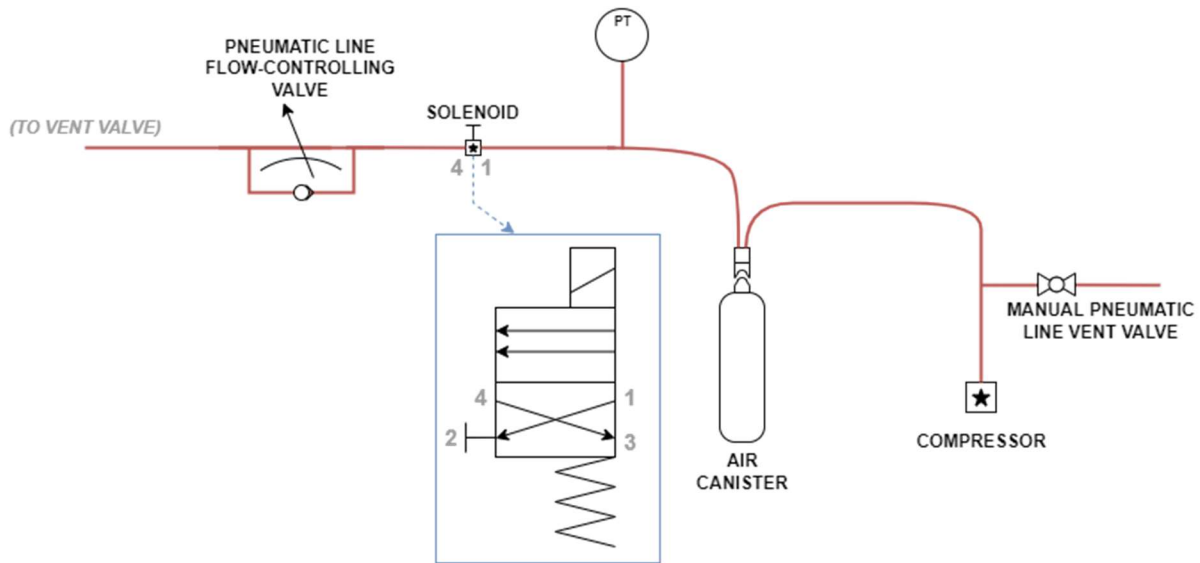


Fig. 27 Vent Valve pneumatic system P&ID

There are also two Raspberry Pi cameras attached to the inside of the body tube surrounding the vent section. These cameras point outward from the rocket and are placed 180° apart to record a 360° video of the rocket during flight. The figure below shows the overall vent section assembly with all major components labeled.

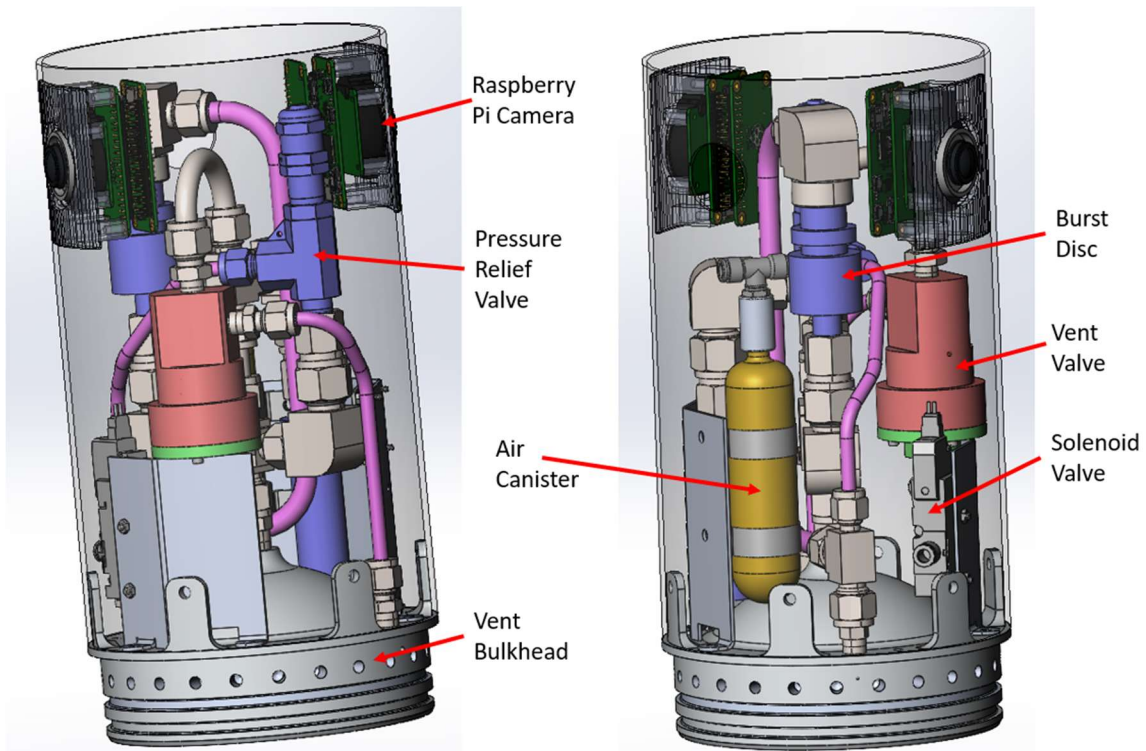


Fig. 28 CAD model of assembled vent section

Vent Valve

The Vent Valve is the team’s SRAD valve that allows air and gaseous nitrous oxide in the ullage space of the oxidizer to be vented. This is an improvement over the permanent vent port used in previous iterations of the rocket. The valve is closed before flight to allow the oxidizer to be pressurized sufficiently before flight.

The valve is a normally-open, pneumatically-actuated shutoff valve. The sealing spool uses a set of X-rings that slide over a side port to seal the flow of oxidizer through the valve. The actuator is a pneumatic piston that is integrated into the spool of the valve, and the body of the piston actuator is integrated into the main body of the valve. This eliminates the need for extra fasteners and seals to combine the valve and the actuator, which saves mass and reduces points where the valve can leak. When pneumatic pressure is lost, the piston returns to its default position using a spring. The figure below shows a cross-section view identifying components of the valve and their materials.

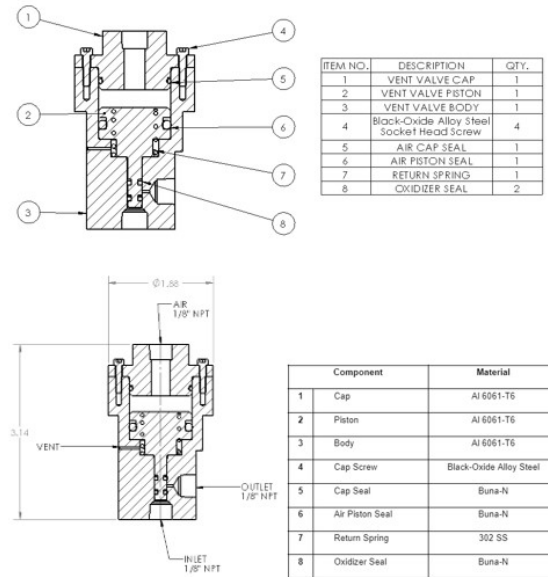


Fig. 29 Cross section of Vent Valve, showing components and their materials, and ports

The air piston side was sized based on the maximum expected N₂O pressure at the valve inlet (1000psi) and the operating pressure of the pneumatic system (90psi). The area ratio required is therefore about 11. Vent Valve has an area ratio of 25, as a factor of safety to be able to control and actuate the valve in case of pressure drops in the pneumatic system, such as due to leaks. The static and dynamic seals' gland geometry and tolerances were obtained from the Parker O-ring Handbook [11].

This valve has been through the following tests to qualify it for flight:

- Hydrostatic test of the oxidizer seals to verify seals do not leak up to 1000 psi
- Shut off test with water, successfully shut off the flow of water
- Shut off test with CO₂, successfully shut off the flow of gas at 600 psi
- Integrated testing with the rest of the propulsion system during a static fire test, successful full cycle test including shut-off of vent to pressurize tanks for engine firing and venting of residual pressure in tanks after firing.

More are included in Appendix C Project Test Reports.

Calculations used in the development of this system may be found in Ref. [2].

B. Aerostructures

Every structural component on the rocket except for the oxidizer tank and boattail is made of SRAD composite parts. The nosecone is a Von Karman shape with a 4:1 fineness ratio. It is made of fibreglass manufactured using a vacuum bag layup process. The tip of the nosecone is a combination of machined steel and aluminum epoxied together to better resist aerodynamic heating. All bodytubes including the parachute bay, upper bodytube, oxidizer tank aft skirt bodytube and combustion chamber bodytube are made of fibreglass manufactured using Vacuum Assisted Resin Transfer Moulding (VARTM). The fin can is made using carbon fibre plates epoxied to a carbon fibre bodytube using high shear strength epoxy. Then, 4 plies of carbon fibre fabric, 3 structural and 1 cosmetic, were epoxied on top using a wet tip-to-tip layup process. The final 2 components, the oxidizer tank and boattail, were both machined out of aluminum and are the only structural components not made of a composite material. The entire structure is monocoque with the oxidizer tank aft skirt supported by longerons meant to resist compression.

The aerostructure components are indicated in the figure below, and more details regarding the dimensions and mass of these components can be found in the table below.

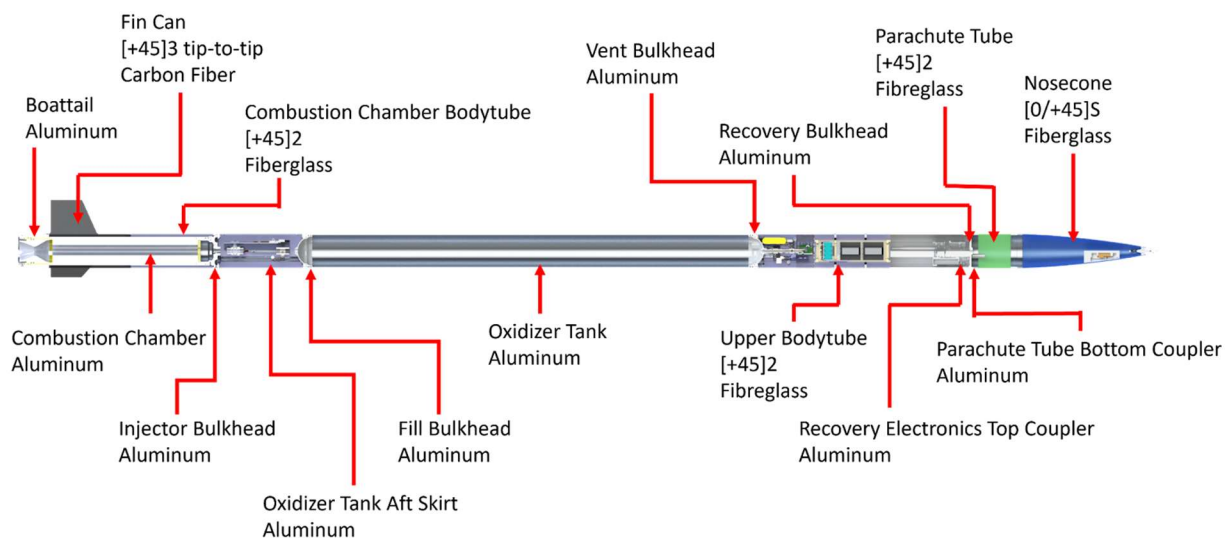


Fig. 30 Aerostructure Layout

Table 5 Mass and Length of Aerostructure Components

Component	Mass (lbm)	Length (in)
Nosecone	1.516	26.813
Parachute Tube	0.800	12
Parachute Tube Coupler	0.300	1.645
Upper Tube Coupler	0.294	1.51
Upper Bodytube	3.182	37.25
Oxidizer Tank + Bulkheads	29.67	83.375
Oxidizer Tank Aft Skirt	1.998	15
Combustion Chamber Bodytube	1.156	15.688
Fin Can	2.914	15.5
Boattail	2.438	5.375
Total	44.268	214.156

7. Loads Analysis

Due to the unusually high aspect ratio of 33.6 of KotS, bending moments induced by in-flight gust loading cannot be neglected. The publicly available BENDIT7 spreadsheet was used to estimate bending moments experienced by the rocket at maximum acceleration (takeoff) and maximum aerodynamic pressure (Max Q). The flight conditions used were taken from OpenRocket simulation data. Thus, stress analysis of components on the rocket during the boost phase considers both bending and axial forces due to acceleration. Due to the uncertainty in the input values and assumptions made in the calculation process, adequately high FOS have been applied to any components that were designed based off the results of the loads analysis. The plots of these results are shown in Figure S1, Figure S2, Figure S3, and Figure S4. See Appendix B Calculations for the loads analysis inputs.

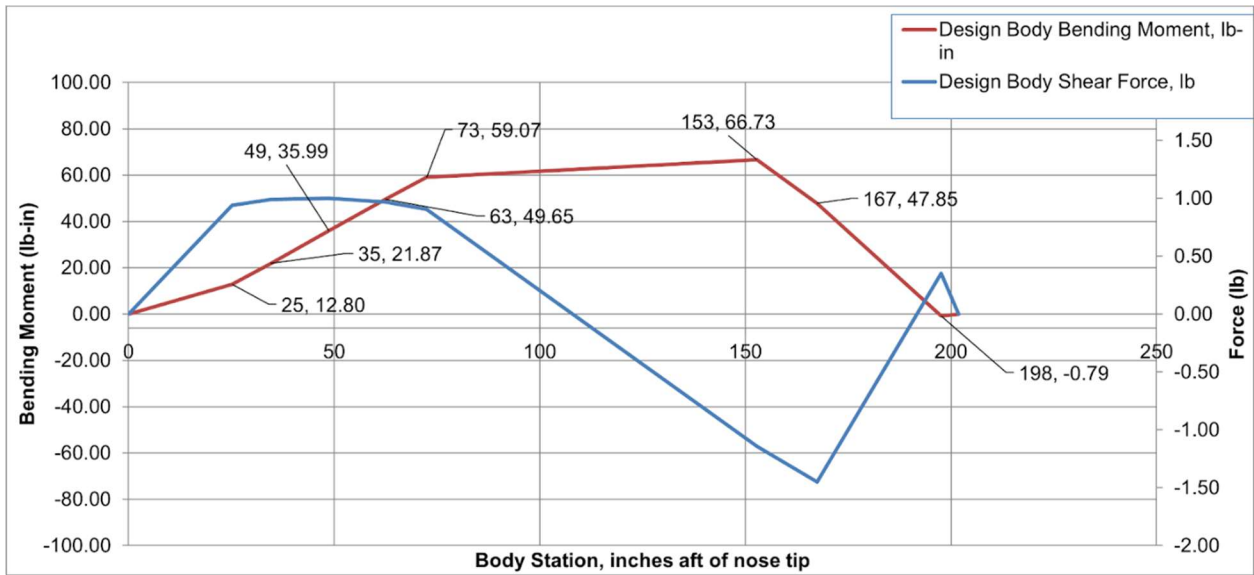


Fig. 31 Body Design Loads at Takeoff

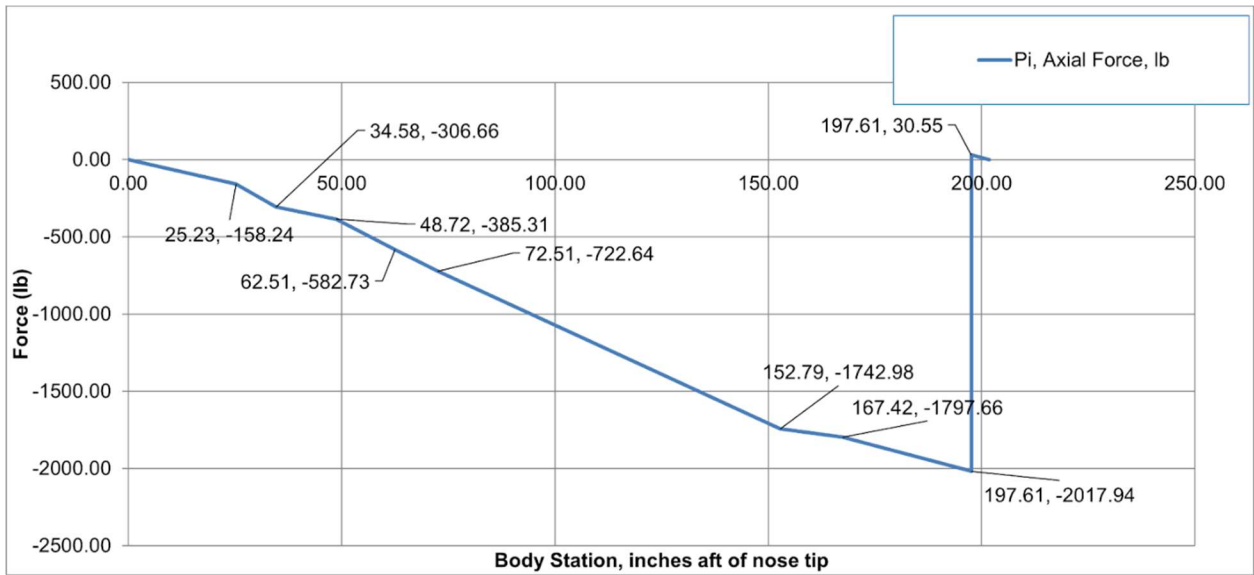


Fig. 32 Axial Force at Takeoff

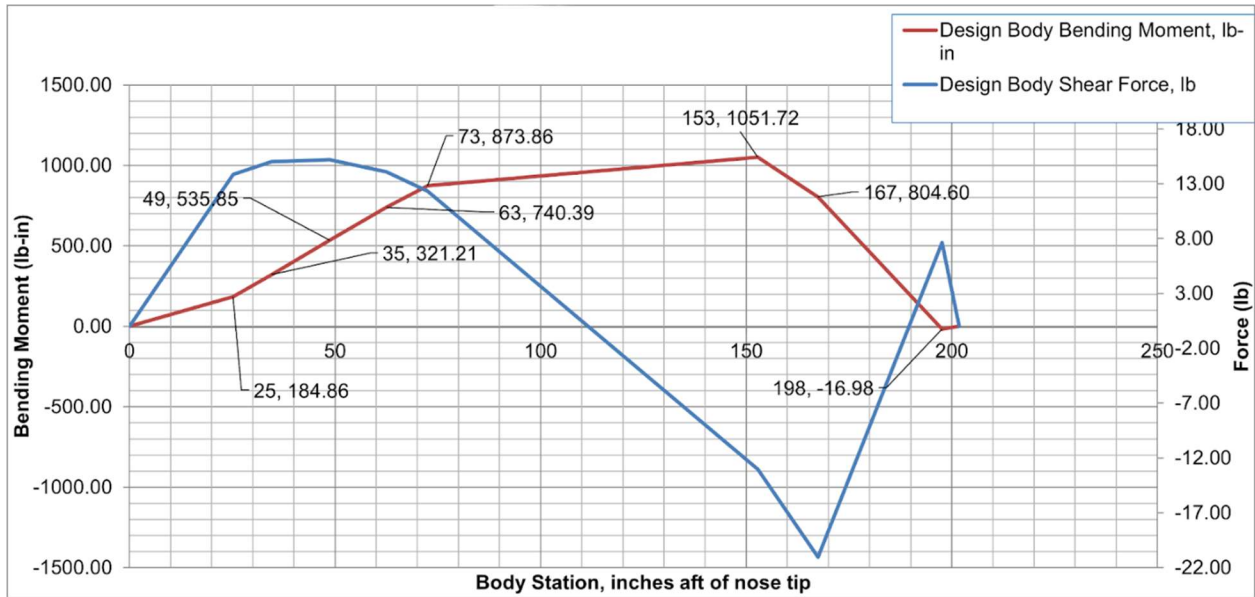


Fig. 33 Bending Loads at Max Q

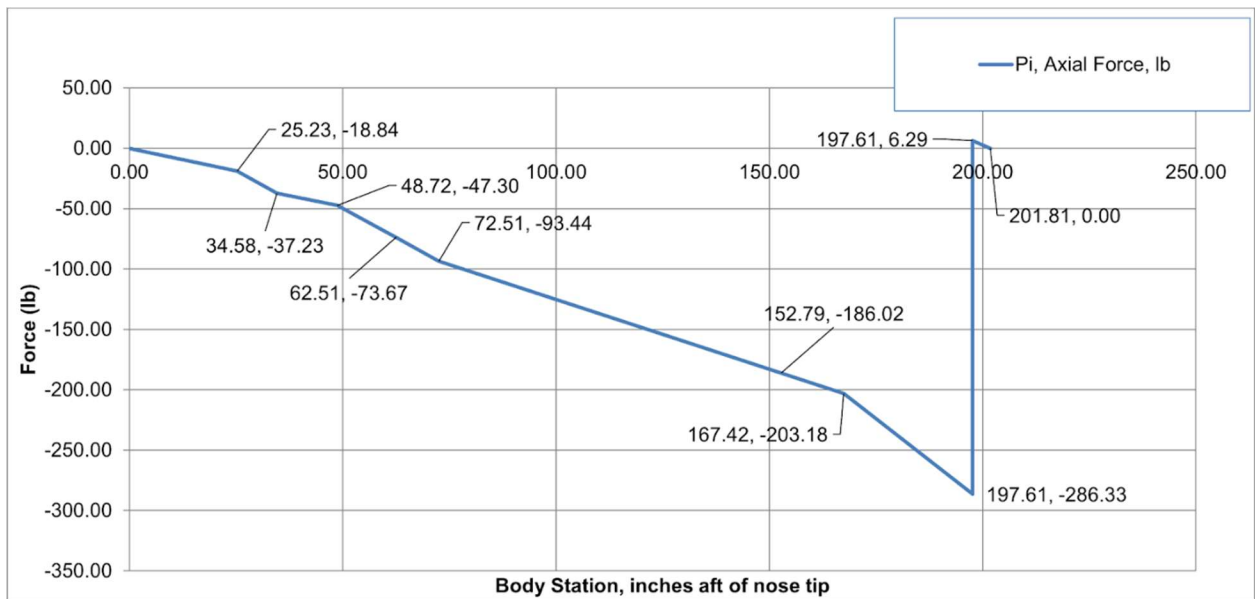


Fig. 34 Axial Force at Max Q

8. *Nosecone*

The fibreglass nosecone is built in a Von Karman shape with a 4:1 fineness ratio optimized for transonic and supersonic flight. It was manufactured in a vacuum bag layup process using a female mold which is shown in Fig. 35. Each of the 2 halves used 4 fibreglass plies arranged in a scarf joint as shown in Fig. 36. The entire mold was left in vacuum as shown in Figure Z to evenly distribute the epoxy, remove excess epoxy and help the nosecone maintain its shape while curing.



Fig. 35 Nosecone Mold Halves

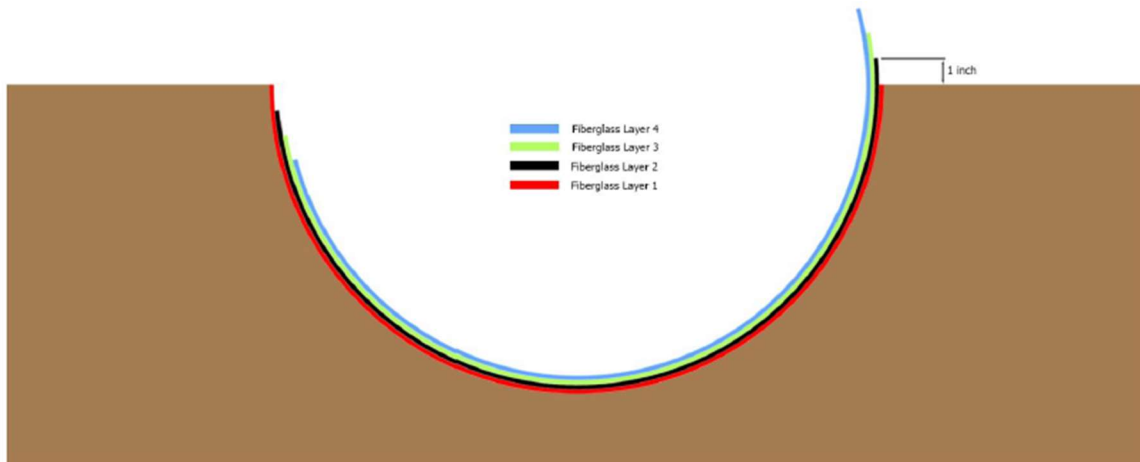


Fig. 36 Scarf Joint

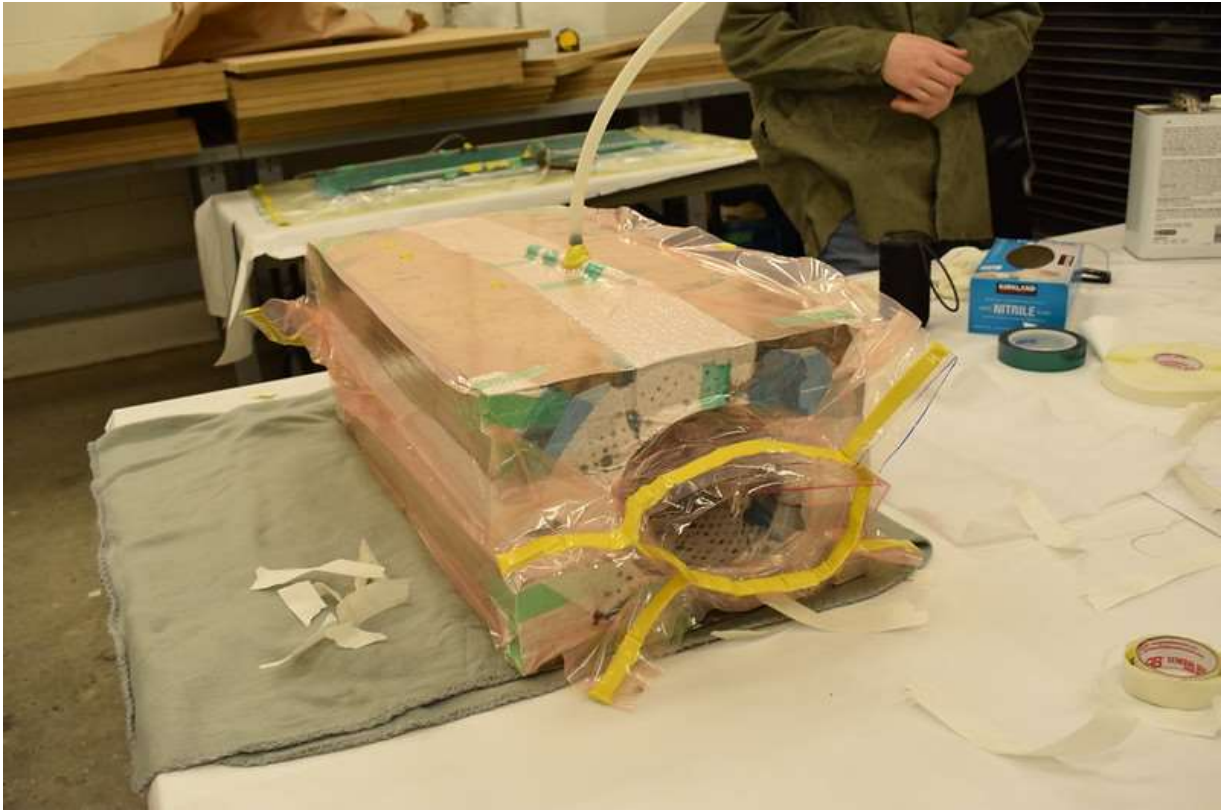


Fig. 37 Vacuum Bag Nosecone Wet Hand Layup

The shape of the nosecone was verified through research and simulation in OpenRocket. It also remains unchanged from Shark of the Sky, the team's 2019 rocket, which had a successful launch at SAC. The nosecone tip is machined stainless steel and aluminum bonded together using epoxy. It is built for wear resistance as well as thermal protection from aerodynamic heating. Inside the nosecone is the parachute and Big Red Bee GPS enclosure used for locating the rocket for recovery after landing. A shear pin coupler is epoxied to the underside of the nosecone to allow it to come off during parachute deployment. The unfinished nosecone for KotS is shown below in Figure A.



Fig. 38 Unpainted Nosecone

9. Composite Bodytubes

KotS is the team's first rocket to implement a completely SRAD composite bodytube construction, further developing our composites knowledge and fabrication capabilities. These SRAD composite bodytubes were designed to be superior to COTS bodytubes in the following ways. The SRAD bodytubes can be made to variable length, increasing material uniformity and reducing manufacturing complications. The second is removing the lead time for shipping, which allowed for greater flexibility and better project planning. Lastly, the stacking sequence of the bodytubes can be tailored to the load case experienced by each specific tube.

To achieve this, the composite bodytubes were manufactured using a Vacuum Assisted Resin Transfer Molding (VARTM) process, also known as resin infusion. Plies of braided fiberglass sleeving were laid out in a female mould using Super 77 spray adhesive. Then, the part was placed under vacuum through poly-tubing attached on one end, with resin allowed to enter from the other via vinyl-tubing. As a result, the resin was pulled through the fiberglass by the vacuum, which ensures an optimal surface finish and low void content. A surface preparation process was done through cleaning, waxing, and Polyvinyl Alcohol (PVA) application to ensure that no contaminants were cured onto the part, and that the bodytubes were released from the mould without damage. The infusion setup process is displayed in Figure X, along with all manufactured bodytubes displayed in Figure Y. Material property characterization of these bodytubes is a work-in-progress, so in the absence of test data, high FOS and non-destructive testing have been employed to ensure all components are unlikely to undergo structural failure. All composite components including bodytubes will be post-cured in a PID controlled curing oven to raise the components' glass transition temperatures above the temperatures expected in the New Mexico desert and fully establish their desired physical properties.

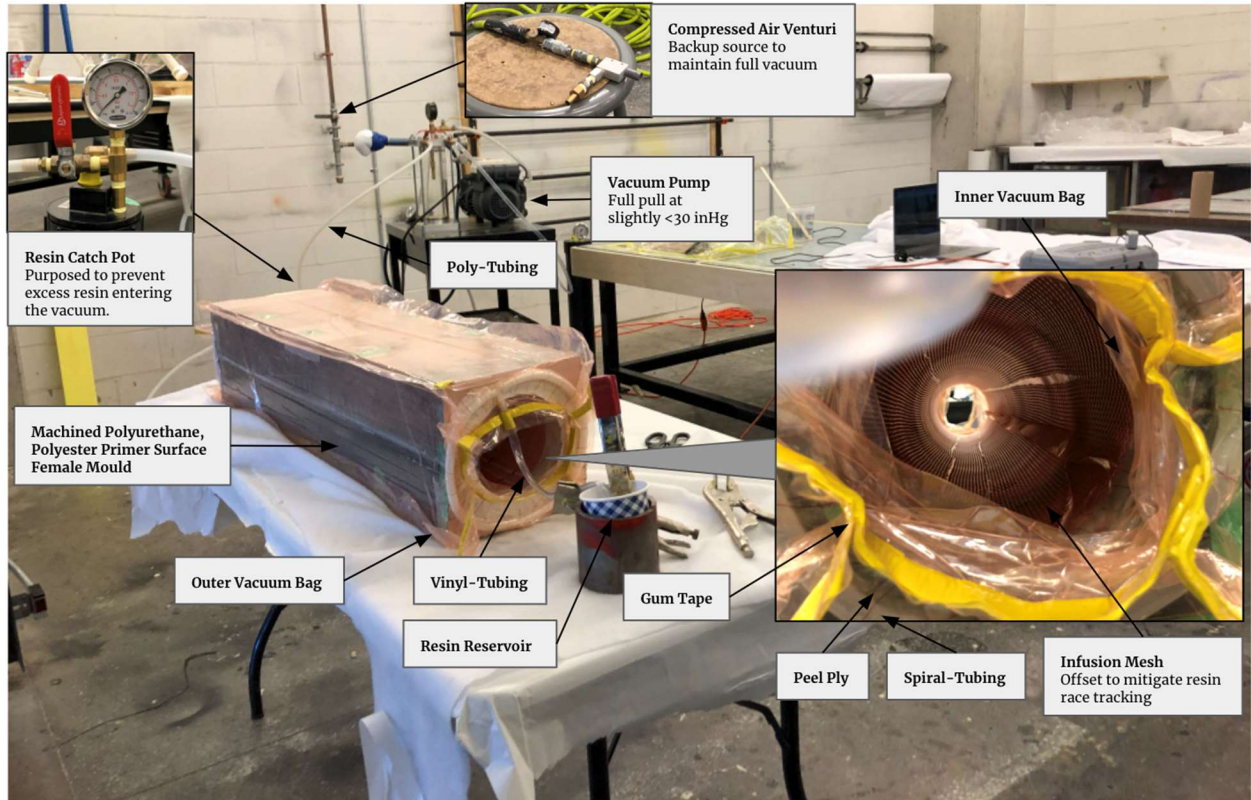


Fig. 39 Resin Infusion Process Setup



Fig. 40 Fiberglass and Carbon Fiber Bodytubes Fabricated Using VARTM

Fiberglass was the material chosen for the upper bodytube of the rocket, which houses the recovery electronics and COTS GPS due to the requirement for RF transparency. Laminate details including stacking sequence and fabric type for all composite components are summarized in the table below. The resin systems used along with calculated Fiber Volume Fraction (FVF) values are summarized in Table 7.

Table 6 Composite Components Summary

Component	Stacking Sequence	Fabric Weight (gsm)	Type of Fabric
Nosecone	[45] ₄	339	Composites Canada Plain Weave Fiberglass, 4HS Fiberglass
Parachute Bay Bodytube	[45] ₂	885	6" OD A&P Braided Sleeve Fiberglass
Upper Bodytube	[45] ₂	885	6" OD A&P Braided Sleeve Fiberglass
Injector Section Fairing (Oxidizer Tank Aft-Skirt Bodytube)	[90/45/90]	664, 80	6" OD A&P Braided Sleeve Carbon Fiber, Textreme 80 Spread-Tow Carbon Fiber
CC-Bodytube	[45] ₂	885	6" OD A&P Braided Sleeve Fiberglass
Fins	[45] ₄	194, 80	2x2 Twill Double Bias A&P Carbon Fiber, Textreme 80 Spread-Tow Carbon Fiber, laid up on COTS 3/16" Thick [0/90] Carbon Fiber Stock
Fin Can Bodytube	[90/45/90]	664, 80	6" OD A&P Braided Sleeve Carbon Fiber, Textreme 80 Spread-Tow Carbon Fiber

Table 7 Resin Systems Used, Fiber Volume Fractions, and Fabrication Method

Component	Resin System	Fiber Volume Fraction (FVF)	Fabrication Method
Nosecone	Aeropoxy PR2032 Resin+ PH3663 Hardener	Not Recorded	Wet Hand Layup Vacuum Bag
Parachute Bay Bodytube	Airstone 780E Resin + 786H Hardener	0.55	VARTM
Upper Bodytube	Airstone 780E Resin + 786H Hardener	0.57	VARTM
Injector Section Fairing (Oxidizer Tank Aft-Skirt Bodytube)	Airstone 780E Resin + 786H Hardener	0.47	VARTM
CC-Bodytube	Airstone 780E Resin + 786H Hardener	Not Recorded	VARTM
Fins	Aeropoxy PR2032 Resin + PH3663 Hardener	Not Recorded	Wet Hand Layup Vacuum Bag
Fin Can Bodytube	Airstone 780E Resin + 786H Hardener	0.47	VARTM

10. Upper Bodytube

The upper bodytube contains the rocket's recovery electronics, payload section, and vent section. A detailed breakdown is given in Figure X. At the top, it is connected to the parachute tube through the recovery bulkhead via a coupler. Two holes 1.178" in diameter were machined in the bodytube for in-flight footage to be captured by the PiCams. This section is reinforced by the payload bay shear ring, a section of epoxied fiberglass tube that locally increases the bending strength of the upper bodytube. The lowest FOS for the upper bodytube is 27.4 at the PiCam holes at Max Q, assuming isotropic material properties.

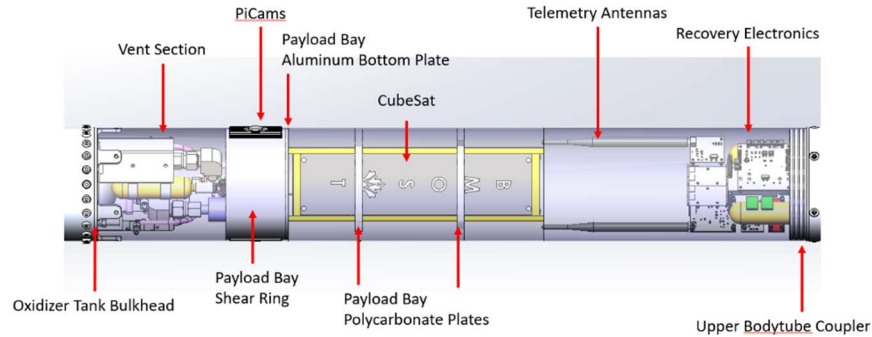


Fig. 41 Upper Bodytube Breakdown

Due to the compact nature of the vent section, PiCams, and payload bay, each hole in the upper bodytube needed to have a high positional accuracy to avoid component interferences. To achieve this a paper template was drawn and printed on A2 paper based on its CAD design and wrapped around the bodytube, as shown in the above figure. This would allow for each feature to be positionally accurate to within 0.5mm. Similarly, the edge of the bodytube could be located using this template, allowing it to be shortened to the correct length.

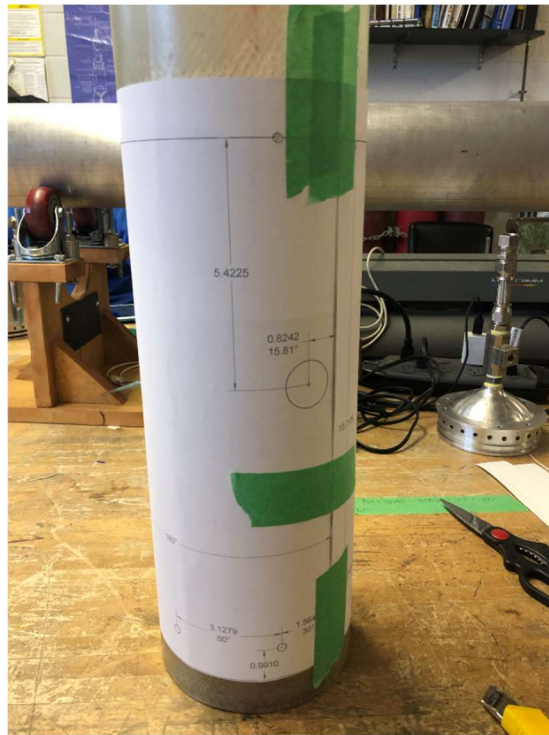


Fig. 42 Template wrapped around upper bodytubeCouplers

The rocket uses radial screw lap joints at the recovery bulkhead and at the top of the oxidizer tank due to their ease of disassembly and manufacturability by team members. When assembled, the couplers are fastened using 6

equidistant ¼-28 button head screws. For each bolted joint, the failure modes of bearing, shear-out, and bolt shear were evaluated. A summary of these calculations can be found in APPENDIX AEROSTRUCTURE CALCULATIONS. The recovery bulkhead couplers are Aluminum 6061-T6, and the lowest factor of safety is 3.6 in a shear-out failure mode of the aluminum under 10g at deployment. At the vent bulkhead, the upper bodytube is fastened to tabs in the oxidizer tank with an aluminum stiffener ring epoxied into the end which ensures a close fit between the bodytube and the vent bulkhead. At this joint, the lowest factor of safety is 9 in a bearing failure mode under 10g of the fiberglass bodytube with the conservative assumption that the aluminum stiffener ring does not contribute to the bearing strength of the holes.



Fig. 43 Recovery Bulkhead CouplersPayload Bay

The payload is secured using 2 centering plates, a bottom plate supported by a “shear ring”, and a side screw. Two non-structural polycarbonate plates, shown in Figure A and Figure B are used to rotationally align the payload. In the previous rocket, this was done using laser cut plywood but those plates were found in an unusable state after the launch at SAC 2019. Polycarbonate was chosen to replace the plywood because the plastic is also a lightweight, easy to machine, and readily available material that is stronger than plywood. It has a tensile strength of 10500 psi compared to plywood’s 5000 psi and a shear strength of 9200 psi compared to 1000 psi of plywood. [X1] [X2] The plates are also designed to allow the CANBus wire and accompanying Harwin connector to route past the payload to the recovery electronics above.

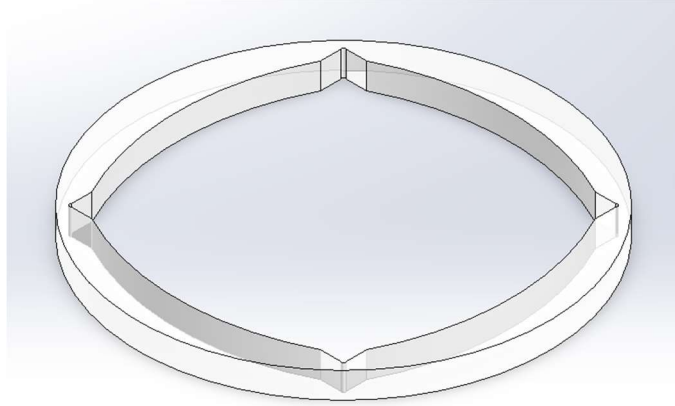


Fig. 44 Payload Bay Top Centering Plate

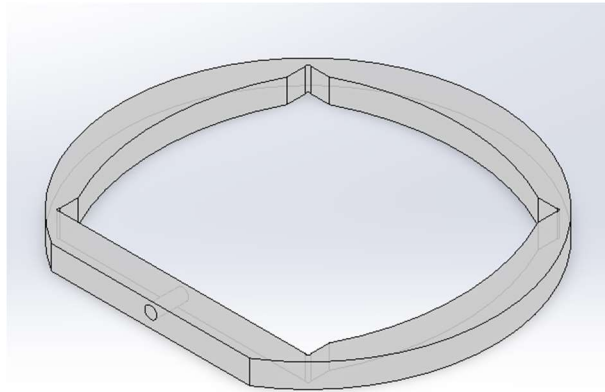


Fig. 45 Payload Bay Bottom Centering Plate

The payload rests on an aluminum bottom plate, shown in Fig. 46, which rests on a fiberglass shear ring cut from excess bodytube. Both support the payload and bear the loads during ascent. The decision to use aluminum for the bottom plate instead of polycarbonate was due to the need for high strength since the rocket experiences higher G-forces ascending than descending and due to space constraints. Aluminum has a higher tensile strength of 45000 psi and shear strength of 30000 psi than polycarbonate. [X3] The geometry is meant to maximize weight savings while still providing the necessary strength to support the payload. A SolidWorks Static FEA simulation was run on the bottom plate under 25 g of acceleration, which is an overestimate of the actual acceleration at deployment. [X4] In addition, the simulation also has 306 lbf applied in 4 areas to account for the force exerted by the payload feet on the bottom plate. The results of this simulation are shown in Figure D and show the maximum stress experienced by the bottom plate is an entire order of magnitude below the yield strength of the aluminum. Therefore, it should not experience failure during flight. The polycarbonate bottom centering plate has a 4-40 screw which prevents the CubeSat from translating upwards. This design was chosen because it is simple, lightweight and easy to assemble. Only one 4-40 screw holds the payload in place during descent. To verify that this design is safe, two failure modes were analyzed: the possibility of a failure of the screw itself and the possibility of the screw tearing out of the polycarbonate plate holding it in place. These calculations are given in Table A and Table B. For the shear failure of the side screw, some assumptions were made. The first is using the Von Mises criterion to get a conservative estimate of the shear strength of the screw based on the manufacturer's given tensile strength. The cross-sectional area of the screw only accounted for its minor diameter and did not include the threads to give a more conservative estimate. The maximum estimated force accounts for the entire weight of the payload, 8.8 lbf, acting on the screw under 25 G's of acceleration. This is the same assumption used in the tear-out calculation.

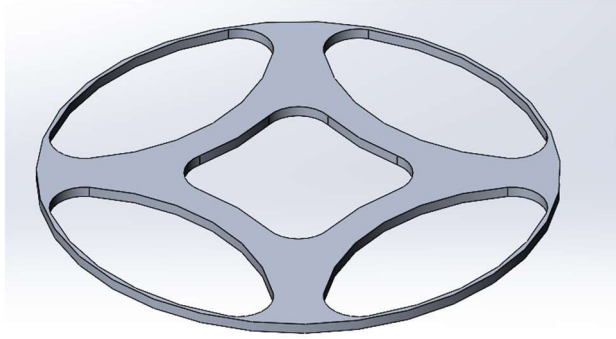


Fig. 46 Payload Bay Bottom Plate

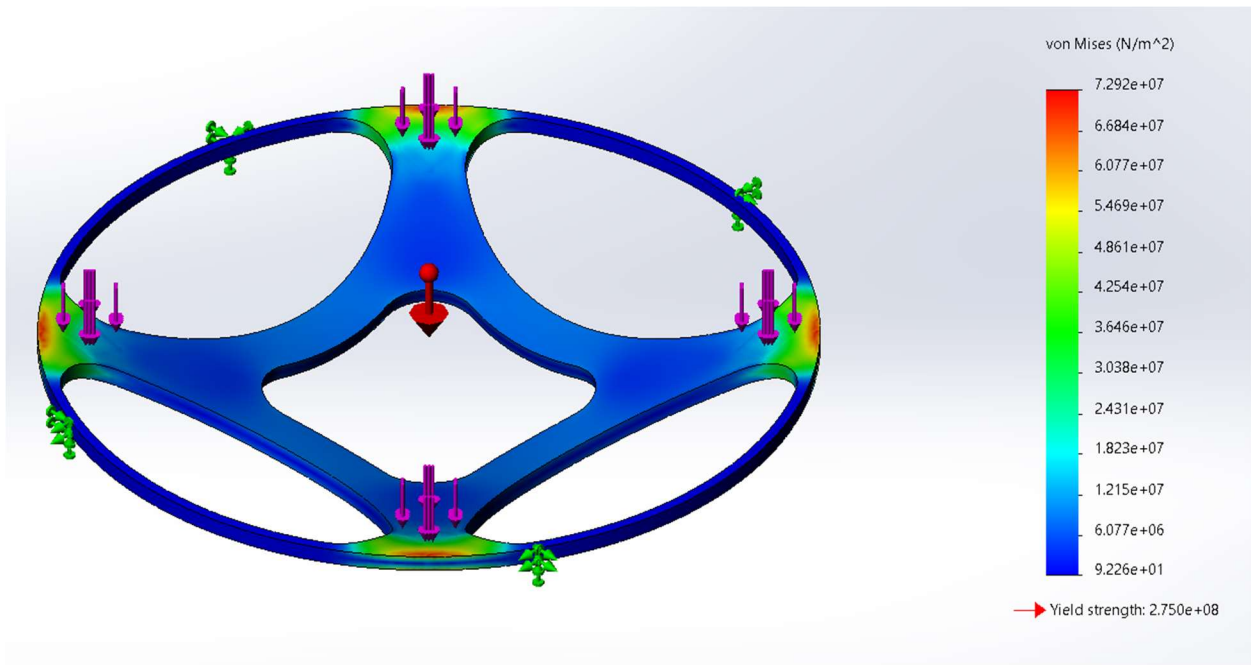


Fig. 47 Bottom Plate Simulation Results

Table 8 Side Screw Shear Failure

Tensile Strength	170,000 psi [X5]
Approximate Shear Strength	98149.55 psi
Screw Cross-Sectional Area	0.005 square inches
Maximum Estimated Force	226.05 lbf
Stress Experienced	59961.91psi
FOS	1.64

Table 9 Tear-Out of Side Screw

Shear Out Area	0.09 square inches
----------------	--------------------

Estimated Applied Force	226.05 lbf
Average Shear Stress	2511.68 psi
Shear Strength of Polycarbonate	9200 psi
FOS	3.66

Although the FOS on the side screw shear failure mode appears low, this number is obtained by assuming 25 G's of acceleration. According to 2019 altimeter data, this acceleration should only be achieved during ascent. During ascent, the bottom plate and shear ring should bear the majority of loading. The engine data only shows a maximum acceleration of around -3 G's during descent which would result in significantly less stress on the side screw. Below the entire assembly is the shear ring. The shear ring is designed to provide additional support to the bottom plate and thus the entire payload. Its secondary purpose is to reinforce the upper bodytube when two holes are drilled in it to allow the PiCams to gather footage of the outside of the rocket during flight. The calculations for the failure of the shear ring, specifically the epoxy bonding it to the bodytube, are given in the table below. One assumption made in the calculations was assuming that the thickness of the entire shear ring was the same as the thickness of material on both sides of the PiCam holes. Another assumption was the there was a complete failure of the payload bay so the CubeSat, both polycarbonate plates, and the aluminum bottom plate would be weighing down on the shear ring. It also assumed 25 G's of acceleration.

Table 10 Shear Ring Failure

Shear Strength (Epoxy)	1600 psi
Outer Surface Area	6.74 in
Estimated Total Weight	12.24 lbm
Maximum Estimated Force	306 lbf
Average Shear Stress	45.42 psi
FOS	35.22

The entire payload bay assembly in CAD is shown in Figure E. To manufacture the payload bay, first the polycarbonate and aluminum plates were cut using a waterjet. The shear ring was cut to length from a spare piece of bodytube. In the bottom centering plate, a clearance hole for the screw was drilled using a drill press. Then both polycarbonate plates were bonded to the inside of the upper bodytube using epoxy. Finally, the bottom plate and shear ring were also bonded into the upper bodytube using epoxy. The entire assembly was left to cure and then the CubeSat was installed to fit check. The manufactured payload bay is shown in Figure F.

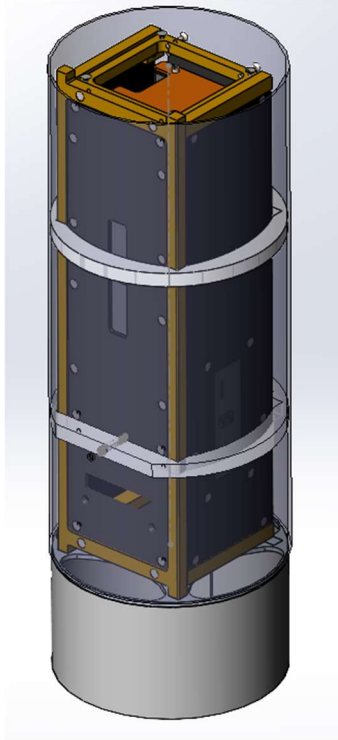


Fig. 48 Payload in Payload Bay

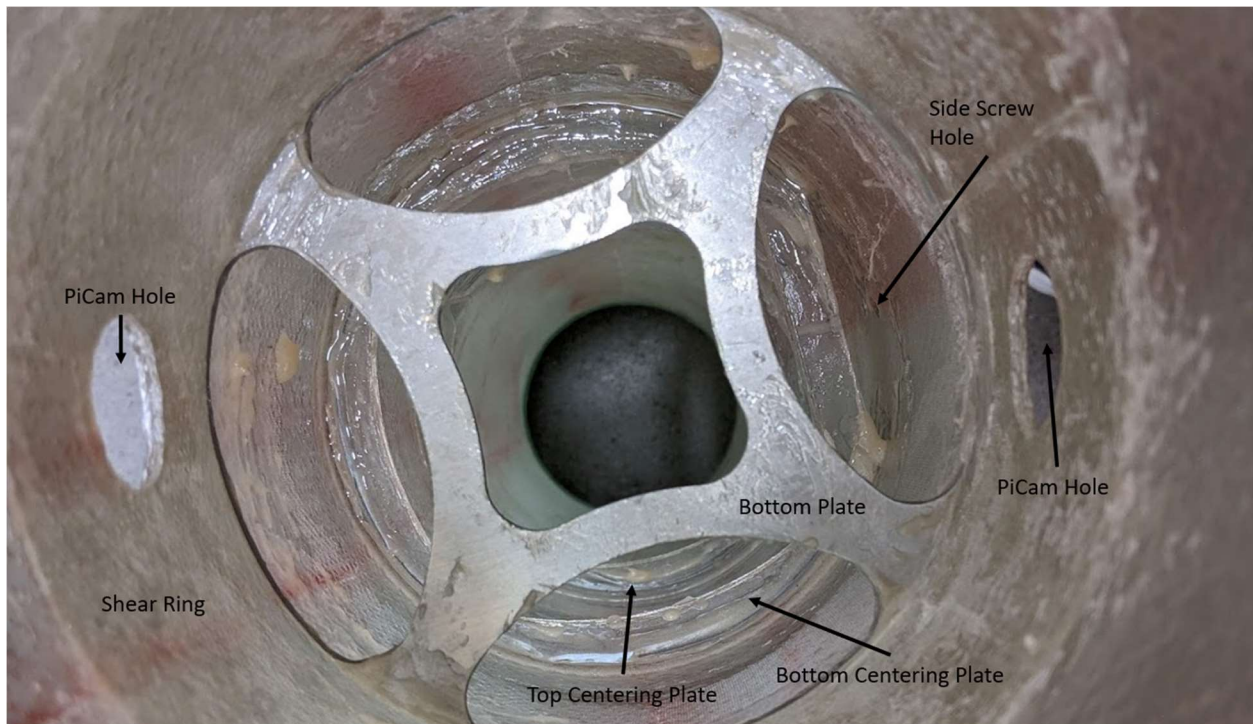


Fig. 49 Manufactured Payload Bay (upside down)

11. Oxidizer Tank

The oxidizer tank aft skirt, shown in Figure S3, is an assembly of 3 longerons located at the injector section that are bolted with 1/4-28 screws to the injector bulkhead on one end, and the fill bulkhead on the other, and transmit thrust from the CC to the rest of the rocket. The design is different from the monocoque fiberglass bodytube used on the

previous rocket, SotS, to improve ease of access to the pneumatic, high-pressure plumbing, and electrical systems contained inside the injector section, facilitate plumbing assembly, and introduce adjustability to compensate for plumbing misalignment through the use of shims on the ends of the longerons. From the results of loads analysis, the lowest FOS is 3.47 in flexural buckling at 6.6 g acceleration experienced at takeoff, assuming an eccentric offset of 0.0729" to account for manufacturing defects. The failure modes are summarized in Table S1 in Appendix Aerostructure Calculations. The boundary conditions used for buckling were pinned-pinned, which is a conservative assumption given that the longerons are bolted on either end. The entire section is covered by fairings cut from a section of SRAD carbon fiber bodytube, fastened to the longerons with 6 4-40 screws on the forward and aft ends. See Appendix A6 for the assembly drawing for the Ox Tank Aft Skirt.



Figure Oxidiser Tank Aft Skirt

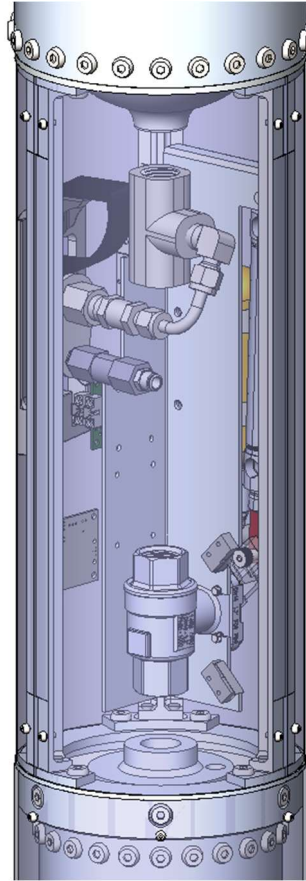


Fig. 50 Oxidizer Tank Aft Skirt CAD

12. Fill Disconnect Hatch

Contained within the oxidizer tank aft skirt section is the fill disconnect hatch. The fill disconnect hatch is the opening through which the ground-based fill system plumbing interfaces with the rocket to fill the ox tank. It uses a torsion spring hinge as well as magnets to remain closed after the fill system disconnects. The hatch and curved arm connecting the hatch to the hinge are 3D printed, while the hinge is a commercially available metal hinge. The design for this system is a work-in-progress.

This design was chosen because it allows for a minimal amount of space to be occupied by the curved arm, minimizing the size of the opening to what is necessary for the fill disconnect system. It also ensures a flush seal with no protruding components when the hatch is closed. The spring provides enough force to close the hatch, but since the spring provides less torque when the hatch is closed, the magnet was added to protect the hatch from opening due to vibrations in flight.

The fill disconnect hatch system is 3D printed to reduce weight and to allow for a more flexible design which would not be as easily achieved using traditional manufacturing methods. 3D printing this component also allows for rapid iteration. For example, version 1 (Figure x1) failed to consider the length and effects of heat-set inserts used to connect the hinge. This caused undesirable deformation of the outside of the hatch surface. In version 3, (Figure x2) the hatch did not close properly due to errors in the assembly procedure. The current version 4 closes reliably, but has slight interferences which will be addressed in the next iteration.



Fig. 51 Version 1 of fill disconnect hatch



Fig. 52 Version 3 of fill disconnect hatch

This system has already undergone several iterations and is nearing its final form. With extensive individual and integration testing with the fill disconnect system and RLCS, it can be ensured that the hatch will close repeatedly and reliably.

13. Fin Can

To determine the optimal fin size and shape, Openrocket software was used to iterate around ten shapes and sizes until most key performance requirements were met. These included ensuring that launch rail velocity was high enough, stability was within 1.5-6 cal, and apogee was maximized. The target launch rail velocity and stability required were taken from the DTEG. Some early iterations are shown in Figure X, Early Fin Iterations.

Shape #1	Shape	Simulation data	Sim 1	Sim 2	
					
	Root chord	16	Min Stability	2.72	1.56
	Tip chord	7.75	Stability off rail	2.79	1.56
	Height	6.2	Max Stability	5.96	5.96
	Sweep length	8.5	Apogee	25840	25920
	Sweep angle	53.9			
Shape #2	Shape	Simulation data	Sim 1	Sim 2	
					
	Root chord	14	Min Stability	1.91	1.56
	Tip chord	8.25	Stability off rail	2.47	1.61
	Height	5.95	Max Stability	5.76	5.77
	Sweep length	7.245	Apogee	25920	26065
	Sweep angle	50.6			
Shape #3	Shape	Simulation data	Sim 1	Sim 2	
					
	Root chord	10	Min Stability	1.54	1.33
	Tip chord	7	Stability off rail	1.61	1.45
	Height	6.04	Max Stability	6.01	6.02
	Sweep length	2.828	Apogee	25550	25690
	Sweep angle	25.1			
Shape #4	Shape	Simulation data	Sim 1	Sim 2	
					
	Root chord	11	Min Stability	1.75	1.65
	Tip chord	11	Stability off rail	2.5	2.02
	Height	6.125	Max Stability	5.97	5.98
	Sweep length	0.5	Apogee	25240	25240
	Sweep angle	4.7			

Fig. 53 Early Fin Iterations

After going through these iterations, a final design was selected with dimensions shown in the figure below.

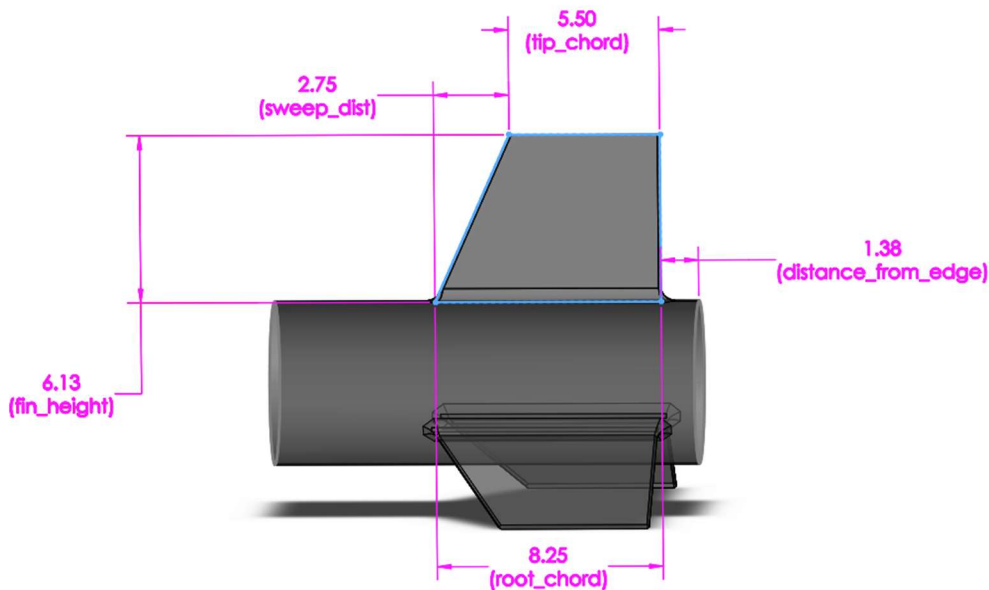


Fig. 54 Fin schematic with dimensions

Using this shape, fin flutter velocity was calculated using a fin flutter boundary equation [x7] to ensure that the flutter velocity would not be reached. A flutter velocity of 2081 ft/s was calculated at Max Q, resulting in a factor of safety of 1.89.

Table 11 Key Fin Performance Values

Fin Flutter Velocity (ft/s)	2081
Velocity at Max Q(ft/s)	1100

To fabricate the fin can, the fins were cut on a CNC router out of commercially available [0/90], 3/16” thick carbon fiber plate stock, and bonded to a section of SRAD carbon fiber bodytube with high shear epoxy. The root fillets were formed using fiberglass reinforced, fumed silica thickened (3-6% by weight) epoxy paste. The position and angle of the fins relative to the fin can bodytube was ensured by using a laser cut alignment jig as seen in Figure X. Lastly, 3 plies of 45-degree 2x2 twill double bias carbon fiber cloth and 1 ply of Textreme 80 spread-tow fabric were laminated onto one side of the fin can using a “tip-to-tip” wet layup and vacuum bagging process. The plies added in the vacuum bagging process increase torsional rigidity, thereby reducing the likelihood of fin flutter. This manufacturing process and stacking sequence are representative of the one used to make the fin can for SotS, which flew successfully at IREC 2019. This process was repeated 2 more times for the other 2 sides of the fin can in a single layup before bagging and pulling vacuum. The fin can was then adhesively bonded to the combustion chamber bodytube through epoxying a machined COTS fiberglass ring, coupled with a wet hand layup using 4 plies of 4HS [0/90] fiberglass cloth. Adhesive bonding for composite components were prioritized since drilling holes into laminates introduces stress concentrations and failure modes specific to composites, such as microcracking and delamination. Refer to Figure X for the wet hand-layup vacuum bag consolidation method done after bonding fins onto the fin can bodytube.



Fig. 55 Bonding Fins Onto Fin Can Bodytube



Fig. 56 Wet Hand-Layup Vacuum Bag Consolidation

After initial curing, a series of epoxy coats were applied followed by surface treatment to reduce drag. This was done by sanding the surface of the fin can with 220 grit sandpaper while paying attention to not sand through the fibers. Then, the surface was prepared using a bonding procedure specified in Appendix X before epoxy was brushed on and allowed to cure. This process was repeated until all noticeable surface imperfections were mitigated. Finally, 400 grit to 800 grit dry sanding, proceeded by 1000 grit to 1500 grit wet sanding was done to yield the final gloss finish seen in the figure below.



Fig. 57 Fin Can Surface Finish

The fin can was then placed in a PID controlled curing oven to post-cure at 90 °C for 1h. The curing schedule is displayed in Figure S5 in APPENDIX CALCULATIONS. All composite components will be similarly post-cured to attain mechanical and thermal properties.

The assembly process to connect the CC-bodytube and fin can was done through adhesive bonding with epoxy resin as according to the above figure. Then a wet hand layup using 4 plies of 4HS 0/90 fiberglass fabric was performed to increase the strength of the bond. This was required as notable circular cracks formed after machining the fiberglass bonded coupler. The joint has a FOS of 31 at max Q assuming isotropic material properties and neglecting the contribution of the butt-joint between the two tubes and the cracked fiberglass to the strength of the joint. To validate the joint, a successful bend test was performed shown in the figure below at 78lbf, equivalent to 1.5x maximum expected gust loading. The weight was applied directly onto the bonded section with the boattail, boattail spacer, and injector bulkhead coupler assembled.



Fig. 58 Fin Can bonded to the CC Bodytube

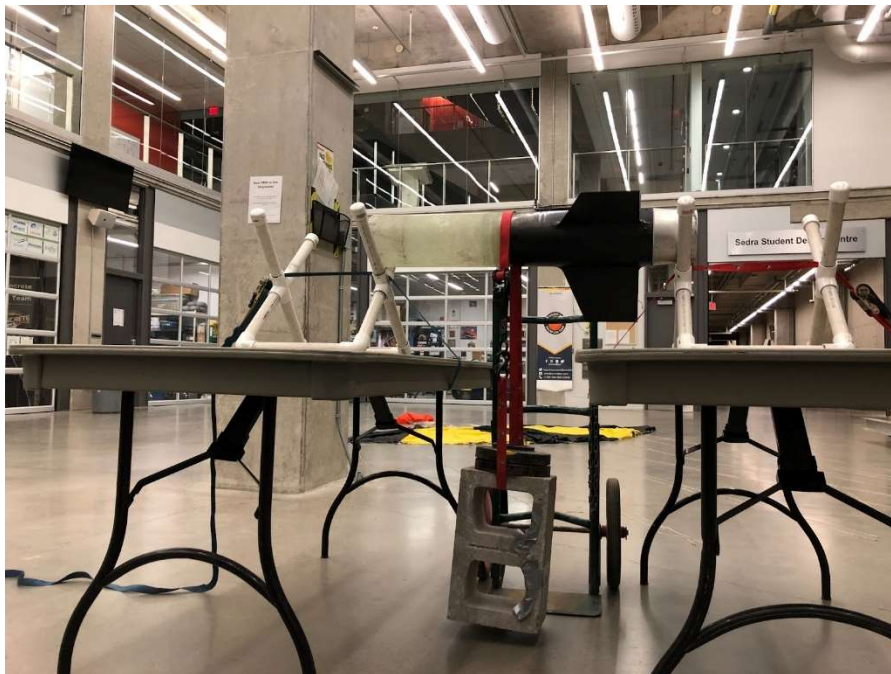


Fig. 59 Load Testing to Validate Loads Analysis

14. Boattail

The conical boattail surrounds the rocket's graphite bell nozzle. The geometry of the boattail and the position of the boattail on the rocket are given in the figures below. Also shown in the figure below is the boattail being secured by bolts to the fin can on the top and a retaining ring which is inside the combustion chamber on the bottom. The boattail is machined out of aluminum and doubles as a heat sink to mitigate thermal loads on the combustion chamber. The primary concern is that the combustion chamber is made of aluminum 6061 T-6 which can anneal and over-age if exposed to high temperatures, thus reducing its strength. A simulation was performed to estimate the effect of the boattail on the combustion chamber temperature and the results were compiled in a previous report done by the team. [X8] The simulation mesh is shown and the results of the simulation are given below in the figures. According to the report, the peak predicted temperature of 228.97°C is approaching the threshold where aluminum 6061 T-6 can anneal

and over-age. However, it concluded that this value is at the lower end of the spectrum and unlikely to have a significant impact on the material properties of the combustion chamber.

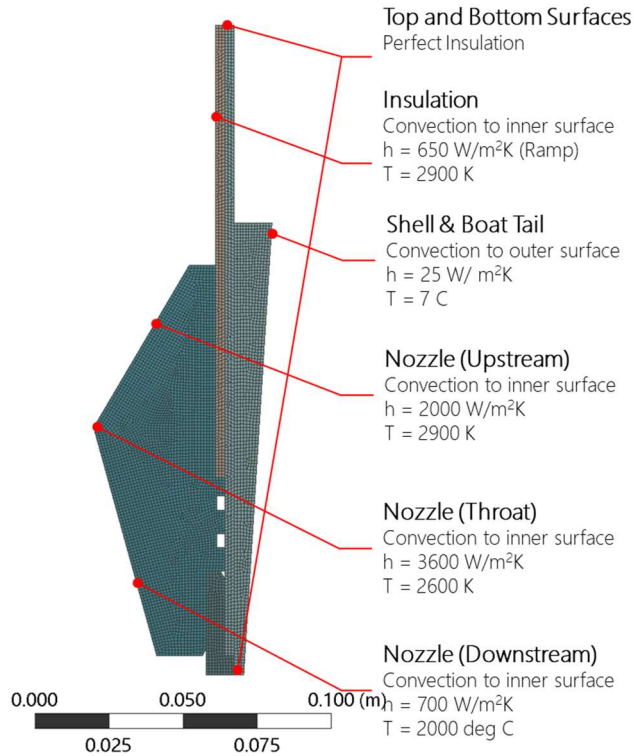


Fig. 60 Model Boundary Condition Summary

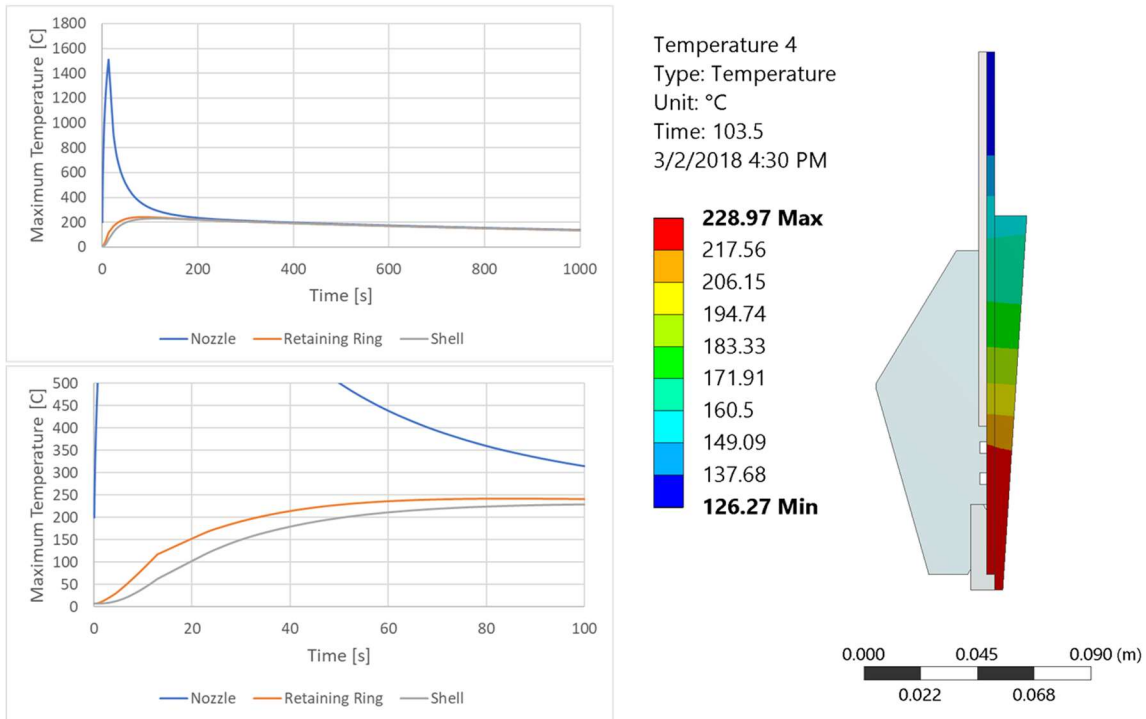


Fig. 61 Boattail Thermal Simulation Results

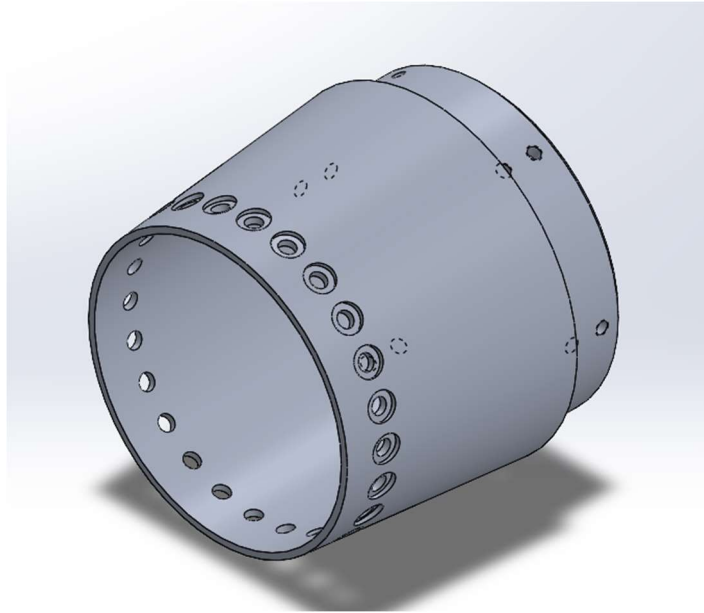


Fig. 62 Boattail

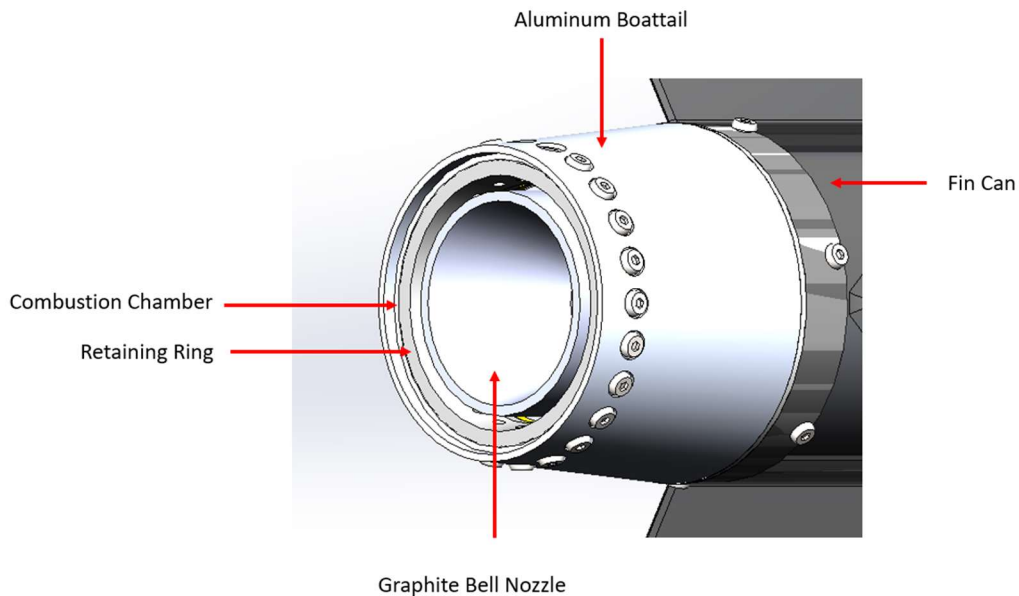


Fig. 63 Boattail on Rocket

C. Recovery

In approaching the design of the Kraken of the Sky recovery system, the main focus was to come up with a system that was well tested and reliable. Following three partial recovery failures at the three previous competitions, all involving hard landings under drogue, special focus was placed to ensure that the new recovery system developed for KotS would be well tested in a variety of representative environments. Additionally, the team wanted to develop a system that would impart less shock on the rocket, as the rapid increase in size in past years had significantly increased the loads the rocket would experience during deployment. The design of a novel, efficient, recovery system was a particularly interesting design challenge to the recovery team.

1. System Overview

The recovery system for KotS is a two-stage, reefing parachute system. The system features a single, semi-elliptical, 12.4 ft diameter reefing parachute, sewn in house out of black and yellow ripstop nylon based on Richard Nakka's design [12]. Upon release at apogee, the main parachute deploys into a reefed state and acts as a drogue, maintaining the descent rate of descent to 112 ft/s. After the disreefing event at 1500 ft AGL, the descent of the rocket is slowed to 29.5 ft/s. Redundant altimeters are used to separate the nose cone using CO₂ pressurization, and to activate redundant pyro cutters for disreefing. Reefing of the parachute is accomplished by constricting the skirt with a thin line that is passed through metal rings. Through extensive testing, the correct reefing ratio to achieve the drag area required was determined. The system also includes a small pilot parachute that is attached to the vent of the main descent parachute. It is a 0.61 m flat parachute that is bright orange in color.



Fig. 64 The KotS parachute

2. Deployment Concept of Operations

A detailed diagram of the entire recovery system in its packed configuration as well as how it proceeds through the nominal deployment events stages can be seen in the figures below.

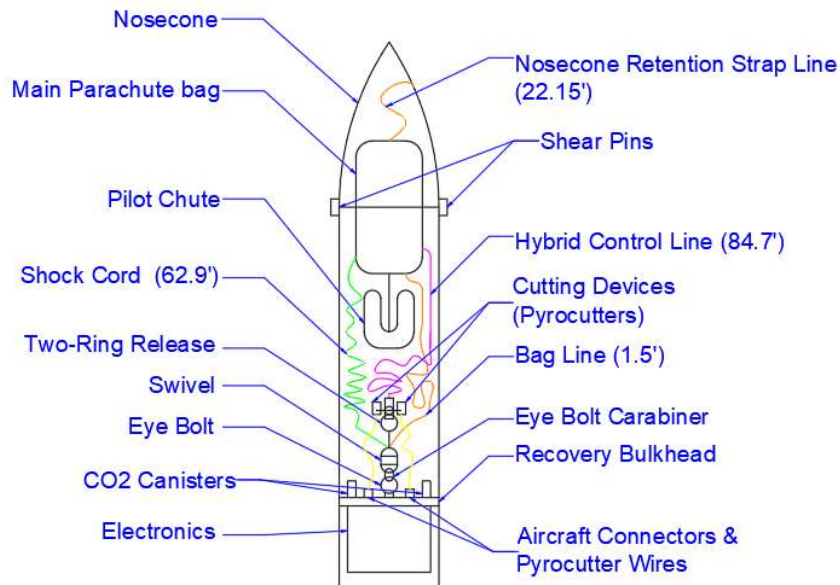


Fig. 65 Diagram of packed recovery section

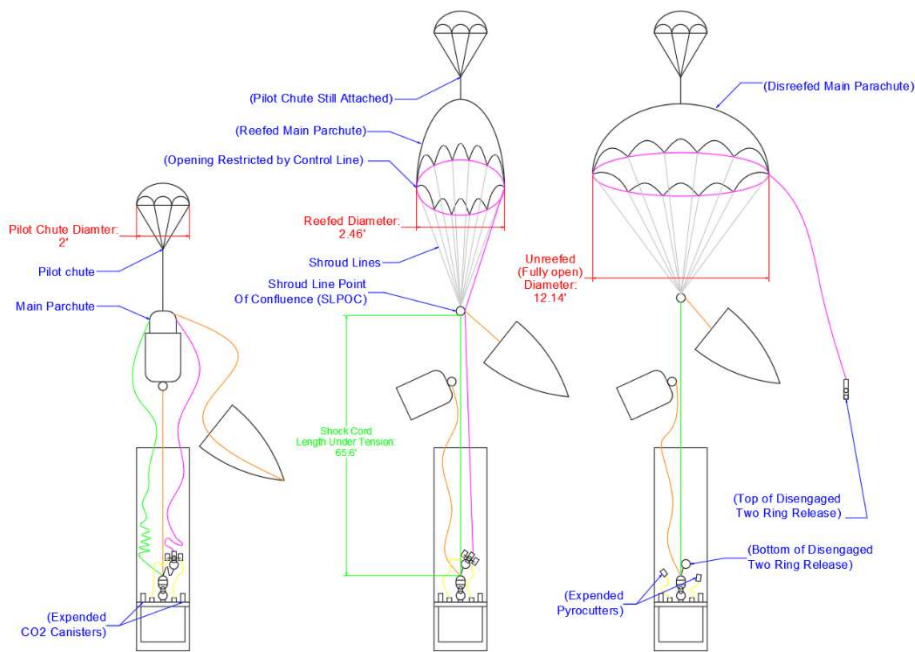


Fig. 66 Recovery deployment concept of operations

At apogee, the avionics will command the CO2 ejectors to fire which will release two 38 g canisters into the parachute bay. This will pressurize the parachute bay and cause the shear pins to break, forcing the nose cone away. The pilot parachute, which is loosely packed, will be released into the airstream, pulling the parachute bag out of the parachute bay and creating tension in the parachute bag line. This pilot parachute will pull out the main parachute from its bag, which is secured to the bulkhead with a shock cord. The main parachute will inflate until the reefing control line that runs parallel to the shock cord becomes taut and prevents further inflation. Due to the strength of Kevlar, the short length of the parachute bay tube, and the aluminum stiffener ring that is epoxied to the end of the parachute bay, neither scissoring of the parachute bay tube nor cutting of the parachute shock cord is a concern. The stiffener ring provides a strong, blunt edge to help distribute any cantilever effect created by the tensioning of the shock cord.

Most of the descent will proceed in this state. Once 1500 ft AGL is reached, the dual, redundant altimeters will command the dual, redundant pyro-cutters to fire and the two-ring release will separate, relieving the tension in the reefing line and thereby allowing the parachute to fully inflate. Full inflation of the parachute will slow it down to the landing speed of 30 ft/s. That would conclude the flight operations of the recovery system, and the state of the system would be maintained through the rest of the descent and to ground impact. A collage of the disreef process from truck testing is shown below, and the more details on the truck testing will be discussed later in Appendix C Project Test Reports.



Fig. 67 Disreefing sequence of the parachute during a 2021 truck test

3. Shock Loading

Much effort has been put into quantifying the loads that the parachute deployment effects impart on the rest of the rocket. In particular, the recovery systems design manual by Knacke section on Shock Load calculations was used to estimate the shock loading under the main at apogee situation, the worst case scenario for shock loading [13]. Despite the fact that shock loads should be reduced with a reefing system, in a worst-case scenario everything can be treated as a full parachute inflation. The formula, that the manual presents, uses a correction factor that it presents in a graph. This graph and the equation are shown in the Fig. 68 below, taken from the manual:

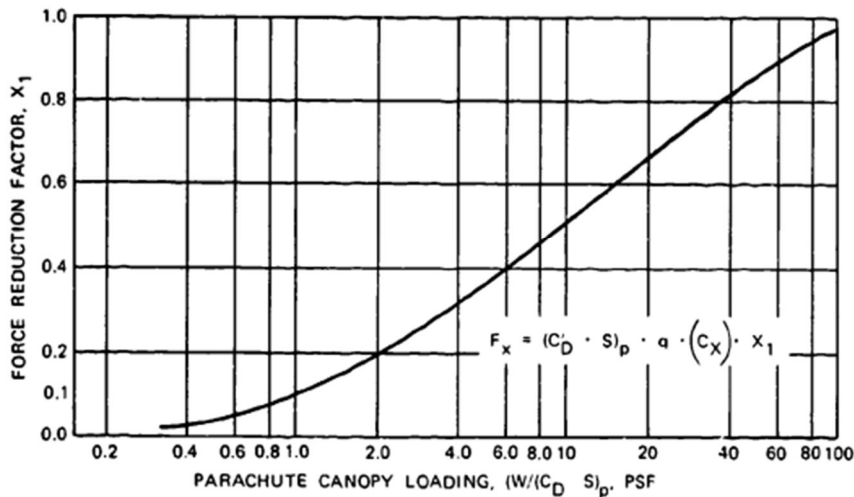


Fig. 68 Opening force reduction factor chart, 5-48 from Knacke [13]

A calculator was written by the team to execute this calculation. However, the uncertainty around the force reduction factor made it very difficult to ascertain what the true forces that would be experienced are. By dividing our parachute drag area by the estimated mass, a rough force reduction factor of 0.1 was ascertained. Based on variation in air density, which will be discussed later in the report, the following shock loading range was calculated.

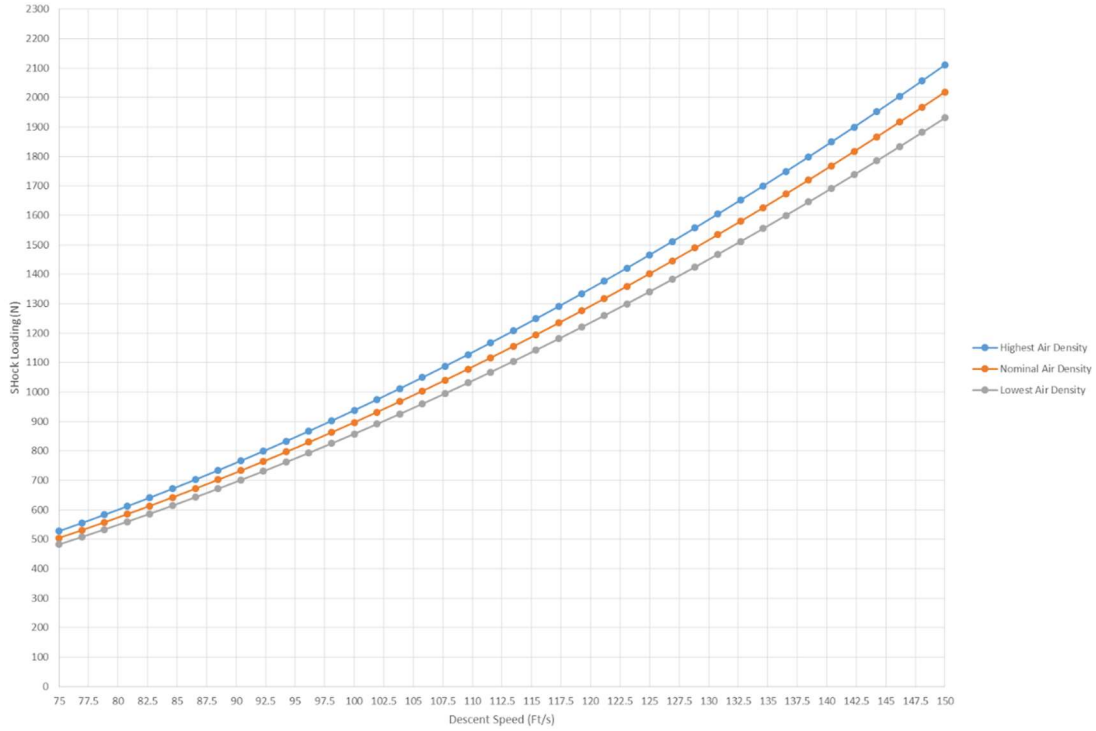


Fig. 69 Shock loading relationship with descent speed, for different air densities

From this, it was determined that the upper limit of shock load that the rocket could experience was around 2200 N, thus this was the minimum value used in the design of the main harness and eyebolt bulkhead. Afterwards, due to the uncertainty in force reduction factors, their variation was also analyzed, with a graph shown below. It was concluded that with sufficient factors of safety there should be no concerns with the system.

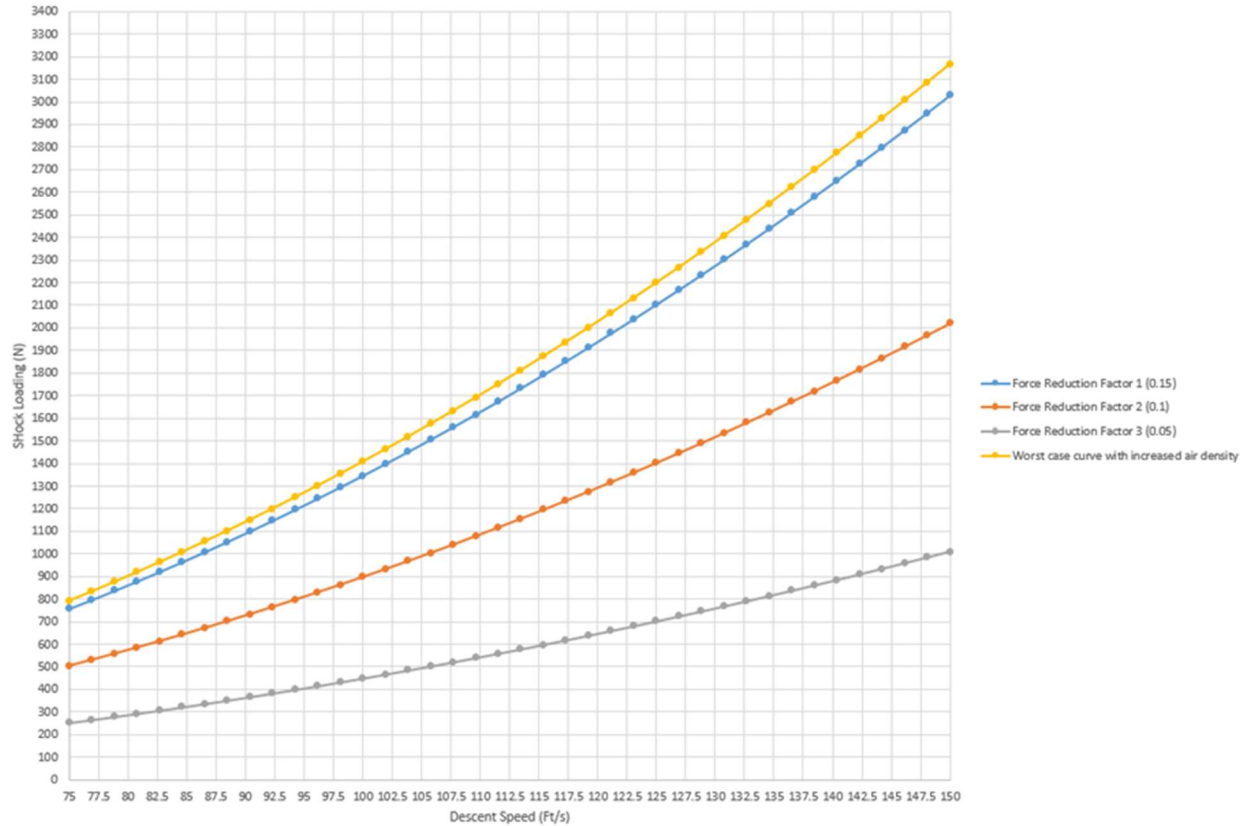


Fig. 70 Shock loading relationship with descent speed, for different force reduction factors

4. Rocket Integration

The recovery section of the rocket consists of two bays, separated by a common bulkhead. The recovery electronics bay sits below the bulkhead, in the rocket's upper bodytube. This section begins at the top of the CubeSat and is enclosed by the recovery bulkhead on top. The recovery electronics are mounted onto two fiberglass plates, called the recovery electronics sled, which are mounted to the bottom of the recovery bulkhead. Below the recovery electronics sled there is some space to provide an RF transparent window for the Live telemetry and GPS antennas mounted on the sled. The recovery bulkhead is secured to the recovery coupler, which consists of two halves that mate together. The bulkhead itself is also keyed to ensure that it is consistently aligned with the rocket. Further discussion of the recovery coupler can be found in the aerostructure section. Further discussion of the design of the recovery bulkhead can be found below in the recovery electronics assembly section.

The parachute bay is the section enclosed between the recovery bulkhead and the nosecone. It consists of the parachute bay tube and the nosecone. Three nylon rivets through an aluminum coupler are used to couple the two sections together. The nylon rivets act as shear pins, as described above. The nosecone section also includes an enclosure for a battery operated BigRedBee GPS. This holder is 3D printed and epoxied onto the side, near the tip. The GPS unit fastens to the top portion of the holder which fastens to the bottom using threaded inserts. In the tip of the nosecone there is a threaded hole into which a $\frac{3}{8}$ " 1300 lb capacity eyebolt is threaded. The figure below shows the KotS recovery section assembly.

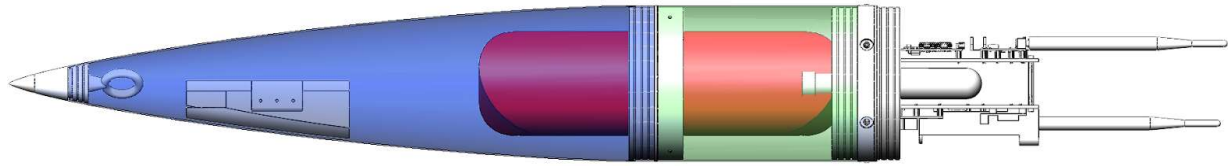


Fig. 71 KotS recovery section assembly

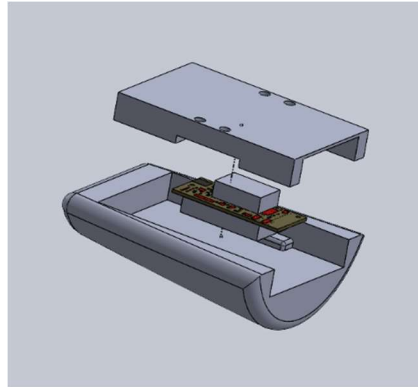


Fig. 72 BigRedBee GPS enclosure

The main parachute and its rigging are packed inside the nosecone and parachute bay tube for space and weight savings. The parachute is folded by repeatedly placing gores on top of each other, like an accordion, and then tightly rolling the resulting triangle into a cylinder. Extreme care is taken to ensure that all of the shroud lines have been routed correctly around the reefing line, and that it all is packed neatly without tangles. The tight parachute bundle is then placed into a parachute bag, reefing rings first, with the pilot parachute hanging out. The parachute shroud lines are taped in little bundles to ensure that they do not tangle but remain easily deployable. The flap is closed over and secured with painters' tape, to ensure that it will easily open when pulled on by the pilot parachute.

Much thought and reasoning has been put into the packing configuration to ensure that the parachute and lines deploy without tangling. Initially into the project, a full-scale drop test was planned to take place using a hired helicopter, in order to fully test all stages of the deployment. Unfortunately, due to logistical and regulatory delays, it wasn't possible to complete the helicopter test in this competition cycle. Instead, this method of folding packing the parachute has been verified in various deployment tests, including from a 60 ft tower drop test, truck testing, and wind tunnel testing.



Fig. 73 60 ft Drop test, conducted at the LiftWerx Test Tower, to characterize the height required to deploy the parachute from its bag

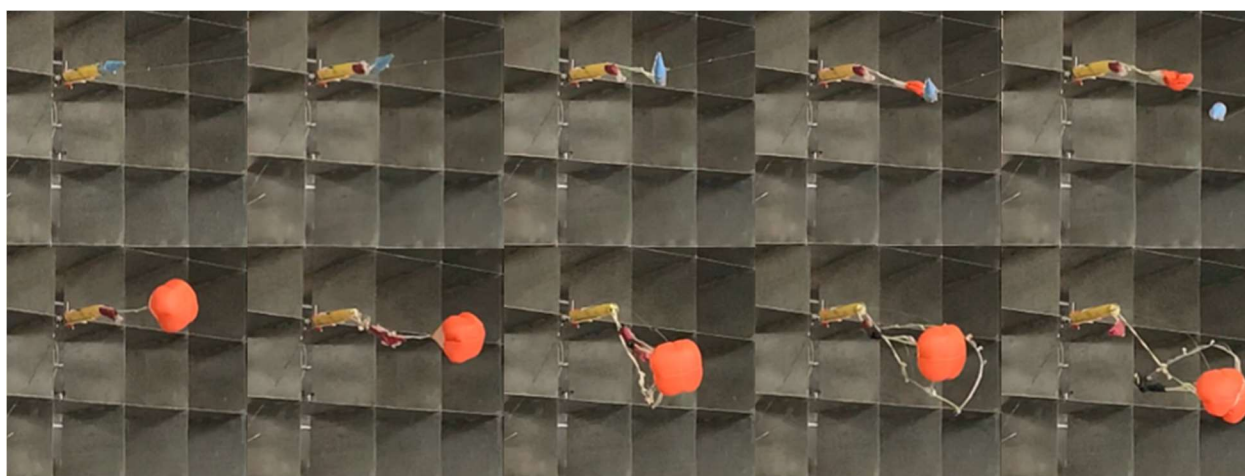


Fig. 74 Deployment sequence, as tested at the University of Waterloo Fire Research Lab Wind Tunnel. Shown is the nosecone detachment via pull cord, pilot parachute ejection and inflation, main parachute bag and line ejection. The last frame shows the deployment

The main Kevlar shock cord is bundled in alternating zig zags with masking tape wrapped around each loop to provide shock dissipation on deployment, and for keeping the lines organized in the rocket. The bundles are loosely secured with rubber bands to control their unraveling and provide a further amount of shock dissipation. The bundles are stowed at the bottom of the parachute tube, directly above the main bulkhead and surrounding the main eyebolt. The Kevlar shock cord is attached to the main eyebolt via a swivel eye which will prevent the main shock cord from getting twisted.



Fig. 75 Partially rigged shock cord

Parallel to the shock cord is the reefing control line that will go up to the canopy. This is packed alongside the shroud line bundles. It is attached to a two-ring release mechanism, which holds the pyrocutters used for disreefing.

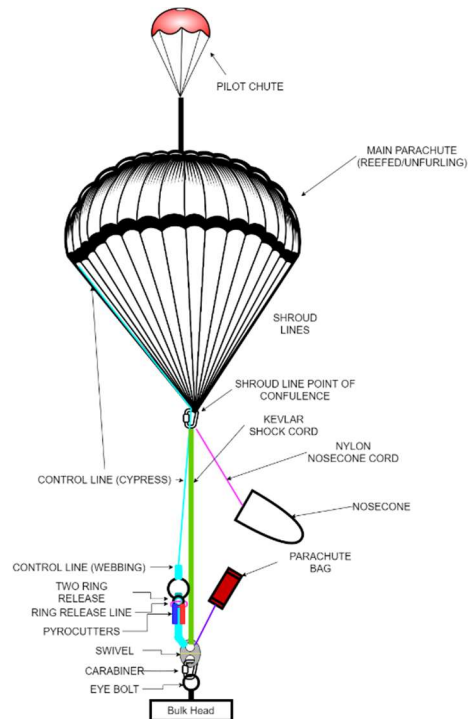


Diagram of the reefing parachute

[STEFANS RIGGING DIAGRAM]

5. Recovery Electronics Assembly

The design and function of the recovery electronics system pertaining to the RocketCAN and the remote arming electronics can be found in the Avionics section of this report.

The recovery electronics and bulkhead assembly were designed to rigidly and efficiently provide mounting to the recovery and telemetry components. The bulkhead was designed to be as lightweight and easy to manufacture as possible, while providing mounting to the CO2 Ejectors, main eyebolt, and panel mount pyrotechnic circular connectors. The bulkhead consists of a 0.33" thick aluminum 6061-T6 plate and features a single row of bolt holes. It is a significant improvement over the previous main deployment bulkhead in terms of weight.



Fig. 76 Old parachute bulkhead on the left (2019), new parachute bulkhead on the right (2022)

The bulkheads geometry was primarily constrained by the components it had to accommodate. It is secured to the recovery coupler assembly with six $\frac{1}{4}$ "-20 socket head cap screws, which are counterbored into the mating coupler. Since this design is statically indeterminate, dynamic analysis was conducted in SolidWorks FEA to verify that the bulkhead could withstand the maximum shock loading as discussed above. In a modal-time history simulation, dynamic load was applied in a curve resembling the expected shock loading curve as covered by Knacke. As an upper limit, a load of maximum 464 lbf was applied to the central eyebolt thread, as calculated and described above in the Shock Loading section. The bolt holes were placed in a fixed condition. The deployment time was taken from similar 2019 flight altimeter data. This analysis showed that the bulkhead experiences a maximum stress of 13 MPa thus has a factor of safety over 20.

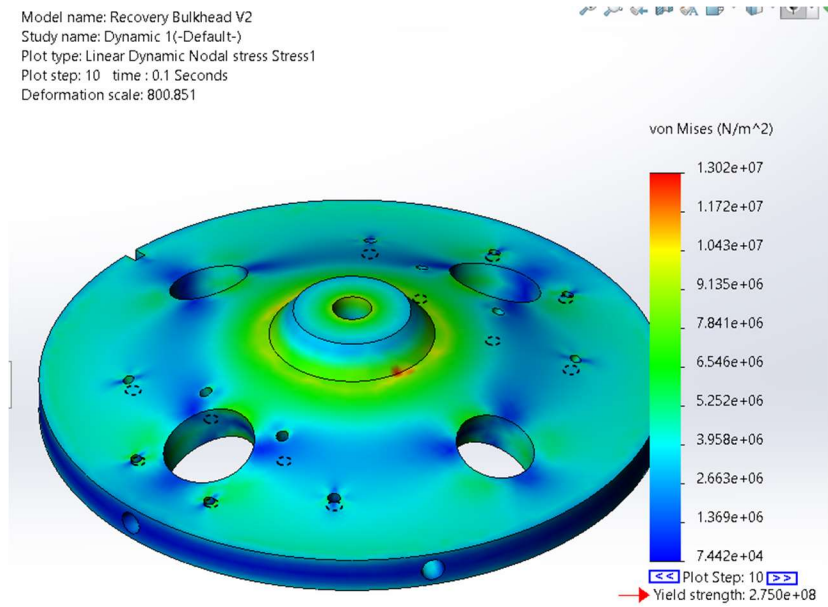


Fig. 77 Results of modal time history simulation on the bulkhead

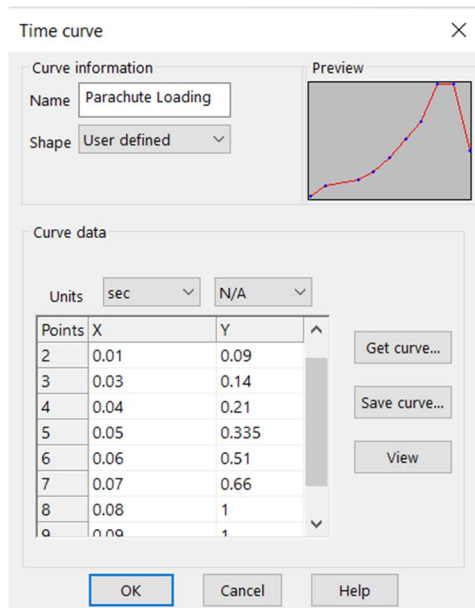


Fig. 78 Parachute loading approximate time history curve, ss input into a SolidWorks Simulation

The circular aircraft-grade connectors on the bulkhead have been graciously donated to the team by Harwin. They are robust and reliable enough to survive the conditions of flight, all while allowing us to pass power to the pyrocutters as needed.

The electronics sled consists of two fiberglass plates which has through-holes waterjet cut to provide mounting for all of the electrical components. It is attached to the bulkhead via four angle brackets with #6 screws. These loads on the screws have been analysed in tensile and shear conditions to ensure that they will be able to survive the accelerations. At the other end of the electrical sled, it is held rigid by two spacer bolts, which ensure that vibrations during flight will not be an issue. All of the mounting screws for this assembly will be secured with thread locking compound to ensure that they do not back out in flight.

The electronics have been placed onto the sled as to efficiently space them for harnessing and to reduce the length of the section. The 9v batteries and lithium polymer battery are secured with zip ties to their battery mounts, to ensure

they do not shift in flight. More details on the recovery electronics components, design, safety, redundancy, and testing can be found in the avionics section.

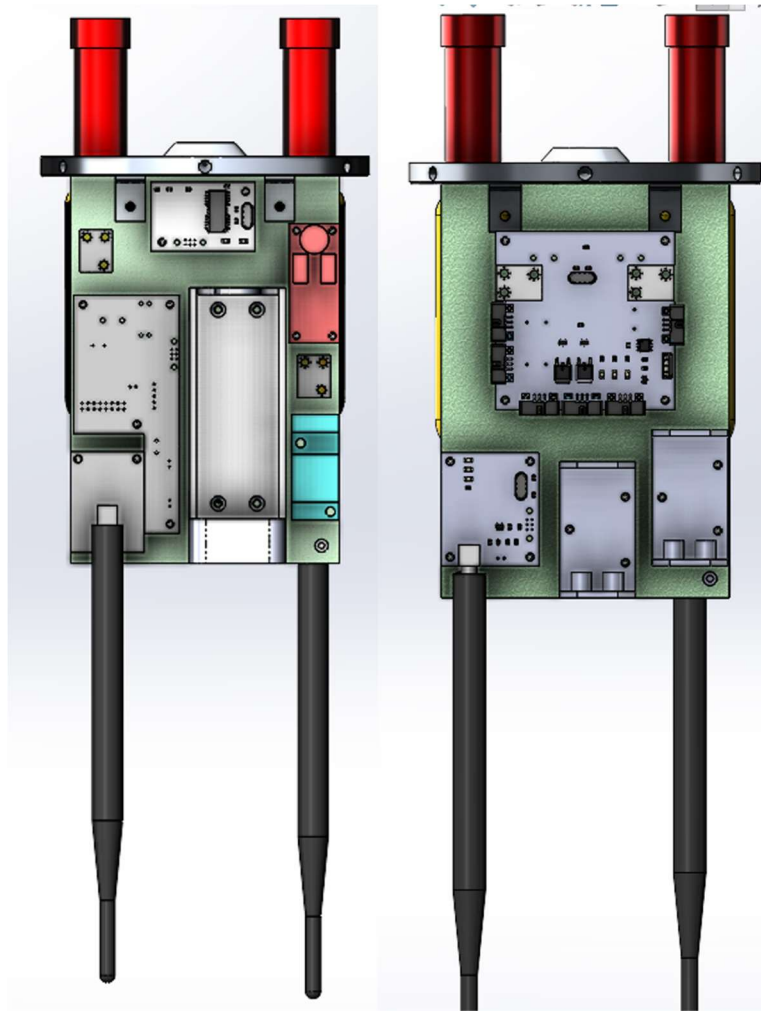


Fig. 79 Recovery electronics sled component placement

6. Reefing Parachute

The main parachute is reefed via a method that was developed based on testing and literature. In the initial research phase of the project, there were three main design concepts considered:

- Skirt reefing, featuring a single line around the parachute skirt and cutting devices attached to the parachute,
- Vent reefing, featuring a line that pulls down the vent through the skirt of the parachute to prevent it from inflating
- And Control line Skirt reefing, featuring a line around the parachute skirt that descends down the shock cord to attach to the main rocket

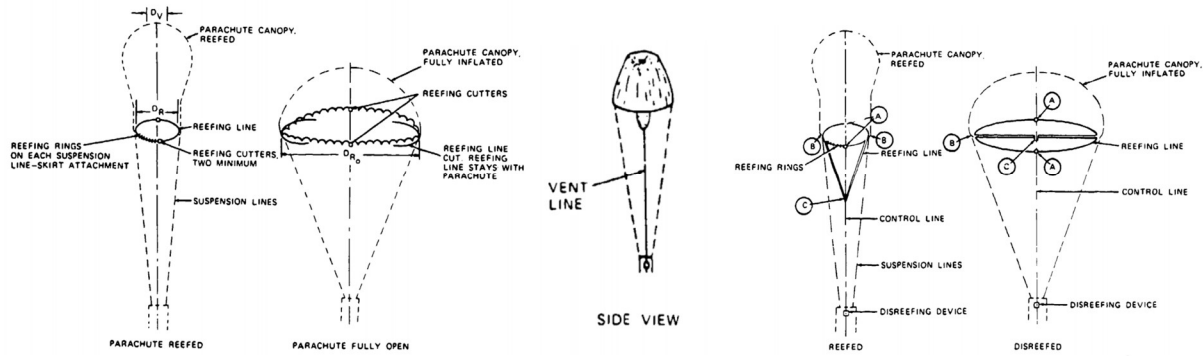


Fig. 80 From left to right: Skirt reefing, Vent reefing, and Control line skirt reefing concepts [13]

Skirt reefing was deemed unfeasible due to the relative size and mass that a standalone cutting device on the parachute would require, and due to the difficulty of ensuring that electrical cables running up the length of the shock cord would be unaffected by the extreme shock loading the parachute experiences. Vent reefing was abandoned due to the relative lack of literature and industry examples that existed to support it. Control line skirt reefing was pursued due to its simpler electrical integration and the amount of literature that existed to support it.

Several methods of routing the control line from the SLPOC (shroud line point of confluence) were conceptualized, in order to be tested on a small-scale truck test. The goal of these scaled tests was to determine the feasibility of the routing concept. They determined which designs provided a consistent shape and consistent disreefing, which designs were easiest to work with, and which designs were least prone to tangling on deployment.

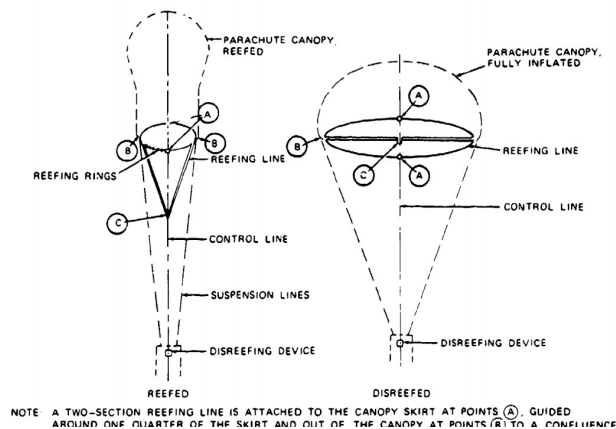


Fig. 81 Control Line Reefing as proposed in Ref. [7,8]

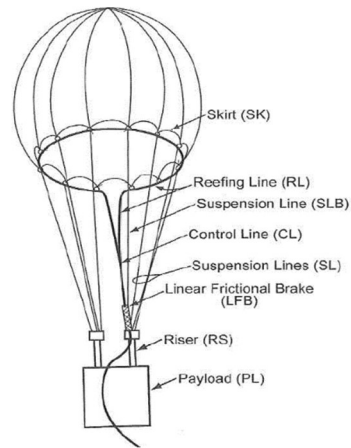


Fig. 82 Continuous-disreefing type control line reefing system as proposed in [15]

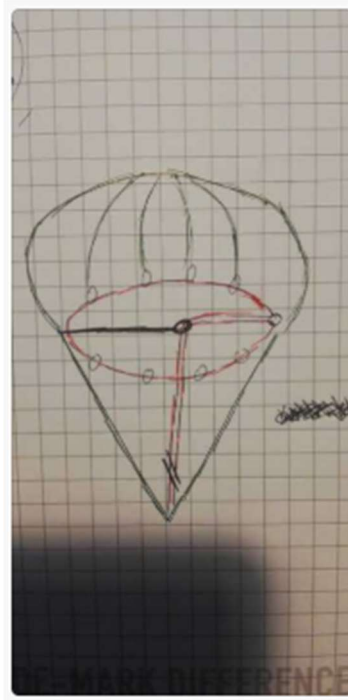


Fig. 83 Modification of vent line reefing as considered by the team

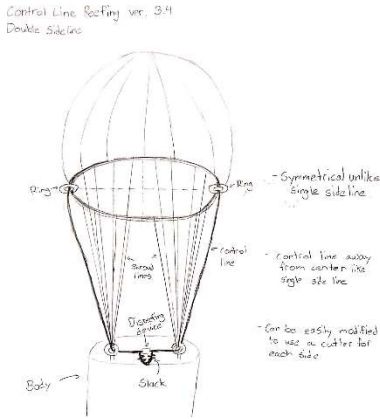


Fig. 84 Dual line reefing system as considered by the team

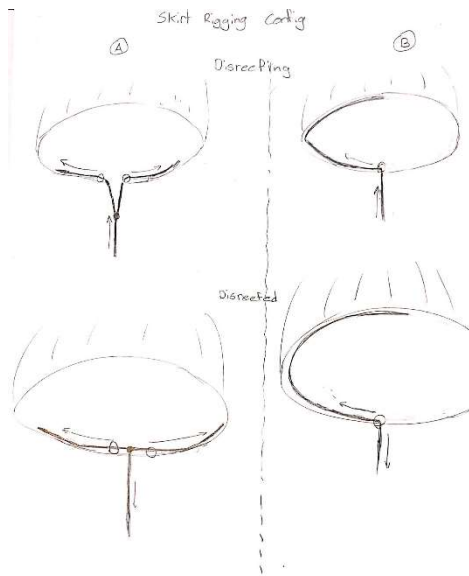


Fig. 85 Modified skirt reefing concept as considered by the team

From small scale testing, it was determined that a single continuous line tied to one point and attached around the entirety of the skirt would be the best option for its relative simplicity. The line would pass down through the SLPOC along the entire length of the shock cord to the rocket booster. This was the design, out of those tested, that presented the least concern for tangling and provided a consistently uniform shape of the parachute. This final design is a slight variation of the design proposed by Sadeck and Lee in Ref. [15]. A disreef sequence of this reefing type is shown below:

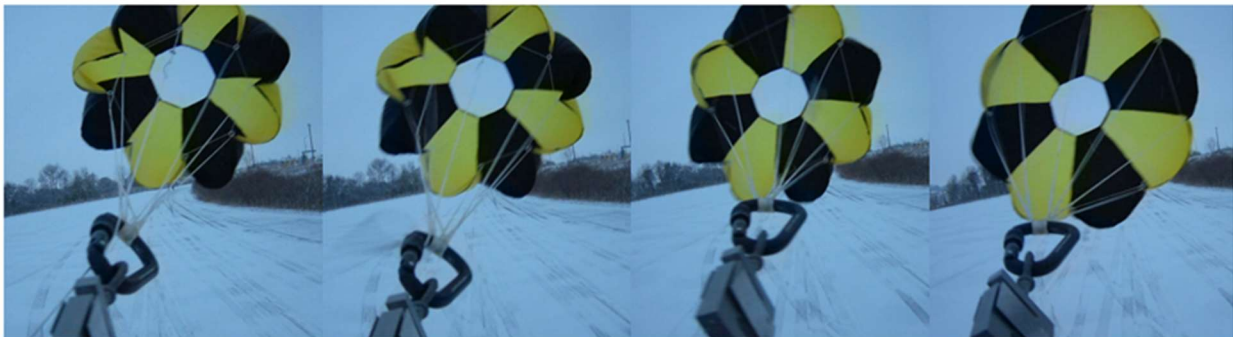


Fig. 86 Disreef sequence on a small-scale parachute

It was chosen that rings would be placed at the inner seam line of each gore for routing of the shroud line around the skirt. This was chosen over a fabric sleeve due to the relatively lower resistance it would provide to the reefing line. The rings were placed at the inside seam line of the gores because they are structurally the strongest points of the parachute construction. They were attached using the same method that the shroud lines are attached to the parachute. The welded rings used are rated to 325 lb.



Fig. 87 Rings at the inner seam line of each gore for routing

The control line passes through all skirt rings and is pulled down to the rocket at one location. When the system is fully taut, the length of the line going around the skirt is less than the inflated perimeter, and the inflation is thus restricted. By varying the length of this line, the descent rate of the rocket is also changed. To determine the correct line length, a line length to drag area curve was to be generated through ground-based parachute truck tests, as was suggested by Knacke [13].

During initial recovery design the dry rocket mass was assumed to be 100 lbs. The specification that our recovery system is designed to is descent speed. As per the IREC DTEG, this speed must be 75-150 ft/s.

It is important to consider the rationale for these limits. The absolute worst case occurs if the overall descent speed is too slow, and the rocket drifts out of bounds into the White Sand Missile Range. This results in the rocket being fully lost, with none of the parts or onboard data being able to be recovered. If the descent speed is too high during the inflated main parachute phase, then the rocket risks impacting the ground too hard, which would result in damage to the rocket.

The last scenario is the rocket traveling too fast during the reefed descent phase. There are three risks associated with this scenario. The first is a significant shock load during the deceleration that occurs at disreef, causing a malfunction in the rigging, resulting in the parachute not being able to be disreefed.

The second risk is that the reefed main does not provide enough drag to stabilize the descent and the rocket tumbles on its way down. In this case, there is an increased possibility of lines being tangled and issues during the disreefing. A disreefing that occurs during a tumbling descent could risk whipping around the body of the rocket violently, which could cause damage to the rocket.

The last is the occurrence of a ‘ballistic re-entry’ as mentioned in the DTEG. In this case, the velocity of the rocket during ascent is maintained through to the descent, creating a parabolic trajectory that also carries the risk of traveling a significant distance and possibly out of bounds. If the descent is very unstabilized, there is also a risk of aerodynamic forces breaking up the rocket.

However, for all of these the descent rate would need to be exceedingly fast, which would generally be outside the margin of error for the system. Regarding the opening shock specifically, the large margins of safety on the strength

of the system components make this not particularly concerning. This range of forces under differing descent rate scenarios are analyzed earlier in the shock loading section.

Thus, the risks that are outlined for the last scenario are not as significant as the risks associated from descending too slowly since. As such, in practical considerations during fabrication rounding should always be done to get a resulting higher descent rate. This was put into practice later in the design.

Since the reefed stage is in effect from 30 000 to 1500 ft AGL. A reasonable target altitude at which the correct speed is to be achieved is thus 1500 ft AGL. At ground level at the launch site, the altitude is roughly 4600 ft. As such, the target altitude becomes 6100 ft. However, to establish the worst case of shock loading and descent speed, it is assumed that it would take roughly 400 ft of altitude for the parachute to disreef fully. As such, an altitude of 5500 ASL is considered. Sea level air density of 0.00237 slugs/ft³ is taken from the table of air densities in Knacke [13]. Air density is mostly constant at a given altitude but does vary with the weather. This was to be taken to account by constructing two worst-case weather scenarios.

In terms of pressure, it was difficult to directly find a value, but one source that was found mentioned that 7 mbar per day is considered a major shift of pressure weather systems [16]. This was thus taken as the pressure variation for the weather scenarios. Through a cursory observation of high-altitude air temperatures using online tracking maps [17], temperature variation was selected to be 10 degrees.

The two extremes are thus considered, and two air densities can be calculated. The highest density would occur at the greatest pressure and lowest temperature, while the lowest one would conversely occur at highest temperature and lowest pressure. For 5500 ft ASL, the nominal air density is 0.002017 slug/ft³. Knowing $\rho = P/RT$, the upper and lower limits on air density were found to be 0.002110 slug/ft³ and 0.01931 slug/ft³.

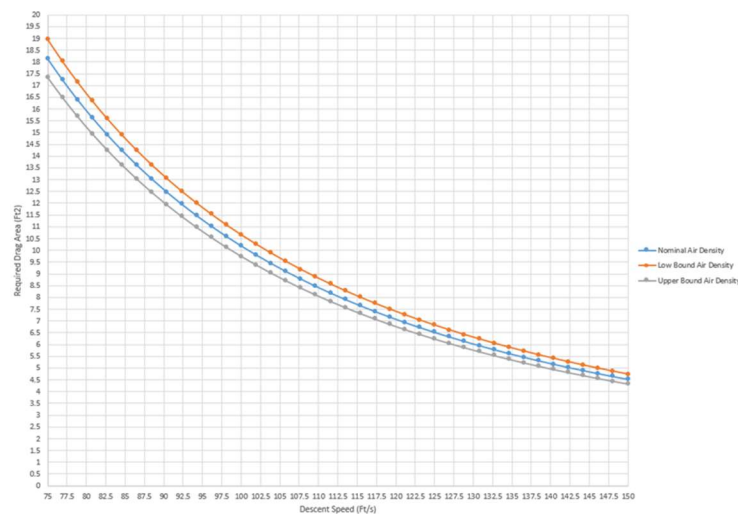


Fig. 88 Rate of Descent vs Required Drag Area for the Nominal, Lower, and Upper air densities

A similar analysis was done to examine the effects of uncertainty in the rocket's mass.

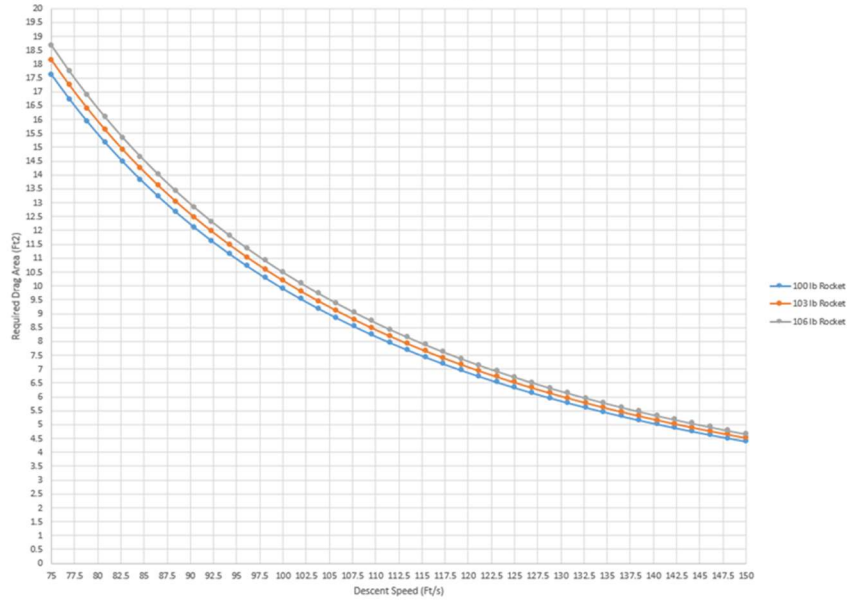


Fig. 89 Rate of Descent vs Required Drag Area for a range of rocket masses

Two non-dimensional numbers were defined by Knacke to relate the drag area of a parachute to the diameter, tau and epsilon. Tau is defined as the reefed diameter divided by the nominal diameter, and epsilon is defined as the reefed drag area divided by the nominal drag area. Through experimental testing, the relationship between tau and epsilon is determined.

Through truck testing, which is discussed in further detail in the project tests appendix, it was found that the disreefed main descent parachute had a drag area of 150 square feet. A mild smoothing algorithm was applied on this data for viewing purposes. Further discussion on this testing can be found in the project test reports appendix.

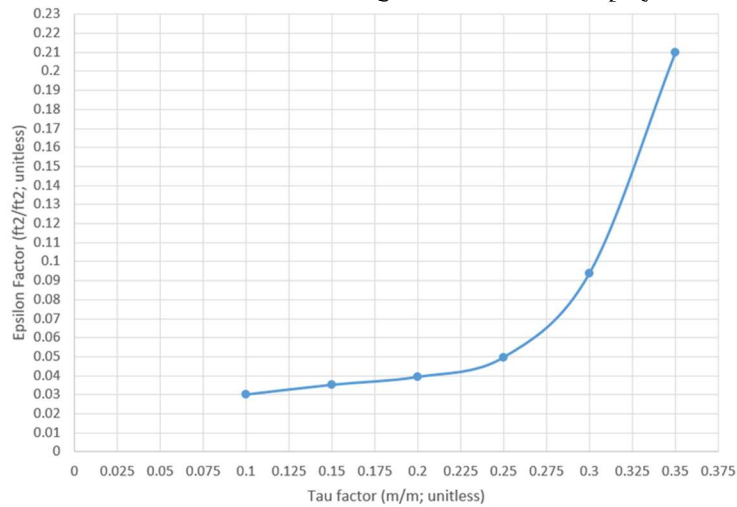


Fig. 90 Tau-epsilon curve

A nominal reefed drag area of 7.5 ft² was chosen based on the analysis of rate of descent with rocket mass and air density which corresponds to an epsilon of 0.05 and a tau of 0.25. This data point was also the best available out of the lengths tested, which also contributed to its choice. This decision allowed us to define the control line length required to constrict the skirt closed such that the parachute falls within competition limits.



Fig. 91 The reefed main parachute undergoing wind tunnel testing

After completing this testing and sizing, the effect of shock loading was then re-examined as detailed above to corroborate the theoretical calculations completed. Wind tunnel testing is also being completed to further verify the testing data.

7. Deployment and Disreefing

The deployment events are controlled by redundant COTS altimeters: the PerfectFilte StratoLogger and the Featherweight Raven 4. Both tie into our avionics system and trigger the CO₂ ejectors along with the cutting devices.

Nosecone separation is carried out using a carbon dioxide canister-based separation mechanism. CO₂ canisters are mounted into ejection cylinders that contain a steel cylinder with a sharp point, a small amount of gunpowder, and an electric match. This cylinder is sealed with epoxy, and the electric match is connected to the drogue output terminals of the altimeter. When the altimeter sends the drogue signal, the electric match ignites, causing the gunpowder to detonate and shoot the puncturing cylinder forward into the CO₂ canister. The sharp point of the cylinder punctures the canister, causing it to eject CO₂ into the parachute bay. The increasing pressure inside this section applies a force to the nosecone, causing the nylon rivets to shear and separating the sections.

These CO₂ ejectors are COTS parts that were provided graciously by Dan Steinhaur at Stein Aeronautics. The nylon rivets used have been previously load tested and characterized to break above 72 lbf. One 38 g cartridge of CO₂ will create enough pressure to break the shear pins with a factor of safety above 2. Two CO₂ ejector systems and two CO₂ cartridges are included in the rocket for redundancy. Note that there is a vent hole located in the parachute bay to allow the rocket to vent out high pressure air on ascent. This has a loose flap over it to provide some sealing during the pressurization of the nosecone section. Additionally, Vaseline is applied at the coupling surfaces of the recovery assembly to provide further sealing. Ground testing is conducted to ensure that a single Co₂ ejector can break the shear pins and separate the section.



Fig. 92 Stein Aeronautics COTS CO2 ejectors



Fig. 93 Ground deployment test setup from 2019

The disreefing mechanism utilizes two redundant pyrocutter which will sever a string that holds a two-ring release closed. This two-ring release is attached to the reefing control line, and when disconnected will allow the reefing control line to ascend and inflate the parachute. The two-ring release prevents the shock of initial inflation from affecting the cutting devices, which are critical for a successful recovery. It consists of a small metal ring that is passed through a large metal ring and tied back with the pyrocutter string through a grommet. It effectively halves the load that the pyrocutter string would otherwise experience. This system is very similar to the two-ring release that has been flown in previous years. CAD of the two-ring release design can be seen below.

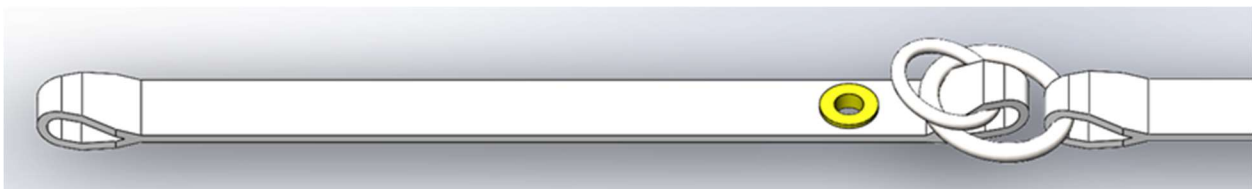


Fig. 94 Two ring release design

The pyrocutter are small cylinders that are bored on one end. They are a COTS part that was sourced several years ago from Prairie Twister Rocketry. They are assembled similarly to the CO2 ejectors, containing a small amount of black powder and an electric match. They contain a small piston with sharp edges, designed to cut a string that passes through it. Previous attempts to use this method of line cutting has been full of issues. They, among a few other factors, contributed to the hard landing of the 2019 rocket, Shark of the Sky. To improve upon these issues, tests were conducted to identify the faults in our use. Firstly, new pyrocutter pistons were made, with significantly sharper edges, and secondly, a new more thorough cleaning method was developed to ensure smooth piston travel. As with the CO2 ejectors, a single pyrocutter being deployed is sufficient to release the two-ring release. Two pyrocutter are flown to create redundancy.



Fig. 95 Two ring release testing

8. System Testing

Further details on recovery testing that has been completed can be found in Appendix C Project Test Reports.

D. Avionics and Electrical Group Support Equipment

1. System Overview

Kraken of the Sky's avionics system is made up of the RocketCAN bus, two dissimilar COTS Altimeters, and an independent BigRedBee COTS GPS tracking module. RocketCAN is a network of independent single-function boards which communicate over a Controller Area Network (CAN) bus, introduced in 2019 on Shark of the Sky. The RocketCAN system has been significantly updated since 2019, including new revisions of every board based on lessons learned with Shark of the Sky, and new systems such as a long-range live telemetry and remote arming of recovery energetics.

The Electrical Ground Support Systems (EGSE) are also all new this year. Our Remote Launch Control System (RLCS) has been significantly upgraded to improve reparability and durability, and a new secondary data acquisition (DAQ) system has also been developed to allow more ground data to be collected for post-flight analysis. The avionics and EGSE systems are summarized in Fig. 96.

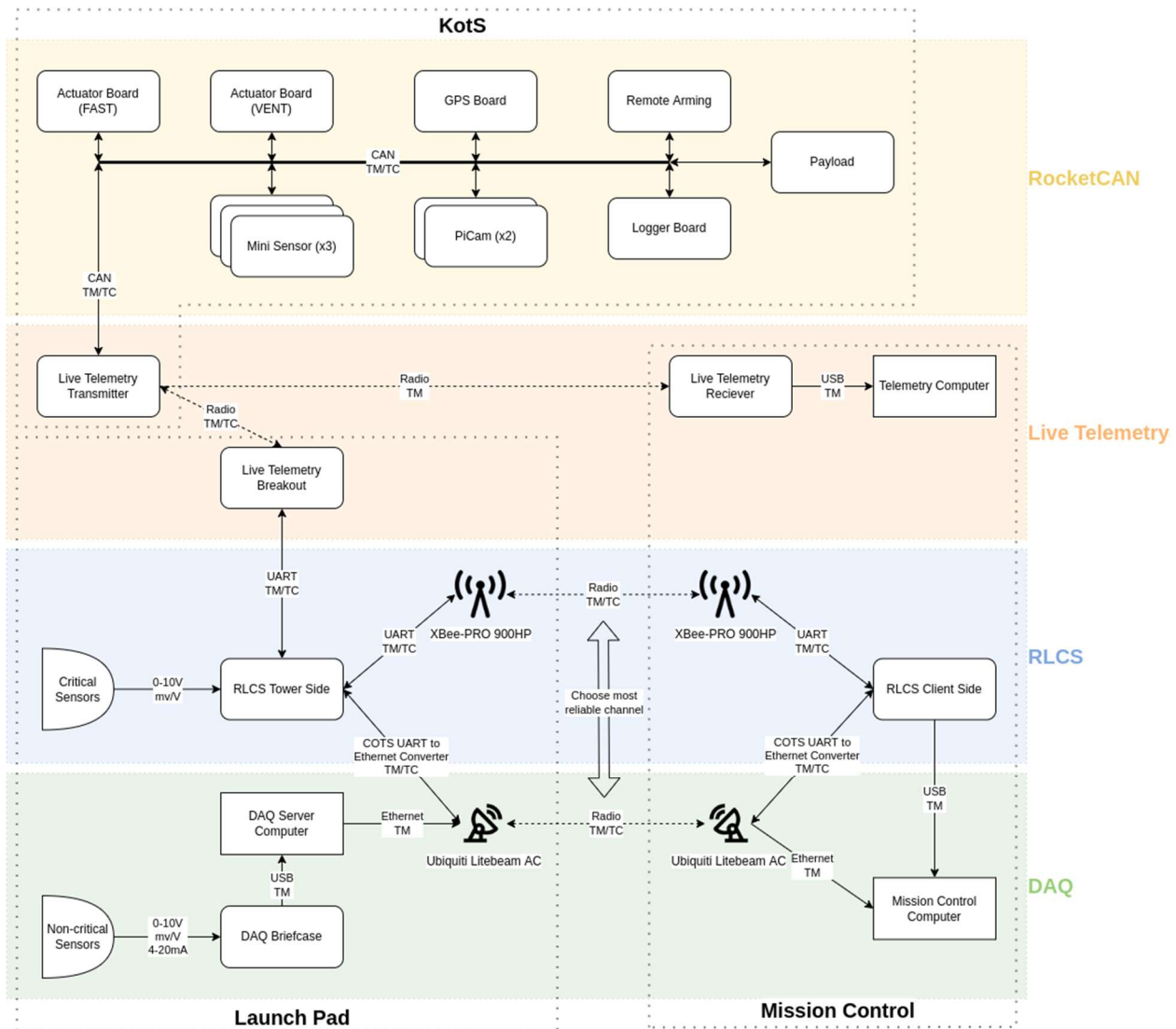


Fig. 96 A block diagram of the RocketCAN system and the EGSE, showing the flow of telemetry (TM) and control (TC) data along with where the components are positioned (dotted outlines)

2. RocketCAN

The avionics modules on the rocket use a Controller Area Network (CAN) bus to communicate. The CAN protocol was primarily selected for its ruggedness; it has strong noise immunity and is suitable for safety-critical outdoor applications. Additionally, CAN is a democratized protocol. There is no bus ‘master’ or ‘slave’ and all boards have an equal opportunity to take control of the bus. This aids the fault tolerance of the system — any individual board can fail without affecting the rest of the bus. Each of the modules can send and receive messages independently using the bus. For example, the Live Telemetry Transmitter (LTT) board can send a message to the vent actuator board to open the vent valve. This modular approach maximizes reliability and robustness and reduces coupling between the different avionics systems. Additionally, if any individual board fails it can quickly and easily be replaced with an identical spare copy. Table 12 gives an overview of the different systems on the rocket.

Table 12 Summary of RocketCAN systems and locations

System Name	Location(s)	Description
Actuator Board	Injector Section, Vent Section	Used to control the pneumatic solenoids for actuating rocket valves. One controls the SRAD injector valve and one controls the SRAD vent valve.

GPS Board	Recovery Electronics Bay	Detects the GPS location of the rocket and relays it over the CAN bus.
Live Telemetry Transmitter	Recovery Electronics Bay	Sends and receives messages from the ground, relaying telemetry and commands to and from other systems on the CAN bus. It also controls and regulates power to the CAN bus, allowing the rest of the bus to be shut off to save energy.
Logger Board	Recovery Electronics Bay	Records all CAN messages to an SD card, including all telemetry and commands for post-flight analysis.
Mini Sensor	Injector Section (2x), Vent Section	Capable of measuring from a pressure transducer and thermistor, as well as an IMU and barometer. Used to measure pressure in the combustion chamber, pneumatic lines, and oxidizer tank, as well as gather pressure and altitude data.
PiCam	Vent Section (2x)	A raspberry pi based camera system with a backpack PCB to control power and recording of the camera via the CAN bus. Two cameras in the vent section are used with 180 degree lenses to capture pseudo-360 degree video of the rocket flight.
Remote Arming	Recovery Electronics Bay	Allows for the redundant COTS recovery altimeters to be armed remotely via the CAN bus, as well as gathering comprehensive telemetry data about the recovery system to ensure correct operation.

Bus Topology and Harness Design

To allow all the RocketCAN systems to communicate there is a harness running from the recovery electronics section down to the injector section connecting each system together. For transport the rocket is assembled in two sections splitting at the vent section. Once at the launch pad it is then joined together. As such there is a mating pair of Harwin Gecko connectors, shown in the figure below, that are used to connect the upper and lower sections of the harness during final integration of the two rocket sections.

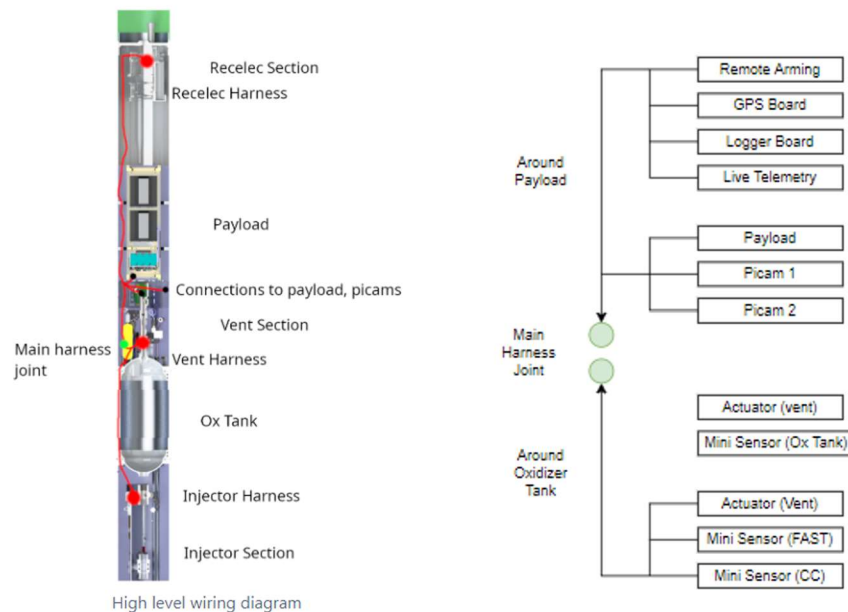


Fig. 97 Left: High level KotS harness diagram. Right: Full harness topology



Fig. 98 Male (G125-FC10605F1-0150L) and female (G125-MC10605M1-0150L) gecko cable assemblies

Electrically, a CAN bus consists of a differential wire pair for communications connecting the modules together in a tree topology. Each end of the bus is terminated with a 120 Ω resistor that ties the high and low lines together when they aren't driven. The RocketCAN implementation includes the CAN bus wire pair, a common ground line, a regulated +5VDC and unregulated +12VDC power lines.

The harness is connected to each system using Harwin Datamate connectors. These connectors, shown in the figure below, along with the gecko connectors above were selected as they are shock resistant and can survive the intense mechanical vibrations experienced during flight thanks to their screw locking mechanism. This has been confirmed through testing, including post-flight analysis of the electrical systems on KotS's predecessor, Shark of the Sky, which had a high-g landing due to a failed main parachute.



Fig. 99 Female Harwin Datamate connector assembly (M80-9410642) with a Male Harwin Datamate PCB mounted connector (M80-5400642) beside it

Since the harness is subject to high loads and wide temperature ranges, particularly the section of the harness which connects the vent and injector sections and runs along the outside of the oxidizer tank, the use of high-quality wire is critical. As such the CAN bus harness is made primarily from 5 conductor shielded cable with Tefzel jacketing, conforming to MIL-C-27500. This is connected to the COTS pre-crimped contacts provided by Harwin, which also use a durable, high temperature PTFE insulation. All connections are made using suitable butt splices and clear heat shrink complying with the IREC DTEG safety critical wiring guidelines.



Fig. 100 Tefzel jacketed cable used for rocket harnessing (M27500-22TG5T14)

RocketCAN Power Systems

The RocketCAN bus is powered by a single 3S 2200mAh lithium polymer battery. The battery is connected through the live telemetry transmitter system, which controls power to the rest of the CAN bus in the form of both a fused but unregulated 12V line directly from the battery for higher power systems such as actuators, and a buck converter that steps down the battery voltage to a stable 5 V which is used to operate the microcontrollers and other digital electronics on the bus. The buck converter delivers up to 2 A of current and is equipped with overcurrent protection. Furthermore, every board on the RocketCAN bus is guarded by a polyfuse, which will automatically disconnect that board from the bus if it has a short circuit. This ensures that an electrical fault on any one of the boards will not affect the operation of the RocketCAN bus as a whole.

Since the rocket must be able to sit for multiple hours on the pad waiting for an opportunity to launch, a long battery life is critical. To allow this the live telemetry transmitter system can shut down the rest of the CAN bus and enter a hibernation mode to conserve battery power. In addition, the cameras, which draw the most power of any system, can be individually shut down to conserve power while the rest of RocketCAN is in operation. Table XXX shows the power consumption, where standby is the power used normally by the system, and active is the power used when the system is live and drawing its maximum amount of power. All of the values have been found experimentally to ensure accuracy, except for live telemetry transmitter since the power requirements of the radio module substantially outweigh those of the rest of the board.

Table 13 CAN Bus Power Consumption

System	Quantity	Standby	Active
Actuator Board	2	130 mW	1010 mW (valve actuated)
GPS Board	1	300 mW	300 mW
Live Telemetry Transmitter	1	480 mW (receiving only)	5260 mW (transmitting)
Logger Board	1	180 mW	180 mW
Mini Sensor	3	170 mW	170 mW
PiCam	2	90 mW	2250 mW (cameras on)
Remote Arming	1	230 mW	950 mW (altimeters on)
	Total:	2140 mW	13720 mW

Based on the power draw, the expected battery life is calculated as shown in the table below. These calculations were performed assuming the rated 24.42 Wh of the 3S Lipo battery, and for the remote arming system (which is powered by a pair of 9V batteries) 4 Wh per battery. The expected battery life for RocketCAN as well as the other electrical systems on the rocket are shown.

Table 14 System battery life

System	Battery Life (Hours)
CAN Bus (Active, Cameras Recording)	1.8
CAN Bus (Active, Cameras Off)	2.6
Live telemetry (Rest of CAN Bus Powered Off)	50.9
Remote Arming (Altimeters Disarmed)	34.8
Remote Arming (Altimeters Armed)	8.4
Big Red Bee COTS GPS Tracker	Well over 10 hours

The avionics systems will draw different amounts of power during different phases of operations, as such the power use in each phase of operations should be estimated and summed to ensure sufficient margins. The table below shows these results.

Table 15 Power schedule and budget

Operations Phase	Estimated Length of Time	RocketCAN	Recovery Electronics	Big Red Bee Tracker (time budget used)
Final integration, flight safety inspection, and transport to launch site	3 hours	1.44 Wh	Off	Off
Tower raising and wait for launch opportunity (assume 5h delay)	6 hours	2.88 Wh	1.38 Wh	6 hours
Fill operations and flight	1 hour	11.55 Wh	0.95 Wh	1 hour
Total Usage		15.87 Wh	2.33 Wh	7 hours
Remaining Margin		8.55 Wh	1.77 Wh (not considering redundant battery)	3+ hours

Common RocketCAN Hardware

Most RocketCAN boards are built around the PIC18F26K83 microcontroller (abbreviated as “PIC18”). The PIC18 is an 8-bit microcontroller running at 12 MHz selected for its low power draw, expansive I/O capabilities including CAN support, low price and high availability throughout worldwide chip shortages. Most of the RocketCAN boards do not perform any complicated processing that would require a larger or more powerful processor, allowing cost savings and simpler embedded code. Some boards such as Logger that need to handle a large amount of data use a 16 bit microcontroller from the dsPIC33 series, selected for its higher clock speed and data bandwidth.

The PIC18 microcontrollers are wired up very similarly across all RocketCAN boards. The MCLR, ICSPDAT and ICSPCLK wires connect to the PICKit3 programmer used to load code onto the boards. OSC1 and OSC2 connect to an external 12 MHz crystal oscillator. CAN_RX and CAN_TX connect to a CAN transceiver such as the MCP2562. Lastly, a number of debugging LEDs are included which will often show board status or a heartbeat indicating the board is alive and well.

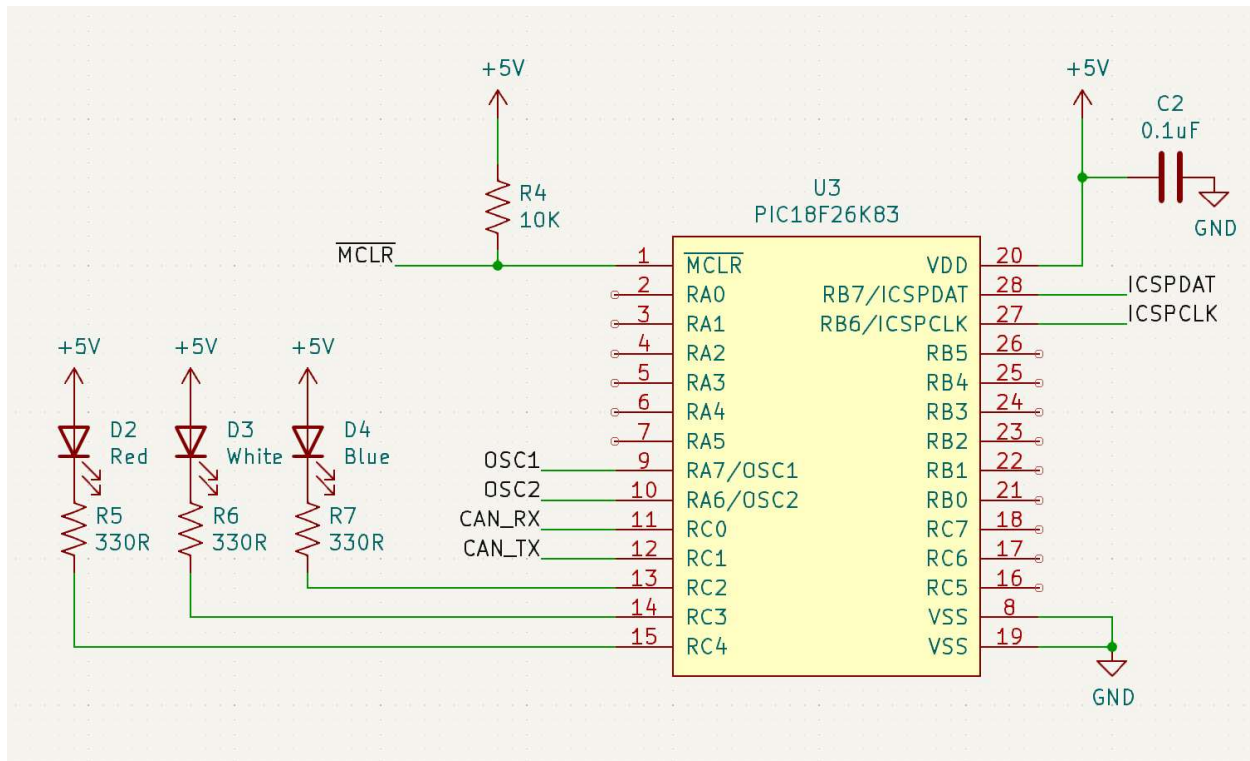


Fig. 101 Schematic of standard PIC18F26K83 connections

Another common fixture on RocketCAN boards is the CAN transceiver. This is a chip that is responsible for converting the differential CANH and CANL signals into digital CAN_TX and CAN_RX signals. The MCP2562 was selected for this purpose due to its ease of use and price. Additionally, drop-in replacements are available should availability become a concern due to ongoing shortages.

The boards are programmed using a PICKit3 which can also act as an in-circuit debugger. It requires three lines to be connected to the microcontroller: MCLR, ICSPDAT and ICSPCLK. These lines along with power and ground are broken out to a Dupont connector placed on each board for ease of programming.

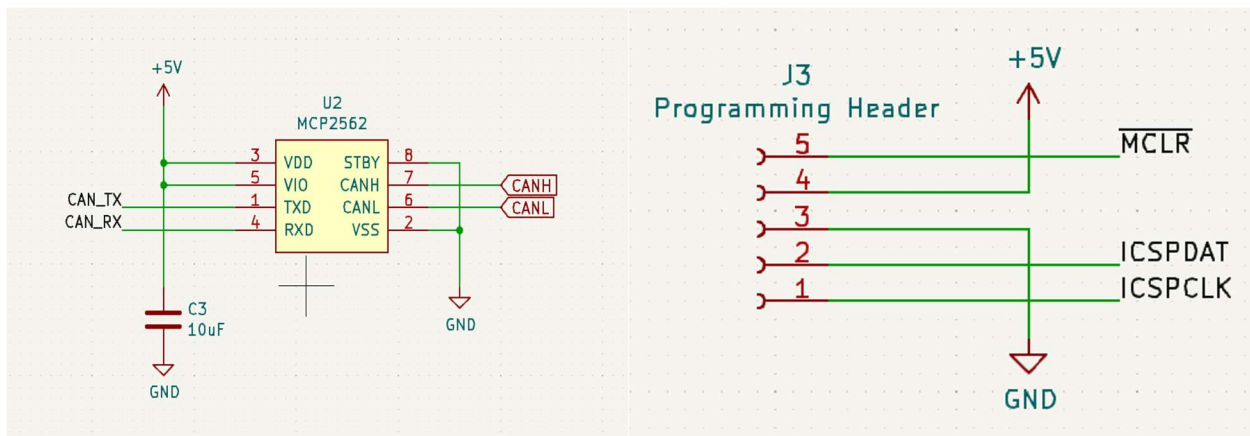


Fig. 102 Schematic of the MCP2562 CAN transceiver and PICKit3 programming header schematic

The last feature common across all RocketCAN boards is the CAN connector and power circuitry. Each board is equipped with a current sensing resistor on the +5 V line which allows it to measure and report how much current it is drawing. The voltage drop across the resistor is amplified by an INA180 current-sense amplifier and measured by

Canlib and Common Software

To handle the intricacies of CAN and ensure a common set of message types, board IDs, and data field formats, all RocketCAN boards use a shared library known as “Canlib” to interface with the CAN bus. Canlib provides functions to build and inspect the various CAN message types, ensuring the format of the data field is well-defined, and abstracts over the specific CAN hardware used which allows its use on the various microcontrollers in the system.

All boards on the CAN bus must fail safely, and the software is an important factor in this. Each board periodically produces a “nominal” status message to indicate that it is still online and functioning correctly. If any of the internal error checks on a board fails the status message will be replaced with an error message indicating the error detected, which will be relayed to the operator over the live telemetry system. Additionally, safety-critical boards will automatically go into an appropriate safe state if an error is detected. For example, if the vent actuator board detects a critically low battery voltage, it will send a low battery warning and open the vent valve in order to safe the rocket. The nature of the safe mode depends on the function of each board, but it is generally a state which will minimize hazards to both the rocket and the human operators. The democratized nature of the CAN bus system means that if any of the boards suddenly stops functioning, the bus will remain online and the other boards on the bus can continue functioning normally.

Actuator Board

Actuator board is responsible for controlling two key actuators in the rocket: the injector valve and the vent valve. These are both pneumatically actuated valves which are controlled by 12 V solenoids. These solenoids are identical and each draw XXX mA, well within the current capabilities of the unregulated Li-Po battery connected to the 12 V line. Additionally, the board supports a pair of limit switches which are used to report the position of the controlled actuator over the CAN bus. The two copies of actuator board are identical, being differentiated only in software by their CAN board ID. This allows for easy hot-swaps if faults are detected with either of the primary copies.

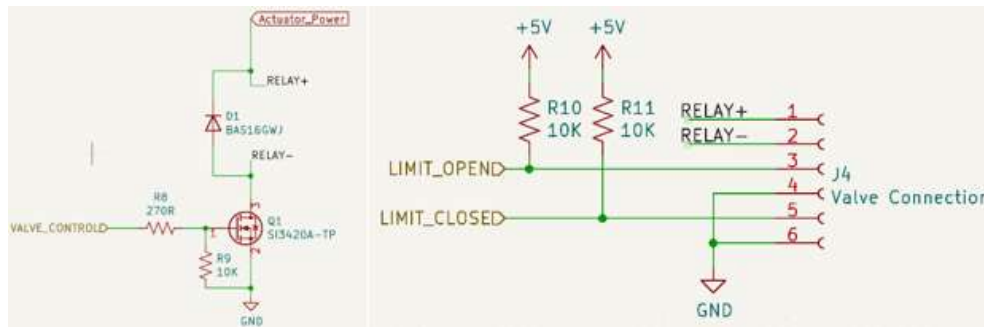


Fig. 105 Schematics of the actuator control circuitry on Actuator board.

Actuator board is designed to fail open. This has the effect of opening the vent valve, where pneumatic pressure is required to close it, and preventing the injector valve from actuating prematurely due to an electrical failure. This is achieved through the use of an N-channel MOSFET in a low-side-switching configuration, which was chosen for simplicity and reliability. A flyback diode is included to prevent voltage spikes from the inductive load of the solenoid. Another of the same shock resistant Harwin Datamate connectors used on the CANBus is used to connect the wiring to the solenoid and limit switches.

Because the GPS module can take up to 30 seconds to obtain a fix on its position when starting up from a cold state, the ability to power the GPS from an external battery was added to this board. Two diodes allow the module to be independently and redundantly from either the auxiliary battery or the CAN bus 5 V line. This allows the GPS module to be powered on before the rest of the RocketCAN bus to ensure a timely fix. In the event of a dead auxiliary battery both the battery voltage and GPS fix state are both reported over the CAN bus so operators can replace the battery or delay until a fix is achieved. However, in order to save on the mass of an auxiliary battery, it was decided that the longer start-up time to achieve a fix was acceptable and an additional battery will not be flown.

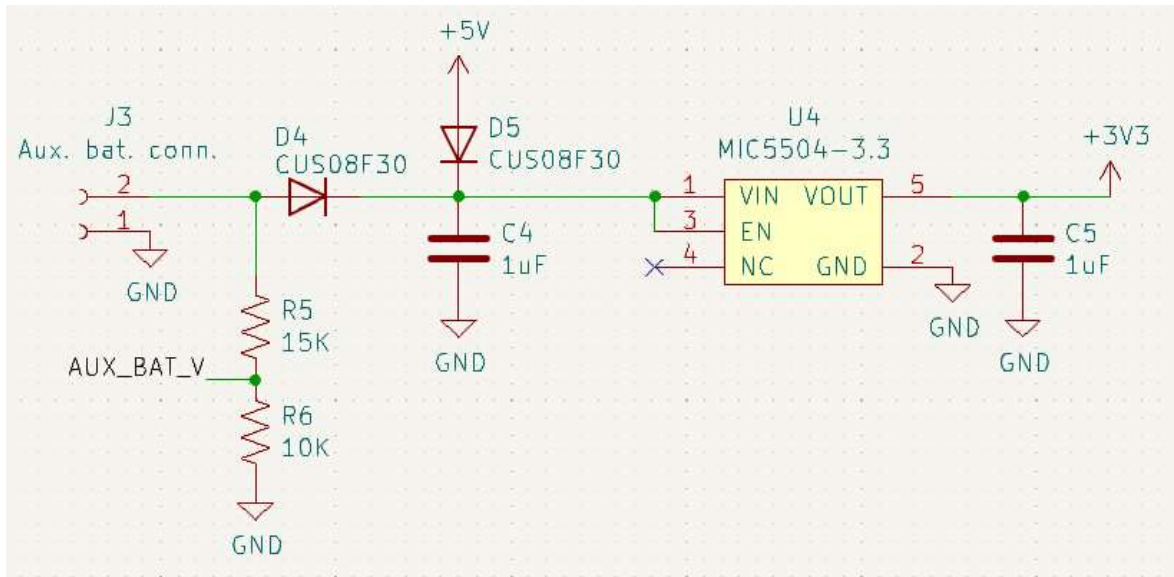


Fig. 108 Schematic of the power supply for the GPS module

Live Telemetry Transmitter

The Live Telemetry Transmitter board (LTT) is the rocket side of the Live Telemetry System. It relays all CAN traffic over a radio link to both the Live Telemetry Receiver (LTR) and the Live Telemetry Breakout (LTB) boards. The LTT can also receive messages from either the LTR or LTB which it then relays over the CAN bus. This allows a computer connected to LTR to obtain real-time telemetry from all of the boards on the rocket, including key parameters such as position and altitude from GPS board or acceleration from Mini Sensor. An operator at the LTR computer can issue CAN commands to control the rocket during launch operations, for example they could start the rocket cameras or reset a specific board that is not functioning correctly.

The RFD 900x modem was selected for this application due to its long range (which has been empirically tested to over 40 km) and ease of use. The modem communicates in the 902 - 928 MHz band and has a transmitting power of 1 W. It acts as a transparent UART link between the connected modules which makes the software very simple. Additionally, the radio module uses a standard 2x8 0.1" connector which lets modules be easily swapped out in the event of any issues.

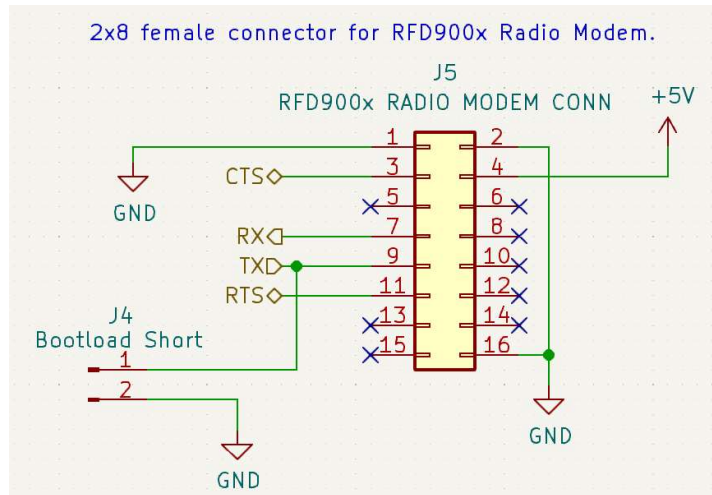


Fig. 109 Connections to the RFD900x Radio Modem

Additionally, LTT regulates and controls power to the rest of the RocketCAN system. In order to allow the rocket to sit on the pad for extended periods of time, all boards except for LTT can be powered down. This is achieved through both high and low side switching in order to ensure that the bus fails depowered, which ensures that the vent valve is open, and the injector valve does not actuate. If power control issues occur there are also jumpers which can permanently enable power to the rest of the bus to ensure the rest of RocketCAN can fly nominally.

The 12 V line is connected through a fuse and current sensing resistor the LiPo battery that powers the bus, this lets it supply high current to components that can tolerate a variable voltage such as actuators. The 5 V line is regulated down from this by a 2 A buck regulator; this is the line that supplies the microcontrollers and voltage-dependent sensors on the bus.

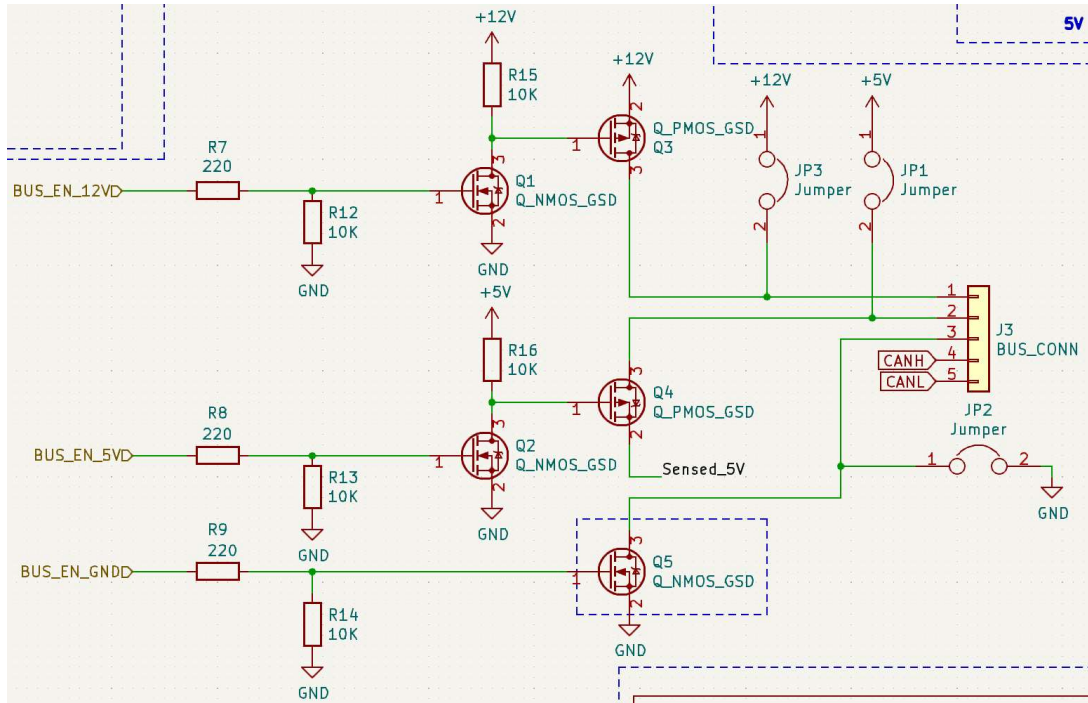


Fig. 110 Schematic of the RocketCAN bus power control circuitry

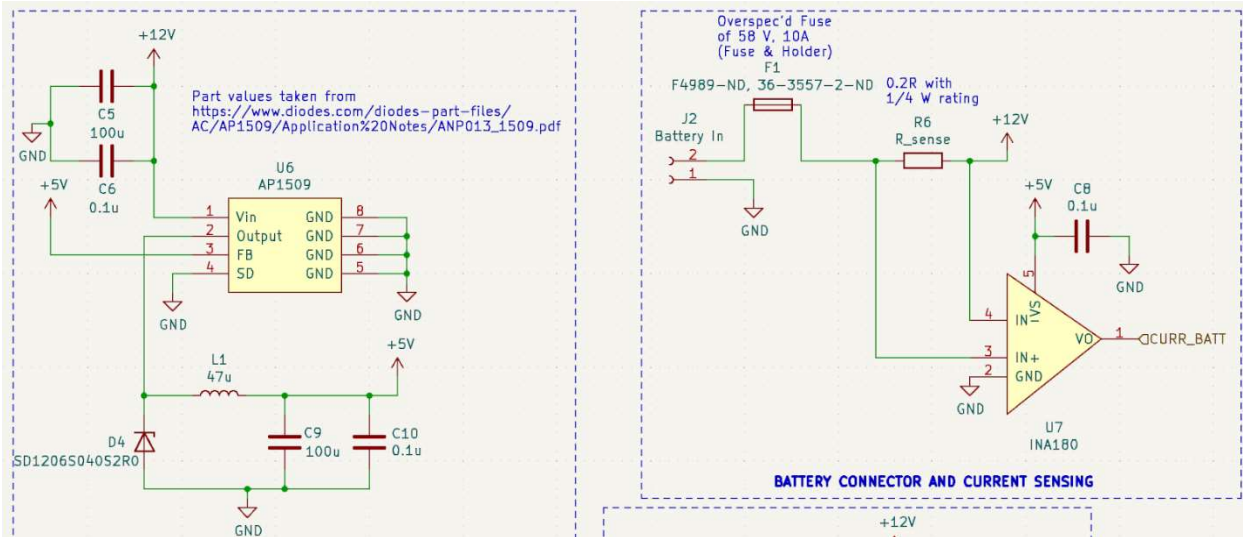


Fig. 111 5 V buck converter and current sensing schematic

Logger Board

Logger board uses a DSPIC33EP512GP502 instead of a PIC18F26K83 as the main MCU due to its fast-processing speed for reliably saving data as it comes in. This MCU also runs on 3.3 V which makes interfacing with the 3.3 V microSD card very easy. It is responsible for saving all the data sent over the CAN bus to a microSD card for post-flight analysis. Of particular interest is the telemetry from the GPS and mini sensor systems which give data on the flight performance of the rocket. Because of the modular nature of our RocketCAN architecture, its function is simple but reliable, and any failure by one board will not result in a loss of information from other boards on the CAN bus. The microSD card is mounted in a vibration-resistant holder that was flight-proven during the launch and hard landing of our rocket Shark of the Sky in 2019. For further logging reliability all data will be transmitted in real-time to the ground through the Live Telemetry System, where it will also be recorded.

Mini Sensor

The purpose of Mini Sensor is to measure various physical parameters during flight and report this data using the CAN bus. It carries a variety of sensors including a magnetometer, two accelerometers, a gyroscope, a barometer and an atmospheric temperature sensor, and includes connectors for an external thermistor and pressure transducer. The data from these sensors is relayed over the CAN bus to be logged by Logger Board and relayed to the ground over the Live Telemetry System.

The magnetometer indicates the strength and direction of magnetic fields, which is useful for determining the direction of flight (relative to Earth's magnetic field). The accelerometers measure the direction and intensity of inertial and gravitational forces experienced by the rocket, which is useful for characterizing engine performance and the load on the rocket throughout flight. The gyroscope measures the angular velocity of the rocket, which is useful for determining the amount of rotation experienced by the rocket during flight. The barometer measures atmospheric pressure, which is useful for inferring the altitude of the rocket. The data from the atmospheric temperature sensor is useful for characterizing the thermal conditions experienced by the rocket during flight. The external pressure and temperature sensors produce data that is useful for characterizing the performance of the engine during flight.

A PIC18LF26K83 microcontroller is responsible for operating all of these sensors and sending the appropriate CAN messages. The data from the accelerometers, magnetometer, barometer, atmospheric temperature sensor and gyroscope are collected by commercial sensor chips and polled using an internal I2C interface. The remaining sensors produce raw analog signals which are polled directly by the microcontroller's built-in analog-to-digital converters.

Pi Cam

The PiCam is a lightweight digital camera system that records in-flight footage and stores it on a microSD card. The rocket has two PiCam units which are both equipped with 180-degree fisheye lenses, which together will capture 360 degree footage throughout flight.



Fig. 112 PiCam board attached to a Raspberry Pi Zero

Each PiCam unit consists of a Raspberry Pi Zero W single board computer, a “Hat” circuit board and a camera module. The Raspberry Pi carries an ARMv6 CPU and a CSI camera adapter. The Pi is linked to the camera via a 20 cm ribbon cable. The camera module supports a 12.3-megapixel SONY IMX477 image sensor and an adjustable lens. The Hat is a circuit board that mates with the Pi’s 40-pin header, and switches power to the Pi. The main purpose of the Hat is to conserve battery power by turning on the Pi (and hence the camera) only when video recording is required and turning the Pi off at other times. Each PiCam system sinks about 0.4 A when recording video, so being able to selectively enable it immediately before flight is critical to maintaining an acceptable battery life. The Pi has a start-up routine which will automatically begin recording video upon boot. The Live Telemetry Transmitter board communicates with the Hat using the CAN bus by sending commands to turn the camera on/off at appropriate times.



Fig. 113 PiCam camera module with 180-degree lens attached (protective cover installed)

Remote Arming

Remote arming is a new system developed for KotS. Its goal is to eliminate the need for operators to climb a step ladder and use a magnet attached to a pole to arm the altimeters while standing directly under the rocket. In addition, it provides valuable instrumentation that allows for constant monitoring of the recovery system health before and during flight, allowing a comprehensive check of the system performance immediately prior to launch. The system communicates via RocketCAN, which in turn receives commands from the operator via RLCS to arm or disarm the system. A block diagram of remote arming is shown in the figure below.

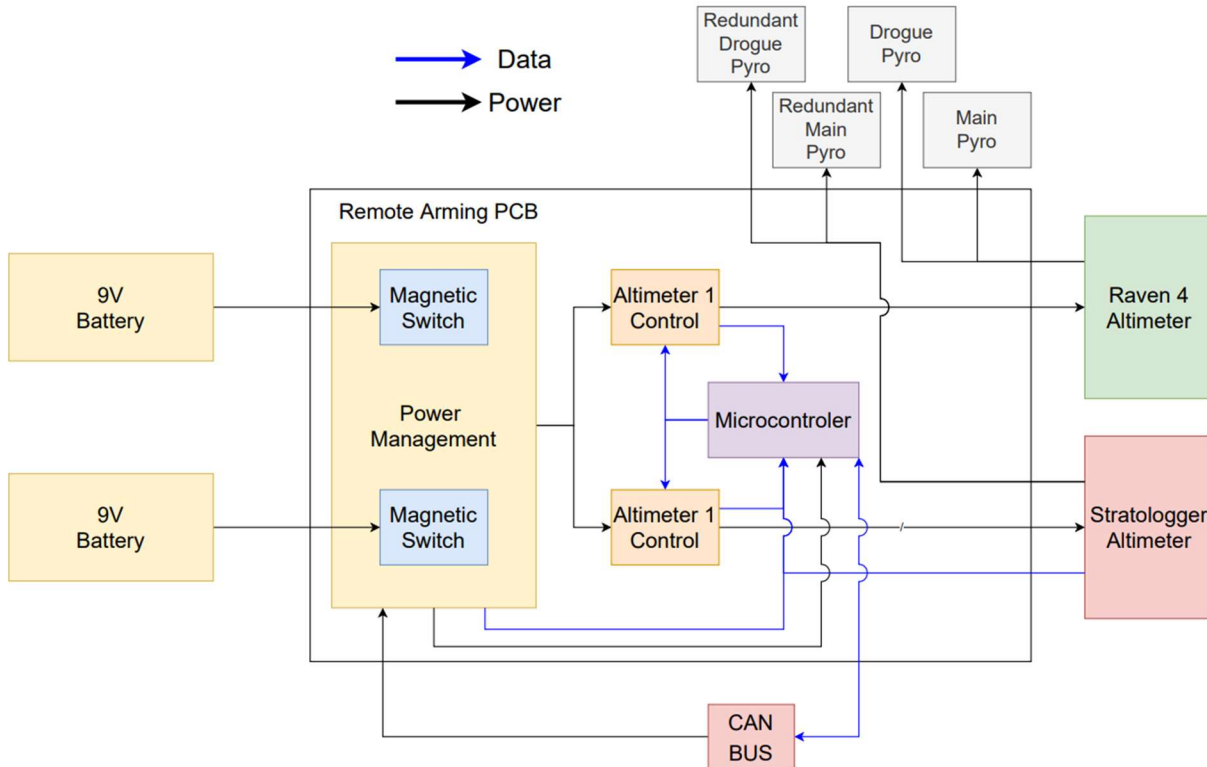


Fig. 114 Remote arming block diagram

Remote arming is a single SRAD PCB, which all the key components of the recovery system are attached to securely, either with screws or screw locking Harwin Datamate connectors. This significantly reduces the complexity of the recovery wiring, reducing the risk of mistakes or faults in the harness such as bad crimps. The complete system is shown below.

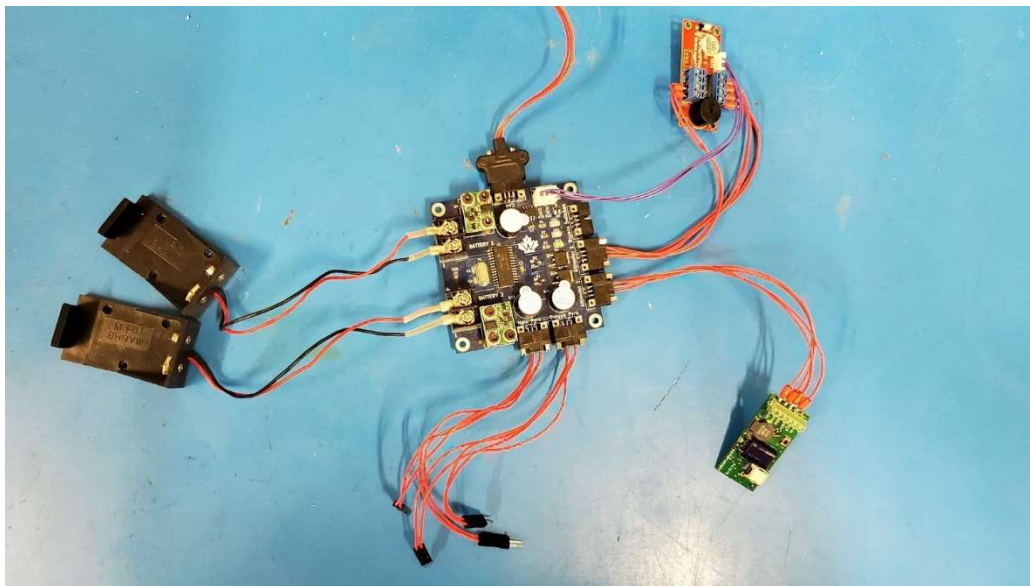


Fig. 115 Complete Remote Arming System

Failing Safely

A key problem for remote arming is to create a system which always fails safe. Most systems on the rocket need to fail safe, however usually this has a well-defined, single meaning. For example, the vent valve should always fail open to ensure there is never an SRAD pressure vessel which cannot be vented. However, for remote arming, failing safely does not always mean the same thing. While the rocket is on the ground, remote arming needs to fail in the disarmed state, as if it fails armed, the pyrotechnics could accidentally be triggered, and an operator could be injured. However, once the rocket launches, the altimeters must stay armed, or the recovery system will fail. As such once in flight the system must fail armed.

It is not possible to design a system which will always fail armed and will always fail disarmed, so a compromise was made. The system has been designed such that it will always fail armed. However, a pair of magnetic switches ensure that the recovery system can always be manually disarmed in the same way that the altimeters have been armed in previous years. In addition, buzzers which are continuously on whenever the altimeters are powered ensure that there is no possibility of personnel approaching the system without knowing it is armed.

Since both arming circuits are controlled by a single microcontroller, several measures have been taken to ensure that it does not cause a single point of failure:

- As shown in Figure XXX, there is a pull up resistor which ensures that if the microcontroller fails or loses power, the circuit will keep the altimeter powered.
- The code on the microcontroller ensures that its default state on power up is armed, as such any temporary loss of power will not result in the altimeters disarming.
- A watchdog timer is used, such that if the main loop is ever hung up, the microcontroller will be reset.
- The microcontroller is powered both by the recovery batteries, and the Rocket's CAN bus, which adds redundancy and reduces the chances of a brown out.

Remote Arming ConOps

Since the logic of remote arming is designed to default to armed, some care must be taken in setting up the system for launch. The procedure is as follows:

- Since the magnetic switch's default state is on, during assembly the 9V batteries should be installed first, the magnetic switches turned off, and then the e-matches should be attached. This is true regardless of remote arming.
- Once the rocket has been full assembled, inspected, and loaded onto the launch rail, but before the rail is raised, the CAN bus should be powered up, remote arming should be commanded to disarm the altimeters, and then a magnet should be used to turn on the magnetic switches, checking the remote arming telemetry to ensure both switches are functioning correctly. The indicator buzzer will also play a repeating tone to indicate both batteries are functioning correctly.

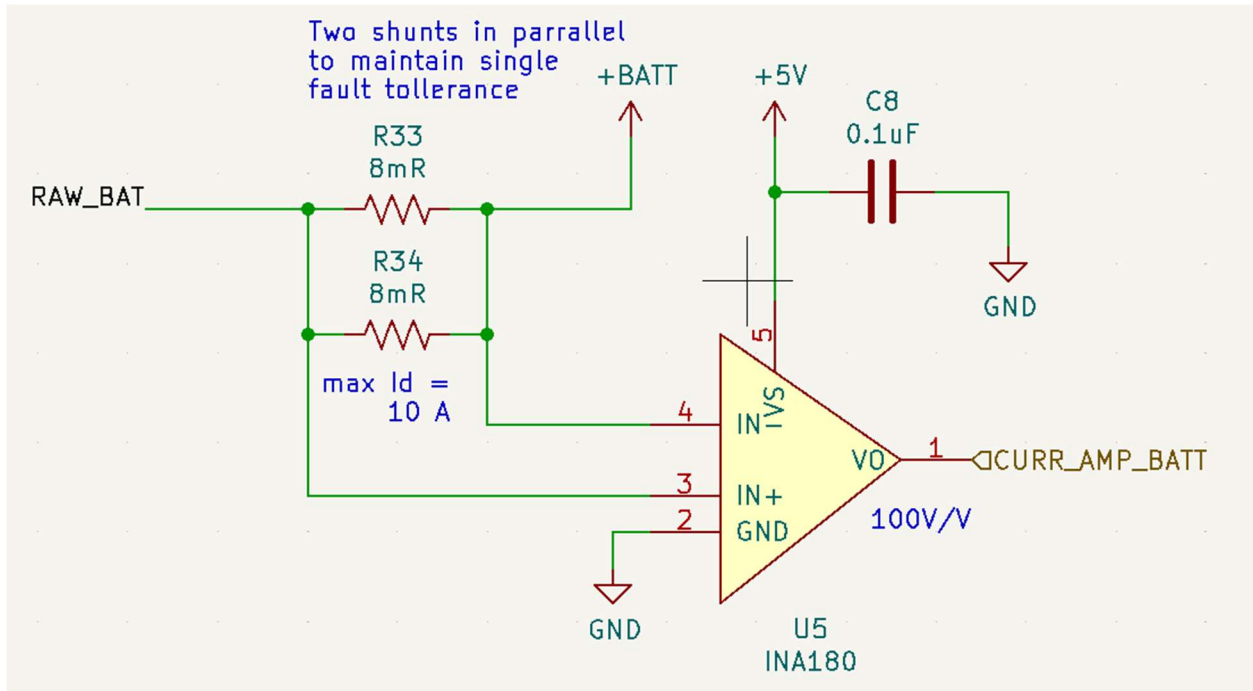


Fig. 117 Recovery batteries current sensing circuit

Altimeter Control

As seen in Fig. 118, power to each altimeter is controlled by an AOD417 P-channel MOSFET, which is in turn controlled by a DMG2302UK N-channel MOSFET to allow the circuit to be controlled with the microcontroller's 5V logic. This high side switching is slightly more complex than if low side switching was implemented with a single N-channel MOSFET but ensuring that the altimeters and remote arming have a shared ground is needed for reading altitude data from the Stratologger. This MOSFET combination has already been flown as part of the injector valve control board for the rocket Shark of the Sky at SA Cup 2019 without issue and continued to function even after the rocket landed under drogue and experienced significant shock loading. The pull up solder jumpers are for use with the Raven 4 altimeter which does not have a dedicated positive pin for the drogue or main e-matches, and as such requires that they are externally connected to power. As mentioned previously, each power control circuit has a buzzer which is on whenever the altimeter is powered. Two different frequencies are used to make it possible to identify which altimeters are powered.

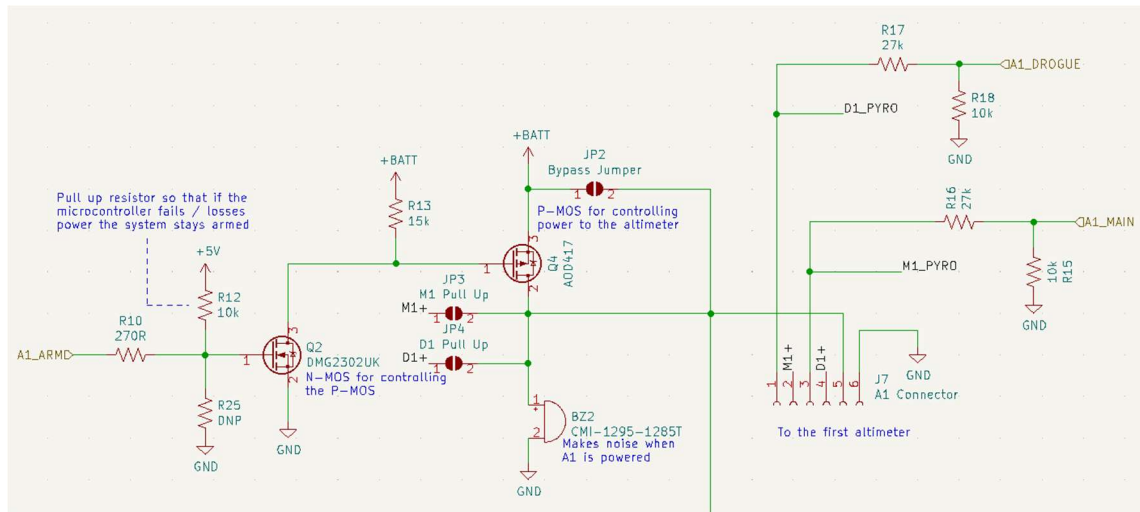


Fig. 118 One of two altimeter arming circuits

Telemetry

Remote arming has a total of eleven different sources of telemetry, the telemetry channels are as follows:

- Battery 1 and battery 2 voltage
- Magnetic switch 1 and switch 2 output voltage
- Voltage reading for all four of the drogue and main e-matches. This voltage reads close to the battery voltage while the altimeters are powered, and the e-matches connected, and close to zero if not. As such it is easy to verify that the recovery system is entirely functional immediately prior to launch.
- Current draw from the 9V recovery batteries, this has a maximum value of 10A so that the current draw of the e-matches firing can be measured. As such the signal is very noisy and imprecise when reading the passive current draw of the microcontroller. This is mitigated via the use of software low pass filters which allow reasonably accurate measurements down to approximately 20mA.
- Current draw from the CAN bus using the same architecture used on all other RocketCAN boards.
- Remote arming parses the UART altitude stream from the Stratologger altimeter and transmits it over the CAN bus so that the altitude can be monitored live during flight. The level shifting circuit can be seen in the figure below.

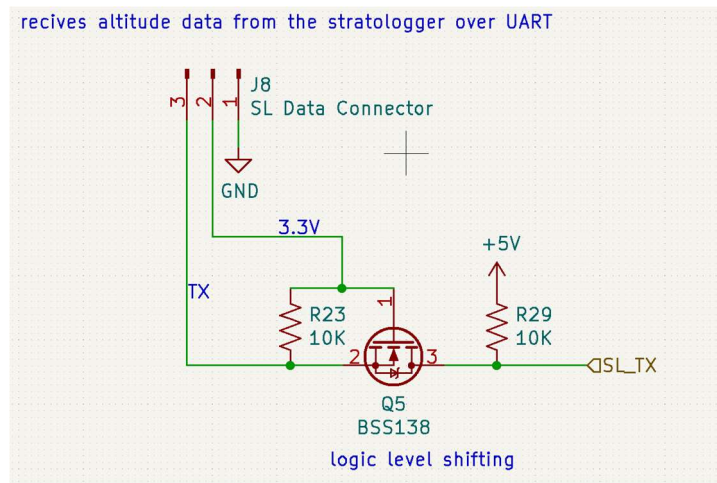


Fig. 119 Stratologger telemetry level shifting circuit

Remote Arming Testing

As of present the remote arming system has undergone full system testing under benchtop conditions. It has also undergone a series of simulated flights where the complete recovery electronics system was put in a vacuum chamber. A partial vacuum was pulled to simulate an increasing altitude, then air was slowly introduced back in to simulate apogee and descent. Referencing an aircraft altimeter, it was confirmed that the drogue channel fired at “apogee”, and the main channel fired at a reading of 1500 ft, as well as that remote arming reported all the correct telemetry. Unfortunately, this test only works with the Stratologger altimeter since its altitude measurement is solely barometer based, while the Raven 4 uses an accelerometer along with the barometer. Both the Raven and Stratologger altimeters were tested with remote arming by connecting them to a computer and using their respective simulated flight tests.

The remote arming system uses a common power bus supplied by two redundant batteries. This single bus provides power to both redundant altimeters. This provides an advantage over the past system which had two isolated redundant systems as it allows for a single battery failure as well as a single altimeter failure without a failure of the recovery system. This was deemed valuable as in 2019 both a battery failure and altimeter failure where experienced, and due to the isolated nature of the systems, this caused both recovery systems to fail. This situation is prevented with the use of a joined power bus. While a joined power bus was deemed valuable for added reliability, a new potential failure mode was identified. It is possible that a short-circuited e-match could cut power to both altimeters leading to a failure. To test this the main parachute pyro line was intentionally short circuited on one altimeter and that channel was fired while monitoring the status of the other altimeter. This test was then conducted with the two altimeters in opposite roles. This test confirmed that the brownout protection capacitors on each altimeter allow them to keep their state in the event of a drop of bus voltage due to a short-circuited e-match on the other altimeter. Therefore, this failure mode does not affect the operation of the other altimeter.

3. COTS Components

While the majority of the KotS avionics suite is SRAD, for the safety critical recovery and tracking systems COTS parts are used.

COTS Recovery Electronics

Per the recommendations and requirements of the DTEG, KotS uses a pair of dissimilar COTS altimeters for recording the maximum altitude achieved and firing the recovery pyrotechnics to deploy the parachute. The first is a Perfectflite Stratologger CF. This barometer-based altimeter was selected due to its low cost and reliability. It has the added benefit of transmitting altitude data over UART throughout the flight. This data is received by remote arming and relayed down to the ground using RocketCAN, allowing for live altitude telemetry.



Fig. 120 Stratologger CF altimeter

The second altimeter used is a Featherweight Raven 4. This altimeter is significantly more advanced and uses a combination of an accelerometer and barometer for altitude estimation. As such, it gathers a large amount of data about the dynamic environment of the rocket throughout flight and provides a valuable redundant source of data for comparison against the data recorded by the SRAD avionics.



Fig. 121 Raven 4 altimeter

To ensure the two redundant recovery systems do not interfere, the Raven 4 is set to fire its charges after the Stratologger has fired. Immediately at apogee the Stratologger is set to fire the drogue pyro to deploy the reefed main parachute by applying a current across the e-match for one second. Then two seconds after apogee, the Raven 4 is programmed to fire the redundant drogue pyro in case of a failure of the Stratologger. When the rocket hits 1,500 ft above ground level, the Stratologger then fires the main pyro to de-reef the parachute, followed by the Raven 4 firing the redundant main pyro at 1,250 ft.

As part of the remote arming system, and for the COTS GPS tracking system, it is important to be able to power systems on and off when the rocket is fully assembled. To allow this Featherweight magnetic switches are used. When a magnet is passed over the outside of the rocket it causes the switch to turn on, and when the magnet is passed over again, the switch turns off.



Fig. 122 Featherweight magnetic switch

COTS APRS Tracking

A BigRedBee tracks and transmits the location of the rocket to assist with discovering the rocket landing site during recovery. The BigRedBee has a built-in GPS receiver which tracks the location of the rocket. The BigRedBee transmits the location of the rocket every 30 seconds using the Automatic Packet Reporting System (APRS) on the 70 cm amateur radio band. The APRS transmitter is tuned to a frequency of 431.0 MHz, which lies within the recommended band plans for digital amateur radio transmissions in the US & Canada. Several team members possess an amateur radio license and are legally permitted to use this band. The APRS transmitter uses a 17 cm quarter-wave monopole antenna with a transmission power of 100 mW (20 dBm). The BigRedBee is powered by a rechargeable single-cell lithium-ion battery which has sufficient energy capacity to operate the BigRedBee for at least 10 hours. The BigRedBee is lightweight, which makes it suitable to be used in the avionics section of the rocket. It can be turned on and off via the use of a magswitch to allow its battery to be conserved.

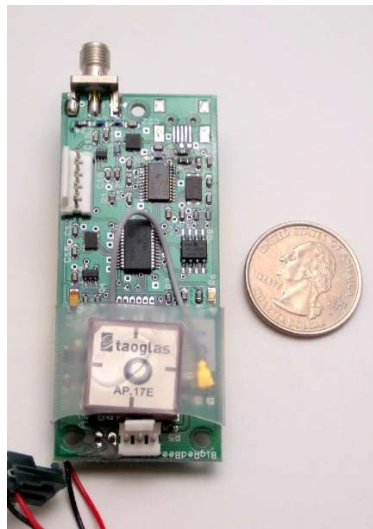


Fig. 123 BigRedBee APRS Transmitter



Fig. 125 Live telemetry transmitter, receiver and breakout

Design Safety

As with all of the systems developed by our team, the LTS is designed to fail safely. As previously mentioned, the LTT controls the power of all the RocketCAN systems. The main safety precaution for the RocketCAN power rails is done through high and low side switching of the power inputs (GND, +5V, and +12V). This ensures any electrical failures will fail with the RocketCAN bus depowered for safe actuation states (vent valve open, injector valve with no actuation). Additionally, solder jumpers are available on all three power rails on the RocketCAN bus, allowing us to permanently enable the rails for all RocketCAN systems. This enables a nominal fly state if there are issues in the switching behavior. The battery input to the LTT is protected by a fuse, and the battery current and voltage is monitored to ensure it does not dip below an acceptable voltage level or draw exceedingly high current.

The LTR has a similar battery safety setup (fuse, voltage and current monitoring) for its external power source. However, the LTR can be powered via USB or a 12V battery, meaning back feeding the power lines was a concern. Thus, schottky diodes are used for each power source to allow flow in only one direction. Additionally, all boards have LEDs which are used to indicate power states, so it is known if any board is in an energized state. All boards also have at least three mounting holes to reinforce the structural safety of the boards in their larger integrated systems. It is important to note the radios will be mounted via their own mounting holes, securing them to mounting plates without permanently attaching them to any of the LTS boards.

Electrical Overview

Live Telemetry Transmitter

The Live Telemetry Transmitter board is an SRAD PCB with an electrical design composed of 2 main subsections all managed by the PIC18F26K83 microcontroller (MCU): power management and radio communication. Power management refers to the regulation of power lines via an LDO (LDLN030G33R) and buck converter (AP1509) for onboard and RocketCAN bus power lines. It also includes battery current and voltage monitoring and RocketCAN bus current monitoring (current sensing using the INA180, voltage sensing through voltage divider). These power electronic circuits are shown in the figure below, as discussed in a previous section. Radio communication is facilitated through the RFD 900x modem, as previously mentioned also. This radio modem connects directly to the LTT via a standard 2x8 0.1" connector, allowing for easy removal and replacement of the radio. The radio communicates with the LTT's main MCU via UART. The PIC18F26K83 was chosen as the main MCU due to its abundant use on the team in various embedded systems and its successful implementation on the previous iteration of our radio communication system for SoS. Additional circuitry on the LTT includes LEDs for debugging and power indication and a MCP2562 CAN transceiver to interface directly to the RocketCAN bus, as shown by the figure below.

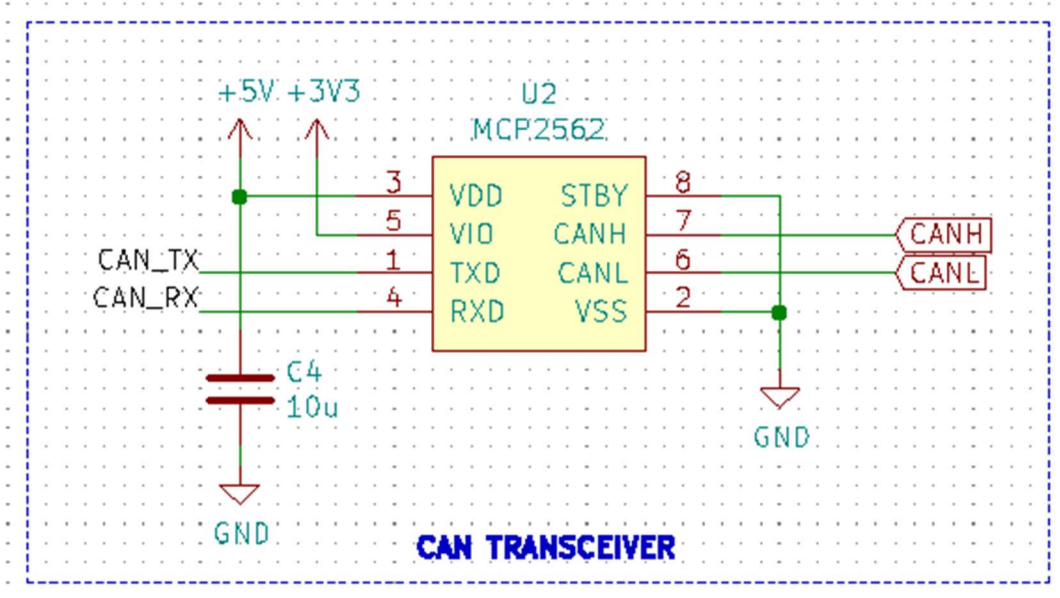


Fig. 126 Live Telemetry Transmitter MCP2562 CAN Transceiver

Live Telemetry Receiver

The Live Telemetry Receiver board is an SRAD PCB with an electrical design broken up into 3 main subsections: power management, radio communication, and USB communication. Similar to the LTT, the LTR power subsystem regulates power through a LDO regulator and buck converter (same part numbers as LTT) in addition to monitoring battery voltage (using a voltage divider) and current sensing (INA180). The radio communication circuitry is connected in the same way as the LTT as well. However, the LTR's MCU required USB support and due to part shortages and a requirement for PIC microcontrollers to be used (for firmware and system consistency), the PIC24FJ64GU205 was chosen. A USB-A 2.0 connector joins the LTR to a laptop for data transmission and optionally power if the RFD 900x does not require as much power for radio transmission. Since the LTR can be powered by either a +12V battery or from a laptop USB-A port, each power input has a Schottky diode in series to prevent back feeding power.

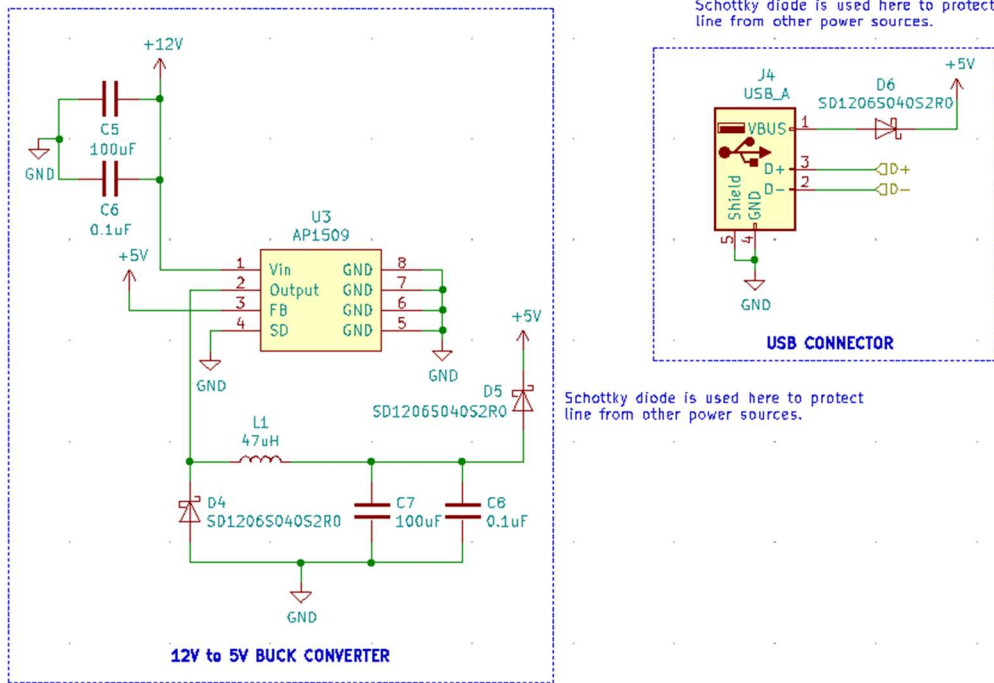


Fig. 127 Live Telemetry Receiver Backfeed Protection via Schottky Diodes

Live Telemetry Breakout

The Live Telemetry Breakout board is an SRAD PCB that is distinct from the previous two LTS boards, as its sole purpose is to make it easy to connect an RFD 900x radio to any of our other embedded systems (most notably RLCS and ST PATS). The board contains two voltage level translators (TXB0106PWR) for converting the +3.3V logic of the RFD 900x modem to +5V logic of other systems. The board also contains a +3.3V LDO regulator (LP5907MFX-3.3/NOPB) for the voltage translators and a power indicator LED. Other embedded systems can easily connect to the LTB via standard 1x6 0.1” pin socket connectors. The entire board circuitry is shown in the figure below.

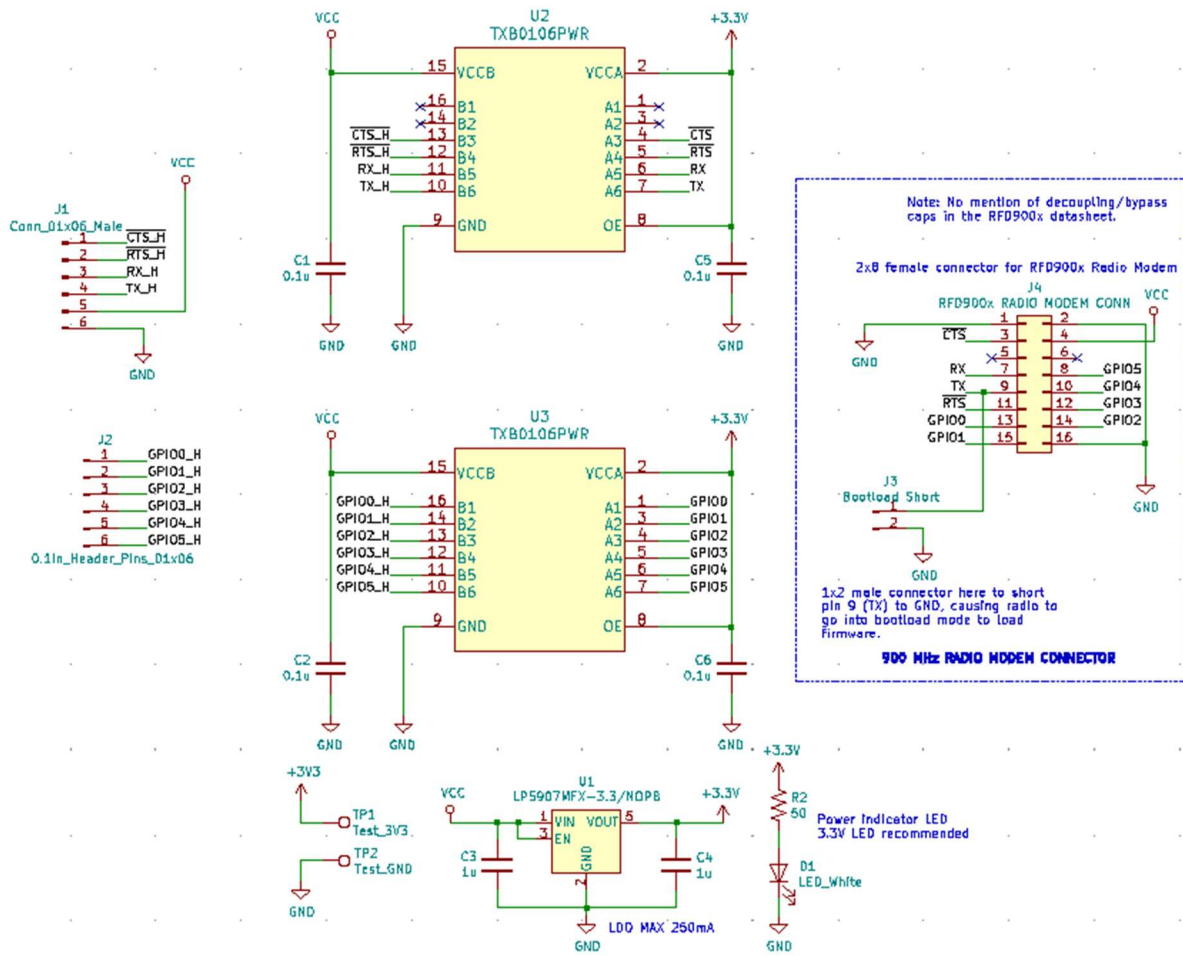


Fig. 128 Live Telemetry Breakout Board Schematic

Testing

The LTS is currently undergoing hardware and software validation testing which is expected to be completed by May 21st. This includes radio communication verification, range testing, and system integration. Power management has already been tested on each board, and the RocketCAN bus power switching logic was also already proven in KotS's predecessor SotS. The RFD 900x radios have already had connectivity verified as well.

The control of the radios from each individual board is to be tested to ensure no inherent radio communication fault exists within our hardware or software designs. A test will consist of connecting a RFD 900x radio to an LTT and either an LTR or LTB, and ensuring the radios are able to connect and communicate with each other via messages being sent back and forth while running their firmware. Messages received from the opposing radio will be analyzed for integrity and data rates (visual confirmation can also be seen on the radios via a green LED which indicates a successful connection and blinks when the radio is transmitting data). This procedure includes testing the connections between the LTT and LTR and the LTT and LTB. The LTT will also be tested for connectivity with both the LTR and LTB at the same time.

The goal of range testing for the LTS is to determine a testable estimate of a distance between the LTT and the LTR/ LTB that still achieves a stable communication link. Range testing consists of taking one of the systems a set distance away from the other and ensuring the communication link between them remains active (where messages are sent between the radio nodes and verified on the receiving end). This testing is highly dependent on location, including the farthest distance testable and what type of obstructions are between the two radios. Given a >40 km area for testing is not feasible for the team (40 km is the empirically derived range of the RFD 900x radios from the manufacturer), a smaller range of 1-5 km will be tested. 1-5 km is an acceptable distance to test should the rocket need to reconnect to our GPS tracking systems if the telemetry link was lost during flight due to range. It is important to note the range

testing is also not completely representative of the conditions of rocket flight, since the testing is occurring horizontally instead of vertically.

System integration is another very important testing procedure for the LTS due to many different systems connecting to various parts of the LTS. As described in other sections of this report, the LTS will undergo systems level integration testing for each of RocketCAN, RLCS, and ST PATS to ensure full functionality with the external systems.

5. *Remote Launch Control System*

The Remote Launch Control System (RLCS) is the primary means of interfacing with the rocket and supporting fill plumbing during launch operations. The main objective of the system is to allow launching the rocket from up to 3,000 ft from the tower. Once the RLCS operator takes control of the launch process, no human intervention should be required at the launch site in any possible error state that requires a human to approach the system. In the event of total failure, the system must put all engine and fill systems into a known safe state so that personnel can approach the rocket without placing themselves in danger.

RLCS is made up of two halves, Clientside and Towerside, which communicate over a radio link formed by a pair of XBEE Pro S3B modules on the 900 MHz band. Towerside is located beside the launch tower and handles actuating motorized valves and interfacing with RocketCAN via Live Telemetry. Clientside is located at mission control and houses switches which map to the various actuators and an LCD to display data to the operator. Both halves are built into weatherproof and robust Pelican cases to protect them from the elements.



Fig. 129 Clientside



Fig. 130 Towerside

System Safety

The entire system is designed to prevent unintended actuation of valves and fail safely. Both Clientside and Towerside have keyed-alike arming and disarming switches respectively, both of which retain the key when turned. This means that whenever the tower is approached the key is removed from Client Side, disarming it, and then inserted into Towerside, also disarming it. In this configuration it is physically impossible to arm Clientside while personnel are at the tower since the key is also physically with them, and even if a fault caused either Clientside or Towerside to unintentionally arm the other half would still be disarmed.

Within Towerside, two relays are required to actuate in order to trigger any action. The relays are wired in series such that one provides power to the actuator and the second determines which direction the actuator should move in. Additionally, to protect against bit flips on the radio link, Towerside only tries to actuate a valve once it has heard two identical valve actuation commands from Clientside. This way, if one command gets randomly corrupted, it will be ignored. The plumbing system is also set up such that if any individual actuator fails the system can still be safely vented.

Clientside and Towerside continually send command and sensor data messages to each other. This means that if either one unexpectedly fails, or the radio link between them drops, both can detect this by noticing silence on the line. If Towerside does not hear from Clientside for 10 seconds, it will automatically set all actuators to a predefined 'safe state' that is baked into its firmware. This means opening all vent valves and closing or de-energizing all others in order to make the system safely approachable by personnel. Clientside will also report any silence of at least 3 seconds to the operator, which could indicate a flakey radio connection or an issue with Towerside.

RLCS controls the following actuators necessary for fill and engine start:

- The Remote Fill Valve, which controls the entry of N₂O into the fill system
- The Line Vent Valve, which opens the fill system to atmosphere in order to vent N₂O
- The linear actuator that triggers the remote disconnect mechanism
- Two nichrome coils inside the engine ignition puck
- The Injector Valve, which controls the flow of N₂O into the combustion chamber, via RocketCAN
- The Tank Vent Valve, which allows the oxidizer tank to be vented of N₂O, via RocketCAN
- Arming of the recovery electronics via RocketCAN

Moreover, RLCS uses sensors to collect the following data, and report that data back to the operator:

- The current state of all valves (open/closed)
- The amount of current flowing through each nichrome coil inside the ignition puck

- The current mass of the rocket, loaded on the rail
- The pressure of oxidizer in the rocket's oxidizer tank
- The pressure of oxidizer in the fill lines
- The pressure of oxidizer in the supply lines
- Data on the status of the remote arming system

Electrical Overview

Clientside is a relatively simple system composed of an Arduino Mega, an LCD, several switches, and a custom PCB that regulates a 3S LiPo down to 5 V for power. Additionally, it exposes a USB port which allows it to send data to a computer for plotting and logging.

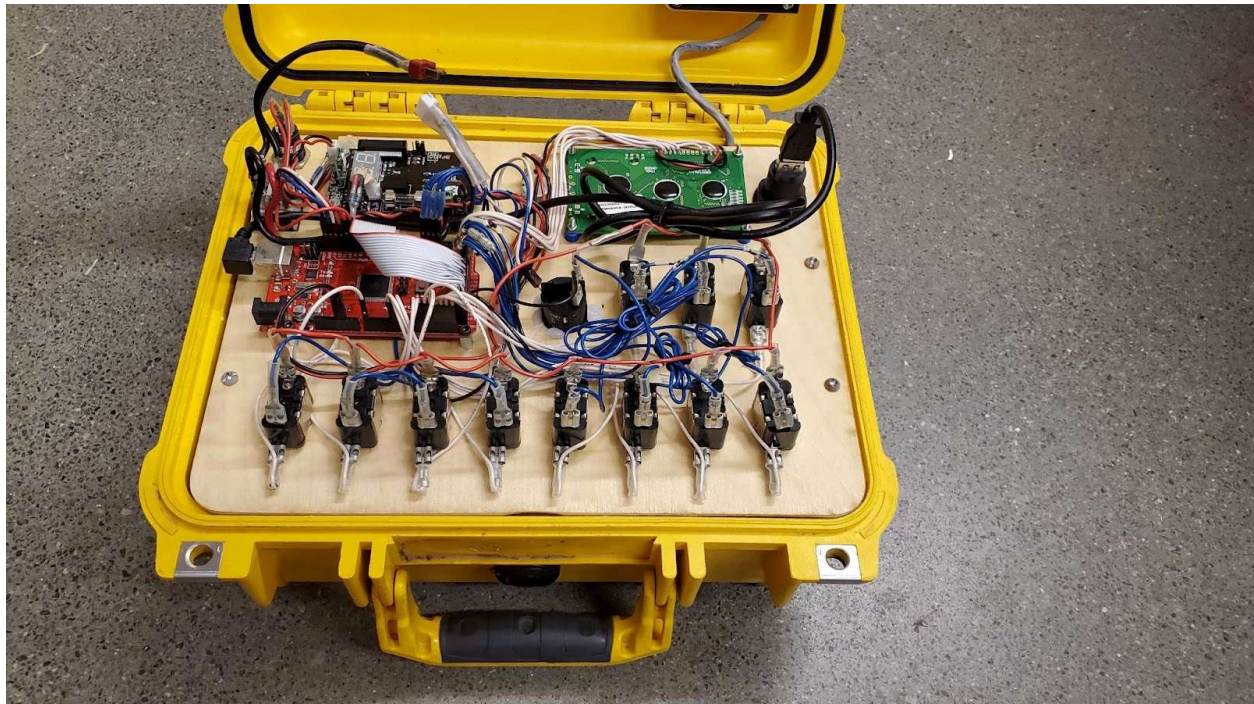


Fig. 131 Electrical internals of Clientside

Towerside is more complicated because it needs to handle the high current draw of motorized valves. It is made up of a set of identical Relay boards connected over an I2C bus to a master Arduino Mega. It additionally contains a copy of I2C Pancake, which interfaces with pressure transducers and load cells on the fill system and launch tower, and Live Telemetry Breakout (LTB) which allows it to interface with the RocketCAN bus through the Live Telemetry System.

The various I2C boards in Towerside are connected over an I2C bus in a daisy-chain configuration. In addition to the two I2C wires SDA and SCL, there is a regulated 5 V line, an unregulated 12 V line, and a ground line. The 5 V line drives the various microcontrollers on the boards and the 12 V line is used to drive the relays on I2C Relay board. The I2C Relay boards additionally have a secondary daisy-chained power connection which uses low-gauge wire and is used exclusively to drive the actuators. This ensures that the high current draw of the actuators does not cause brown outs on the MCU power lines.

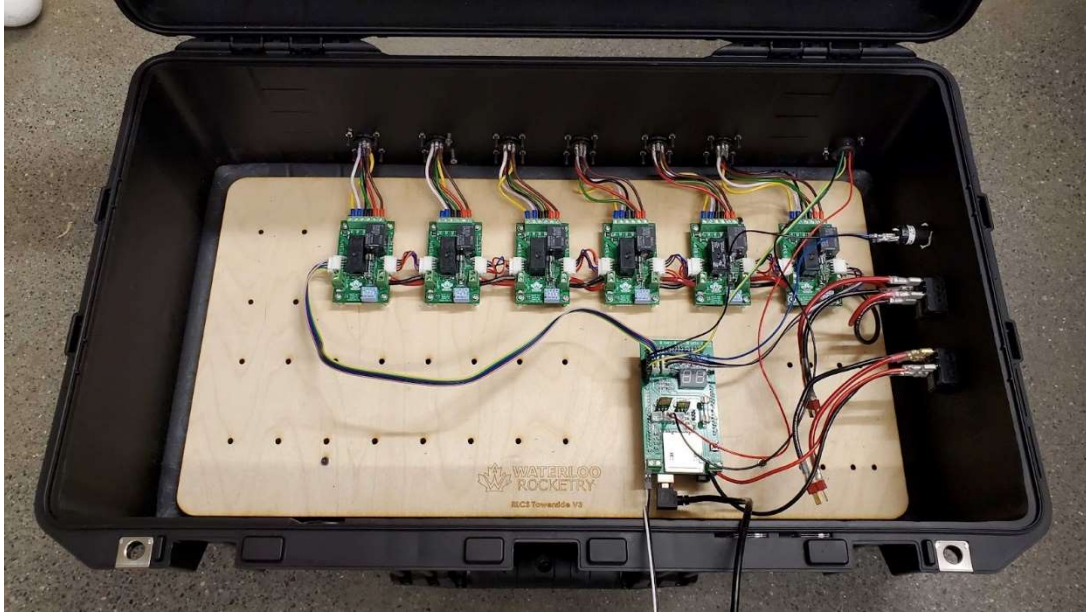


Fig. 132 Electrical internals of Towerside

The main purpose of Relay board is to operate the motorized valves that control the flow of oxidizer into the rocket during fill operations. Each Relay board is connected to one motorized valve. Relay board also detects the states of limit switches built into the valves, which are activated whenever the motor shaft arrives at a fully closed or fully open state. These limit switches indicate the current position of the motor shaft; this information is provided to human operators at mission control so that the operators are continually aware of the current position of every motorized valve in the system. Accurate tracking of the states of each of the launch control devices is critical for safety. In addition to operating motorized valves, the Relay board can also apply an electric current to an ignition coil to ignite the engine. The typical ignition current is approximately 5 A. The Relay board is equipped with a current-sense amplifier which continually measures the current sunk through whatever actuator or coil is connected. These measurements are reported to the human operators at mission control so that the operators are aware of the current flowing to the motors and ignition coils. Thus, if any of these electrical devices are malfunctioning, the human operators can easily identify the faulty component and take appropriate action.

Relay board uses a pair of relays to control actuation direction and power to the actuator independently. This requires two actions to be taken in order to actuate a valve or fire an ignition coil (where the coil is wired to the normally open contacts of the direction relay).

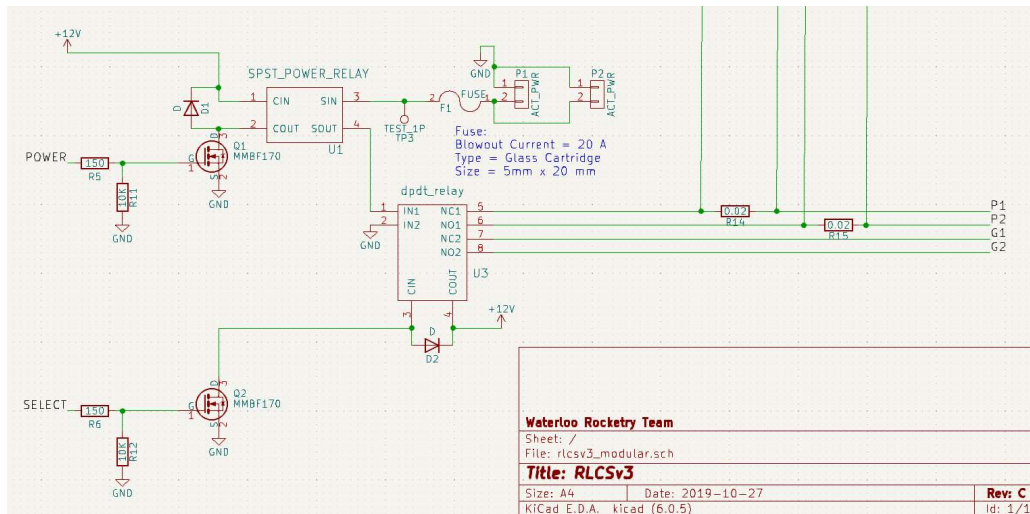


Fig. 133 Relay board actuator control circuitry

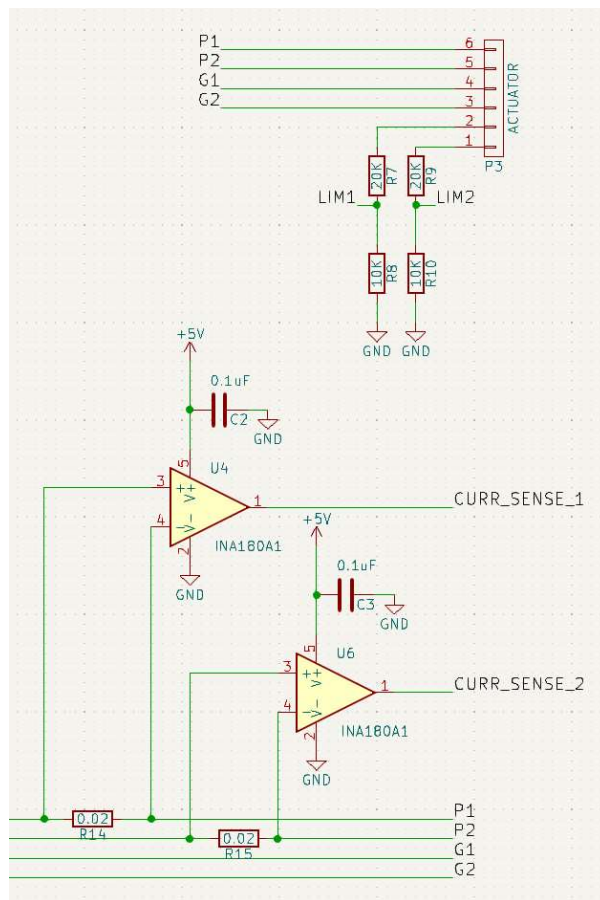


Fig. 134 Relay board actuator connector and current sensing schematic

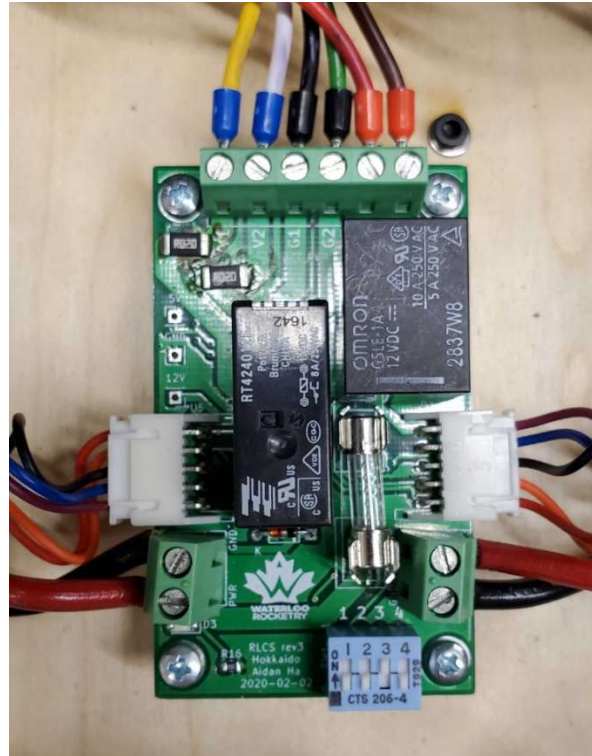


Fig. 135 I2C Relay board

The I2C Pancake board is designed to interface with the ground sensors during fill operations. I2C Pancake is equipped with three strain gauge and two pressure transducer interfaces. It has on-board instrumentation amplifiers which are used to read the analog measurements from each of the strain gauge sensors connected to the board. The strain gauges are load cells which can measure the mass of the rocket in order to determine the amount of N2O in the oxidizer tank. The pressure transducer ports are connected to gas pressure sensors attached to the filling lines which measure the pressure of gasses in the lines. The results of these measurements are sent using the daisy chained I2C bus to the Arduino in the Towerside box. The data is then relayed to Clientside over the radio link so that human operators can track the state of the fill plumbing.

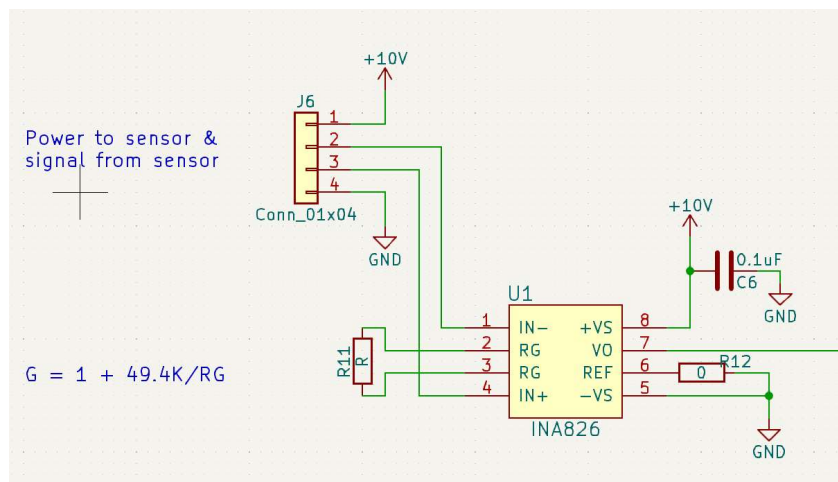


Fig. 136 I2C Pancake strain gauge amplifier schematic

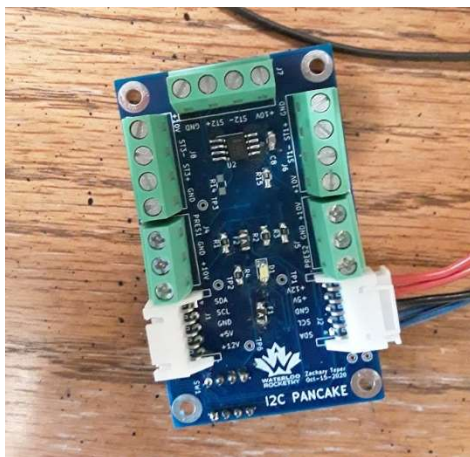


Fig. 137 I2C Pancake board

6. Data Acquisition System

The goal of the Data Acquisition (DAQ) system is to provide a more convenient and accurate method of obtaining ground sensor data during fill and launch operations. It will also allow data to be plotted and logged in real time on a computer in a more readable manner than the LCD on Clientside. This is made possible this year due to the recent ruggedization and remote capabilities of our static fire data acquisition system, which will be used effectively unchanged at competition. The system is built into a weather- and shock-proof Pelican Air case. A computer connected to the case over USB relays the sensor data over a pair of Ubiquiti Litebeam AC long range ethernet antennas to a second computer at mission control, which plots and logs the data in real time.

This new iteration of the DAQ system has been fully qualified at both cold flows and parachute tests and will be used at the upcoming static fire. So far, no reliability or range issues have been observed with the pair of Ubiquiti Litebeam AC antennas used, and preliminary range testing suggests that they will have more than the required 3000 ft of range required for competition. However, should this not be the case, RLCS is also fully capable of handling the entire required ground data acquisition on its own. Range verification will be conducted at competition to determine which system will handle the ground sensor data; whichever proves more reliable will be used.

The heart of the DAQ system is a National Instruments USB-6218 Multifunction I/O Device (the “NI module”). It supports up to 32 analog input channels with a sensitivity down to 4.8 μV . This makes it suitable for both 0-5 V / 4-20 mA sensors and mV/V strain gauges such as load cells with no external amplification. Sensors are wired into the NI module through a set of DIN rail terminal blocks for ease and reliability of configuration. Sensors with a 4-20 mA signal are supported by placing a 100-ohm resistor between the negative sensor wire and ground, and measuring the voltage drop across the resistor which will vary linearly with the current. Thermistors are also supported with the same internal resistor configuration forming a voltage divider with the external thermistor.



Fig. 138 Connector ports on DAQ system

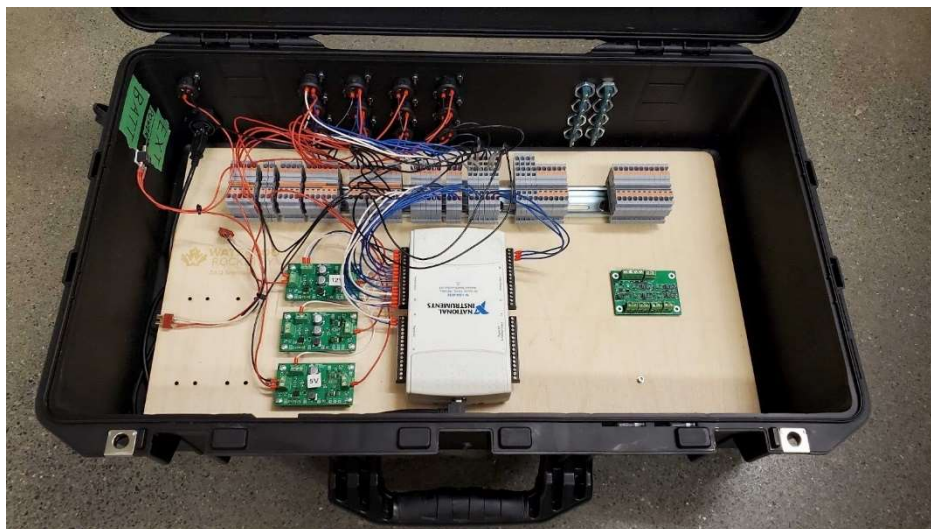


Fig. 139 Internals of DAQ system

Once the sensor voltages are collected by the NI module, they are passed over USB to a connected computer. This computer then relays them in real time over an ethernet link to a computer at mission control, which plots and logs the data. Since ethernet cables have a maximum length of only 100 m, the Ubiquiti Litebeam AC antennas were selected to act as a transparent link which can span the distance between the launch tower and mission control.

Power to the sensors is delivered by a DAQ Power Board, a custom PCB designed for ultra-low output noise. This is achieved by a dual step-down design where a high-efficiency buck converter regulates the input voltage down to 2 V above the desired output voltage and the final regulation is achieved by a pair of less efficient but ultra-low-noise linear dropout regulators (LDOs). Three copies of this board power the +5 V, +10 V, and +12 V power rails within the DAQ system. The output noise of the board was too low to be measured accurately but is at most 10 μ V peak to peak.

DAQ Power board was designed for 1 A output at a configurable voltage between 5 and 15 V. To achieve this a 1 A buck converter is followed by two 500 mA LDOs which share the output load. Additionally, pairing up the LDOs reduces the output noise by a factor of 1.4. To allow optimal efficiency of the LDOs, the feedback pin of the buck converter is actively controlled by one of the LDOs. This lets the LDO choose its own input voltage optimally and eliminates a secondary manual configuration of the boost converter.

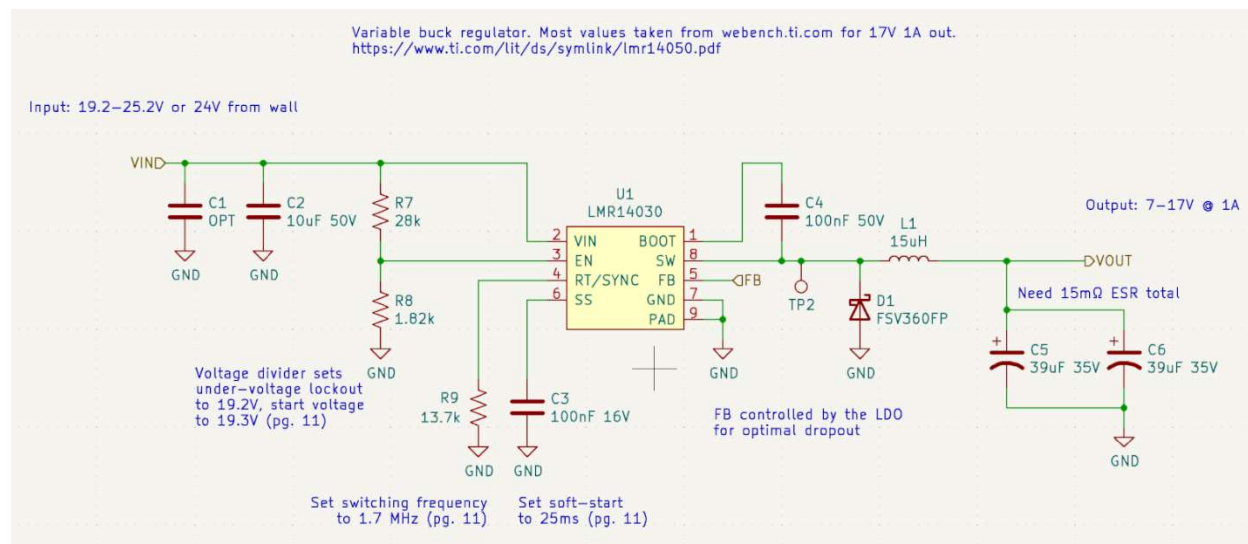


Fig. 140 Schematic of the buck regulator on DAQ Power board



Fig. 142 ST PATS local GPS and compass test

The microcontroller used in ST PATS is Adafruit Feather M0 Adalogger. It has great support for all the other Adafruit components used on board. Additionally, the board supports multiple hardware serial connections, making it easy to communicate with USB, GPS, and radio telemetry. For more, logs can be saved to an external storage via on-board SD card slot. The Adalogger has a built-in battery regulator and charger, providing a safe way to use and charge LiPo batteries.

As known by most, Earth is not flat. Therefore, the direction of the rocket cannot be calculated with 2D Euclidean geometry directly. To overcome this, the program projects the rocket coordinates from latitude and longitude into polar coordinates using azimuthal projection, centered at the current location. The direction can then be calculated by subtracting the compass heading from the polar coordinate heading.

E. Payload

Galactic cosmic rays (GCRs) are high-energy subatomic particles that post significant adverse effects to human health and flight electronics, particularly in space [18]. Materials used in industry such as lead, steel, and concrete offer satisfactory GCR shielding for space missions, albeit with high mass costs. Creating adequate, lightweight GCR shielding is a prevalent challenge in the aerospace industry as permanent, manned missions beyond Low-Earth Orbit are continued to be sought after.

The payload will analyze GCR shielding materials for aerospace applications such as protective coatings for electronics. Boron-nitride nanotube (BNNT) composites have significant potential due to their gamma and neutron shielding characteristics [19]. Research has shown that boron nitride incorporated into polymer composites offer improved yield strength, bulk modulus, and toughness when compared to neat polymers [20]. Metal oxide impregnated acrylic coatings also have potential as a lightweight, low-cost alternative for shielding electronics from GCRs while providing protection from moisture, dust, and sudden temperature changes [21]. Sample specimens of each type of material are shown in the figure below.

The objective of this payload is to incorporate samples of both materials and radiation detectors into the rocket to measure their GCR shielding efficacy during flight. This experiment will seek to experimentally validate theoretical modeling of these coatings and investigate the radiation shielding properties of the coatings. GCR shielding efficacy will be evaluated by measuring radiation levels inside the rocket with silicon photomultiplier (SiPM) -scintillator pairs. Unshielded detectors will be implemented as experimental controls alongside the shielded detectors. A general system architecture of the payload is illustrated in the block diagram in Figure #.

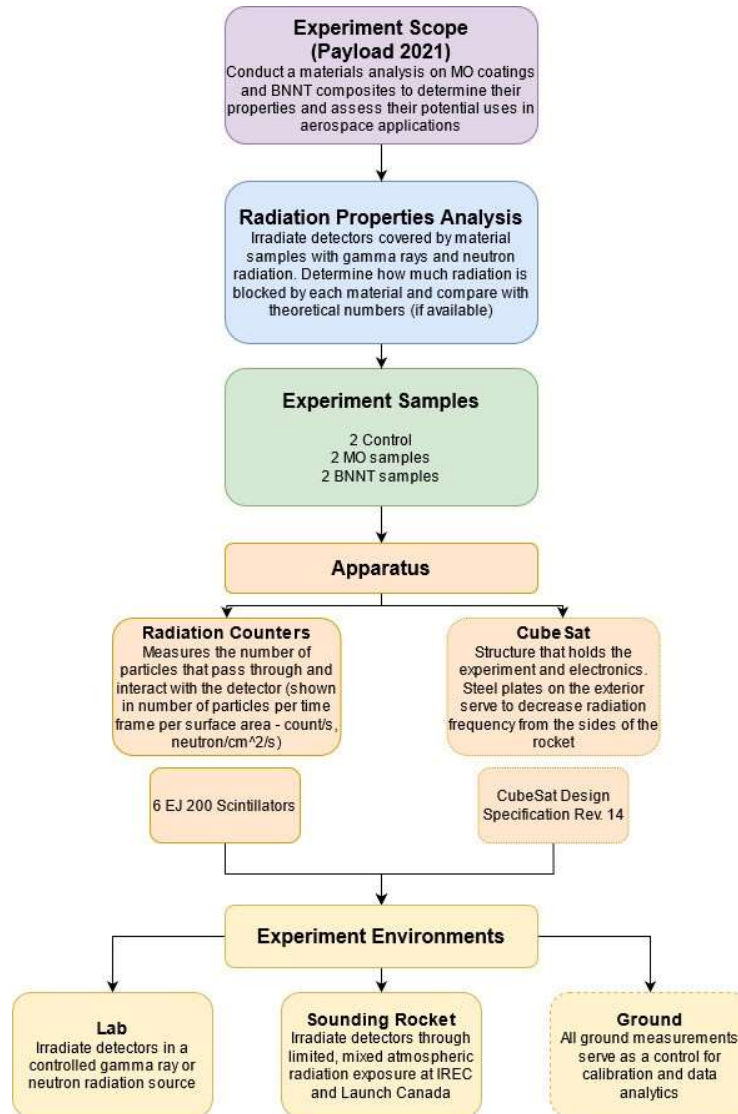


Fig. 143 System overview of the payload including objectives, apparatus and operating environments

To calibrate the performance of the radiation detection hardware and also gain additional data on the material samples, radiation tests will be conducted through a partner lab at the University of Waterloo once all PCBs have been assembled and tested in ambient environments. These lab tests will use a 0.2-0.5 mCu sample of Ba133 that emits gamma radiation at 100-300 keV.

1. Electrical Hardware

As visualized in the figure below, the electronics will be controlled by a main board, which will be armed via RocketCAN at launch. Two payload detector boards will be connected to the main board via an internal payload CANBus. The Minisensor board will measure interior conditions of the CubeSat to improve the context analysis of experimental data.

Payload Electronics System

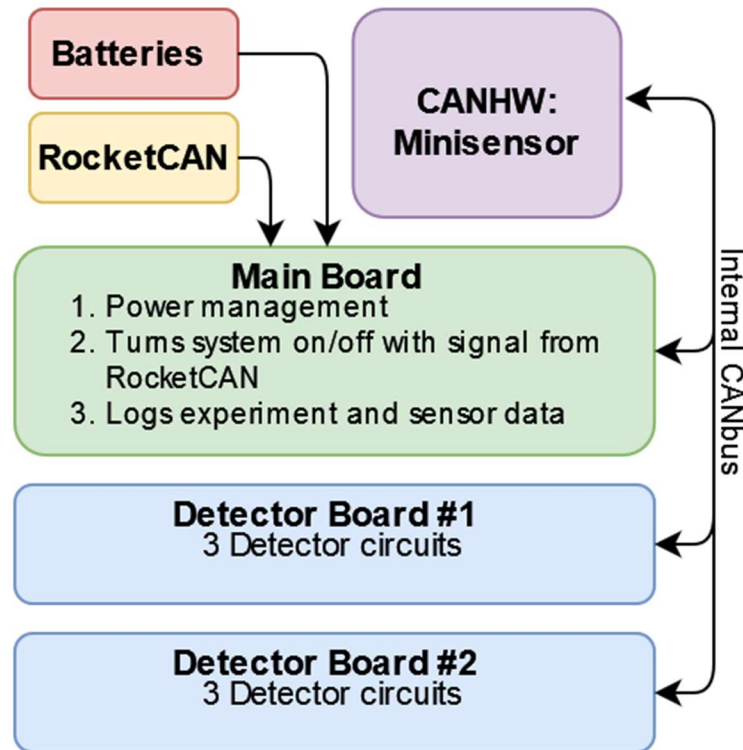


Fig. 144 Payload electrical system architecture

In order to detect the radiation spikes using the photomultiplier-scintillator pairs, the “detector circuit” located on the detector board was designed and tested in parallel, through inspiration (but heavily modified) from the circuit in [22]. The detector circuit consists of several stages: transimpedance amplifier, filtration, second-stage amplification, peak detector and comparator. The transimpedance amplifier converts and amplifies the current signal received from the SiPM into a voltage signal. The peak detector extends the length of the signal so the PIC18F26K83 on the detector board has more time to take an ADC sample. The comparator goes high whenever the voltage level of the second stage amplification goes above a set level. This triggers an interrupt, which informs the MCU to take several ADC samples from the output of the peak detector. This combination of comparator and ADC values will allow for some noise-induced false pulses to be filtered out during post-processing, as well as the separation of two spikes that may occur within the same peak detector pulse. The data from the ADC, along with a number representing which detector was triggered will be sent to the main board via the internal CANBus.

To keep the noise-sensitive detector circuit isolated from noise, the power supplied ended up being quite complicated. First of all, the SiPMs need a +36V power line to bias the devices. That was made using a +37V buck regulator on the main board, and a +36V linear regulator on the detector boards to reduce noise. Furthermore, the MCUs required a 5V line, and so did the detector circuit. In order to keep noise off the detector electronics, the MCUs operate on a 5.3V, and a linear regulator on the detector circuits cleans the power supply and brings it down to 4.7V, which is used to power the amplifiers. Finally, the SD card operates off 3V3, which was generated using another linear regulator. . In order to communicate with the SD card using SPI, a level shifter was added between the SD card and the MCU.

2. Electrical Hardware Testing

The signal conditioning circuit used to detect the radiation underwent several stages of development and testing. It was first prototyped on a breadboard, which was deemed to be a mistake because the wires would come loose, and capacitance on the breadboard pins made the entire system behave unpredictably. Finally, a prototype PCB was designed, built and tested, seen in the figure below. The prototype board featured a larger board and a smaller, detachable board. The larger board had the power supplies, microSD card and PIC18F26K83, so further system

functionality could be tested before the flight boards were made. Several versions of the smaller boards were made with different op-amp layouts so the performance of different op-amps could be tested.

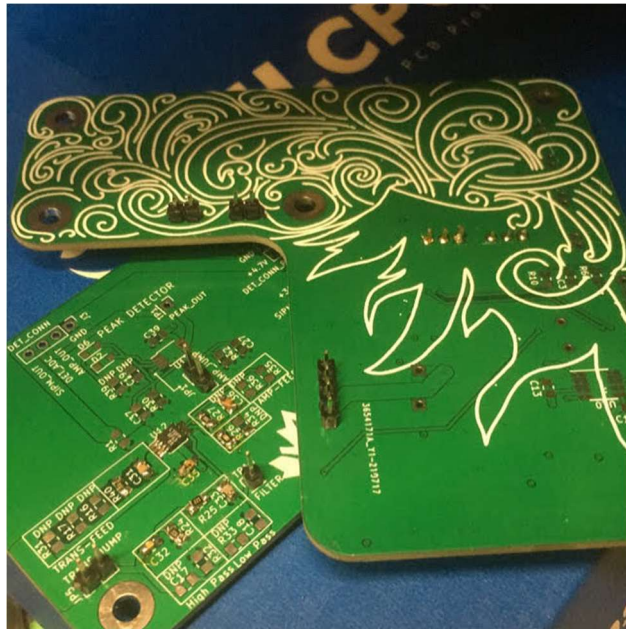


Fig. 145 Payload detector circuit prototype PCB

The figure below shows the amplified signal in yellow, and the filtered and peak detected signal in green from the prototype board.

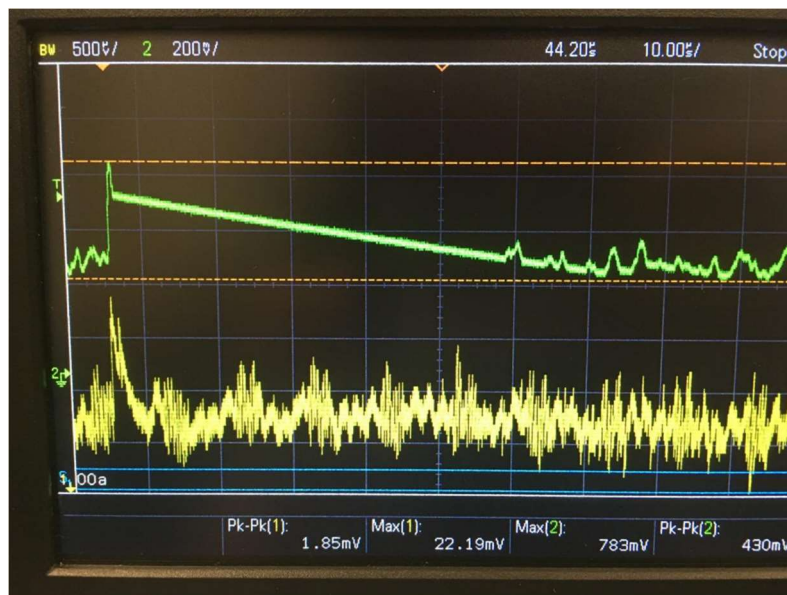


Fig. 146 Yellow signal: amplified output from SiPM, Green signal: Output from peak detector

The testing on the prototype board included observing the radiation spikes on an oscilloscope, testing the filtering and peak detection capabilities and efficiencies of the detector circuits, making sure the SiPM bias voltage ripple was at an adequate level as to not interfere or surpass the radiation peak signals, and ensuring that relevant data of the radiation spikes was being properly logged onto the microSD card. The three smaller circuit boards were individually tested, and one was selected for use in the final design based on the performance of the chosen op-amp and op-amp configuration, which varied on each of the three circuits.

After the power board and detection circuit board PCBs were developed based on the testing results of the prototype board, additional hardware testing was required. Firstly, the software for the microcontroller units on the power board was tested to ensure proper communication to the rocket's CANBus, as well as the payload's internal CANBus to ensure proper logging of data from the detector board to the microSD card on the power board. In addition, the power supplies, such as the buck regulator, boost regulator, low-dropout regulators, and the MOSFET used as a power switch to connect and disconnect power to the detection circuit board were all tested and observed to ensure proper voltage levels and low voltage ripple using a voltmeter and oscilloscope respectively. These two parameters are crucial to the proper operation of the silicon photomultipliers and the ability to isolate the bias voltage noise from radiation spikes during the radiation peak detection stage of the circuit.

In the flight set-up the detector boards will detect radiation pulses and send data packages with the magnitude and a number representing which detector measured the pulse to the main board to be logged on an SD card. The main board is still undergoing final qualification testing, but so far, all power supplies are functional, and CANBus messages have been transmitted and received. For the final validation testing of the payload hardware, the power board, detection board, batteries, and silicon photomultipliers will be fully assembled, connected, and tested to ensure that the entire system is operating together as expected with full functionalities.

3. CubeSat Design

The payload will be housed within a student designed 3U CubeSat, in accordance with the CubeSat Design Specification Rev. 14; the CubeSat will not be deployed during flight [23].

The CubeSat design can be broken up into three major components: structure, Systems Module, and Scintillator Module. The structure is the skeleton of the CubeSat and as a free-standing structure, it does not require any internal modules to support it. This eases assembly as internal modules can be easily slid out from the side to be serviced when necessary. The Systems Module houses the power management hardware for the payload: this includes the Papa board and CANHW daughter boards all on a PCB stack, and battery mount. The Scintillator Module carries the scintillator detectors, material samples and detection circuitry located on Mama board. Assembly drawings for these modules are included in the Appendix G Engineering Drawings.

Ansys FEA verified preliminary flight worthiness of an early CubeSat design iteration. The three internal modules of the CubeSat were approximated with point masses and fixed moments of inertia. The point masses were set through a weight budget and moments of inertia were calculated assuming a rectangular prism of constant density occupying each of the three modules.

Static structural analysis verified structural integrity during the boost phase of rocket flight. OpenRocket sims had predicted a maximum acceleration during boost of 7.1G, and previous accelerometer data during flight of UXO measured 10G. Thus, static structural analysis was conducted with a 15G axial acceleration, the results shown in the figure below. Maximum von Mises equivalent stress is well below yield of aluminum and thus the design is expected to withstand rocket boost.

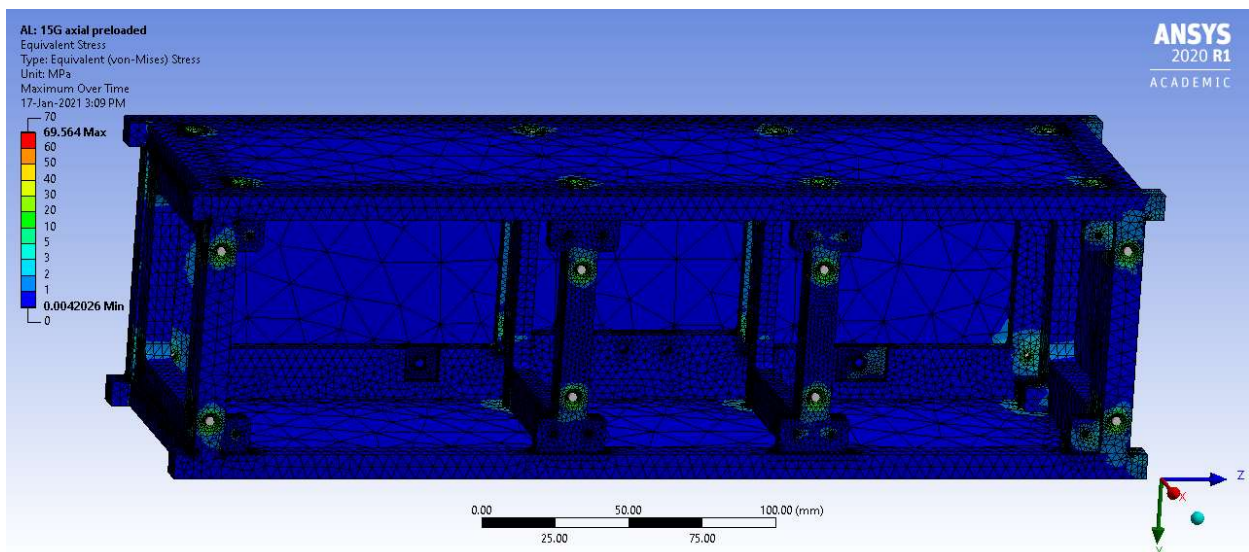


Fig. 147 Von-Mises stress plot of CubeSat under 15G acceleration in Z-axis

Modal analysis was conducted to investigate dynamic behavior of the CubeSat to detect risks of dynamic coupling with the rocket. The results of the modal analysis are shown in the figure below. The modal frequencies of CubeSats should be greater than 100 Hz [x21, x22]. This decouples the dynamic behavior of the CubeSat from that of the rocket and prevents vibratory resonance. The first three modal frequencies at 718 Hz, 833 Hz, and 834 Hz contribute negligibly to the dynamic behavior of the system because of their low ratios of effective mass to total mass. The modes at 886 Hz, 981 Hz, and 1025 Hz are the first major nodes with significant effective mass participation factors. All 6 of these modes have frequencies significantly greater than 100 Hz, thus the structure is predicted to be dynamically sound.

Ratio of Effective Mass to Total Mass

Mode	Frequency [Hz]	X Direction	Y Direction	Z Direction	Rotation X	Rotation Y	Rotation Z
1	718.36	4.6519e-002	5.2206e-005	2.1221e-004	1.7483e-006	9.8817e-004	1.5306e-003
2	833.26	8.2769e-008	8.3179e-002	2.9197e-005	6.0052e-003	2.1e-006	2.4345e-003
3	836.77	1.1713e-003	5.3348e-003	1.7189e-003	3.0078e-004	3.7391e-004	1.6153e-004
4	885.66	0.76722	2.7553e-004	5.6106e-002	3.5954e-005	0.21115	5.0235e-005
5	981.35	1.5871e-003	0.70445	4.2903e-003	0.14802	6.0236e-004	9.1032e-002
6	1025.1	4.2986e-002	4.4586e-003	0.90445	9.2256e-004	2.2898e-002	1.9574e-004
7	1189.8	4.7506e-003	1.1178e-003	1.728e-004	9.596e-004	1.1011e-003	5.1862e-003
8	1265.6	4.2297e-005	3.3446e-004	6.3726e-004	4.9138e-003	4.5174e-005	4.3256e-003
9	1279.	1.5744e-005	7.1207e-004	3.5216e-004	1.4762e-002	4.8509e-007	1.5827e-002
10	1297.3	7.2059e-011	8.492e-004	3.9791e-005	2.3033e-005	1.419e-006	6.164e-003
11	1309.5	3.9163e-006	6.0898e-004	4.2787e-005	6.3693e-005	1.3757e-005	5.0401e-003
12	1547.8	3.1084e-003	1.2697e-004	1.578e-004	8.285e-005	3.5047e-002	6.1222e-005
13	1592.9	1.9785e-004	1.3328e-003	8.6665e-005	1.5026e-003	9.7709e-003	1.09e-002
14	1634.9	5.6124e-005	2.8811e-002	5.2433e-005	6.1316e-002	8.2343e-004	0.56778
15	1709.9	4.7587e-007	1.618e-003	8.0625e-006	8.4359e-003	1.7722e-003	9.2866e-003
16	1735.5	9.6935e-004	1.7186e-004	2.9668e-003	1.5551e-003	1.7934e-003	1.2027e-003
17	1761.5	5.5056e-005	9.2562e-003	1.2207e-005	0.10948	8.6044e-004	3.5591e-002
18	1848.	1.1969e-002	2.9453e-007	3.6155e-003	2.1992e-004	0.41079	6.1355e-009
19	1904.4	7.8048e-005	2.3456e-004	2.396e-005	2.1951e-002	4.5152e-003	2.1704e-003
20	1968.6	1.2514e-005	6.4855e-003	2.7663e-005	0.18577	9.6036e-004	3.0846e-002
21	1992.7	1.9413e-007	3.6956e-003	6.6851e-006	2.4832e-002	2.1096e-004	1.9472e-002
22	2263.7	3.9508e-004	1.6002e-004	6.332e-005	2.1376e-005	3.5269e-005	3.7428e-004
23	2293.7	2.433e-004	1.1323e-005	6.15e-007	2.8592e-003	2.534e-005	7.7648e-004
24	2301.5	1.7203e-006	4.6907e-004	2.3428e-005	7.0444e-006	8.433e-004	1.3994e-003
25	2318.	1.3775e-005	6.2842e-003	2.1154e-006	1.1745e-002	6.3692e-005	2.7802e-004
Sum		0.8814	0.86003	0.9751	0.6058	0.70469	0.81209

Figure # Modal analysis results of CubeSat

Further analysis with the latest structure was not conducted due to time and resource limitations. The primary difference is the deletion of one X-Y brace to increase internal volume for the experiment modules. The change in structure was not deemed a significant risk to the static and dynamic behaviour of the CubeSat because the factor of safety during boost acceleration was already significant, and because the first significant modal frequency was over 7 times that of the minimum recommended 100 Hz, respectively.

The scintillators will be housed in 3D printed enclosures, that will be printed in black with 100% infill to block light, and then coated with a layer of black enamel spray paint. The material samples will be mounted on one end of the scintillators, and the SiPMs will be mounted on the other as seen in the figure below. There will be two layers of scintillators, each with one BNNT sample, one metal oxide sample, and one control. To help shield radiation in directions not covered by the material samples, some of the side panels of the CubeSat were manufactured in steel. To prevent rust, the CubeSat cover panels were powder coated flat black by our sponsor, Demtool, while the structure was anodized gold by our sponsor Waterloo Electroplating & Metal Finishing. These finishes were chosen based on the condition of cost and the fact that our CubeSat would not experience outgassing during flight or operation due to the rocket's projected altitude.



Fig. 148 Scintillators and enclosures (left) SiPMs (right)

The final CubeSat design was manufactured by CNC and assembled as shown in the figure below. Final qualification of the design and tolerances have been conducted. In Fig. 149 below, the CubeSat is displayed with the 3D printed enclosure for the scintillators



Fig. 149 Assembled CubeSat displayed along with scintillator enclosure

4. Material Samples

BNNT-TPU samples were prepared and packaged at the National Research Council facility in Ottawa. Raw BNNT was dispersed in methanol, before being added to a solution of TPU in acetone. The resulting TPU coated BNNT was filtered in a process adjacent to papermaking to form a sheet. The sheet was cut, and the smaller

segments were stacked and hot pressed into one billet to form the final sample as seen in the figure below. The final material is similar to paper with a web of TPU-coated BNNT forming the structure. For the higher BNNT sample, there is no matrix of TPU, rather there is void space between the BNNT fibers.



Fig. 150 BNNT TPU sheet cut and pressed into a final sample

Metal oxide samples were prepared and packaged in-house in Waterloo. Raw metal oxide powder acquired from Ereztech LLC was dispersed in MG Chemicals 419D conformal coating before being mechanically agitated to create a homogenous mixture. Parchment paper strips were dipped and coated into the mixture before being hung up to dry and cure. Thin paper strips about 0.05 mm thick were used as a medium due to their poor abilities to shield radiation in small quantities [24]. The resulting paper-coated samples can be cut to size and assembled within the payload above the detectors.

5. Experiment Simulation

In addition to the physical experiment to be carried out at launch, a software simulation of the experiment is performed prior to the launch. The software simulation serves as a preliminary overview of the dosages of each particle anticipated to be absorbed by the scintillator under different scintillator coatings during the flight. The simulation software is written in C++ and built with the Geant4 platform to allow for tracking simulated subatomic particles in a user-defined geometry [25]. The simulation software operates under a Monte Carlo approach, whereby a set of possible outcome events are recalculated with bounded random numbers as the attribute of each event [26]. The program first defines the environment of the experiment by modeling the CubeSat geometry and materials; then, by generating and tracking a predicted set of subatomic particles based on our projected altitude with random momentum profile in the simulated environment, radiation dosage absorbed by the scintillator can be calculated by accumulating the particle energy level colliding with the scintillator object [27]. This process can then be displayed by a visualization driver, as shown by Fig. 151.



Fig. 151 Placeholder visualization driver

By running the simulation program with input specification matching the approximate flight profile of the payload, a set of dosage data for each scintillator in a set was obtained and shown by **Table K** below. These results will serve as expected output from the payload at the launch to verify the results we obtain from the physical system.

Table 16 Scintillator simulation data

Scintillator	Gamma Radiation Dose Detected
Lower - Paper	0.02533 picoSV
Lower - MO	0 picoSV
Lower - BNNT	0 picoSV
Upper - Paper	12.8302 picoSV
Upper - MO	12.4856 picoSV
Upper - BNNT	12.8018 picoSV

F. Mechanical Group Support Equipment

6. Launch Tower

The launch tower is a modular structure consisting of five sections of steel lattice mounted on a base of square steel tubing. When fully erected at an angle of 5° from vertical, the tower reaches a total height of 39 ft. The launch tower provides support for the 1515 aluminum extrusion launch rail, which guides the rocket during the first few seconds of unstable flight. The tower also acts as a mounting structure for other GSE subsystems, including RLCS and DAQ components.

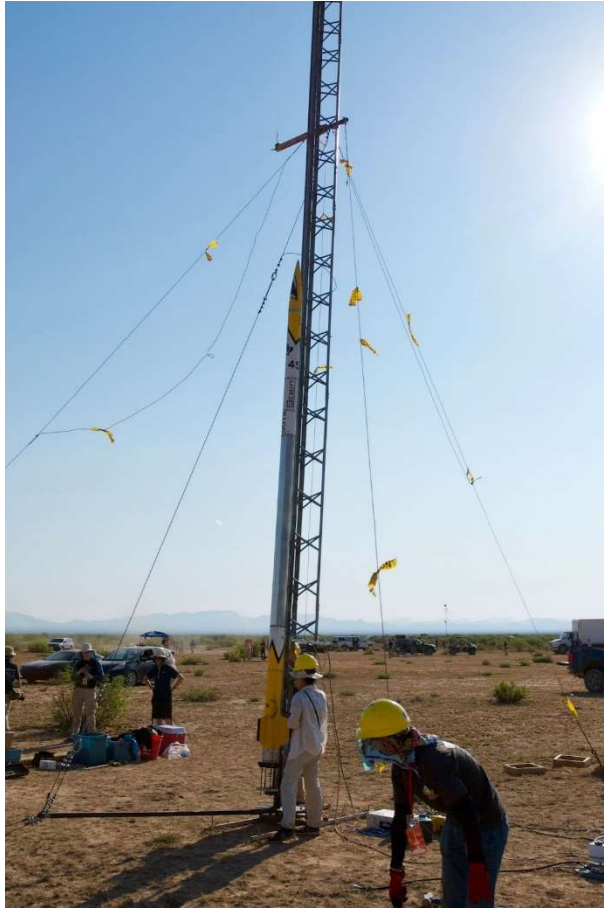


Fig. 152 Waterloo Rocketry launch tower with 2019 rocket Shark of the Sky

7. Tower Stability

It is critical both for the safety of the rocket and personnel that the tower cannot tip over. To prevent this the base of the tower is secured by staking rebar through its 4 steel legs and into the ground. To protect against lateral loads such as wind, there are three guywires which attach midway up the launch tower and are mounted to the ground using helical ground anchors. Each guywire is tensioned using a turnbuckle to ensure the lines are always properly tensioned.

8. Tower Raising

In order to raise the launch tower to a vertical position, a gin pole assembly is used as shown in the figure below. The gin pole is a steel arm that is mounted to the base of the tower, perpendicular to the tower axis. A steel cable runs from the end of the gin pole to a cross member midway up the tower, and a separate steel cable runs from the end of the gin pole to a motorized winch away from the tower. When the winch is powered, force is transmitted through tension in the steel cables to the cross member on the tower; this results in a moment of the tower base, causing it to rotate upwards. As the tower rises, operators keep tension on the guywires to ensure the tower remains stable. Once upright, the three guy-wires are secured to ensure that any wind or other forces do not cause it to tip.



Fig. 153 Raising the launch tower to a vertical position

9. Fill Disconnect

The launch tower additionally provides mounting features for the remote-disconnect mechanism. Due to the nature of hybrid fill operations, it is necessary that a mechanism exists to disconnect the fill line from the engine prior to launch. In addition, the rocket uses pneumatics to actuate the vent and injector valve. The rocket has sufficient compressed air storage onboard for the expected operations, however pneumatic systems are prone to small leaks, so to ensure sufficient air pressure during long delays on the pad, the compressed air supply is disconnected using the same mechanism right before launch. Disconnect is accomplished using a spring-loaded system secured with quick connect fittings. The female quick connect fittings, attached to the end of the fill hose, is mounted to an aluminum arm that pivots around a bracket mounted to the tower; the other end of this arm is connected to two tension springs. During fill, the female fitting is connected to the male quick connect fitting on the rocket. The release mechanism consists of a linear actuator controlled by RLCS, a bracket inserted between the male and female quick connect fittings, and a mounting structure to secure the linear actuator to the arm. Once fill has concluded, the linear actuator retracts to pull the bracket, which also pulls the collar on the female fittings, allowing the fittings to disconnect. Pulled by the tension springs, the fill arm pivots away from the rocket and pulls the fill hoses from the fill ports.

10. Ground Plumbing

The ground plumbing is responsible for filling the rocket with oxidizer and providing vent/abort pathways for safing the fill cylinders and isolating them from the rocket when necessary. As the entire plumbing setup is in contact with nitrous oxide at some point throughout oxidizer fill, it is sanitized as per Part Sanitation for Oxidizer Service. All COTS plumbing components used are rated to at least the maximum expected operating pressure, and any SRAD plumbing is rated and tested as per the DTEG requirements for SRAD pressure vessels and plumbing. The plumbing, shown in the figure below, is arranged to prevent need of any personnel coming in proximity to the engine once fill of the rocket commences, for safety reasons; all the high-risk actuations are done using motorized valves controlled by the Control Operator from mission control. Refer to A Propulsion for the plumbing layout of the flight vehicle.

Two N_2O supply cylinders are used to ensure enough propellant is available, and to prevent time-costly swaps of cylinders in the event of a temporary vent or abort. The cylinders are isolated using check valves to prevent contamination from backflow, and the ground plumbing block's connection to the rocket is isolated with a check valve to prevent backflow. At no point in time does pressurized oxidizer get trapped in a section of the plumbing that requires an operator to approach the plumbing and manually loosen a fitting — there is a safe vent pathway for each section and subsection of plumbing at any point during the rocket's fill and launch operations. Even if any motorized valves fail and/or actuators lose connection to mission control, there is no need for any operators to get closer than 100 ft to the rocket and plumbing after rocket fill begins.

Throughout the rocket's fill operations, pressure and temperature transducer data is relayed to mission control for review by the launch operations team. Data from pressure transducers is used to confirm pressurization, leaks, and safing/venting of plumbing sections, and is monitored by a dedicated operator at mission control, who is trained in data acquisition and operation. Any leaks in plumbing are addressed per the operations procedure, and as directed by the Operations Lead.

When the plumbing is first pressurized, the "fill block" is leak-tested in isolation before the oxidizer tank fill begins. That is, GV-1 and GV-2 remain closed until the block is shown to not leak, and then GV-1 is opened with MV-1 closed and operators retreat to mission control. PI-1, an analog pressure gauge, is used to corroborate pressure readings from PT-1 (a pressure transducer) and serves as a method of evaluating system pressurization independently of the electrical system for redundancy purposes. A description of each plumbing component can be found in the table below.

Table 17 Description of labelled components from P&ID (Fig. 154)

Component	Description
SC-1, SC-2	Nitrous oxide supply cylinders
CV-1, CV-2	Supply cylinder shutoff valves
CK-1, CK-2	Supply cylinder backflow prevention check valves
CK-3	Rocket fill check valve
PT-1	Fill block pressure transducer
PI-1	Fill block analog pressure gauge
MV-1	Motorized rocket fill valve
GV-1	Manual series fill valve
GV-2	Manual parallel fill valve
GV-3	Manual rope-actuated (100 ft rope length) line vent valve

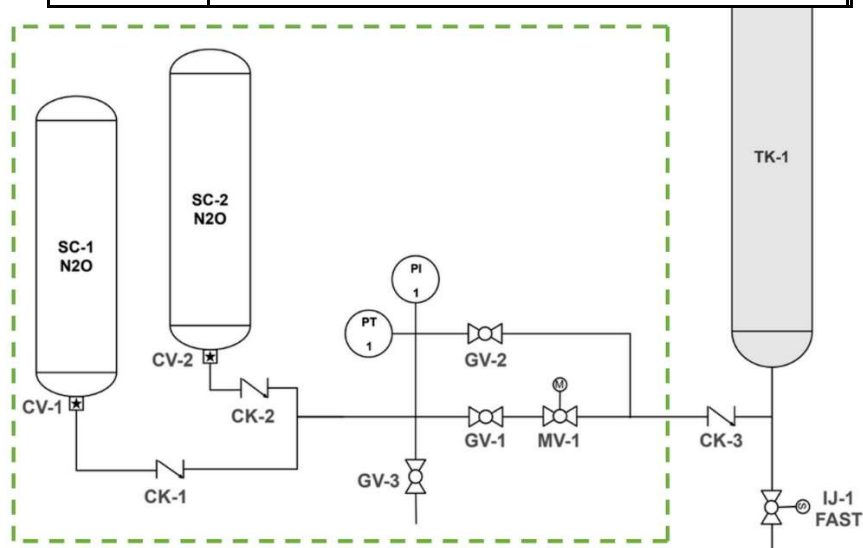


Fig. 154 P&ID showing ground side plumbing (confined in dashed lines). Ground plumbing is isolated from the rocket using fill disconnect prior to launch.

IV. Mission Concept of Operations Overview

G. Flight Plan

The mission concept of operations (CONOPS) of Kraken of the Sky is made up of 9 phases, beginning with pre-launch operations and ending with vehicle recovery. The main stages are shown in the following figure, with a more in-depth chain of events below.

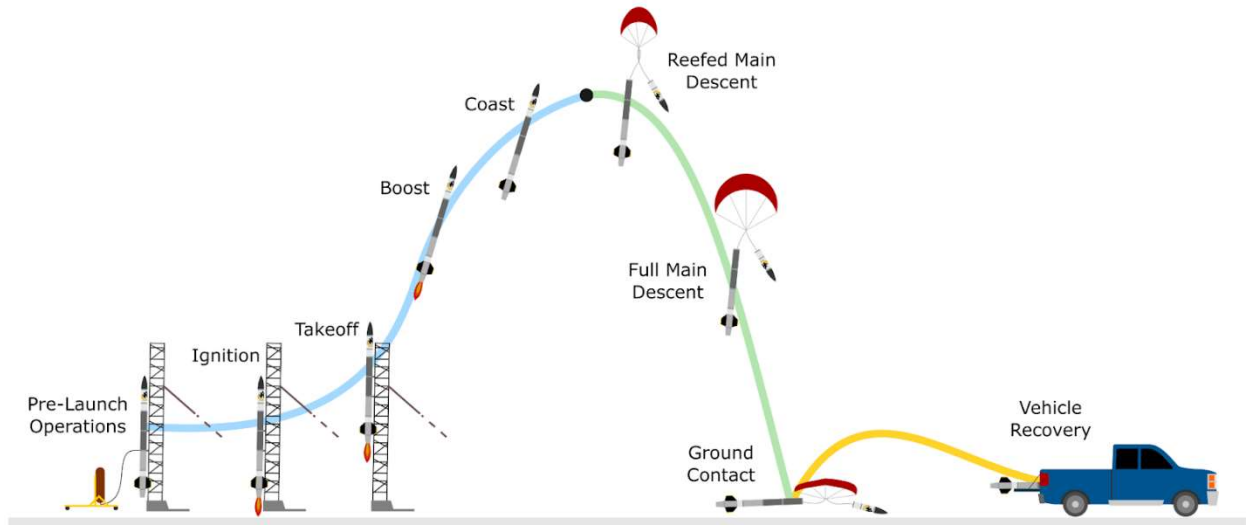


Fig. 155 KotS Nominal CONOPS

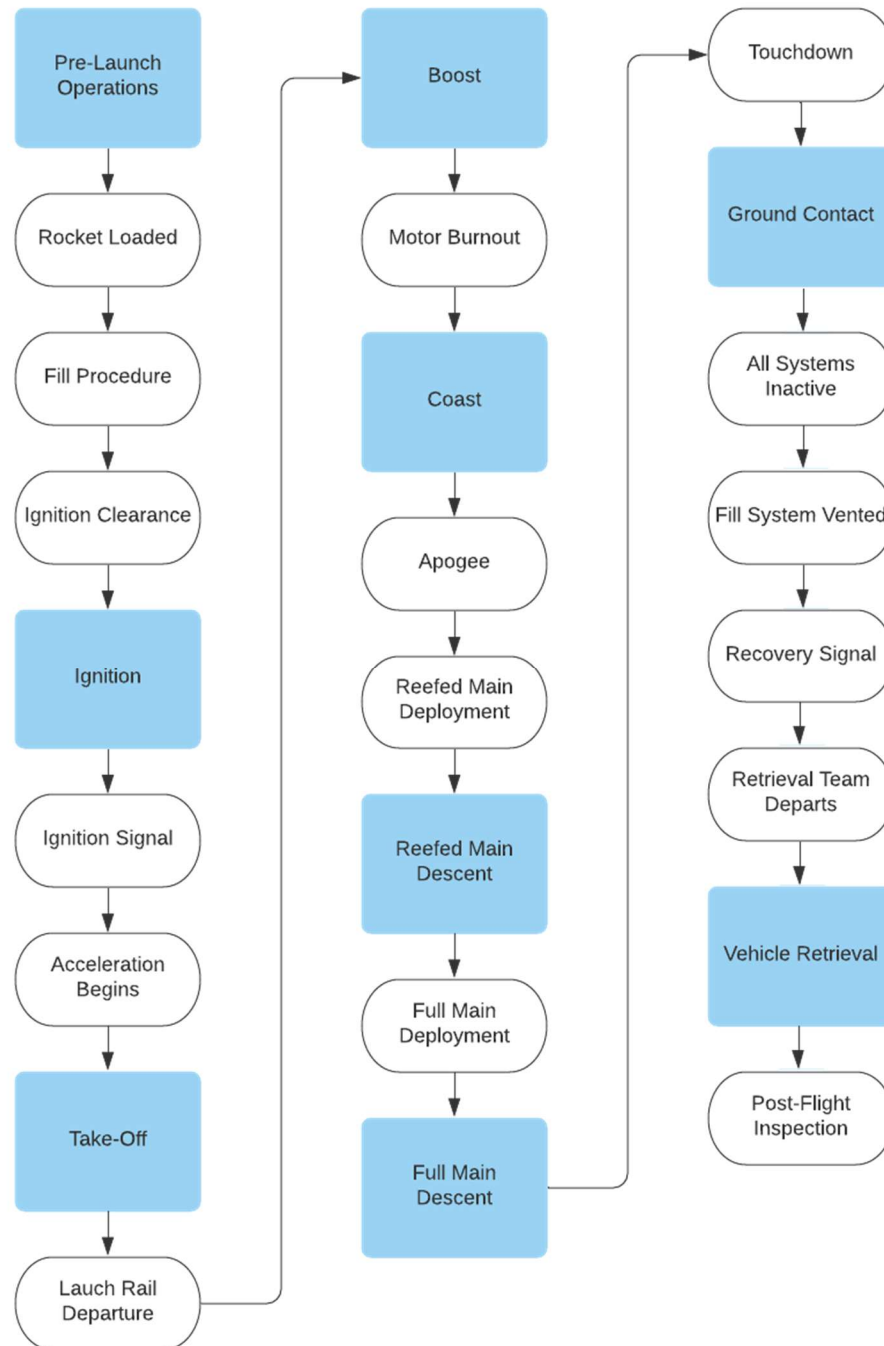


Fig. 156 CONOPS Chain of Events

A. Pre-launch Operations

Pre-launch operations begin when the rocket and launch tower have been fully assembled. KotS then departs for the launch site and is loaded onto the launch rail upon arrival. The tower is then raised. All team members return to base apart from the primary and secondary operators, as outlined in the fill procedure, who don the necessary personal protective equipment. The operators perform the required system verifications and arm the recovery system, then retreat to the minimum safe distance before the remote fill procedure commences. Throughout fill, the remote launch control system (RLCS) and the data acquisition system (DAQ) provide feedback on the rocket mass and pressures from the fill lines and oxidizer tank. The

fill arm is disconnected when fill is complete, which is indicated by the rocket reaching a predetermined mass and oxidizer tank pressure. The first stage ends when clearance to begin ignition is received.

B. Ignition

The ignition phase begins when the signal is sent to the primary ignition puck. When the puck ignites successfully, the injector valve is opened, and the propellant ignites. The payload, recovery and avionics systems continue to acquire data. The ignition phase ends when KotS begins to accelerate.

C. Take-Off

The take-off phase begins as the rocket accelerates up the launch rail. KotS reaches the end of the rail with a velocity of 92 ft/s. This velocity corresponds to a static stability margin of 1.71 calibers, which is sufficient to keep the rocket stable and on the correct flight path. The recovery system, avionics board and payload experiment will continue to acquire data.

D. Boost

The boost phase begins when the rocket departs the launch rail. The engine will continue to burn for approximately 30 seconds, reaching a maximum velocity of 1,112 ft/s, or Mach 1.04, at an altitude of 22,100 ft. The recovery, avionics and payload systems will continue to acquire data. This phase ends at motor burnout.

E. Coast

The coast phase begins following motor burnout, at which point the engine stops producing thrust and the rocket begins to decelerate. At the time of burnout, the static stability margin is 5.8 calibers. The rocket is predicted to reach an apogee of 25,916 ft after coasting for 13 seconds, approximately 44 seconds after engine ignition. The maximum stability margin reached is 6.62 calibers.

F. Reefed Main Descent

When KotS reaches apogee, the altimeters will detect a decrease in altitude and trigger deployment of the main parachute, which opens initially in a reefed state. This will slow descent to a constant velocity of 113 ft/s. The avionics and payload systems will continue to acquire data, and the propulsion system will remain inactive.

G. Full Main Descent

The altimeters detect that a pre-set altitude of 1,500 ft AGL has been reached and trigger a disreefing event, expanding the main parachute to its full size. This will slow descent to a constant 30 ft/s. The recovery system will track the rocket's position as it descends. The avionics and payload systems will continue acquiring data, and the propulsion system will remain inactive. This phase ends when KotS touches down on the ground.

H. Ground Contact

This phase begins when KotS makes contact with the ground, and the vehicle and parachute come to rest. This action renders all systems inactive, with the exception of the payload and avionics, which will continue to acquire data.

At the launch site, the fill system is safed using RLCS and the primary and secondary operators approach from the minimum safe distance in order to complete the venting procedure. The phase ends when the fill system has been vented, indicated by all sensors in the lines and tanks reading atmospheric pressure.

I. Vehicle Recovery

The vehicle recovery phase begins when a recovery route is planned, and a retrieval team is formed. When the retrieval team has received safety kits and permission to depart, they proceed to the received location. When they arrive at this location, a primary damage inspection is done. If any energetics failed to discharge during the flight, they are safely disarmed by trained personnel. KotS is then returned to mission control for a full post-flight evaluation.

H. Flight Simulations

The team primarily uses OpenRocket, an open-source 6-DOF RK-4 simulator that uses the Extended Barrowman method to calculate the aerodynamic properties of the rocket. The launch rail length is measured from the topmost launch lug. All initial launch conditions are taken at White Sands, NM in June. A custom .rse engine file, generated using Static Fire 4 CC load cell and ox tank mass data, was used in the model to accurately represent the shifting CG

of the engine throughout the burn and the thrust curve. To verify that the off-rail-velocity of 92 ft/s is sufficient to maintain a static stability margin of >1.5 calibers, 5 simulations shown in Table 18 were run with the lowest observed margin at x calibers. Table 19 summarizes key flight parameters. Plots of altitude, stability margin, velocity, and acceleration can be found in Appendix A System Weights, Measures and Performance Data.

Table 18 Stability margin of rocket

Simulation Number	Minimum Stability Margin
1	2.08
2	1.71
3	2.23
4	1.9
5	1.76

Table 19 List of flight characteristics

Flight Characteristic	Value	Unit	Comments
Launch Rail Length	260	in	Measured from Vent Bulkhead
Liftoff Thrust to Weight Ratio	6:1	unitless	Based off SF4 data
Launch Rail Departure Velocity	92	ft/s	
Stability Margin Range	1.71-6.62	cal	
Maximum Velocity	1141	ft/s	
Maximum Acceleration	218	ft/s ²	
Target Apogee	30,000	ft	
Predicted Apogee	25,916	ft	
Dry Mass	105.28	lbm	
Wet Mass	163.28	lbm	NOS + Fuel Grain

Due to the unusually high aspect ratio of KotS, body lifting forces at nonzero angle of attacks must be considered. The extended Barrowman method used by OpenRocket to estimate CP does not consider body lift. In order to mitigate reductions in stability due to body lift, the fins were sized such that the distance between the CG and CP was at least 1.5 calibers and fulfilled the rule of thumb of 10%-20% of total rocket length for high aspect ratio rockets. On KotS, the shortest distance between the CG and CP is 15% total rocket length.

Trajectory analysis was performed using a combination of wind speeds at 7.33 ft/s and 16 ft/s which are at the 25th and 75th percentiles, with wind blowing to the East and West, with the launch rail angled East.

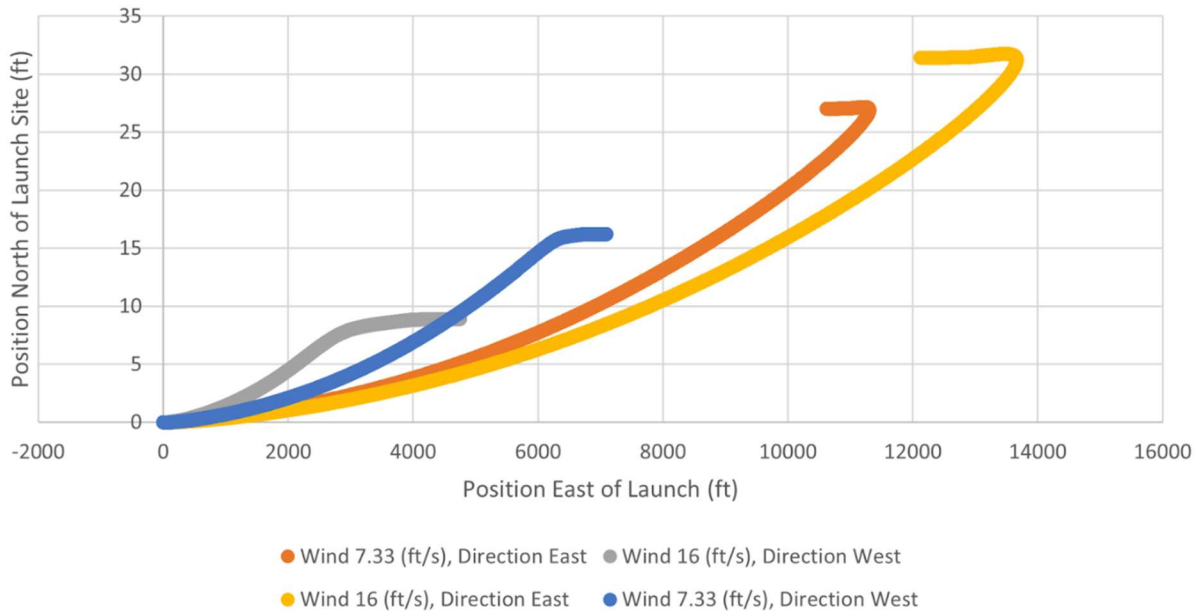


Fig. 157 Trajectory of rocket

V. Conclusion and Lessons Learned

Although the team underwent several large changes over the past design cycle, both with respect to project management and technical projects, the strong focus on iteration and learning from previous designs is still prevalent. It has remained the philosophy of the team to innovate and push forward the design of our launch vehicle and supporting equipment.

A. Technical Lessons Learned

11. Reliability and Simplicity

The underlying principles of every design are to maintain, whenever possible, a system that is both simple and reliable. There are a number of factors that lead into these philosophies; other than being generally good engineering principles, they are even more applicable to a group of students who are attempting to build naturally complex series of integrated systems in a relatively short time frame. Simple systems are easier to design, easier to troubleshoot, and easier to learn - which is especially important on a team with a high turnover rate, as we continue to both gain new members and lose alumni every year. Simplicity is prerequisite to reliability. Canadian teams such as ours often have one launch opportunity a year, at our competition. It is important to design systems that will work in unfamiliar conditions and circumstances, and that we can trust to get us in the air and bring us down safely.

12. Training Procedure

One thing that became evident during the pandemic was the importance of proper training procedures. In order for new members to succeed at the technical challenges presented to them in the process of developing a rocket, it is important to provide them with the technical foundation required to start learning on their own. The team runs regular training sessions for skills such as plumbing sanitation and assembly, PCB design and fabrication, and use of software like GitHub, KiCad and SolidWorks. Providing a simple way for team members to learn these skills has proven to be a great benefit to the team, as the team members have carried and extended these skills into the projects that they develop.

13. Design Reviews

2022 marks the first year that the team was able to successfully run a complete critical design review of the integrated design, including reviews from our advisors and alumni. This marked a major milestone and provided many insights into our design in a very productive review session. Design reviews are at the center of all good quality iterative design, and their importance cannot be understated. Each system and project done for the rocket undergoes a preliminary project proposal, as well as 1-2 intermediate design reviews, and then the final critical design review of the entire rocket. These give an opportunity for the project leads to receive feedback from the rest of the team, as well as address any integration concerns. As a bonus, they provide an opportunity for new members to learn about projects

more in depth, or for team members working on other systems to learn about the parts of the rocket that they are not directly responsible for.

B. Team Management and Operational Lessons Learned

14. The Importance of Documentation and Knowledge Transfer

Although Waterloo Rocketry has existed for over 10 years, the proper documentation of our systems is a relatively new development. In the past most knowledge on the team was gained through hands-on experience, and a lot of the time older members would teach newer members about the rocket's projects through in person conversations and messages on Slack. The logic was to build the rocket first, and write about it later. In hindsight this was flawed, and there were ways to do both, but it was easy to justify under the pressure of deadlines and trying to make it to a launch opportunity. Then the pandemic happened, and all of a sudden the team couldn't rely on in person explanations of systems. We struggled to onboard new members without extensive hardware, in-person training, and tests to show them. What was once easy to push to the side was staring us in the face, and it didn't appear to be going away anytime soon: our documentation was severely lacking. The issues were only compounded with the graduation of 2 classes between the start of the lockdown and the full return to in person activities; many of our older members left the team without being able to fully hand off their knowledge. It was evident that change was required.

Over the past 3 years, led in many ways by our new members, the team has implemented a number of strategies to document and better analyze the systems we build. Design documents for each project outline the goals, requirements and design choices. Tests are summarized in post-test documents, and the analysis of anomalies is recorded more easily for future reference. Reports, such as this one, are given more time and care in an effort to compile a complete, detailed insight to the rocket and its supporting infrastructure. There is still more to be done, but the change is evident. Waterloo Rocketry was determined not to lose sight of our goals and motivations during the pandemic, and proper documentation and knowledge transfer will help us continue to ensure that we will not.

15. Team Cohesiveness and the Relation to Successful Integration

The other major change brought about by the COVID-19 pandemic was the inability of the team to gather and hold events. The cohesiveness of the team has always been one of its strongest points, and we pride ourselves on the friendships that are built here. A number of online events, such as games nights on discord, were held in an attempt to keep everyone involved and interested in the team. Overall, these online events were relatively successful, but the importance of in person activities and work cannot be understated. There was an obvious positive change in the team when we returned to campus full-time, with unrestricted access to our work bay.

This is important for several reasons, certainly having access to our equipment again was a relief, but it was also a relief from a managerial standpoint. The rocket is made up of its separate components, but in flight it functions as a single entity. Systems rely on each other for function and need to be properly integrated in order to ensure success. The teams that do this best are the ones that are cohesive. When the team can work together, they will create systems that work together, and in person work provides a space for team members working on different subsystems to meet and discuss how their projects will be integrated. Although this is still possible to achieve online, it occurs much more naturally in person. Over the past design cycle, Waterloo Rocketry has made it a conscious effort to ensure integration success. Regular meetings were held to discuss integration concerns and issues as they arose and have proven to be successful overall. As the rocket comes together in the final stages, it is obvious that there was a conscious effort made to integrate and accommodate the design and requirements of each subsystem.

16. Management of Team Growth and the Importance of In-Person Engineering Experience

Over the past couple of years, the team has grown steadily, and is now at over 50 people. As the primary goal of the team is to provide interesting opportunities and experiences to anyone who'd like to participate, this growth is certainly welcome. However, learning how to manage a growing number of team members, projects, and resources has been a challenge unto itself. In some ways, the extended design cycle that has arisen from IREC being delayed has presented new opportunities to the team that may have otherwise been too complicated or time consuming for a 1-year design cycle. We have been able to simultaneously develop a more complex version of the hybrid rocket which we have been iterating on for the past 5 years, as well as begin development of a liquid engine, which we hope to fly at IREC in 2023.

While remote, the team struggled to find work for the many new students joining university for the first time, wanting to get involved with design teams. We added a number of design projects to our scope in order to continue to produce work while being unable to have full access to our manufacturing and testing equipment and facilities. This means that the return to in person work has provided many tasks for new members, and the management of the large number of people on the team has begun to feel more natural, and in many ways simpler. There is interesting

work to be done, and there are interested people to do it. We have been able to show up close how our systems function and fit together; how and why they are designed and built and tested. Having more older team members around the bay consistently has lent itself well to the training of the next generation of the team, and the future looks bright.

Appendix

A. System Weights, Measures and Performance Data

Table 1 Vehicle Mass Budget

Subsystem	Components	Mass Budget (lbm)	Margin	Source
Aerostructures	Nosecone & coupler	3.09	+/- 5%	CAD
	Bodytubes and Structures	5.51	+2%	CAD
	Fin Can + boattail	5.95	+2%	CAD
	Ox Tank Aft Skirt	5.95	+5%	CAD
Recovery	Parachute + rigging	12.79	+/-1%	Measured
	Recovery electronics	3.53	+/- 5%	CAD
Payload	Cubesat	9.70	0%	CAD
Vent	Vent valve + electronics	9.92	+/- 5%	CAD
Propulsion	Oxidizer tank + bulkheads	29.67	+/-2%	Measured
	Injector valve + electronics	3.97	+5%	CAD
	Combustion Chamber assembly	15.43	+5%	Measured
Total Dry Mass Budget		105.51		
Total Wet Mass Budget		167.33		

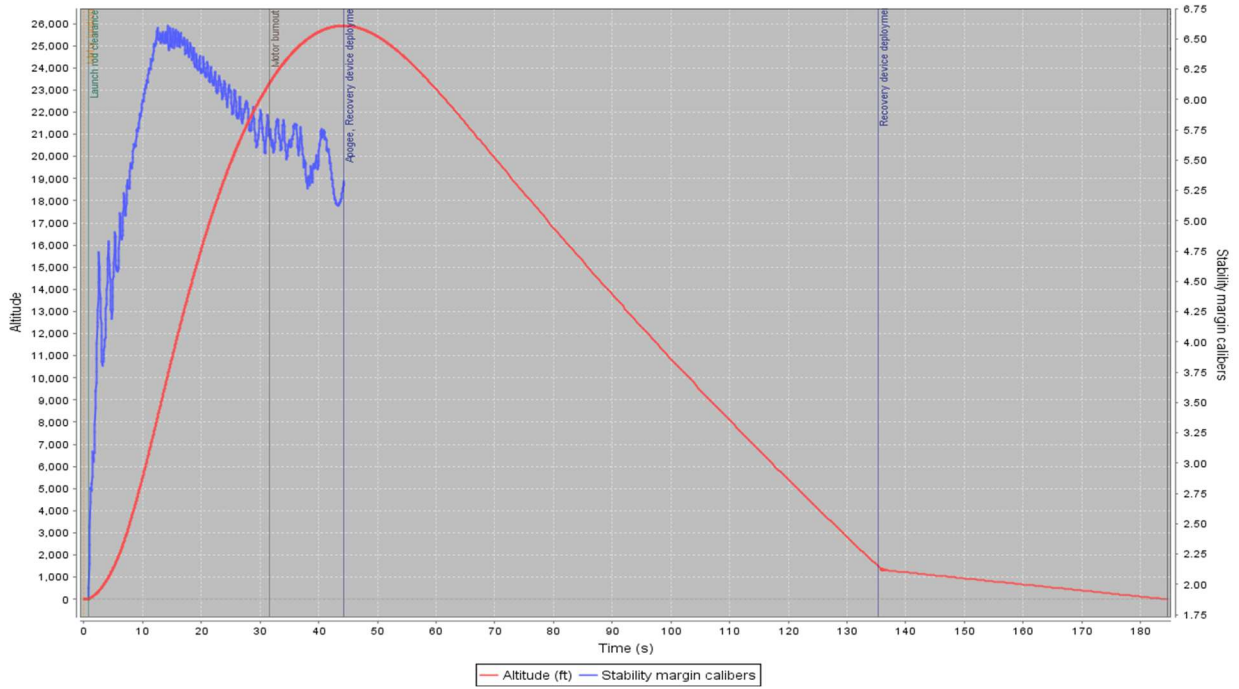


Figure 1 Flight simulation plot of time vs altitude

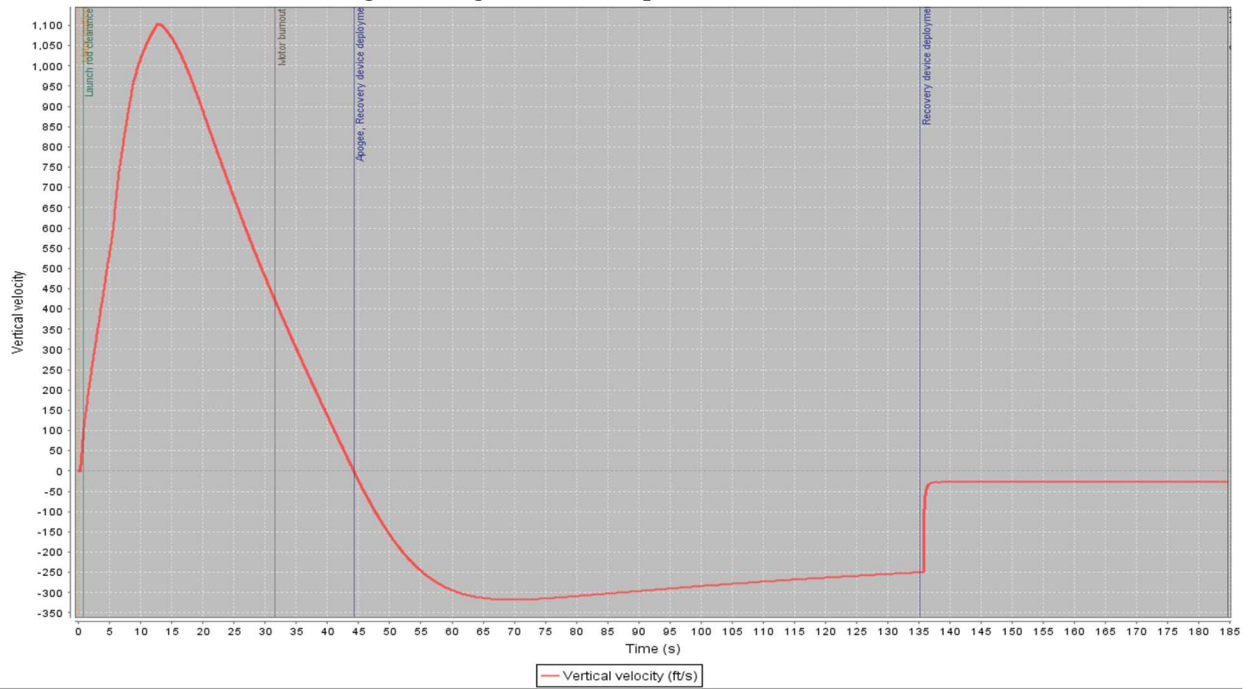


Figure 2 Flight simulation plot of time vs vertical velocity

Simulation 1
Custom

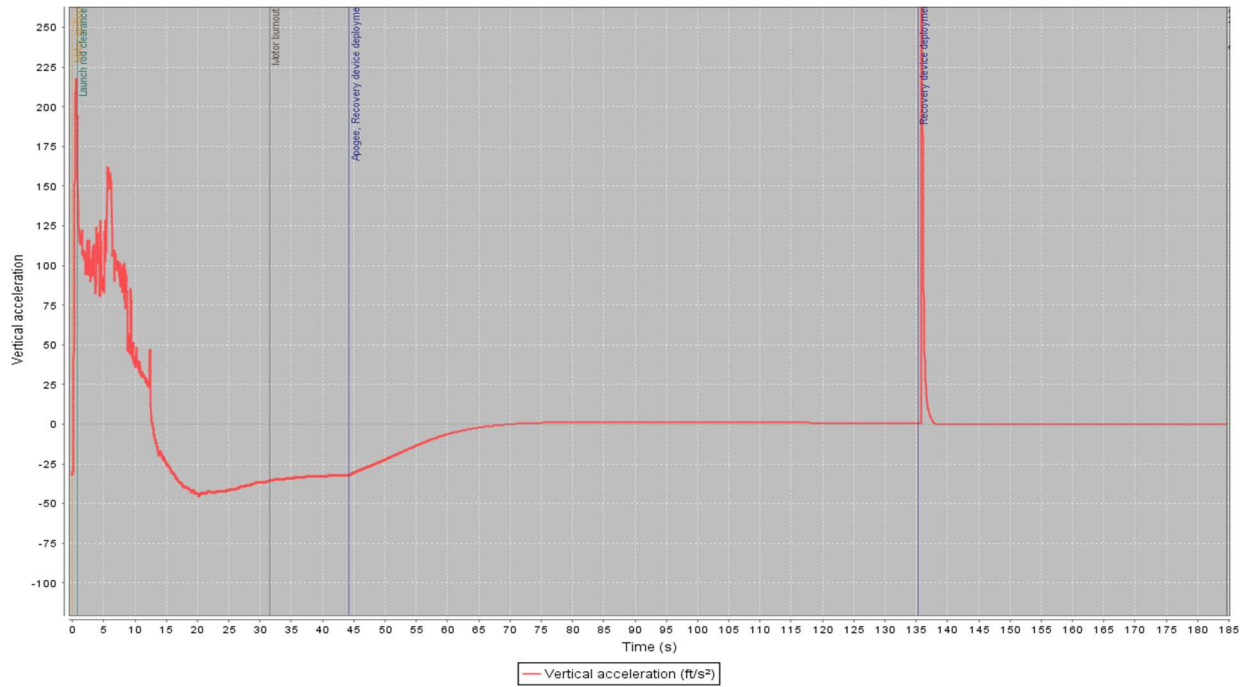


Figure 3 Flight simulation of time vs vertical acceleration

B. Calculations

17. Load Analysis Inputs

Table 2 Aerostructures BENDIT7 loads analysis inputs – flight conditions

Flight Conditions							
Altitude, ft AGL	Launch Altitude, ft	Launcher Length, ft	Mach Number	Flight Speed, fps	q, Dynamic pressure, lb/ft ²	Sref, Aerodynamic reference area, ft ²	Reference Length, Max Body Diameter, in
7.202427822	3910.761155	26	0.05	50.80052493	2.44208305	0.19590317	6
Pr (no failure)	Axial Acceleration, a, ft/sec ²	Thrust, lb	1 σ C.G. Lateral Offset, ft	1 σ Thrust misalignment angle, rad.	Body Station of Nozzle Throat, in	Element where the thrust is applied	Analysis Condition Right after ignition?
0.999	215.7250656	1276.847354	0.00984252	0.002	201.5748031	9	TRUE
I _{xx} , Roll Moment of Inertia, sl-ft ²	E, Nose Shell Modulus of Elasticity, psf	Element to use as base for nose aeroelastic effect	Nose Static Aeroelastic Effect?	N, number of fin panels	1σ gust amplitude, fps	Gust Longitudinal Autocorrelation Length, ft	Body-Fixed Response Roll Amplification Factor
0.140800613	3.89E+05	5	TRUE	3	45.27559055	1000	1
Roll wavenumber options 1 = Total roll revs 2 = Percentage of Boost	First Stage Roll Option (1, 2 or 3)	Option 1 - Stage 1 Roll Revolutions in Boost	Option 2 - Stage 1 Roll wave number as percentage of Stage 1 Pitch Revs		Second Stage Roll Option (2 or 3)	Option 2 - Stage 2 Roll wave number as percentage of stage 2 Pitch Revs	
	1	4	30.00%		2	30.00%	

Table 3 Aerostructures BENDIT7 loads analysis inputs – body profile data (finless)

Body Profile Data (Finless)								
Element Counter	Element Contents	xi, Element aft face body station, inches from nose tip	Ri, Element body external radius at body station xi, in	wi, Element weight (finless), lb	Element C_{Noi} (finless), per radian	Element Xcpi, (finless) from element front, in	Element C_{Noiv} per radian	Element Xcpi, from nose tip, in
0	0	0	0					
1	Nose	25.228	6	7.45	2	11.038	1.999330463	11.038
2	Parachute Bay	34.584	6	7.276	0	4.678	0	29.906
3	Recovery Elec	48.724	6	3.981	0	7.07	0	41.654
4	Payload Bay	62.514	6	10.427	0	6.895	0	55.619
5	Vent Section	72.514	6	7.82	0	5	0	67.514
6	Ox Tank	152.794	6	78.827	0	40.486	0	113
7	OTAS + FAST +	167.419	6	6.787	0	7.206	0	160
8	Combustion C	197.609	6	39.581	0	15.581	9.34	190
9	Boattail	201.809	5.25	2.486	-0.469	2.391	-0.469	200

Table 4 Aerostructures BENDIT7 loads analysis inputs – first stage fin data

First Stage Fin Data							
Fin spar attachment element	C_R root chord, in	C_T tip chord, in	B exposed semispan, in	Γ , LE sweep, deg	$1\sigma \delta$ (fin), rad	Number of elements along the fin span	
8	12	6.25	6.5	51.84	0.004	50	
Fin panel weight, lb	Root Chord LE Body Station, in, xF	Fin α and δ Center of Pressure Body Station, in	Fin Alone Airfoil C_{Noi} , per rad	Single Panel C_{Noi} , rad ⁻¹	Total Tail Assembly C_{Noi} (with Vortex Interference [only 2 stage]), rad ⁻¹	Fin ass'y Xcpi, from the root chord LE, in	
0.685659197	96.25	190	9.34	9.21633811	9.34	93.75	
Trailing Vortex Strength, (1/U) $d\Gamma/d\alpha$, (only 2 stage), in	Trailing Vortex Spanwise Location at Stage 1 (only 2 stage), in	Image Vortex Spanwise Location at Stage 1 (only 2 stage), in	Roll Wavenumber, λ_{Rv} , rad/ft	Mean Fin Cant Angle, δ_F , rad	CLp, per rad	Cldelta, per rad	
60.47150662	8.618544662	1.129471434	0	0	-53.06964826	11.42411362	

Table 5 MaxQ Aerostructures BENDIT7 loads analysis inputs – flight conditions

Flight Conditions							
Altitude, ft AGL	Launch Altitude, ft	Launcher Length, ft	Mach Number	Flight Speed, fps	q, Dynamic pressure, lb/ft ²	Sref, Aerodynamic reference area, ft ²	Reference Length, Max Body Diameter, in
7.202427822	3910.761155	26	0.05	50.80052493	2.44208305	0.19590317	6
Pr (no failure)	Axial Acceleration, a, ft/sec ²	Thrust, lb	1σ C.G. Lateral Offset, ft	1σ Thrust misalignment angle, rad.	Body Station of Nozzle Throat, in	Element where the thrust is applied	Analysis Condition Right after ignition?
0.999	215.7250656	1276.847354	0.00984252	0.002	201.5748031	9	TRUE
I_{xx} , Roll Moment of Inertia, sl-ft ²	E, Nose Shell Modulus of Elasticity, psf	Element to use as base for nose aeroelastic effect	Nose Static Aeroelastic Effect?	N, number of fin panels	1σ gust amplitude, fps	Gust Longitudinal Autocorrelation Length, ft	Body-Fixed Response Roll Amplification Factor
0.140800613	3.89E+05	5	TRUE	3	45.27559055	1000	1
Roll wavenumber options	First Stage Roll Option (1, 2 or 3)	Option 1 - Stage 1 Roll Revolutions in Boost	Option 2 - Stage 1 Roll wave number as percentage of Stage 1 λ_{Rv} (rev/ft)	Second Stage Roll Option (2 or 3)	Option 2 - Stage 2 Roll wave number as percentage of stage 2 λ_{Rv} (rev/ft)		
1 = Total roll revs 2 = Percentage of 1	1	4	30.00%	2	30.00%		

Table 6 MaxQ Aerostructures BENDIT7 loads analysis inputs – body profile data (finless)

Body Profile Data (Finless)								
Element Counter	Element Contents	x_i , Element aft face body station, inches from nose tip	R_i , Element body external radius at body station x_i , in	w_i , Element weight (finless), lb	Element $C_{N\alpha i}$ (finless), per radian	Element X_{cpi} , (finless) from element front, in	Element $C_{N\alpha v}$ per radian	Element X_{cpi} , from nose tip, in
0	0	0	0					
1	Nose	25.228	6	7.45	2	11.038	1.999330463	11.038
2	Parachute Bay	34.584	6	7.276	0	4.678	0	29.906
3	Recovery Elec	48.724	6	3.981	0	7.07	0	41.654
4	Payload Bay	62.514	6	10.427	0	6.895	0	55.619
5	Vent Section	72.514	6	7.82	0	5	0	67.514
6	Ox Tank	152.794	6	78.827	0	40.486	0	113
7	OTAS + FAST +	167.419	6	6.787	0	7.206	0	160
8	Combustion C	197.609	6	39.581	0	15.581	9.34	190
9	Boattail	201.809	5.25	2.486	-0.469	2.391	-0.469	200

Table 7 MaxQ Aerostructures BENDIT7 loads analysis inputs – first stage fin data

First Stage Fin Data						
Fin spar attachment element	c_R root chord, in	c_T tip chord, in	B exposed semispan, in	Γ_{LE} sweep, deg	$1\sigma \delta$ (fin), rad	Number of elements along the fin span
8	12	6.25	6.5	51.84	0.004	50
Fin panel weight, lb	Root Chord LE Body Station, in, xF	Fin α and δ Center of Pressure Body Station, in	Fin Alone Airfoil $C_{N\alpha}$, per rad	Single Panel $C_{N\alpha}$, rad ⁻¹	Total Tail Assembly $C_{N\alpha}$ (with Vortex Interference [only 2 stage]), rad ⁻¹	Fin ass'y X_{cpi} , from the root chord LE, in
0.685659197	96.25	190	9.34	9.21633811	9.34	93.75
Trailing Vortex Strength, $(1/U) d\Gamma/d\alpha$ (only 2 stage), in	Trailing Vortex Spanwise Location at Stage 1 (only 2 stage), in	Image Vortex Spanwise Location at Stage 1 (only 2 stage), in	Roll Wavenumber, λ_R , rad/ft	Mean Fin Cant Angle, δ_F , rad	CLp, per rad	Cldelta, per rad
60.47150662	8.618544662	1.129471434	0	0	-53.06964826	11.42411362

18. Bodytube Infusion Characterization

To better understand resin flow behaviour under vacuum, a characterization infusion was performed to experimentally derive permeability constants of various fabrics used. This was done by setting up a half-mould infusion that closely reflected the actual full infusion procedure. At measured intervals from the inlet, data for flow front distance, time, and temperature were recorded. Plotting and linearly interpolating these data points, permeability constants were obtained for each fabric tested. These values were then inputted in a calculator based on Darcy’s Law formula for volumetric flowrate through a porous medium to compute estimated infusion time. Through this process, certain flow control measures could be taken to mitigate manufacturing defects such as dry spots, without fear of exceeding the resin’s pot life. Refer to Darcy’s Law equation used to derive vacuum permeability in the table below. See Figure X for an example of linear interpolation performed to obtain the slope of flow front position vs. time. See Figure Y for the composites calculator computing an estimated infusion time of 841 seconds vs. actual infusion time of 889 seconds. These deviations are attributed to assumptions made; Further development will continue in order to consider the change in resin viscosity and temperature over time to yield more accurate results.

Table 8 Darcy’s Law Equations

Arrangement	Solve For Variable	Equation
Darcy's Law Equation	Q, Volumetric Flowrate (m ³ /s)	Q=kApL
Rearranged	K, Permeability Constant (m ²)	k=m ² p
Rearranged	t, Time (s)	t=VLkAp

Time Elapsed (S)	Distance Traveled (inches) = FF position	FF Position (m)	FF Position Sq. (m ²)	FF Position Sq./Time	Average Slope m=x ² /t
93	3.7	0.09398	0.0088322404	0.00009497032688	
153	6	0.1524	0.02322576	0.0001518023529	0.0002398919933
213	9.7	0.24638	0.0607031044	0.0002849911005	0.0006246224067
281	12.25	0.31115	0.0968143225	0.0003445349555	0.000531047325
327	15.2	0.38608	0.1490577664	0.000455834148	0.001135727041
380	19	0.4826	0.23290276	0.000612902	0.001581981011
443	22	0.5588	0.31225744	0.0007048700677	0.001259598095
523	24.2	0.61468	0.3778315024	0.0007224311709	0.00081967578
624	27.4	0.69596	0.4843603216	0.0007762184641	0.001054740784
744	30	0.762	0.580644	0.0007804354839	0.0008023639867
808	33	0.8382	0.70257924	0.0008695287624	0.001905238125
889	36	0.9144	0.83612736	0.0009405257143	0.001648742222

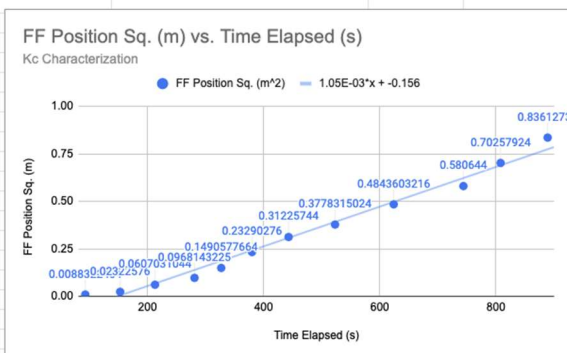


Figure 4 Flow Front Position Vs. Time Linear Interpolation

Enter Data:		Units	Auto Calcs:		Units
Body Tube Radius (R1):	3	in	Body Tube Radius S.I.:	0.0762	m
Body Tube Length (L):	37	in	Body Tube Length S.I.:	0.9398	m
Stacked Fiber Thickness (B):	0.00127	m	Cross-sectional Area (A):	0.0006029819001	m ²
Desired/Estimated Fiber Volume Fraction (Vf)	50	%	Volume of Bodytube (V):	0.0005666823897	m ³
Absolute Pressure on Vacuum (Δp):	30	inhg	Total Surface Area (TSA):	0.893619176	m ²
Resin Viscosity (μ):	225	cP	Specific Surface Area (S):	1576.931262	m ⁻¹
			Absolute Pressure on Vacuum S.I.:	101591.7	Pa
			Resin Viscosity S.I.:	0.225	Pa s
			Porosity In Decimal (φ)	0.5	pu*10 ⁻²
			Kozeny Constant (C)	5.367849	
			Average Fiber Permeability (Kc)	0.000000005813713128	m ²
Estimated Infusion Time:	841.1657524	s	Measured Infusion Time	889	s (Half mould)
	14.01942921	min	Measured Fiber Permeability	0.000000005813713128	
			Experimental FF Position Sq. vs. Ti	0.000372	(Full 3rd infu.)
				0.00105	(Half mould)
				0.000633	(Full 2nd infu.)

Figure 5 Infusion Time Calculator

Table 9 Coupler Calculations

Component	Failure Mode	FOS
-----------	--------------	-----

Recovery Electronics Top Coupler	Bearing	10.4
Recovery Electronics Top Coupler	Shear-out	3.6
Recovery Electronics Top Coupler	Bolt Shear	8.8
Vent Bulkhead	Bearing	20.1
Vent Bulkhead	Shear-out	10.8
Vent Bulkhead	Bolt Shear	13.0
Upper Bodytube	Bearing	9.0

Table 10 Ox Tank Aft Skirt Failure Modes

Component	Failure Mode	FOS
Longeron	Flexural Buckling - e=0.0729"	3.47
Longeron	Flexural Buckling - No Eccentricity	4.78
Longeron	Torsional Buckling	4.96
Longeron	Compressive Yielding	11.26
Longeron	Tensile Yielding	20.62
Fill Bulkhead, Injector bulkhead Coupler, Longeron	Thread Shear	76.83
Injector Bulkhead	Shear-out	34.04
Injector Bulkhead Coupler	Bearing	12.84

Fin Flutter Equation

$$V_f = a \sqrt{\frac{G}{1.337A^3 P(\lambda+1)2(AR+2)\left(\frac{L}{c}\right)^3}} \quad (x1)$$

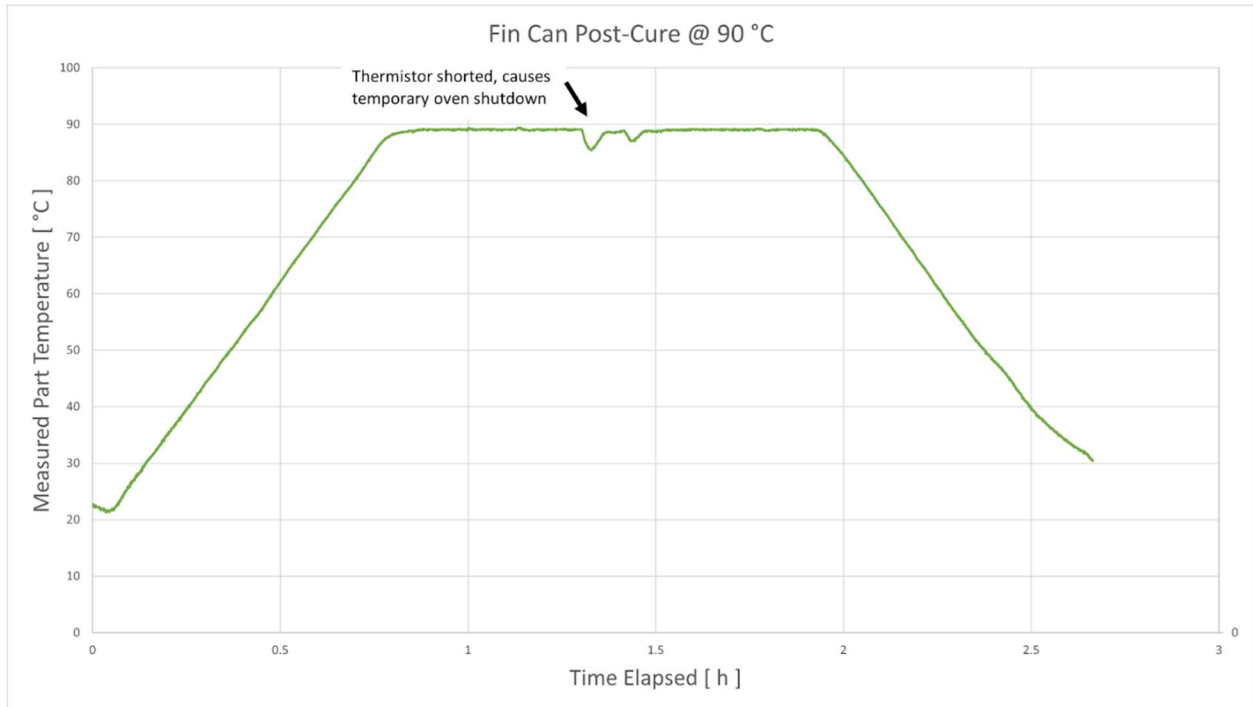


Figure 6 Post-Cure Schedule of the Fin Can

C. Project Test Reports

19. Recovery System Testing

Parachute development testing

This competition cycle has seen a series of truck testing, drop testing, and wind tunnel testing campaigns. The primary purpose of the truck tests were to allow the team to test a parachute when unable to access the wind tunnel due to COVID-19. A system was designed and built to adapt a loadcell and anemometer, attached to a parachute, into the hitch of a pickup truck, which would then be driven around a test track to gather data.



Figure 7 truck testing with the full scale parachute.

This testing allowed for the verification of the rigging and disreefing on the flight parachute. An image of a disreefing collage can be seen in the figure below. A number of tests were performed in this configuration, and the parachute was thoroughly characterized. At this point, it was also calculated that in order to descend at our target speed, a drag area of 7.5 ft² was required for the parachute



Figure 8 Disreefing sequence on the full-scale parachute.

Using the wind speed and the known desired drag area, a ‘target force’ at each instant in time was calculated. The data from the load cell measuring the actual force of the parachute could be visually inspected and compared to the target force for similarity. While more sophisticated data analysis strategies were attempted, they proved to be unstable. The graph of the data obtained for the final size of reefing parachute can be seen in the figure below.

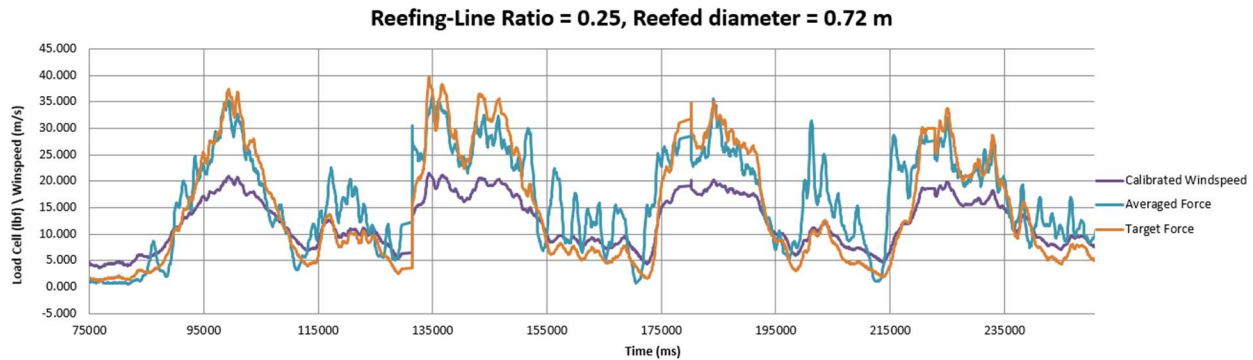


Figure 9 Data of the parachute behavior with the selected reefing length

As discussed previously, the parachute relies on a smaller parachute to pull it out of the bag due to the lack of a drogue. The release of the pilot parachute can be tested through ground tests, but it could not be verified that it would possess enough strength to pull the main parachute out. In the “Parachute Systems Design Manual” [REF X2 from recovery section], it is recommended that the extraction force of the pilot parachute be at least four times the weight of the parachute assembly that it is to extract. However, due to the flexibility of our system in regards to the time of the drogue deployment this meant that the parachute was sized to be relatively small. In order to verify that the parachute would indeed deploy, a drop tower test was performed.

The parachute was packed into a drop test article and taken up to the top of a 60 foot drop tower. For ease of testing, the main parachute was wrapped with tape, as this test was only looking at the extraction capabilities of the pilot parachute. With the pilot parachute dangling out, the test article was thrown off the tower. Even over the short drop distance, the pilot parachute was able to successfully extract the main parachute from its bag. A collage of this can be seen below.



Figure 10 Pilot Parachute test drop from 60 ft test tower

The final confirmation of the system was supposed to be the helicopter drop test, where a drop test article with functioning avionics and a deadweight simulating the mass of the rocket would be dropped from a helicopter, ideally from an altitude of around 1.5 km. We had reached an agreement with a helicopter company, prepared test procedures and equipment when we ran into regulatory difficulties with the airspace. Due to time constraints, the helicopter test will not be going ahead for the 2022 competition cycle.



Figure 11 Team members inspecting the test helicopter.

Fortunately, due to restrictions with the COVID-19 pandemic winding down, the team has recently been able to get access to the University of Waterloo Fire Research Lab Wind Tunnel. At the time of writing, wind tunnel tests are ongoing to determine the optimal packing configuration and fine-tune the reefing ratio. These tests are also incredibly valuable to eliminating the chances of tangling during deployment, as already multiple instances of possible tangling have been identified and rectified.



Figure 12 Reefed Parachute testing in the Fire Research Lab Wind Tunnel

Pyrotechnic and deployment development testing

There have been multiple campaigns of pyrotechnic tests in order to develop and validate methods for separating the reefing control line from the body of the rocket.

There were initial pathfinding experiments to design a device coined a “pyromelter”. It was to be a small metal tube, with the control line passing through it, that would have Richard Nakka Experimental solid fuel (RNX) cast inside. It would be ignited with either nichrome or an e-match, and would melt the control line while it was being burned. The pyromelter was ultimately abandoned due to reliability issues.



Figure 13 Pyromelter test article ready for ignition

The design was reverted back to use pyrocutters and a two ring release. Subsequently there were several tests conducted to ensure that the existing pyrocutters that we had on hand would work reliably and that the two ring release design would work with them.



Figure 14 Two ring release undergoing testing

System validation testing

System validation testing involves testing the recovery system deployment sequence in a representative environment. As of the writing of this report, this has not yet been completed for the KOTS recovery system.

The planned configuration for the ground deployment test will be to assemble the recovery module and lay it out horizontally. The altimeter will be programmed to simulate an ascent, apogee, and descent. At apogee, the CO₂ canisters will be punctured, separating the nosecone from the parachute bay. At a simulated altitude of 1500 ft AGL,

the pyrotechnic cutters will be actuated, allowing the two-ring release to deploy. The main parachute will be pulled out of its bag and will be verified to have disreefed. This will verify successful pyrotechnic actuation.

There is also ongoing discussion about possibly conducting this testing in the wind tunnel, which would allow a full simulation of the deployment sequence in order to verify packing configuration.

20. SRAD Propulsion Testing

Cold Flow Testing

Several cold flow tests have been conducted in order to validate components of the propulsion system, including the vent valve, the injector, and the injector valve. For each test, liquid CO₂ was used as a proxy for N₂O. The test setup was functionally identical to the Kismet plumbing configuration in the following section, save the combustion chamber and nozzle. Operational conformity to design intent for all systems being tested is the main success criterion.

21. Static Fire Testing

Static Fire 6

On May 14th, 2022, Waterloo Rocketry will conduct the 6th static fire (SF6) of the Kismet hybrid engine. The test will be used to validate the current iteration of the Kismet engine, which will fly at IREC 2022. The objectives of the test, in order of criticality, are as follows:

- Collect data to confirm the apogee of the Kraken of the Sky (KotS) rocket through simulation
- Validate the use of the parabolic graphite nozzle

An update will be available upon completion of the test.

Static Fire 5

On Sunday, July 18th, 2021, Waterloo Rocketry conducted the 5th static fire (SF5) of the Kismet hybrid engine. This test was the sole one performed so far for the 2020/2021/2022 competition cycle, due in part to the ongoing COVID-19 pandemic. The objectives of the test, in order to criticality, were as follows:

- Collect data to confirm the apogee of the Kraken of the Sky (KotS) rocket through simulation
- Validate the use of the Ghost Pepper 3D printed nozzle
- Validate the use of the FAST injector valve
- Validate the use of the oxidizer vent valve

The primary objective of the test, confirming the apogee of KotS through simulation, was to ensure that the rocket was capable of reaching its predicted 26,000 ft apogee. This was of particular importance due to the underperformance of its predecessor, SOTS, which was predicted to reach a similar apogee but in practice reached only 15,500 ft. It should, however, be noted that this is thought to have been due to an underfill of oxidizer in the tank at competition, as the load cell was oversaturated and fill data could not be relayed to the ops team.

The secondary objective, validation of the 3D printed “Ghost Pepper” nozzle, was set to replace the regular graphite nozzle in order to save weight and test a novel cooling method. More details on the design of the nozzle are available in the technical report [REFERENCE TO STEFANS REPORT]. The tertiary and quaternary goals were to provide a secondary validation of the FAST injector valve and SRAD oxidizer vent valve, which had been previously tested in cold flows. An additional goal was to validate the use of the new test site, nicknamed “Texas”.

Two previous SF5 attempts, as well as the unnamed liquid engine test, were slowed greatly or called off due to unseen difficulties with Texas, including lack of running water, electricity, and warm shelter, along with inclement weather, among other things.

A number of improvements were made to the test site in order to increase the efficiency of testing. These included mounts to attach the oxidizer fill plumbing to the walls of the shipping container, as well as increased fire fighting measures such as the inclusion of 2 smaller B class fire extinguishers that were readily available to the operating technicians, in addition to the large D class extinguisher that is normally present.

In order to find solutions for potential problems that could arise on test day, a dry run of the static fire was performed one week prior to the test using CO₂ as an analogue for NOS. Due to COVID-19 restrictions, the test crew was limited to 10 people. However, the dry run was overall successful, with a timeline as follows:

- 9:00 AM: met at the work bay
- 10:15 AM: got to the test site
- 2:00 PM: setup complete
- 3:30 PM: started ops
- 5:00 PM: had most items packed up
- 7:00 PM: everything returned, bay cleaned

In the end, a smaller number of people allowed new members who attended to receive thorough training in one or two critical systems. Overall, this made the setup run smoother during the static fire. A number of issues were caught and addressed during the dry run, including ops procedure corrections, items that were forgotten during packing, and some minor issues with DAQ and RLCS.

Summary of Operations

Setup was completed at approximately 3:15 PM, followed by a subsequent operations briefing which ended at 3:30 PM. Small changes were made to the procedure prior to leak check. No leaks were found, and fill started at approximately 5:45 PM. The SRAD vent valve performed nominally.

The FAST injector valve performed nominally, and the engine was fired at 850 psi with 46 lbs of NOS in the oxidizer tank. Nominal burn occurred for the first 1-2 seconds after firing began.

After that, the printed nozzle began to burn through at the throat and quickly burned any part of the nozzle below the initial portion of the converging section. In addition the post combustor liner began to unravel during the burn. Eventually this led to the lower end of the CC melting off of the engine. 3 noticeable fires, all small in size, were started in the area at the front of the test site. Primary and secondary re-entered the test area after the burn had ended in order to extinguish them out of an abundance of caution, even though through observation of live drone footage it didn't appear that the fires could sustain themselves. The test area was monitored using a drone to ensure that no other fires were started, and the site was safed within minutes.

When it came time to detach the supply cylinder from the system, primary and secondary observed a liquid dripping from approximately the connection between the fill line and the supply cylinder, evaporating as soon as it hit the mat below, along with significant frosting on the plumbing. The cylinder was vented out of caution, and afterwards the liquid was no longer observed. The test concluded without incident at approximately 6:45 PM. Teardown was completed at approximately 9:00 PM.



Figure 15 Kismet engine firing

Printed Nozzle Burnthrough

At approximately 1.5 seconds after burn starts, the water in the nozzle appears to reach its boiling point. For the next 0.5 seconds, the nozzle appears to function perfectly; water is boiled into steam which is released through the vent ports, and the reservoir reaches pseudo-equilibrium. However, as it continues to boil the steam pushes liquid water out of the vent ports, causing the nozzle to use up its coolant much faster than expected. Approximately 2 seconds after firing, the nozzle runs out of coolant and burns through at the throat, as thermal simulations would predict when no coolant is present.

Liner Unravelling

After the nozzle burned through the liner unraveled, leaving the lower portion of the cc exposed, at which point the unprotected section melted. It is possible that the unraveling was due to a sharp edge in the liner, where the combustion gases could catch. It is unclear if the failure of the liner was related to the failure of the nozzle, however there are no clear correlations and as such the design of the liner, particularly the sharp leading edge is suspected as the reason for the failure.

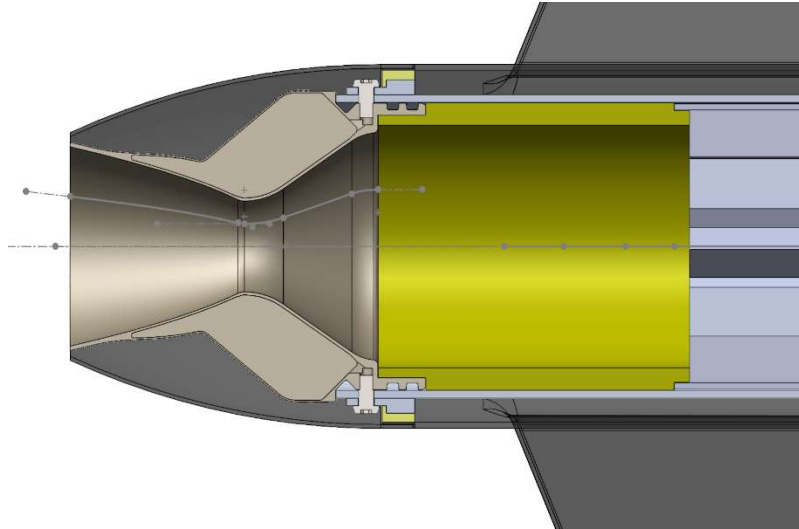


Figure 16 Printed nozzle geometry with sharp liner edge

As there is likely insufficient time to redesign the Ghost Pepper nozzle and perform another static fire, it was recommended that the project be abandoned for the current competition cycle. As of September 2021 the engine has been remade and converted back to the previous iteration, which used a graphite nozzle.

Data collected from SF5 and SF4 is shown below. SF4 data was taken from a static fire of the previous engine iteration, which will be reverted back to for the 2022 competition cycle. Note that only the first 3 seconds is given for the SF5 data, since the data is only being used to analyse the potential cause of failure modes that occurred during the test, as opposed to a full analysis of the complete burn.

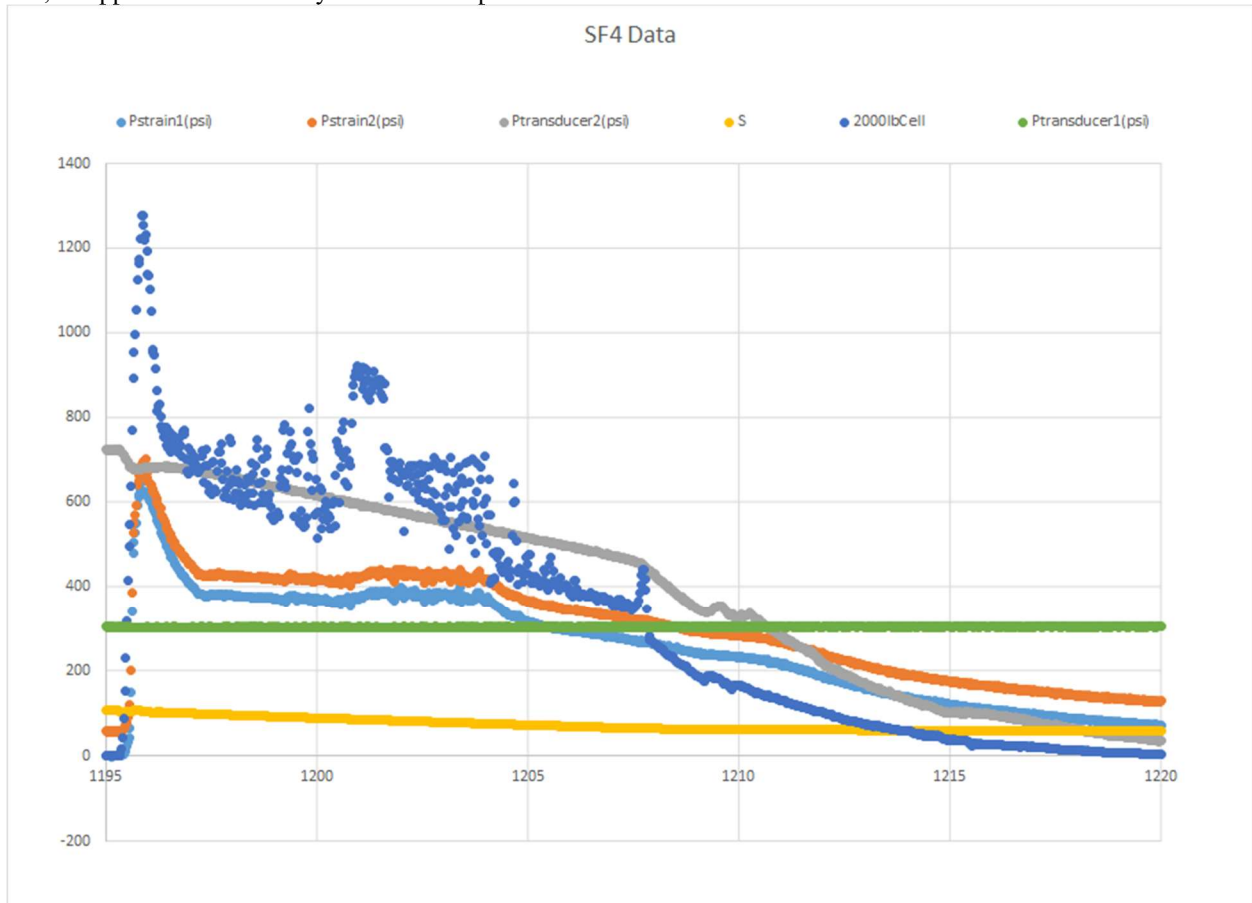


Figure 17 SF4 Data

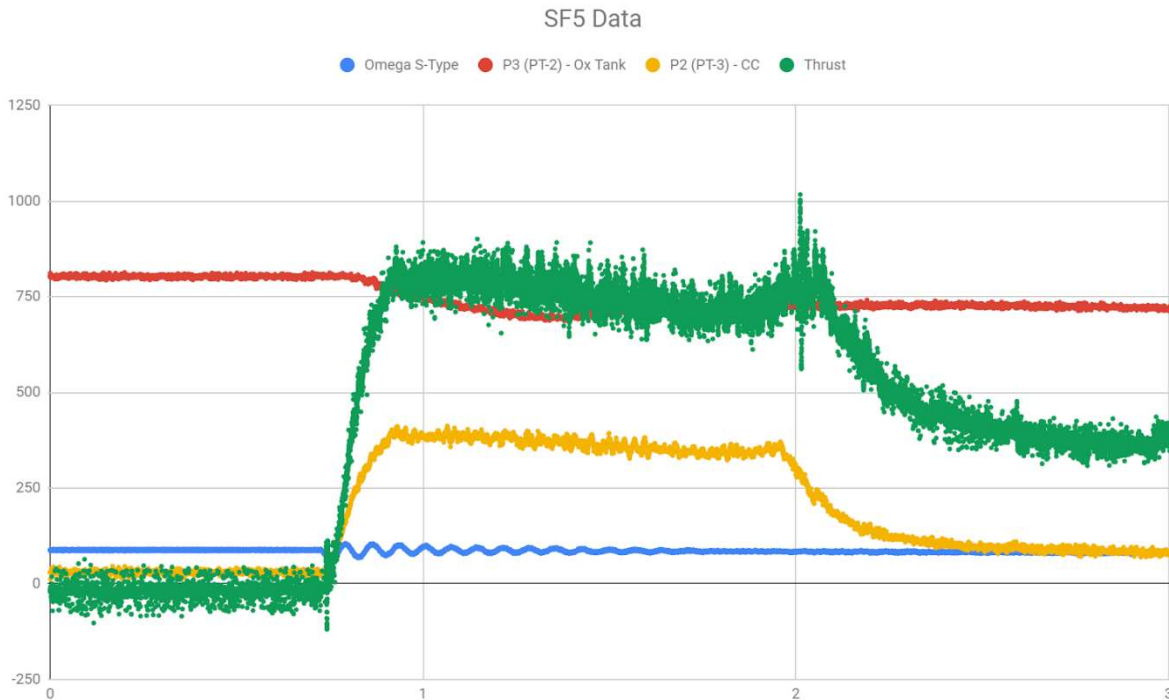


Figure 18 SF5 Data

SF5 was unsuccessful in two of the four objectives set for the test. Unfortunately, the failure of the Ghost Pepper nozzle meant that the data obtained could not be applied to flight simulations. As well, the implementation of a new nozzle will mean that the engine setup tested in SF5 cannot be used as a validation of the flight engine.

Objectives 3 and 4 were met, as the oxidizer vent valve and injector valve performed nominally during the static fire.

Although SF5 failed to meet some of its objectives, the test should not be considered unsuccessful. SF6 will be performed in order to gather test data on the current iteration of the engine. As well, the team learned a number of valuable lessons in testing at the new site - this test was the first to be performed at Texas that was not canceled or delayed significantly. The training and knowledge gained from this attempt will prove incredibly valuable in future testing endeavors.

22. SRAD Pressure Vessel Testing

Hydrostatic Testing

SRAD components required to hold pressure, including the combustion chamber and oxidizer tank, are hydrostatic tested at 1.5 times their operating pressure. The test is performed when the component is fabricated, as well as prior to and after any cold flow or static fire testing. All included fittings are teflon taped, and the component being tested is hooked up to a water pump. Using the pump, the pressure is raised to 1.5 times the maximum expected operating pressure of the component. The pressure gauge attached to the pump is observed. A pressure drop of less than 2% over 10 minutes is deemed acceptable.

D. Hazard Analysis

Table 11 Hazards Analysis

Hazard	Possible Causes	Likelihood Rationale	and	Mitigation Strategy	Risk After Mitigation
--------	-----------------	----------------------	-----	---------------------	-----------------------

Unintended gunpowder ignition	Gunpowder comes in contact with spark, electrical or otherwise.	Medium Risk; Gunpowder must be used during the final assembly of the recovery pyrotechnics, which include electronics.	Gunpowder is kept in the original container inside a sealed ammunition box at all times except for during final assembly, at which point only the two recovery technicians are present, wearing appropriate PPE. Batteries are not plugged in when gunpowder is exposed.	Low Risk
Recovery CO2 canister bursting	CO2 Canister is inadvertently punctured.	Low Risk; Canisters are used during the final assembly of the recovery pyrotechnics and contain very high pressure CO2.	CO2 canisters are stored in a sealed ammunition box except for during final assembly, at which point only the two recovery technicians are present, wearing appropriate PPE.	Minimal Risk
Lithium polymer (Lipo) battery fire	Battery is overcharged, short circuited, or punctured.	Medium Risk; Multiple Lipo batteries used across systems and in close contact with technicians.	All Lipo batteries are stored in a sealed ammunition box, and securely mounted in all systems when in use. Only correct 3S lipo chargers are used for charging. All systems are appropriately fused directly after the battery in case of shorts.	Low Risk
Accidental ignition puck ignition	Substantial electrical charge or heat source applied to ignition puck.	Low Risk: The ignition puck stores a very large amount of chemical energy and cannot be extinguished, but requires a substantial activation energy to ignite.	Pucks are stored in a sealed ammunition box until final engine assembly, after which electrical leads are covered at all times. Engine is kept away from any significant heat source.	Minimal Risk
Accidental e-match ignition	Exposure to electrical charge or heat source.	Medium Risk: E-matches store a small amount of chemical energy that could cause burns, and require relatively small charges to ignite.	E-matches are securely stored until final assembly, at which point only the two recovery technicians are present, wearing appropriate PPE. Leads are kept shorted until final assembly to prevent discharged through the body of the e-match.	Low Risk
Electric shock	Exposure to high voltage sources or creation of low-impedance paths and exposure to medium voltages.	Medium Risk: Electric shock can cause a serious risk of injury or death, but high voltage systems are avoided and all SRAD systems use voltages of 24V or less.	All high voltage systems are COTS and CSA approved. Electronics are never handled with wet hands, and batteries are disconnected before work is done on electrical circuits.	Minimal Risk

Launch tower falling on personnel	Tower is raised or secured incorrectly.	High Risk: If the launch tower were to fall it would pose a serious risk of injury or death due to its large height and weight.	Tower raising procedure is tightly controlled and followed, no personnel are ever under the tower during raising, all personnel wear hard hats during operations.	Low Risk
Contact or inhalation of toxic composite materials	Large variety of harmful dust and vapors formed during many airframe manufacturing activities.	High Risk: Most of the byproducts generated are some combination of irritants, toxins, and carcinogens, often with acute long term effects.	All Chemical MSDS are carefully tracked, and reviewed before use. Standard operating procedures are followed, and appropriate PPE is used.	Low Risk
Nitrous Oxide decomposition	Given sufficient catalyst or activation energy, nitrous can explosively decompose.	High Risk: In the unlikely event that decomposition occurs, it would likely cause a substantial explosion that could cause huge amounts of harm.	Only nitrous compatible materials are used for any system that may come in contact with nitrous. Careful sanitation and inspection procedures are followed for all plumbing. Procedures are designed to minimize time spent by operators near nitrous, and only COTS parts are used in systems that are pressurized during operator presence.	Minimal Risk
Contact with Nitrous Oxide	Leaky fittings, incorrect plumbing usage.	Very High Risk: Nitrous oxide is an asphyxiant, stored under very high pressures, and due to phase change during expansion, can reach very low temperatures. All of which pose a significant hazard to operators .	Procedures for working with nitrous are very clearly written, reviewed, and practiced. All functions related to nitrous are done remotely if possible. Operators wear appropriate PPE including safety glasses, face shields, shop coats, and thermal gloves. A secondary operator is present whose role is to keep the primary operator safe in the event of an anomaly.	Low Risk
Injury due to compressed air; direct or accelerated debris	Leaky fittings, incorrect plumbing usage.	Medium Risk: High velocity compressed air, or particles accelerated by it can easily cause injury, particularly to eyesight.	All personnel in the area where compressed air is being used must wear safety glasses and be aware of the pressurized system. Systems must be carefully operated according to procedures.	Low Risk
Injury due to misuse of power tools or other	Incorrect use of tools or bad process.	High Risk: Almost all rocket components are manufactured by students. Most machines	General machine shop training plus specific machine training required to use machines. Standard operating procedures	Low Risk

machine shop equipment		and power tools used have the capability for serious injury if misused.	required for any new tools or processes. Full time staff available to advise on best usage and safety	
Pinching or abrasions during rocket assembly.	Careless or rushed assembly, sharp edges on parts.	Medium Risk: There are many tight interfaces and parts that must fit together during assembly of the rocket. May of which could have sharp edges, pinch points, and other sources of injury.	All parts should be sufficiently de-burred to prevent sharp edges. Assembly procedures written for each system and practiced. Great care taken during flight hardware assembly.	Low Risk
Dehydration	The desert is very hot, and members are working long strenuous days.	Very High Risk: Members are working hard and sweating a lot, staying properly hydrated requires a larger amount of water than is intuitive.	Ensure large stockpiles of available water, ensure team members follow a strict hydration schedule and that each member is consuming sufficient water.	Medium Risk
Sunburn	Members are spending large amounts of time in direct sunlight for multiple days.	Very High Risk: Direct sunlight in the middle of the desert in the summer can very quickly cause sunburn, and members may not realize until badly burnt.	Ensure large stockpiles of available sunscreen for members, and enforce strict application schedules. Encourage members to wear fully covering clothing when possible.	Medium Risk

E. Risk Assessment

The following section details the risks to personnel, the launch vehicle, and associated equipment that may occur during the mission of operations of Kraken of the Sky. The following table provides a rating for probability of occurrence, severity, and detectability. For each risk, the ratings are multiplied to give a risk priority number (RPN). An RPN of under 30 is considered acceptable.

Rating	Occurrence (OCC)	Severity (SEV)	Detectability
5	Highly likely to occur	Hazardous without warning	Undetectable with training
4	Moderately likely to occur	Hazardous with warning	Moderately detectable with training
3	May or may not occur	Major system loss of functionality	Easily detectable with training
2	Moderately unlikely to occur	Minor system loss of functionality	Moderately detectable without training
1	Highly unlikely to occur	Little to no effect	Easily detectable without training

Failure Mode	Possible Effects	Potential Cause	Mitigation Strategies	O	D	S	RPN
				C	E	E	
<i>Pre-Launch Operations</i>							
Rocket ignites during preparations	Injury to surrounding personnel	Premature activation of ignition circuit	Ignition circuit requires arming locked out system, manual depression of ignition button for several seconds, and independent activation of injector valve.	1	3	3	9
	Cannot complete launch, primary mission goal failure		Oxidizer is not present in fill system during initial preparations.				
			Ignition circuit is not armed until immediately prior to fill.				
Rocket falls from launch rail during launch preparations	Injury to surrounding personnel	Stopping mechanism fails to support the weight of the rocket	Tower is raised with the rocket on top, with the tower structure and gin pole supporting the rocket during erection	2	2	4	16
	Damage to rocket	Rail buttons rip out of bulkhead	Launch rail is kept level to avoid stress on rail buttons				
			All personnel involved in launch tower erection wear hard hats				
Nitrous oxide escapes from the supply plumbing during fill procedure	Freezing of body parts, unconsciousness, or other bodily harm	Leaks in valves, fittings, or hoses	Plumbing components have been tested without failure and have adequate factors of safety	2	3	2	12
		Premature activation of remote	Check valve is rated to well over				
		Failure of oxidizer tank check valve	All plumbing components are visually inspected during assembly				
		Fill line does not adequately depressurize upon disconnect	Remote disconnect system requires power supply connection and activation of arming switch				
			During remote fill procedure, all personnel are to remain well away from supply plumbing				
Personnel are to remain well away from fill line following disconnect prior to launch							
Explosion of oxidizer tank during fill procedure	Blast or flying debris causing injury	Overpressurization due to clogging of the vent	Pressure relief valve is installed for overpressurization	1	3	2	6
	Cannot complete launch, primary mission goal failure		Oxidizer tank fails to hold normal operating pressure				
		All open ends of plumbing are covered during assembly, only uncovered before launch					
		Oxidizer tank is designed to rupture laterally instead of radially, minimizing flying debris					
Oxidizer tank is pressure tested to 1.5x expected maximum operating pressure							
Rocket ignites during fill procedure	Injury to nearby personnel	Premature activation of ignition circuit	All personnel are to remain well away from the rocket during fill procedure	1	3	3	9
	Cannot complete launch,		Ignition circuit requires activation of a key switch and an emergency stop button prior to arming				

	primary mission goal failure		Ignition circuit is not armed until launch personnel receive confirmation from range safety personnel				
Operators are no longer able to control the valves onboard the rocket	Loss of injector control	Radio contact loss between RLCS operator and rocket	All connections are terminated properly to avoid potential intermittent shorts				
		CAN module failure on radio or valve boards	The bus is off for most of the day, minimizing quiescent current draw				
		Microcontroller failure on radio/valve boards	Vent valve is designed to open if unable to re-establish radio contact	2	2	2	8
	Loss of vent control	Main battery runs out and bus goes down	Injector valve is designed to remain in current state upon radio contact loss If microcontroller goes down, vent valve board is hardwired to open the valve				
Vent valve closes and cannot be opened again	Loss of primary venting method	Solenoid valve fails closed	Loss communication to valve causes it to fail open				
			If launch abort is required, open injector valve very slightly. If this fails, allow oxidizer tank to overpressurize and rupture burst disk.	2	2	1	4
			The vent board continuously measures its battery voltage and is programmed to open the valve if the battery is low.				
Feedback from fill sensing system is lost	Unable to confirm fill level of tank	CAN module failure on fill sensing board	Full scale test of system is performed prior to flight				
			Pressure sensors, load cell data, and thermistor located at vent valve will provide enough data to determine fill level of rocket	3	2	2	12
Ignition Phase							
Engine does not ignite when command is given ("hang fire"), but does ignite when team approaches to troubleshoot	Injury to personnel	Primary igniter is activated, but gives no visual or electrical confirmation	Ignition relies on continuous delivery of current over several seconds, activated when operator holds down ignition button.				
			Primary igniter produces a great deal of dark smoke for visual confirmation of successful ignition				
	Cannot complete launch, primary mission goal failure	Electrical ignition signal is delayed	Display on RLCS indicates that ignition circuit is active, personnel do not approach during this time.	2	1	4	8
			All ignition control systems are to be disarmed prior to approach by personnel Personnel are not to approach the rocket if the oxidizer tank contains NOS				
Takeoff Phase							
Rocket deviates from	Contact with personnel causing severe injury, death	Failure of launch tower components	Off the rail velocity and stability are simulated prior to launch and deemed acceptable				

nominal flight path at takeoff	Cannot complete launch, primary mission goal failure	Unexpectedly low off-the-rail velocity resulting in low stability	Thorough inspection of all launch tower components occurs before assembly	2	1	5	6
			Launch tower is directed away from basecamp				
Explosion of combustion chamber or oxidizer tank during engine burn	Blast or flying debris cause injury to personnel	Backflow of gases from the combustion chamber into the oxidizer tank	Engine components have been designed with high factor of safety	2	1	3	6
		Clogging of nozzle due to bundled ignition wires	Injector has been designed for 50% pressure drop to minimize potential backflow				
		Fuel grain inhomogeneity causing breach of G11 liner or clogging of nozzle	Minimal, thin wires are used for ignition				
	Cannot complete launch, primary mission goal failure	Failure of hex bolts used to connect bulkheads, oxidizer tank, or combustion chamber	Fuel grain casting is done through strict procedure and visually inspected prior to assembly				
			All personnel remain well away from launch pad during launch				
			Oxidizer tank and combustion chamber are designed to rupture laterally instead of radially, minimizing flying debris				
Boost Phase							
Explosion of combustion chamber or oxidizer tank during engine burn	Blast or flying debris cause injury to personnel	Backflow of gases from the combustion chamber into the oxidizer tank	Engine components have been designed with high factor of safety	2	1	3	6
		Clogging of nozzle due to bundled ignition wires	Injector has been designed for 50% pressure drop to minimize potential backflow				
		Fuel grain inhomogeneity causing breach of G11 liner or clogging of nozzle	Minimal, thin wires are used for ignition				
	Cannot complete launch, primary mission goal failure	Failure of hex bolts used to connect bulkheads, oxidizer tank, or combustion chamber	Fuel grain casting is done through strict procedure and visually inspected prior to assembly				
			All personnel remain well away from launch pad during launch procedure				
			Oxidizer tank and combustion chamber are designed to rupture laterally instead of radially, minimizing flying debris				
Rocket deviates from nominal flight path during engine burn	Contact with personnel at high speeds causing severe injury, death	Unexpectedly high wind gusts	Rocket flight is simulated with high winds and does not experience significant deviation	2	1	3	6
			Fins are designed to maintain a static stability margin of between 1.5 and 6.0 cal throughout flight				
	Cannot complete launch, primary mission goal failure	Tail fins become damaged during launch	Tail fins are unobstructed during ascent on tower				
			All participants are aware of launch and can take cover if necessary A maximum allowed wind speed is set for launch				
Coast Phase							

Rocket deviates from nominal flight path	Contact with personnel at high speeds causing severe injury, death	Unexpectedly high wind gusts	Rocket flight is simulated with high winds and does not experience significant deviation	2	1	3	6
			Fins are designed to maintain a static stability margin of between 1.5 and 6.0 cal throughout flight				
	Cannot complete launch, primary mission goal failure	Tail fins become damaged during launch	Tail fins are unobstructed during ascent on tower				
			All participants are aware of launch and can take cover if necessary A maximum allowed wind speed is set for launch				
Reefed Main Descent							
Parachute fails to deploy, rocket comes in contact with personnel	Severe injury to personnel, death	Failure of altimeters	Altimeters are commercial components	2	2	3	12
		Insufficient pressure in the recovery bay to break shear bolts	Two altimeters are used for redundancy				
	Cannot complete launch, primary mission goal failure	Pilot chute fails to pull out main parachute	All decoupling systems are ground tested prior to launch				
		Line tangles due to incorrect packing	Recovery system is tested in a wind tunnel prior to launch				
Parachute disreefs at or near apogee, rocket drifts into unexpected area	Cannot recover vehicle	Parachute disreefs early	2-ring system is rated to well above expected stress	2	3	2	12
	Contact with personnel or equipment causing injury or damage	2-ring system breaks under load when reefed parachute is deployed	All decoupling systems are ground tested prior to launch				
			Rings are checked for signs of wear prior to launch				
Full Main Descent							
Parachute fails to disreef	Contact with personnel or equipment causing injury or damage	Pyrocutters fail to cut line	Avionics and disreefing mechanism are tested prior to launch	3	2	2	12
		Disreefing line becomes tangled and keeps parachute from fully deploying	All decoupling systems are ground tested prior to launch				
Rocket airframe separates into multiple assemblies	Injury to personnel due to high speed contact with falling component	Failure of recovery lines, resulting in component freefall not slowed by parachute	All recovery lines in system are designed for use with parachutes	2	1	4	8
			All participants are aware of launch and can take cover if necessary				

F. Assembly, Preflight, Launch, and Recovery Checklists

Waterloo Rocketry Procedure Oxidizer Component Sanitation

Basics:

Description	This document outlines the procedures to sanitize any component that contacts nitrous oxide. The purpose of doing so is to minimize the likelihood of explosions and other dangerous releases of energy as a result of chemical reactions occurring between components and oxidizer.
Location	E5 1008 – Rocketry Bay
SOP Created	Sept 2016
SOP revised	March 2021
Manual location	Google Drive, physical copy should be in SOP binder on the back of the door.
Authorized Trainers	Delaney Dymont, Aaron Leszkowiat, Hamza Abuabah, Shirley Kong

Safety Summary:

Significant hazards	Exposure/ingestion to/of chemicals Electric shock
Administrative Controls	All work shall be done at the sink and/or at the designated sanitation station.
Engineering Controls	None
PPE Required	Nitrile gloves, close toed shoes, safety glasses or goggles (goggles preferred).
Relevant MSDS	<ul style="list-style-type: none">• See list of equipment below
Accident procedures	In case of spill into work area, use spill kit to clean up the spill if the chemical is hazardous. Otherwise, clean the spill using paper towel. In case of spill onto persons, follow instructions presented in the MSDS.

Equipment and Materials (Chemicals bolded):

- Hand tools for component disassembly
 - o Screwdrivers
 - o Wrenches
 - o Tweezers
 - o Cups
 - o Clean trays
 - o Small metal picks
- Toothbrush or small bottle brush for small components
- Larger pipe brush for oxidizer tank
- Functioning sink
- Deionized water
- Ultrasonic cleaner

Standard Operating Procedure – Waterloo Rocketry Team
Oxidizer Component Sanitation

- Simple Green
- Cleanroom bags
- Clean plastic cups (for cleaning solution and water)
- Aluminum foil
- PPE equipment as noted above
- Component plugs/caps
- Paper towel
- CLR
- Tape
- Nitrogen Gas Cylinder
- Air hose

Pre-start Checklist:

1. Ensure at least 2 people are on hand
2. Connect the air hose to the nitrogen gas supply cylinder
3. Open the overhead door
4. Prepare ultrasonic cleaner
 - Inspect the ultrasonic cleaner for cleanliness
 - Closely inspect the ultrasonic cleaner tank for any signs of mineral deposits within the tank. Clean the tank as needed with the appropriate cleaner, as per manufacturer's instructions.
5. Inspect cleaning solutions
 - Ensure it has not exceeded shelf life
 - No signs of leaks or contamination
6. Gather appropriate materials from checklist above
7. Notify
 - Notify team members in the area
 - Notify Team lead and/or safety captain

Setup Checklist:

1. Don all PPE as listed above.
2. Lay aluminum foil over work area and trays
3. Dilute necessary cleaning solutions using tap water, according to the manufacturer instructions. For the correct quantity of solution, see the next section on cleaning procedure by component type.
4. Wash necessary tools (i.e. metal picks, tweezers, toothbrush).

Cleaning Procedure by Component Type:

Oxidizer Tank

1. This procedure may be done at the sink located in the SDC common area to provide more space.
2. Remove any rust by scrubbing with CLR.
3. Rinse loose dirt/dust off of the outside and inside of the oxidizer tank using tap water.
4. Prepare 1/3 to 1/2 bucket of diluted cleaning solution, as per manufacturer instructions.
5. Using a pipe brush and bucket of Simple Green cleaning solution placed inside the sink, scrub the inside of the oxidizer tank for 15 minutes. Be mindful of even coverage and use a cup or similar to frequently coat the inside of the tank with the cleaning solution.

Standard Operating Procedure – Waterloo Rocketry Team
Oxidizer Component Sanitation

6. Rinse the tank thoroughly with deionized water (4 minutes is usually an appropriate amount of time).
7. At this point the inside of the tank should NOT contact any other material (i.e. paper towel). Shake the tank to remove excess water.
8. Dry the oxidizer tank using nitrogen gas.
9. Place aluminium foil around the ends of the tank, ensuring to cover all bolt holes, and secure in place with tape.
10. Store tank in a safe location.
11. Attach label to the tank indicating date/time of cleaning, and by whom.

Hoses

1. Remove residual Teflon tape or other debris from hose ends.
2. Remove any visible rust from the hoses by scrubbing with CLR.
3. Rinse any potential debris from hoses by running tap water through them. Ensure the water exiting the hose appears clean before continuing.
4. Prepare approximately half a cup to one cup of cleaning solution according to manufacturer's instructions, depending on the size of the hose.
5. Cap one end of the hose with your thumb, and pour the cleaning solution in the other end.
6. Cap the other end with your other thumb and swing the hose around gently, ensuring even coverage with the cleaning solution.
7. Dump the cleaning solution out of the hose and into the sink.
8. Run deionized water through the hose, until the water comes out clean.
9. Use nitrogen gas to flush the hose of excess water.
10. Cap the ends of the hose with aluminium foil, and secure with tape.
11. Label hose (date/time cleaned and by whom), and store safely.

Valves

1. Disassemble valve with reference to the manufacturer specifications, being careful to document reassembly instructions and to not lose components.
2. Remove any rust by scrubbing with CLR.
3. Rinse away loose surface dust/dirt using tap water.
4. Prepare roughly a cup's worth of cleaning solution as per manufacturer instructions.
5. Clean each component thoroughly using a toothbrush and cleaning solution.
6. Rinse components with deionized water.
7. Use nitrogen gas to dry components.
8. Reassemble valve.
9. Cover open ports on the valve with aluminum foil.
10. Place the valve in a cleanroom bag. Label (date/time cleaned and by whom), and store safely.

Fittings and Miscellaneous small components

1. Remove any rust by scrubbing with CLR.
2. Rinse away loose surface dust/dirt using tap water.
3. Fill the ultrasonic cleaner tank with lukewarm water and cleaning solution in the appropriate ratio, based on the cleanliness of the fittings. Do not exceed the 'MAX' fill line indicated on the inside of the tank.
 - a. Recommended ratio for Simple Green: 1 part simple green and 3 parts water.
4. Place the basket supplied with the ultrasonic cleaner inside the tank.
5. Set the timer to one of the preset times: 90, 180, 280, 380, or 480 seconds.

Standard Operating Procedure – Waterloo Rocketry Team
Oxidizer Component Sanitation

6. If necessary, the heater feature may be turned on. It will take 30-60 minutes for the water in the tank to heat up.
7. Start the ultrasonic cleaner and leave it for the set time. The cleaning cycle may be stopped if there is an issue inside the cleaner.
8. Once cycling is complete, take the basket out of the ultrasonic, and drain the ultrasonic by pouring out one of the corners. Rinse the tank if needed.
9. Rinse components using deionized water.
10. Dry components using nitrogen gas.
11. Place caps/plugs on open ports on the component, or if no cap/plug exists cover with aluminum foil.
12. Place the component in a cleanroom bag. Label (date/time cleaned and by whom), and store safely.

Sensors / Gauges

1. Ensure that the sensor can be cleaned using the materials prescribed (sensor dependent). Modify the following procedure accordingly.
2. Rinse away loose surface dust/dirt using tap water.
3. Prepare roughly a cup's worth of cleaning solution as per manufacturer instructions.
4. Clean each component thoroughly using a toothbrush and cleaning solution, including the corresponding cap or plug if it exists.
5. **Do NOT clean the inside sections of the sensors. They contain sensitive electronics and you WILL damage them.**
6. Rinse components using deionized water.
7. Dry components using nitrogen gas.
8. Place caps/plugs on open ports on the component, or if no cap/plug exists cover with aluminum foil.
9. Place the component in a cleanroom bag. Label (date/time cleaned and by whom), and store safely.

Bulkheads

1. Remove any rust by scrubbing with CLR.
2. Rinse away loose surface dust/dirt using tap water.
3. Prepare roughly a cup's worth of cleaning solution as per manufacturer instructions.
4. Clean each component thoroughly using a toothbrush (or other appropriate tool) and cleaning solution.
5. Rinse components with deionized water.
6. Use nitrogen gas to dry.
7. Wrap bulkhead in tinfoil.
8. Place the component in a cleanroom bag. Label (date/time cleaned and by whom), and store safely.

Cleanup/Takedown Procedure:

1. Ensure the nitrogen gas supply cylinder is closed.
2. Ensure that components are safely stored according to their respective procedures, and are clearly labelled (date/time of cleaning, and by whom).
3. Rinse cleaning supplies used.
4. Rinse out the Ultrasonic cleaner, wipe it dry, and store in a cool, dry place.
5. Dispose of aluminium foil used as table and tray covering.
6. Remove PPE.

Standard Operating Procedure – Waterloo Rocketry Team
Oxidizer Component Sanitation

Additional Notes for Ultrasonic Cleaner

- Use lukewarm or room temperature water only
- Avoid getting water on the control panel or any electronic components in the ultrasonic cleaner
- To avoid overheating, avoid using the ultrasonic cleaner continuously for more than 30 minutes
- Do not use corrosive solutions inside the tank. Only use authorized cleaning solutions
- Only turn on the ultrasonic cleaner when there is fluid inside
- Do not turn the ultrasonic cleaner on unless there is water/solution inside the tank
- When the ultrasonic cleaner is no longer being used, clean the tank, wipe it dry, and store the ultrasonic cleaner in a cool and dry place.

Combustion Chamber Assembly

Note o-ring sizes: 242 between nozzle and liner, 246 between liner and aluminium chamber

1. Ensure injector bulkhead and inside of injector are sanitized.
2. Align fuel grain to injector ports. (at least align one star corner to one injector port)
3. Align bulkhead holes on injector bulkhead to retaining ring holes to help the alignment in the previous step.
4. Mark alignment using a sharpie.
5. Make sure the nozzle is cleaned (using a toothbrush), and all the old o-rings are removed.
6. Install o-rings on the nozzle (size: 236) with o-ring lubricant.
7. Place a layer of tape above the o-rings to prevent contact with caulking. Ensure that the tape does not contact the o-rings.
8. Place nozzle on retaining ring.
9. Apply high temperature caulking on female lip of fuel grain.
10. Use a popsicle stick to evenly spread the caulking.
11. Add a little caulking on the male end of the nozzle.
12. Use a popsicle stick to evenly spread the caulking.
13. Put nozzle liner on nozzle
14. Add a little caulking on the end of the nozzle liner.
15. Use a popsicle stick to evenly spread the caulking.
16. Join fuel grain and the nozzle together.
17. Clean excess caulking using paper towel.
18. Ensure the caulking didn't get over the O-ring.
19. Align combustion chamber to the retaining ring.
20. Put fin can on the bottom of combustion chamber. Do not screw it in!
21. Take off the tape on the nozzle o-rings.
22. Slide the combustion chamber and fin can onto the fuel grain assembly.
23. Make sure no component of fuel grain assembly rotates.
24. Rotate the fin can until the bolt hole for rail button and the pre-marked fill port location are 90 degrees apart clockwise.
25. Screw the fin can in using Eleven ¼"-28 (long ones) and a ¼"-28 (super long one) with rail button.
26. Ensure that the rail button is between two fins.
27. Install the break link adapter onto the retaining ring. Ensure the break link adapter is mounted opposite the rail button.
28. Join the end of ignition wiring to a thin tube using masking tape.
29. Pass this tube through the fuel grain and nozzle while making sure not to damage the nozzle.
30. ENSURE that you do not pull on the ignition wiring.
31. Get two pieces of wooden 2x4 to support the engine so as to not compress the ignition wiring under the weight of the engine.
32. Apply caulking to the male end of the fuel grain.
33. Use a popsicle stick to evenly spread the caulking.
34. Apply caulking to the female end of the spacer.
35. Use a popsicle stick to evenly spread the caulking.
36. Press the spacer onto the fuel grain.
37. Check continuity on both ignition cables to ensure good assembly.
38. Slide the fiberglass sleeve on the injector bulkhead.
39. Install combustion chamber external o-rings (size: 236) onto injector bulkhead with o-ring lubricant.
40. Apply caulking to the male end of the spacer.
41. Use a popsicle stick to evenly spread the caulking.
42. Apply caulking to the female end of the injector bulkhead.
43. Use a popsicle stick to evenly spread the caulking.
44. Make sure the alignment between injector bulkhead and combustion chamber is correct.
45. Ensure to use the correct (longer) O-ring fillers
46. Insert oxidizer tank assembly onto the engine assembly.
47. Check if any of the O-rings ruptured during installation through the bolt holes.
48. Fasten with twelve ¼"-28 screws (short ones)

49. Check if the O-ring fillers ruptured after installation.
50. Check continuity on both ignition cables to ensure good assembly.
51. Strain relief the ignition cables by using masking tape to connect it to the outside of the engine.
52. Close the nozzle end of the engine using a ziploc bag and masking tape.
53. Short the igniters to ensure they do not accidentally ignite during transport.

Oxidizer Tank Assembly

Notes:

- Use gloves for installation to avoid contamination
- Apply PTFE tape to all pipe fittings

Procedure:

1. Sanitize everything that will contact oxidizer (ref. Sanitation Procedure)
2. Inspect all components for damage. Dents, digs, or deep scratches larger than 1cm should be noted and evaluated more closely for impact to seal quality. Note that extrusion marks on the tank do not apply.
3. Record the dip tube length and insert it on vent bulkhead
4. Install o-rings on both bulkheads using o-ring lube
5. Place bolt hole plugs into one end of tank, secure and check for any plugs protruding inside the tank.
6. Slide bottom fill bulkhead into place, ensuring the holes align while inserting
7. Remove plugs and bolt fill bulkhead into place, tightening all 12 ¼-28 fasteners in a star pattern and checking for ripped o-rings. DO NOT OVERTIGHTEN to avoid stripping the threads.
8. Place bolt hole plugs into holes on the top side of the tank, secure and check for any plugs protruding inside the tank.
9. Slide vent bulkhead into place, ensuring the holes align.
10. Remove plugs and bolt vent bulkhead into place, tightening all 12 ¼-28 fasteners in a star pattern and checking for ripped o-rings. DO NOT OVERTIGHTEN to avoid stripping the threads.
11. Cap both ends of the tank if not immediately assembled to injector and vent valves.

Recovery System Setup Procedures

Inspection

1. Ensure all components are undamaged
2. Ensure that all pyrotechnics and batteries are disconnected and shorted before starting

Wiring

1. Ensure that all pyrotechnics and batteries are disconnected and shorted before wiring
2. Check that all circuit components are properly mounted to the sled with proper spacers, screws, and nuts
3. Ensure all switches are in the energized position
4. Check continuity between batteries and altimeters
5. Turn all switches to the non-energized position
6. Check batteries for full capacity (nominal 9 V)
7. Install batteries correctly in battery holders
8. Plug in camera

CO2 System Installation

1. Ensure all ejection device wires and batteries are disconnected from the electronics bay before proceeding
2. Ensure the two CO2 ejection devices are installed into the bulkhead
3. Install two 38 gram CO2 cylinders into the ejection devices, using two washers to ensure CO2 vent holes are unobstructed. Use Teflon tape on the threads of the CO2 cylinder when connecting

GPS System

1. Ensure GPS battery is fully charged
2. Ensure GPS is functional after connecting battery
3. Turn GPS system off by waving magnet over the magnetic switch

Sled Installation

1. Ensure all wires are tucked away to prevent pinching during installation
2. Ensure the CO2 cylinders are installed into the CO2 ejection device
3. Ensure that the batteries are installed in the battery holder

CO2 Ejector Setup

1. Place igniter and wires inside igniter cylinder and center igniter in cylinder using tissue paper
2. Place epoxy on igniter wires so that when the igniters are pulled, the wires do not pull out of the igniter cylinder
3. Ensure igniter is placed so that it is flush with the rim of the cylinder that touches the puncturing cylinder
4. Place aluminium foil on the working surface
5. Place a separate piece of aluminium foil on the working surface for holding and pouring the gunpowder
6. Place avionics assembly on the first aluminium sheet with the injector body opening upwards such that the entire body is grounded
7. Place O-ring on puncturing cylinder and lightly lubricate with spray silicone lubricant making sure to wipe off excess lubricant
8. Place puncturing cylinder in injector body
9. Fill puncturing cylinder to the rim with FFFF gunpowder
10. Ensure igniter leads remain shorted
11. Place O-ring on igniter cylinder and lubricate
12. Place igniter cylinder on top of puncturing cylinder and push down until igniter cylinder is flush with injector body
13. Ensure gunpowder vent holes are clear of obstructions and cover lightly with masking tape
14. Run igniter wires through body cap and screw cap on tightly
15. Check for movement of the igniter wires
16. If moving, take apart and reseal igniter so that it is seated firmly in place

Pyrotechnic Cutter Setup

1. Slide an O-Ring into the bottom of the cutter to act as a bumper for the piston
2. Insert recovery dual ring rope through the hole of the cutter
3. Trim excess rope
4. Insert shearing piston
5. Insert black powder
6. Insert E-match
7. Install o-rings to act as seal
8. Slide hex screw over E-match leads and screw into cutter

Parachute Section Assembly

1. Seat the main recovery bulkhead against the parachute tube coupler
2. Ensure that all recovery lines are free and not tangled
3. Ensure that the 9 V batteries are disconnected
4. Fold the main parachute, gore by gore, in an accordion-style pattern
5. Fold the main parachute vertically in half
6. Roll the main parachute from the top towards the main parachute lines
7. Pack the rolled parachute into the parachute bag so that the main parachute lines extend from one of the open corners
8. Secure the main parachute lines over the parachute bag cover using the elastics
9. Use the carabiner to connect the main parachute line to the main coupling line
10. Connect the two-ring release mechanism and secure using the dual ring rope
11. Secure the pyrotechnic line cutters to the primary recovery line using electrical tape
12. Connect the pyrotechnic leads to the connectors on the primary recovery line
13. Pack the parachute bag into the parachute bay and push it towards the engine end
14. Fasten the eyebolt to the top of the vent bulkhead with a lock washer and Loctite
15. Wrap a fireproof cloth around the pyrotechnic line cutters to protect main parachute and recovery lines from the black powder burn
16. Connect the circular connector from the primary recovery line to the avionics module

17. Pack the remaining recovery lines into the parachute bay
18. Confirm that the altimeters are off
19. Make all appropriate electrical connections at the avionics terminals
20. Insert the 9V batteries into their mounts
21. Fasten the electronics sleds onto the main recovery bulkhead
22. Connect the altimeters to the circular connectors using the screw terminals
23. Check continuity between parachute bay connector pins and altimeter
24. Wrap a fireproof cloth around the igniter cylinders to protect recovery lines and parachutes from the black powder burn
25. Connect the upper bodytube to the main recovery bulkhead
26. Apply a layer of grease to nosecone and parachute tube coupler
27. Place the nosecone coupler over the parachute tube coupler
28. Secure the nosecone and parachute tube module together with shear pins

LAUNCH TOWER OPERATIONS

Assembly Checks

- Ensure all 1/4" cable clamps are torqued to 4 3/4 lbs.ft (57 lbs.in) minimum
- Ensure all 3/16" cable clamps are torqued to 3 3/4 lbs.ft (45 lbs.in) minimum
- Ensure that there are a minimum of 2 threads sticking sticking out the end of the turnbuckles
- Ensure that cable assemblies are at least the lengths specified in the "Gin Pole Mechanism Drawings"
- Ensure that the "Connecting Wire ASY" and "Puller Wire ASY" are assembled onto the long gin pole. A section of the "Puller Wire ASY" will not be connected to the winch; this is what should be on the gin pole
- Have the hand drill set on low speed. Max rpm on low speed is 600 rpm, which is also the rpm rating of the winch
- Ensure there is sufficient lubrication on winch gears

Launch Pad Installation Procedure

Estimated time: 10 min

Technicians Required: 2

Tools Required:

- Sledgehammer
- Strike plate
- Level measurement device

1. Identify a fairly flat piece of land, unobstructed by plants
2. Place the launch pad on the ground. If the ground is soft, place several 2x4's underneath the pad, evenly spaced
3. Level the launch pad by adding/removing ground as required. Max of 2deg tilt is acceptable
4. Drive stakes through each corner of the launch pad legs, leaving about 1"-2" sticking out
5. *End of procedure*

Gin Pole Installation

Please see drawings for assembly details

Estimated Time: 1 min

Technicians Required: 3

Tools Required

- Adjustable wrench/ratchet wrench x2
- Long Gin Pole section

1. Ensure the pad is rotated to “tower vertical” position
2. Disassemble the bolt and nut on the Short Gin Pole (already installed on the pad)
3. Slide the Long Gin Pole onto the Short Gin Pole
4. Use the bolt and nut to fasten the sections together, and tighten with wrenches
5. *End of procedure*

Ground Anchor Installation

Please see drawings for geometry

Estimated Time: 25 (5 min per anchor). Time is reduced with more technicians and hammers

Technicians Required: 1 (per sledgehammer)

Tools Required

- Sledgehammer
- Short stake
- Medium stake
- Long stake
- Strike plate
- Measuring tape (at least 22')
- 5x ground anchors

PPE

- Safety glasses (per sledgehammer)

1. Locate a point 18' away from the pivot point of the launch tower. Line up this point with the gin pole (installed on the tower)
2. Use the short stake, strike plate, and sledgehammer to drive two anchors vertically down at this location. Switch to the medium, then long stake when there is insufficient length of rod
3. Leave 2" of cable sticking out of the ground, close enough that they can be routed to attach at a single point
4. Pull on the cable to lock the anchor in the ground
5. Locate three points 16' away from the pivot point of the launch tower, in the geometry shown in "Guy Wire Schematic"
6. Drive at one anchor at each point.
7. *End of procedure*

Winch Installation

Please see drawings for details

Estimated Time: 30 sec

Technicians Required: 1

1. Ensure the cable on the winch is fully retracted
2. Snap the carabiner on the winch frame to the both ground anchors. Ensure the winch cable is facing the pad
3. Ensure the carabiner is twist locked
4. Extend the winch cable until it reaches the "Puller Wire ASY", which is installed on the gin pole
5. Snap the carabiner from the "Puller Wire ASY" onto the winch cable
6. Ensure the carabiner is twist locked
7. *End of procedure*

Tower Installation Procedure

Estimated Time: 30 min

Technicians Required: 3

Tools Required

- Hand drill with $\frac{5}{8}$ " socket and adapter
- Winch handle

PPE

- Gloves x1 pair (for holding the wire on the winch)
1. Locate the turnbuckle on the "Connecting Wire ASY" closest to the gin pole. Leave 2 inches of threads sticking out either end
 2. Place technician #1 at the winch. This technician should have the hand drill/handle
 3. Place technician #2 between the winch and the gin pole. This technician should hold the winch wire with gloves
 4. Place technician #3 at the pad, holding the gin pole
 5. Unwind the winch, and rotate the gin pole until it hits the launch pad
 - a. Technician #1: Use the hand drill/winch to unwind the winch cable
 - b. Technician #2: Keep tension on the winch cable
 - c. Technician #3: Rotate the gin pole to keep tension on the wire
 6. Install the tower (see "Tower Assembly Procedure") onto the launch pad
 7. Install any other GSE required for the tower before it is lifted
 8. Snap the carabiner from the "Connecting Wire Assembly" to the "Cable Mount Assembly" on the tower
 9. Tighten the turnbuckle on the connecting wire assembly to prevent slack
 10. *End of procedure*

Tower Raising Procedure

Estimated Time: 2 min (based on test)

Technicians Required: 6

Tools Required

- Hand drill with 5/8" socket and adapter for the socket
- Winch handle
- Wooden rod (for adjusting wire)

PPE

- Gloves x4 pairs (for handling the wire)
- Hard hat x2
- Safety glasses x7

1. Place technicians #1 to #2 at each guy wire, pulling with the tower rotation direction. Gloves should be worn
2. Place technician #3 at the guy wire, pulling against the tower rotation direction. Gloves should be worn
3. Place technician #4 and #5 at the launch pad. Hard hats should be worn
4. Place technician #6 and #7 at the winch. Technician #6 should have the hand drill. Technician #7 should have gloves and the wooden rod
5. **Ensure there are no people under the tower**
6. Lift the tower
 - a. Technicians #1 to #2: Keep light tension on the guy wires to prevent the tower from swaying side to side. Walk towards the ground anchors. **Do not wrap the wire around your back. If the tower falls, you will be dragged along with it. Keep the wire in front of you. Hold it and the turnbuckle with two hands**
 - b. Technician #3: Hold the wire, do not pull
 - c. Technician #4 and #5: Keep your hands on the rocket and watch for any hoses/wires. Make sure they are secure
 - d. Technician #6: Use the hand drill/handle to wind the wire on the winch
 - e. Technician #7: Use the wooden rod to correct the fleet angle on the winch, ensuring the wire is winding neatly
7. Observe the tower as it approaches the vertical position
 - a. Technicians #1 to #3: Hook your turnbuckle into the ground anchors if possible
 - b. Technicians #4 and #5: Get ready to support the tower as it lands
 - c. Technician #6: Slow down
 - d. Technician #7: Keep correcting the fleet angle
8. The tower is vertical
 - a. Technicians #1 and #2: Tighten your turnbuckles.
 - b. Technician #3: Tighten your turnbuckle.

- c. Technician #6: Remove your drill/handle from the winch. Install the locking bracket on the gin pole. Then, locate the turnbuckle on the end of the gin pole (part of the "Connecting Wire Assembly") and loosen it. Bring the cable to the launch pad and secure it there, away from the rocket and surrounding systems
 - d. Technician #4, #5, #7: You are on standby.
9. *End of procedure*

References

1. Gin Pole Mechanism Drawings:
<https://drive.google.com/open?id=1rt5yeW1eY-8Mm6EDkKu2cCEj6esZ8aQX>
2. Guy Wire Schematic:
https://drive.google.com/open?id=1qoH6KCie765ZaYR5V8Le4__bvGB_x37_
3. Tower Assembly Procedure:
<https://drive.google.com/open?id=1nEuWRCcT0XX4UjCyDY5CeUoVsdslygwFoTTsf7Xvpps>



Shark of the Sky Hybrid Rocket 2019 IREC

Launch Operations Procedures

Compiled on 2022-05-09

Background and Reference

Contents

This document contains two nominal procedures:

- **N1**, *Final Setup and Pre-Launch Checks*, comprises the final checks and tests performed on the Remote Launch Control System (RLCS) prior to rocket launch, as well as avionics systems arming.
- **N2**, *Fill and Launch Operations*, comprises steps for oxidizer fill and rocket launch.

Additionally, this document contains five abort procedures:

- **A1**, *Abort Procedure - Leak At Supply Plumbing*, is used if a plumbing leak is detected when the supply cylinder is initially opened.
- **A2**, *Abort Procedure - Low Supply Pressure*, is used if the oxidizer pressure is below the acceptable limit for launch.
- **A3**, *Abort Procedure - High Supply Pressure*, is used if the oxidizer pressure is above the acceptable limit for launch.
- **A4**, *Abort Procedure - Leak At Fill Plumbing*, is used if a plumbing leak is detected during manual fill leak checks.
- **A5**, *Abort Procedure - Remote Disconnect or Ignition Failure*, is used if the remote disconnect or ignition systems fail, necessitating a full vent of the oxidizer tank.
- **A γ** , *Abort Procedure - Voice Contact Loss*, is used if the operators at the launch site lose the ability to communicate with the operators at launch control.

Personnel Required

The launch operations team consists of four personnel:

- 1 The **Operations Director [OPS]** is stationed at Launch Control. **OPS** directs operations procedures and communicates with the other launch personnel.
- 2 The **Control System Operator [CONTROL]** is stationed at Launch Control and is responsible for operation of RLCS, including remote fill, disconnect, and ignition.
- 3 The **Primary Fill Operator [PRIMARY]** is initially stationed at the Launch Tower and carries out all tasks occurring at the Launch Tower. **PRIMARY** engages the remote disconnect system, arms the vehicle recovery deployment system, connects the ignition wires to the rocket, and operates all manual valves during the manual portion of fill.
- 4 The **Secondary Fill Operator [SECONDARY]** is the backup for **PRIMARY**, and communicates with **OPS**. If **PRIMARY** becomes incapacitated, **SECONDARY** is responsible for removing them from danger.

Sign-Off

To be completed by all test personnel after reading and familiarization with procedures

- 1 **Operations Director [OPS]** _____
- 2 **Control System Operator [CONTROL]** _____
- 3 **Primary Fill Operator [PRIMARY]** _____
- 4 **Secondary Fill Operator [SECONDARY]** _____

[N1] Final Setup and Pre-Launch Checks

Prior to Start

- 1 Ensure that the following procedures are complete:
 - 2 Rocket Assembly procedure
 - 3 RLCS Setup procedure
 - 4 Launch Tower Setup procedure
- 5 Ensure that all personnel as defined above are available and have completed the sign-off.
- 6 Ensure that the following personnel have walkie-talkies and communication is functional:
 - 7 **OPS**
 - 8 **CONTROL**
 - 9 **PRIMARY**
 - 10 **SECONDARY**
- 11 Ensure that **OPS** is in possession of the system control key.
- 12 Ensure that the client-side RLCS box is powered off.
- 13 Ensure that the locations of Launch Control, Launch Tower, and the Minimum Safe Distance are clearly defined.

Launch Control	Launch Tower	Minimum Safe Distance

Nominal Procedure

- 1 **PRIMARY**: Confirm that the following valves are initially closed:
 - 2 Cylinder Valve
 - 3 Remote Fill Valve
 - 4 Parallel Fill Valve
 - 5 Series Fill Valve
 - 6 Line Vent Valve
 - 7 Parallel Vent Valve
- 8 **PRIMARY**: Confirm that the ignition connectors are disconnected from the rocket.
- 9 **SECONDARY**: Confirm that the voltage across the ignition connectors is 0 V.
- 10 **OPS**: Give the system control key to **CONTROL**.
- 11 **CONTROL**: Confirm that all actuator controls are in the off/closed state:

- 12 Remote Fill Valve
- 13 Line Vent Valve
- 14 Remote Disconnect
- 15 Primary Ignition
- 16 Secondary Ignition
- 17 Injector Valve
- 18 **CONTROL**: Engage the key switch and enable actuators.
- 19 **CONTROL** and **SECONDARY**: Confirm that all actuators actuate as intended:
 - 20 Remote Fill Valve
 - 21 Line Vent Valve
 - 22 Remote Disconnect
 - 23 Injector Valve
- 24 **CONTROL** and **SECONDARY**: Confirm that the ignition voltage is 12 V when the ignition button is fired:
 - 25 Primary Ignition
 - 26 Secondary Ignition
- 27 **CONTROL**: Confirm that all DAQ readings are displaying appropriately.
- 28 **OPS**: Record the resting DAQ values:

[M] Dry Mass (lbs)	[P1] Supply Pressure (psi)	[P2] Fill Line Pressure (psi)	[P3] Oxidizer Tank Pressure (psi)

- 29 **CONTROL**: Remove the system control key and give it to **OPS**.
- 30 **PRIMARY**: Arm recovery avionics using remote arming.
- 31 **PRIMARY**: Arm remote disconnect by connecting the springs and fill adapter.
- 32 **PRIMARY**: Connect the ignition connectors to the rocket.

[N2] Fill and Launch Operations

Prior to Start

- 1 Ensure that the following procedure is complete:
- 2 **N1**, *Final Setup and Pre-Launch Checks*
- 3 Ensure that all personnel are available and have completed the sign-off.
- 4 Ensure that the following personnel have walkie-talkies and communication is functional:
- 5 **OPS**
- 6 **CONTROL**
- 7 **PRIMARY**
- 8 **SECONDARY**
- 9 Ensure that **PRIMARY** and **SECONDARY** are wearing face shields and have no exposed skin.
- 10 Ensure that **PRIMARY** is wearing thermal gloves.
- 11 Ensure that **OPS** is in possession of the system control key.

Nominal Procedure

- 1 **SECONDARY**: Confirm that no personnel other than **PRIMARY** and **SECONDARY** are within the Minimum Safe Distance.
- 2 **OPS**: Confirm that the actuator key switch is disabled and that only **OPS** is in possession of the system control key.
- 3 **OPS**: Confirm that the Range Safety Officer and Launch Control Officer have given clearance to proceed with fill procedures.
- 4 **CONTROL**: Confirm that the RLCS client-side box is on and displaying DAQ information.
- 5 **PRIMARY**: Confirm that the following valves are initially closed:
- 6 Cylinder Valve
- 7 Remote Fill Valve
- 8 Parallel Fill Valve
- 9 Series Fill Valve
- 10 Line Vent Valve
- 11 Parallel Vent Valve
- 12 **OPS**: Confirm that the Pressure Relief Valve is initially closed.
- 13 **OPS**: Confirm that the Injector Valve is initially closed.
- 14 **PRIMARY**: Slowly open the Cylinder Valve through $\frac{3}{4}$ of a turn.
 - If leaks are observed:
- 15 **OPS**: Proceed to procedure A1.
- 16 **PRIMARY**: Communicate the supply line pressure as visible on the Pressure Gauge.

- 17 • If the supply line pressure is below 800 psi:
 - OPS**: Proceed to procedure **A2**.
- 18 • If the supply line pressure exceeds 1000 psi:
 - OPS**: Proceed to procedure **A3**.
- 19 **CONTROL**: Confirm that the supply line pressure as read by **PRIMARY** agrees with the supply line pressure [P1] measured by the DAQ system.
- 20 **OPS**: Record the resting rocket dry mass and supply pressure:

[M] Dry Mass (lbs)	[P1] Supply Pressure (psi)

- 21 **PRIMARY**: Open the Series Fill Valve.
- 22 **PRIMARY** and **SECONDARY**: Retreat 100 ft from the fill system.
- 23 **OPS**: Give the system control key to **CONTROL**.
- 24 **CONTROL**: Confirm the following valves are closed:
 - 25 Remote Fill Valve
 - 26 Remote Vent Valve
- 27 **CONTROL**: Engage the key switch and enable actuators.
- 28 **CONTROL**: Open the Remote Fill Valve.
- 29 **CONTROL**: Confirm the following pressures are increasing:
 - 30 [P2] Fill line pressure
 - 31 [P3] Oxidizer tank pressure
- 32 **CONTROL**: Close the Remote Fill Valve.
- 33 **CONTROL**: Confirm the following pressures are stable:
 - 34 [P2] Fill line pressure
 - 35 [P3] Oxidizer tank pressure
 - 36 • If the pressures are decreasing:
 - OPS**: Proceed to procedure **A4**.
- 37 **CONTROL**: Open the Remote Vent Valve.
- 38 **CONTROL**: Confirm the following pressures are atmospheric:
 - 39 [P2] Fill line pressure
 - 40 [P3] Oxidizer tank pressure
- 41 **CONTROL**: Disengage the key switch and disable actuators
- 42 **PRIMARY** and **SECONDARY**: Retreat to the Minimum Safe Distance.

- 43 **SECONDARY**: Confirm that **PRIMARY** and **SECONDARY** are at the Minimum Safe Distance.
- 44 **PAUSE POINT**
- 45 **CONTROL**: Confirm that all actuator controls are in the off state:
 - 46 Remote Fill Valve
 - 47 Line Vent Valve
 - 48 Remote Disconnect
 - 49 Primary Ignition
 - 50 Secondary Ignition
 - 51 Injector Valve
- 52 **CONTROL**: Engage the key switch and enable actuators.
- 53 **CONTROL**: Open the Remote Fill Valve.
- 54 **CONTROL**: Monitor the RLCS display for rocket mass and oxidizer tank pressure.
- 55 **CONTROL**: Confirm the vent valve thermistor has shown a temperature drop.
- 56 **OPS**: Proceed only when the following is true:
 - 57 Rocket mass [M] plateaus
 - 58 Oxidizer tank pressure [P3] is within the acceptable limits
- 59 **CONTROL**: Close the Remote Fill Valve.
- 60 **CONTROL**: Open the Remote Vent Valve.
- 61 **CONTROL**: Confirm that the fill line pressure [P2] is atmospheric.
- 62 **CONTROL**: Actuate Remote Disconnect.
 - If Remote Disconnect fails to actuate:
 - 63 **OPS**: Proceed to procedure **A5**.
- 64 **PAUSE POINT**
- 65 **OPS**: Perform pre-launch checks:
 - 66 Request clearance for launch from the Launch Control Officer.
 - 67 Confirm that all members are aware of launch.
- 68 **CONTROL**: Perform engine startup procedure:
 - 69 Arm the Primary Ignition switch.
 - 70 Hold down the Fire button until the Primary current reading drops to 0 A.
 - In the event of a failed ignition (current drop not observed within 1 minute):
 - 71 **CONTROL**: Disarm the Primary Ignition switch.
 - 72 **CONTROL**: Arm the Secondary Ignition switch.
 - 73 **CONTROL**: Hold down the Fire button until the Secondary current reading drops to 0 A.
 - In the event of a second failed ignition (current drop not observed within 1 minute):
 - 74 **CONTROL**: Disarm the Secondary Ignition switch.
 - 75 **OPS**: Proceed to procedure **A5**.
- 76 **CONTROL**: Start the engine by opening the Injector Valve.

- 77 **ALL**: Observe the rocket during takeoff, ascent, and recovery:
 - 78 First vehicle motion
 - 79 Launch rail departure
 - 80 Engine burnout
 - 81 Payload deployment
 - 82 Drogue parachute deployment
 - 83 Main parachute deployment
 - 84 Approximate recovery area/direction
- 85 **CONTROL**: Disarm RLCS:
 - 86 Disable actuator control by removing the system control key.
 - 87 Give the system control key to **OPS**.
- 88 **OPS**: Confirm that RLCS is disarmed and **OPS** is in possession of the system control key.
- 89 **OPS**: Proceed only when clearance is received from the Launch Control Officer to approach the Launch Tower.
- 90 **PRIMARY** and **SECONDARY**: Approach the Launch Tower.
- 91 **PRIMARY**: Close the Cylinder Valve.
- 92 **PRIMARY**: Open the Parallel Vent Valve.
- 93 **PRIMARY**: Slowly open the Parallel Fill Valve.
- 94 **PRIMARY** and **SECONDARY**: Retreat 20 ft from the fill system.
- 95 **OPS**: Give the master key to **CONTROL**
- 96 **CONTROL**: Engage the key switch and enable actuators.
- 97 **CONTROL**: Open the Remote Fill Valve.
- 98 **CONTROL**: Confirm that the supply line pressure [P1] is atmospheric.
- 99 **PRIMARY**: Disconnect the supply line from the supply cylinder.
- 100 **PRIMARY**: Replace the cap on the nitrous oxide supply cylinder.
- 101 **OPS**: Proceed with teardown and disassembly.

Abort Procedures

[A1] Abort Procedure - Leak At Supply Plumbing

- 1 **PRIMARY**: Close the Cylinder Valve.
- 2 **PRIMARY**: Slowly open the Parallel Vent Valve.
- 3 **PRIMARY**: Slowly open the Parallel Fill Valve.
- 4 **CONTROL**: Confirm the following pressures are atmospheric:
 - 5 [P1] Supply pressure
 - 6 [P2] Fill line pressure
- 7 **PRIMARY**: Disarm the system:
 - 8 Disconnect the ignition leads from the rocket.
 - 9 Detach the torsion springs from the disconnect mechanism.
 - 10 Disarm the recovery electronics system using the magnetic switches.
 - 11 Disarm the payload using the transponder.
 - 12 Disconnect the fill line from the supply cylinder.
 - 13 Replace the cap on the nitrous oxide supply cylinder.
- 14 **OPS**: Revisit plumbing setup.

[A2] Abort Procedure - Low Supply Pressure

- 1 **PRIMARY**: Close the Cylinder Valve.
- 2 **PRIMARY**: Slowly open the Parallel Vent Valve.
- 3 **PRIMARY**: Slowly open the Parallel Fill Valve.
- 4 **CONTROL**: Confirm the following pressures are atmospheric:
 - 5 [P1] Supply pressure
 - 6 [P2] Fill line pressure
- 7 **PRIMARY**: Allow the supply cylinder to warm up.
- 8 **OPS**: Revisit **N1**.

[A3] Abort Procedure - High Supply Pressure

- 1 **PRIMARY**: Close the Cylinder Valve.
- 2 **PRIMARY**: Slowly open the Parallel Vent Valve.
- 3 **PRIMARY**: Slowly open the Parallel Fill Valve.
- 4 **CONTROL**: Confirm the following pressures are atmospheric:
 - 5 [P1] Supply pressure
 - 6 [P2] Fill line pressure
- 7 **PRIMARY**: Disarm the system:

- 8 Disconnect the ignition leads from the rocket.
- 9 Detatch the torsion springs from the disconnect mechanism.
- 10 Disarm the recovery electronics system using the magnetic switches.
- 11 Disarm the payload using the transponder.
- 12 Disconnect the fill line from the supply cylinder.
- 13 Replace the cap on the nitrous oxide supply cylinder.
- 14 **OPS**: Revisit cylinder cooling methods.

[A4] Abort Procedure - Leak At Fill Plumbing

- 1 **CONTROL**: Close the Remote Fill Valve.
- 2 **CONTROL**: Open the Remote Vent Valve.
- 3 **CONTROL**: Confirm the following pressures are atmospheric:
 - 4 P2: Fill line pressure
 - 5 P3: Rocket Tank pressure
- 6 **PRIMARY** and **SECONDARY**: Return to plumbing setup
- 7 **PRIMARY**: Close the Cylinder Valve.
- 8 **PRIMARY**: Slowly open the Parallel Vent Valve.
- 9 **PRIMARY**: Slowly open the Parallel Fill Valve.
- 10 **CONTROL**: Confirm the following pressures are atmospheric:
 - 11 [P1] Supply pressure
 - 12 [P2] Fill line pressure
- 13 **PRIMARY**: Disarm the system:
 - 14 Disconnect the ignition leads from the rocket.
 - 15 Detatch the torsion springs from the disconnect mechanism.
 - 16 Disarm the recovery electronics system using the magnetic switches.
 - 17 Disarm the payload using the transponder.
 - 18 Disconnect the fill line from the supply cylinder.
 - 19 Replace the cap on the nitrous oxide supply cylinder.
- 20 **OPS**: Revisit plumbing setup.

[A5] Abort Procedure - Remote Disconnect or Ignition Failure

- 1 **CONTROL**: Monitor the RLCS display for rocket mass and oxidizer tank pressure as the oxidizer tank vents.
- 2 **OPS**: Proceed only when the following is true:
 - 3 Rocket mass is equal to the pre-launch recorded mass
 - 4 Oxidizer tank pressure [P3] is atmospheric
 - 5 The Launch Control Officer has given clearance to approach the Launch Tower.
- 6 **PRIMARY** and **SECONDARY**: Approach the Launch Tower.

- 7 **PRIMARY**: Close the Cylinder Valve.
- 8 **PRIMARY**: Open the Parallel Vent Valve.
- 9 **PRIMARY**: Slowly open the Parallel Fill Valve.
- 10 **PRIMARY** and **SECONDARY**: Retreat 20 ft from the fill system.
- 11 **OPS**: Give the system control key to **CONTROL**
- 12 **CONTROL**: Engage the system control switch and enable actuators.
- 13 **CONTROL**: Open the Remote Fill Valve.
- 14 **CONTROL**: Confirm the following pressures are atmospheric:
 - 15 [P1] Supply pressure
 - 16 [P2] Fill line pressure
- 17 **PRIMARY**: Disarm the system:
 - 18 Disconnect the ignition leads from the rocket.
 - 19 Detach the torsion springs from the disconnect mechanism.
 - 20 Disarm the recovery electronics system using the magnetic switches.
 - 21 Disarm the payload using the transponder.
 - 22 Disconnect the fill line from the supply cylinder.
 - 23 Replace the cap on the nitrous oxide supply cylinder.
- 24 **OPS**: Proceed with teardown and disassembly.

[Aγ] Abort Procedure - Voice Contact Loss - For Launch Control Operators

- 1 **CONTROL**: Remove the system control key from the client side box.
- 2 **OPS**: Attempt to regain communication with the operators at the pad:
 - 3 Send "**OPS** to **SECONDARY**, **OPS** to **SECONDARY**, **SECONDARY** please come in".
 - 4 If contact is restored:
 - 4 Return to normal operations.
 - 5 Check batteries in radio.
 - 6 Check that radio is set to the proper channel.
 - 7 Check that radio volume is high enough.
 - 8 Wait 30 seconds, then send message again.
 - 9 If contact is restored:
 - 9 Return to normal operations.
 - 10 **OPS**: Wait 30 seconds.
 - 11 **OPS**: Send "**OPS** to **SECONDARY**, **OPS** to **SECONDARY**, going to full abort. I say again, going to full abort."
 - 12 **OPS**: Inform the ESRA official that launch operations will be aborted.
 - 13 **OPS**: Wait for operators to return from pad.
 - 14 **OPS**: Proceed with teardown and disassembly.

[Aγ] Abort Procedure - Voice Contact Loss - For Launch Pad Operators

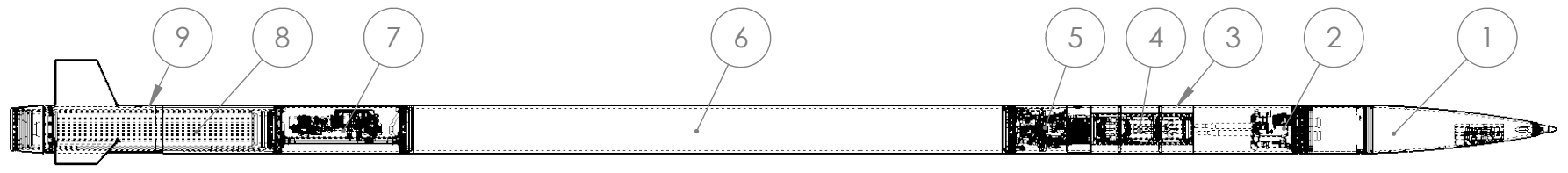
- 1 **SECONDARY**: Attempt to regain communication with the operators at launch control:
- 2 Send "**SECONDARY** to **OPS**, **SECONDARY** to **OPS**, **OPS** please acknowledge".
 - 3 If contact is restored:
 - 4 Return to normal operations.
 - 4 Check batteries in radio.
 - 5 Check that radio is set to the proper channel.
 - 6 Check that radio volume is high enough.
 - 7 Wait 30 seconds, then send message again.
 - 8 If contact is restored:
 - 9 Return to normal operations.
- 9 **SECONDARY** and **PRIMARY**: Approach the rocket, listening for hisses coming from fill system
- 10 **PRIMARY**: Close the Cylinder Valve.
- 11 **PRIMARY**: Slowly open the Parallel Vent Valve.
- 12 **PRIMARY**: Slowly open the Parallel Fill Valve.
- 13 **SECONDARY** and **PRIMARY**: Return to launch control.

G. Engineering Drawings

6 5 4 3 2 1

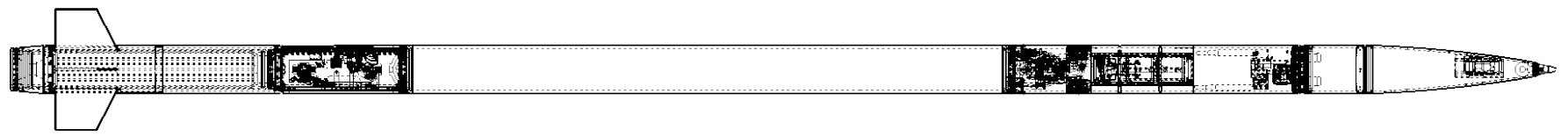
REVISION HISTORY			
REV	DESCRIPTION	DATE	AUTHOR
00	INITIAL RELEASE	2022-05-13	R.K

D



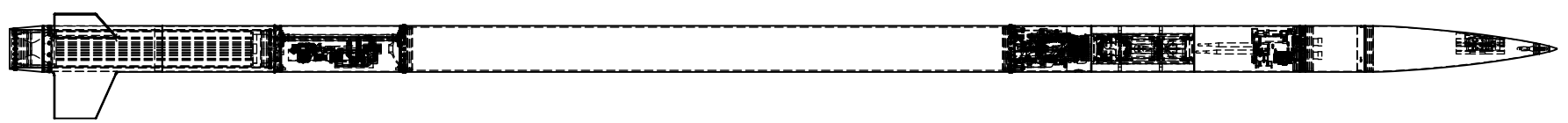
D

C



C

B



B

ITEM NO.	DESCRIPTION
1	RECOVERY SECTION ASSEMBLY
2	RECOVERY ELECTRONICS ASSEMBLY
3	UPPER BODYTUBE ASSEMBLY
4	PAYLOAD ASSEMBLY
5	VENT SECTION ASSEMBLY
6	OXIDIZER TANK ASSEMBLY
7	OXIDIZER TANK AFT SKIRT ASSEMBLY
8	COMBUSTION CHAMBER ASSEMBLY
9	FIN CAN ASSEMBLY

UNLESS OTHERWISE SPECIFIED:
 DIMENSIONS ARE IN INCHES
 REMOVE BURRS AND SHARP EDGES
 TOLERANCES:
 LINEAR: 2 DECIMALS: ±0.010"
 3 DECIMALS: ±0.005"
 ANGULAR: ±1°



NAME	DATE
R. KOBETS	2022-05-13
MATERIAL: VARIOUS	
FINISH:	
WEIGHT:	103.39 LBS

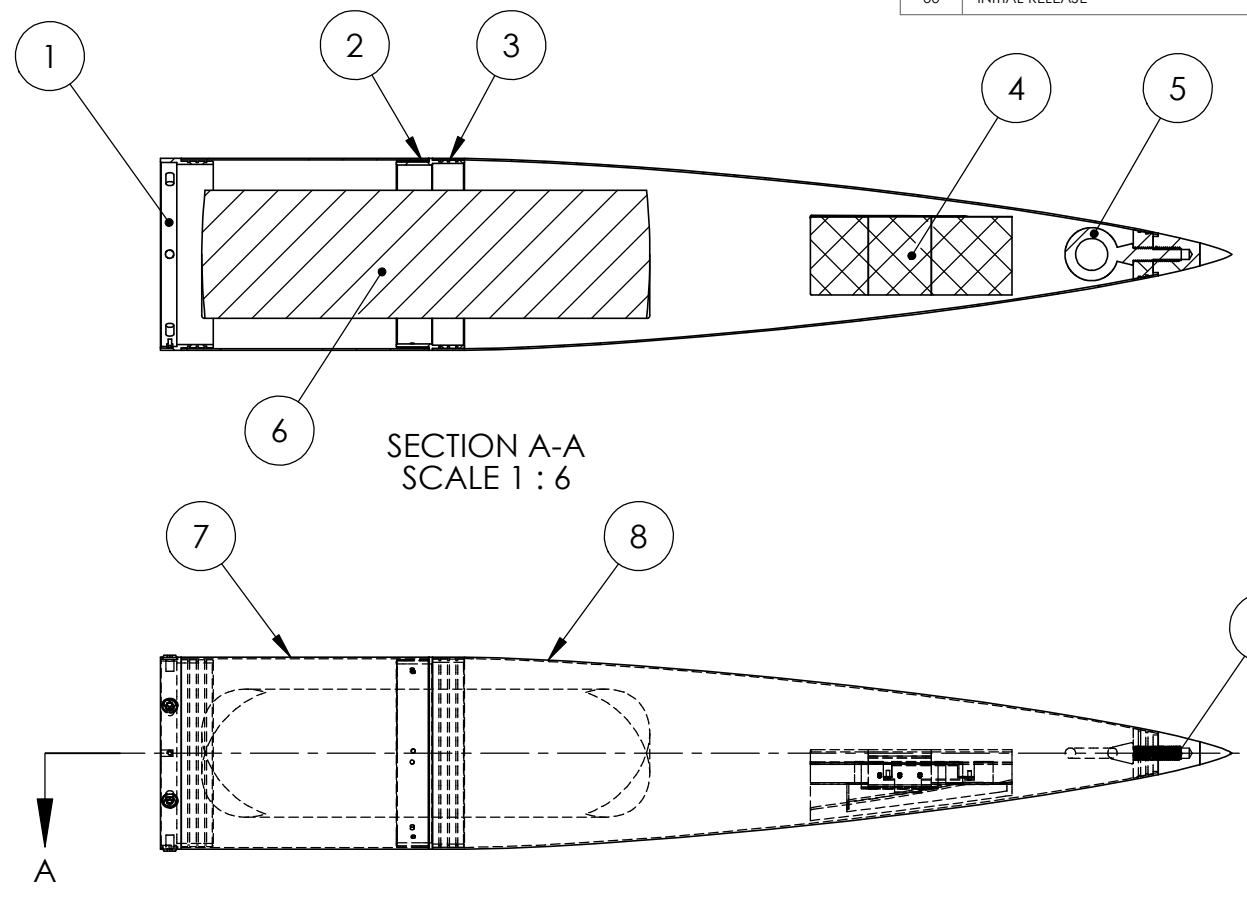
DESCRIPTION: KRAKEN OF THE SKY ROCKET ASSEMBLY		
SIZE	DRAWING NUMBER:	REVISION
A	22-WR-KOTS	00
SCALE: 1:48		DO NOT SCALE DRAWING
SHEET 1 OF 1		

A

A

6 5 4 3 2 1
 SOLIDWORKS Educational Product. For Instructional Use Only.

REVISION HISTORY			
REV	DESCRIPTION	DATE	AUTHOR
00	INITIAL RELEASE	2022-05-08	A.L



ITEM NO.	DESCRIPTION	QTY.
1	PARACHUTE BAY BOTTOM COUPLER	1
2	PARACHUTE TUBE STIFFENER	1
3	NOSECONE SHEAR PIN COUPLER	1
4	BIGREDBEE GPS	1
5	EYEBOLT	1
6	MAIN PARACHUTE BAG	1
7	PARACHUTE BAY TUBE	1
8	NOSECONE	1
9	NOSECONE TIP	1

UNLESS OTHERWISE SPECIFIED:
DIMENSIONS ARE IN INCHES
REMOVE BURRS AND SHARP EDGES
TOLERANCES:
LINEAR: 2 DECIMALS: ±0.010"
3 DECIMALS: ±0.005"
ANGULAR: ±1°

DRAWN	NAME	DATE
	A. LEW	2022-05-08
MATERIAL:		
FINISH:		
WEIGHT: _____ LBS		

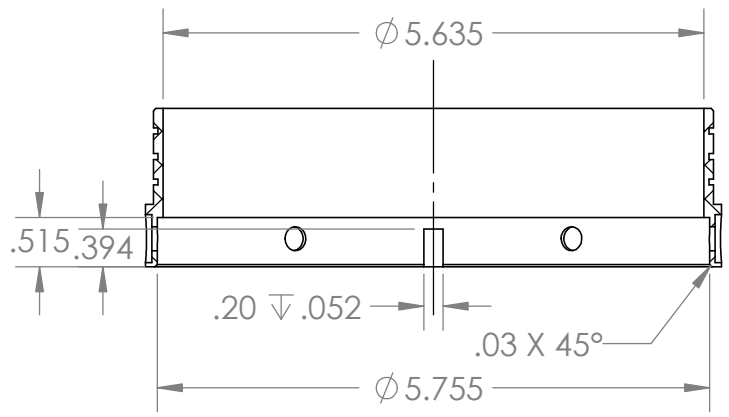
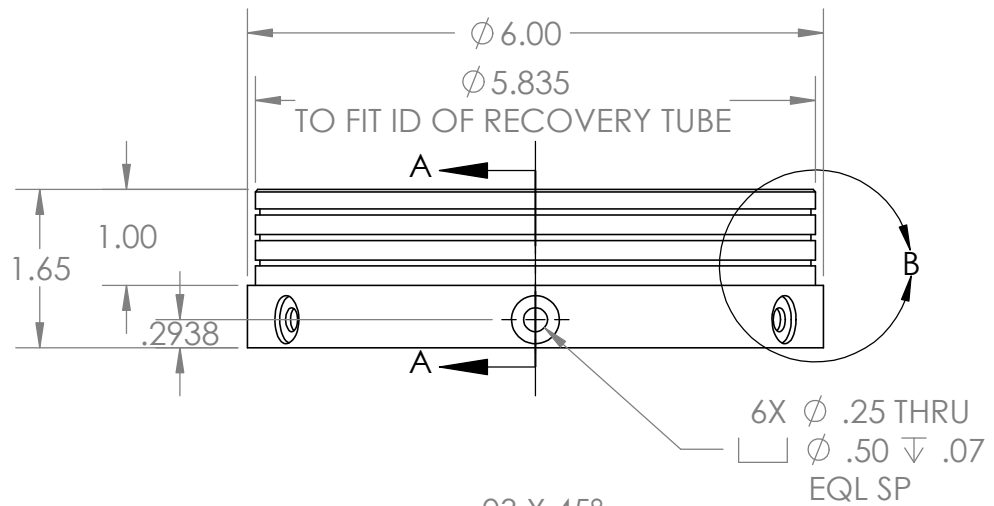
WATERLOO ROCKETRY

DESCRIPTION: RECOVERY SECTION ASSEMBLY		
SIZE A	DRAWING NUMBER: 22-RC-017	REVISION 00
SCALE: 1:6		DO NOT SCALE DRAWING
SHEET 1 OF 1		

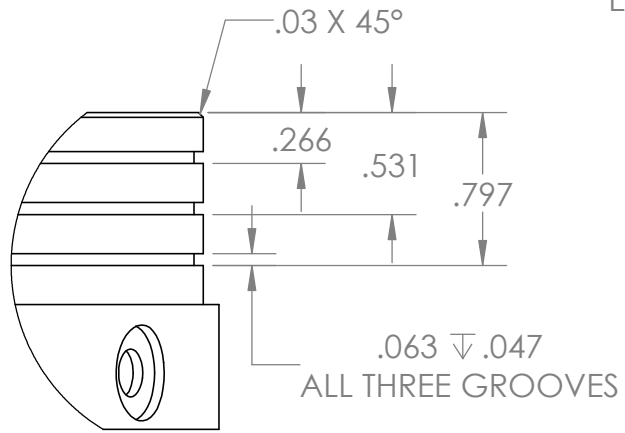
REVISION HISTORY			
REV	DESCRIPTION	DATE	AUTHOR
00	INITIAL RELEASE	2021-11-20	A.LEW
01	REDUCED THICKNESS OF EPOXIED SIDE TO .1IN	2021-12-22	A.LEW



SCALE 1:5



SECTION A-A



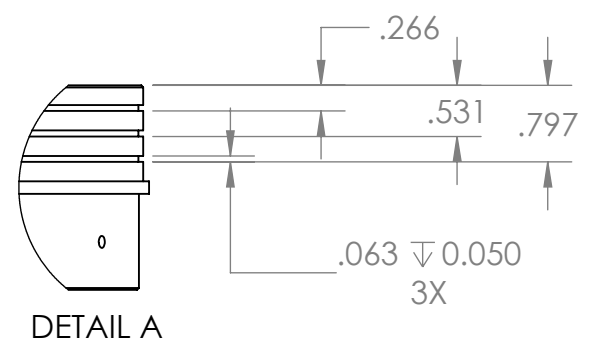
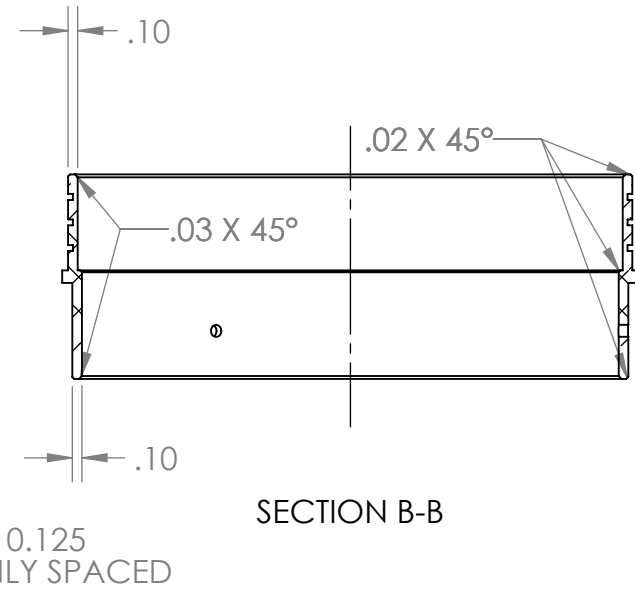
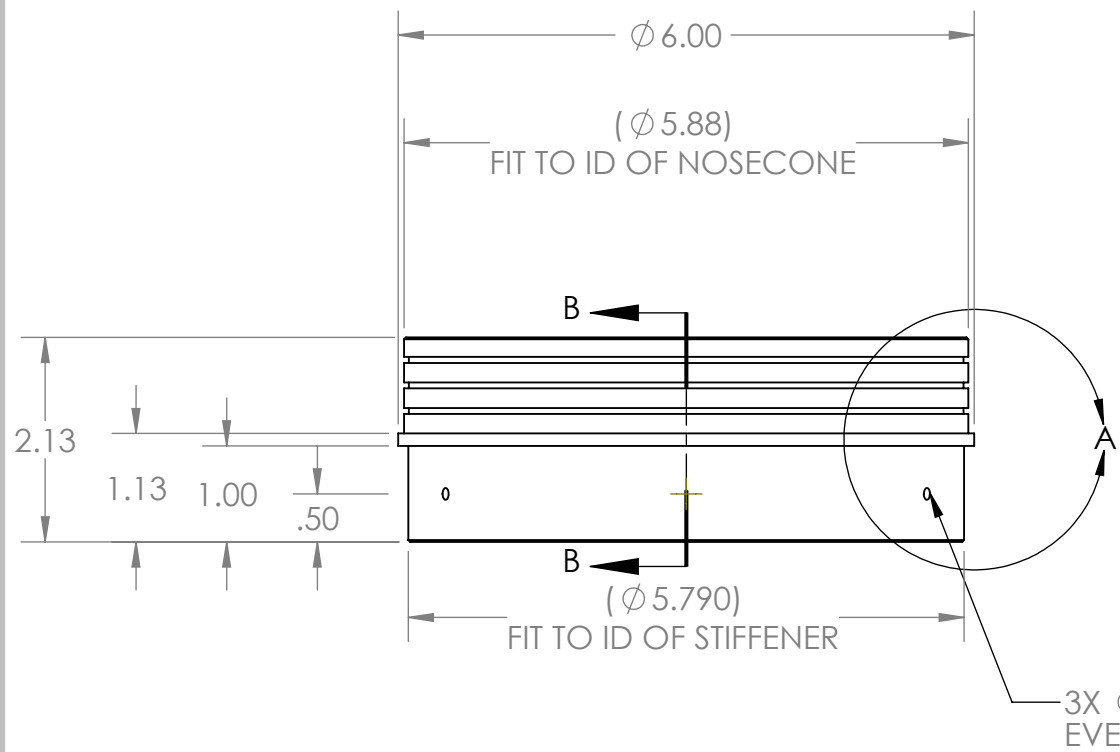
DETAIL B
SCALE 1:1

UNLESS OTHERWISE SPECIFIED:
 DIMENSIONS ARE IN INCHES
 REMOVE BURRS AND SHARP EDGES
 TOLERANCES:
 LINEAR: 2 DECIMALS: $\pm 0.010''$
 3 DECIMALS: $\pm 0.005''$
 ANGULAR: $\pm 1^\circ$



DRAWN: A.LEW		DATE: 2021-11-20	DESCRIPTION: PARACHUTE TUBE BOTTOM COUPLER	
MATERIAL: 6061-T6			SIZE: A	DRAWING NUMBER: 22-AF-005
FINISH: AS MACHINED			REVISION: 01	
WEIGHT: 0.38	LBS	SCALE: 1:2	DO NOT SCALE DRAWING	SHEET 1 OF 1

REVISION HISTORY			
REV	DESCRIPTION	DATE	AUTHOR
00	INITIAL RELEASE	2021-11-27	S. A-C
01	REVISED TO REDUCE AMOUNT OF MATERIAL	2021-12-14	S. A-C



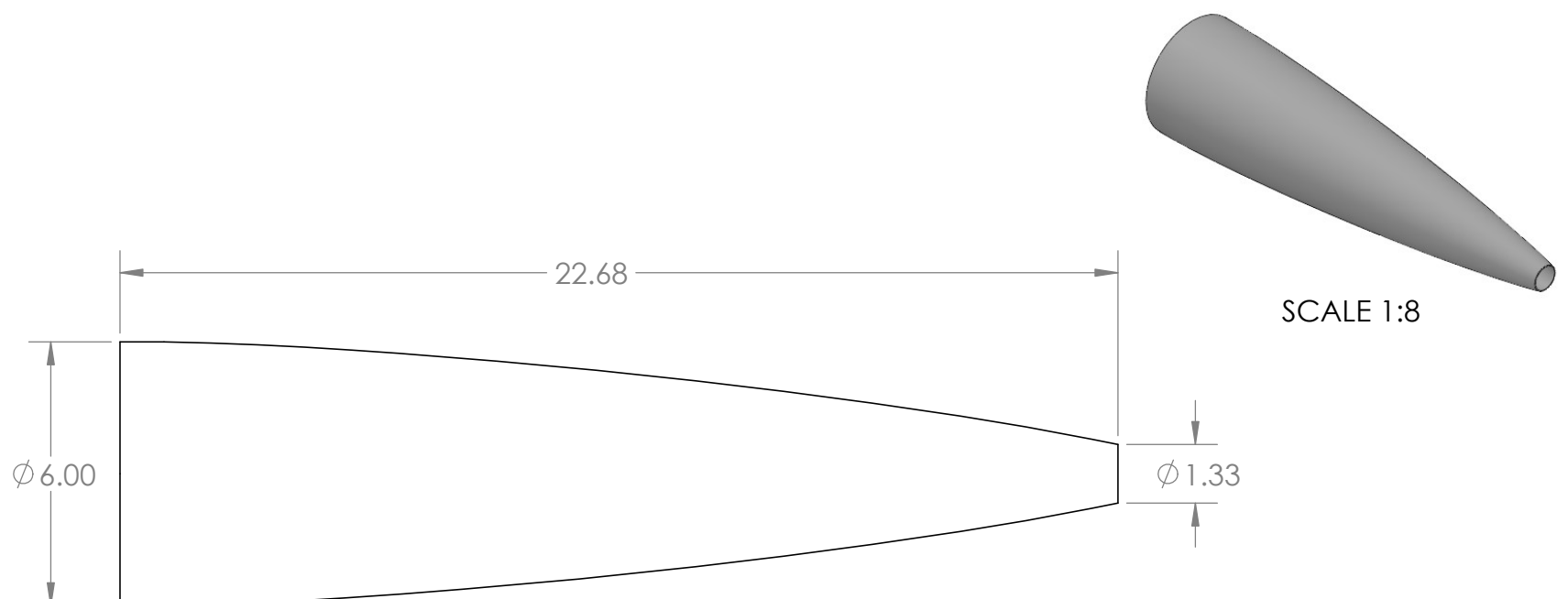
NOTE: MANUFACTURE WITH PARACHUTE TUBE STIFFENER

UNLESS OTHERWISE SPECIFIED:
 DIMENSIONS ARE IN INCHES
 REMOVE BURRS AND SHARP EDGES
 TOLERANCES:
 LINEAR: 2 DECIMALS: $\pm 0.010''$
 3 DECIMALS: $\pm 0.005''$
 ANGULAR: $\pm 1^\circ$



DRAWN: S. A-C		DATE: 2021-11-27	DESCRIPTION: NOSECONE COUPLER	
MATERIAL: 6061-T6 (SS)			SIZE: A	DRAWING NUMBER: 21-RC-013
FINISH: AS MACHINED			REVISION: 01	
WEIGHT: 0.38	LBS	SCALE: 1:2	DO NOT SCALE DRAWING	SHEET 1 OF 1

REVISION HISTORY			
REV	DESCRIPTION	DATE	AUTHOR
00	INITIAL RELEASE	2022-05-10	A.L



UNLESS OTHERWISE SPECIFIED:
 DIMENSIONS ARE IN INCHES
 REMOVE BURRS AND SHARP EDGES
 TOLERANCES:
 LINEAR: 2 DECIMALS: $\pm 0.010''$
 3 DECIMALS: $\pm 0.005''$
 ANGULAR: $\pm 1^\circ$



**WATERLOO
ROCKETRY**

DRAWN	NAME	DATE	DESCRIPTION:
	A.LEW	2022-05-10	NOSECONE
MATERIAL:			SIZE
FINISH:			DRAWING NUMBER:
WEIGHT:			REVISION
LBS			00
SCALE: 1:4		DO NOT SCALE DRAWING	
SHEET 1 OF 1			

6

5

4

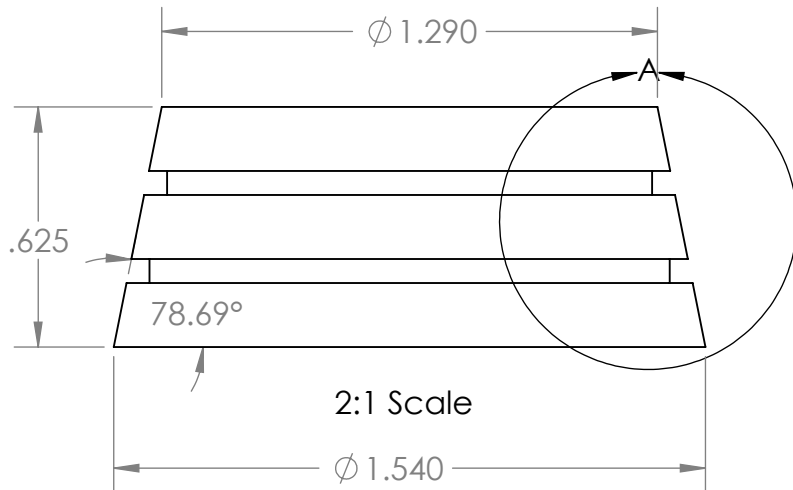
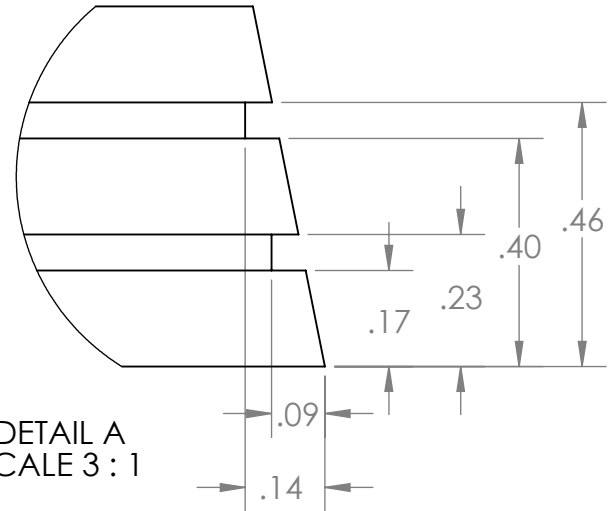
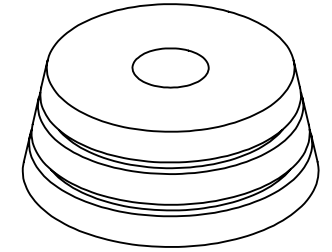
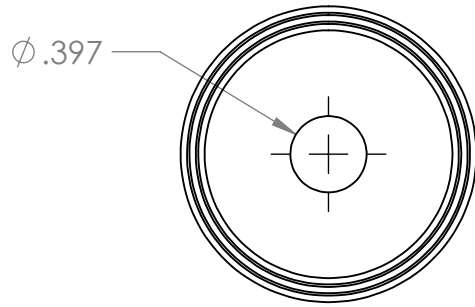
3

2

1

REVISION HISTORY

REV	DESCRIPTION	DATE	AUTHOR
00	INITIAL RELEASE FOR 2019 - SOTS	2019-05-22	R.K
01	DIAMETER CHANGE FOR 2021 - KOTS NOSECONE	2021-12-15	S.K



UNLESS OTHERWISE SPECIFIED:
 DIMENSIONS ARE IN INCHES
 REMOVE BURRS AND SHARP EDGES
 TOLERANCES:
 LINEAR: 2 DECIMALS: $\pm 0.010''$
 3 DECIMALS: $\pm 0.005''$
 ANGULAR: $\pm 1^\circ$

DRAWN	NAME	DATE
SHIRLEY KONG		2021-12-15

MATERIAL:
6061-T6

FINISH:
AS-MACHINED

WEIGHT: 0.0858 LBS



**WATERLOO
ROCKETRY**

DESCRIPTION:
NOSECONE TIP SPACER

SIZE	DRAWING NUMBER:	REVISION
A4	22-AF-006	01

SCALE: 1:1 SHEET 1 OF 1

6

5

4

3

2

1

D

D

C

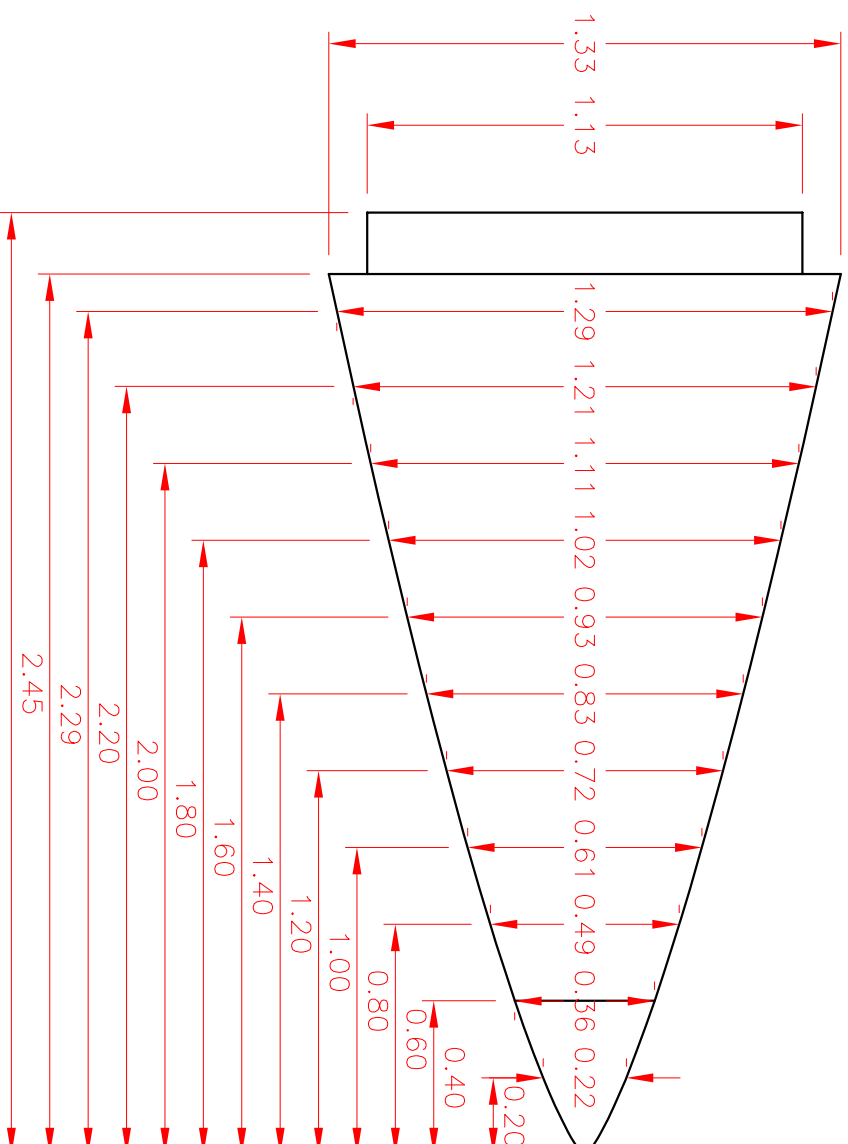
C

B

B

A

A

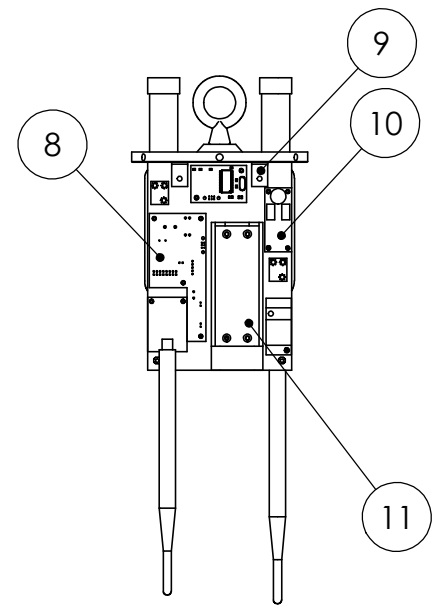
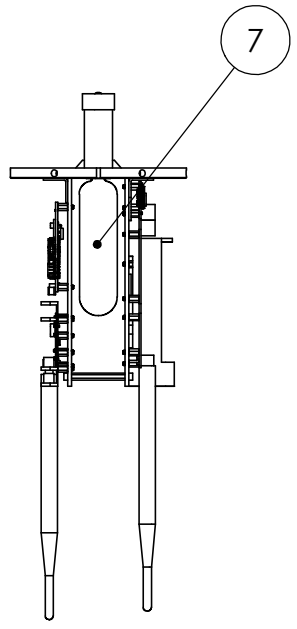
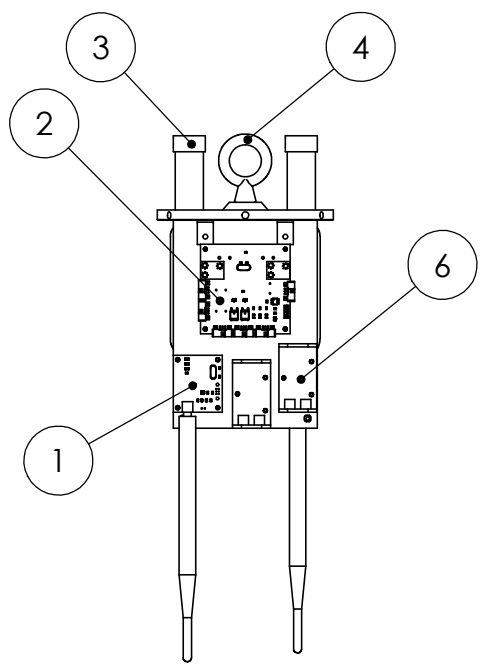
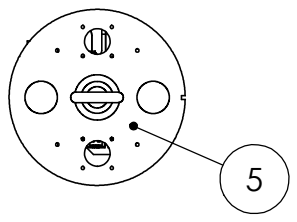


All dim in inches.

Size: A

Scale: 2:1

REVISION HISTORY			
REV	DESCRIPTION	DATE	AUTHOR
00	INITIAL RELEASE	2022-05-08	A.L



ITEM NO.	DESCRIPTION	QTY.
1	GPS	1
2	REMOTE ARMING BOARD	1
3	CO2 EJECTOR	2
4	EYEBOLT	1
5	RECOVERY BULKHEAD	1
6	9V BATTERY HOLDER	2
7	CO2 CYLINDER	2
8	TELEMETARY TRANSMITTER	1
9	L BRACKET	4
10	STRATOLOGGER	1
11	LIPO (12V) BATTERY HOLDER	1

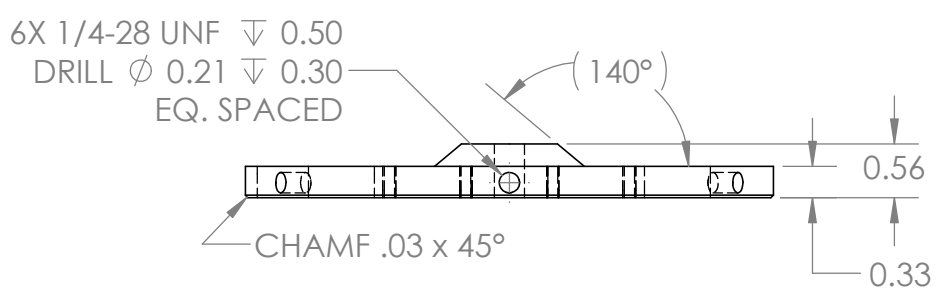
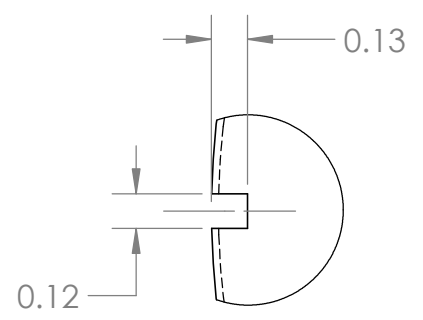
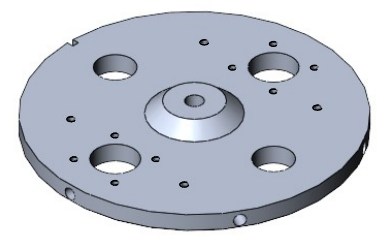
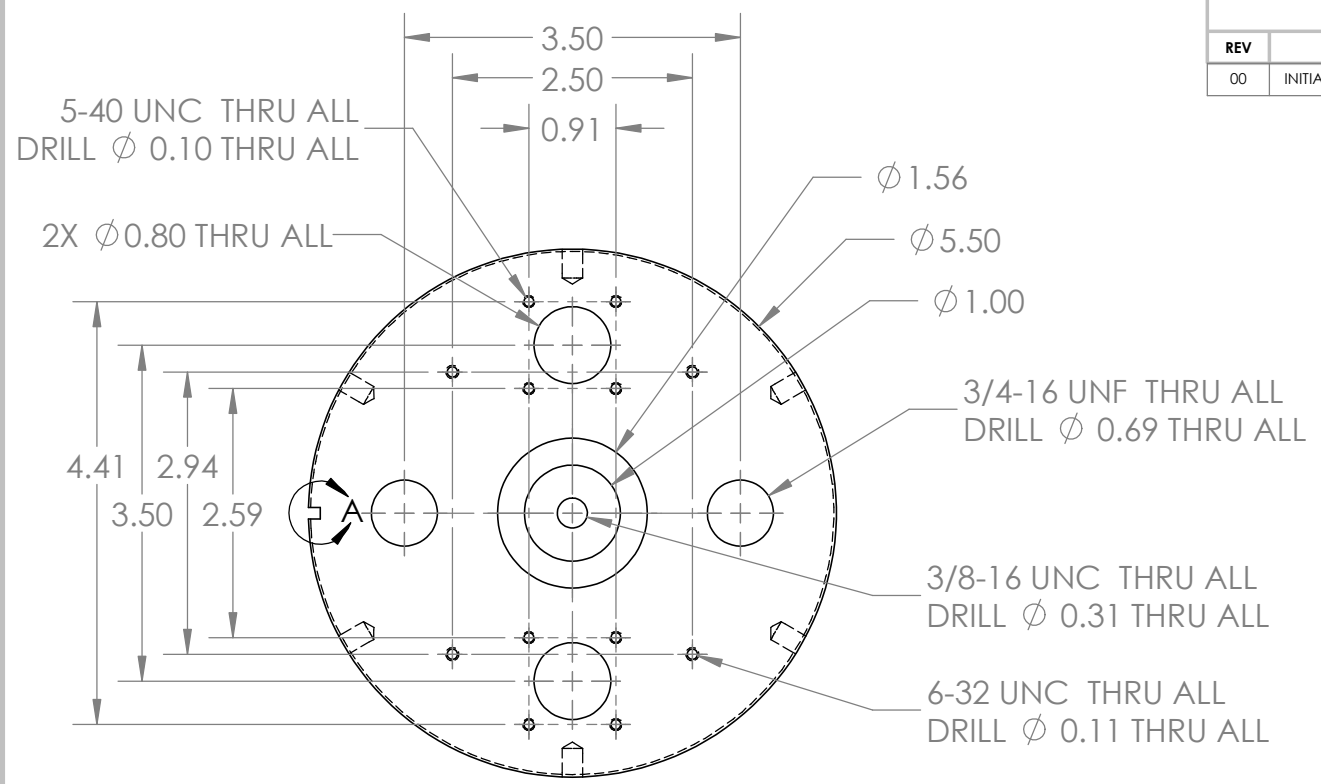
UNLESS OTHERWISE SPECIFIED:
 DIMENSIONS ARE IN INCHES
 REMOVE BURRS AND SHARP EDGES
 TOLERANCES:
 LINEAR: 2 DECIMALS: ±0.010"
 3 DECIMALS: ±0.005"
 ANGULAR: ±1°

DRAWN	NAME	DATE
	A. LEW	2022-05-08
MATERIAL:		
FINISH:		
WEIGHT:	4.36	LBS

WATERLOO ROCKETRY

DESCRIPTION: REEFING RECOVERY ELECTRONICS ASSEMBLY		
SIZE: A	DRAWING NUMBER: 22-RC-018	REVISION: 00
SCALE: 1:6	DO NOT SCALE DRAWING	SHEET 1 OF 1

REVISION HISTORY			
REV	DESCRIPTION	DATE	AUTHOR
00	INITIAL RELEASE	2022-07-01	R.K



UNLESS OTHERWISE SPECIFIED:
DIMENSIONS ARE IN INCHES
REMOVE BURRS AND SHARP EDGES
TOLERANCES:
LINEAR: 2 DECIMALS: ±0.010"
3 DECIMALS: ±0.005"
ANGULAR: ±1°

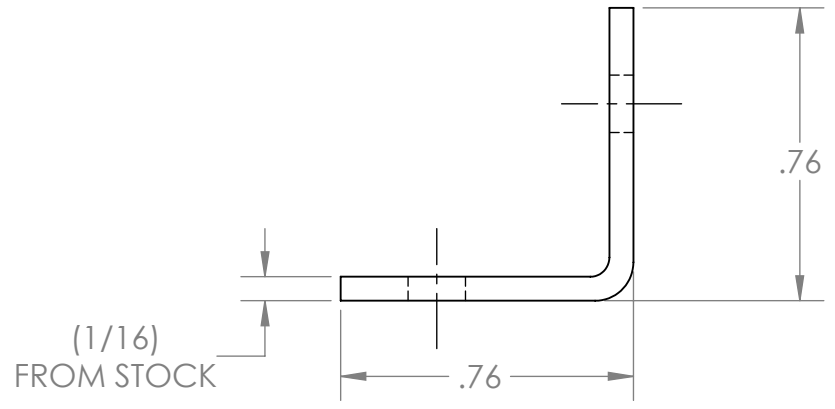
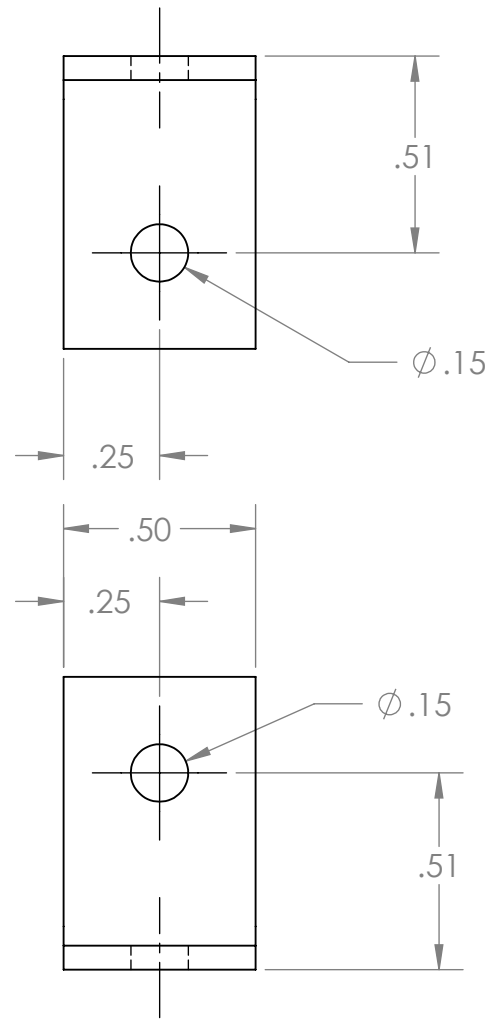
NAME	DATE
R. KOBETS	2022-01-07
MATERIAL:	6061-T6 (SS)
FINISH:	BRUSHED
WEIGHT:	0.71 LBS



WATERLOO ROCKETRY

DESCRIPTION: RECOVERY BULKHEAD		
SIZE: A	DRAWING NUMBER: 22-RC-016	REVISION: 00
SCALE: 1:2	DO NOT SCALE DRAWING	SHEET 1 OF 1

REVISION HISTORY			
REV	DESCRIPTION	DATE	AUTHOR
00	INITIAL RELEASE	2021-11-29	S. A-C
01	REMADE FOR ALUMINUM ANGLE	2021-12-22	S. A-C

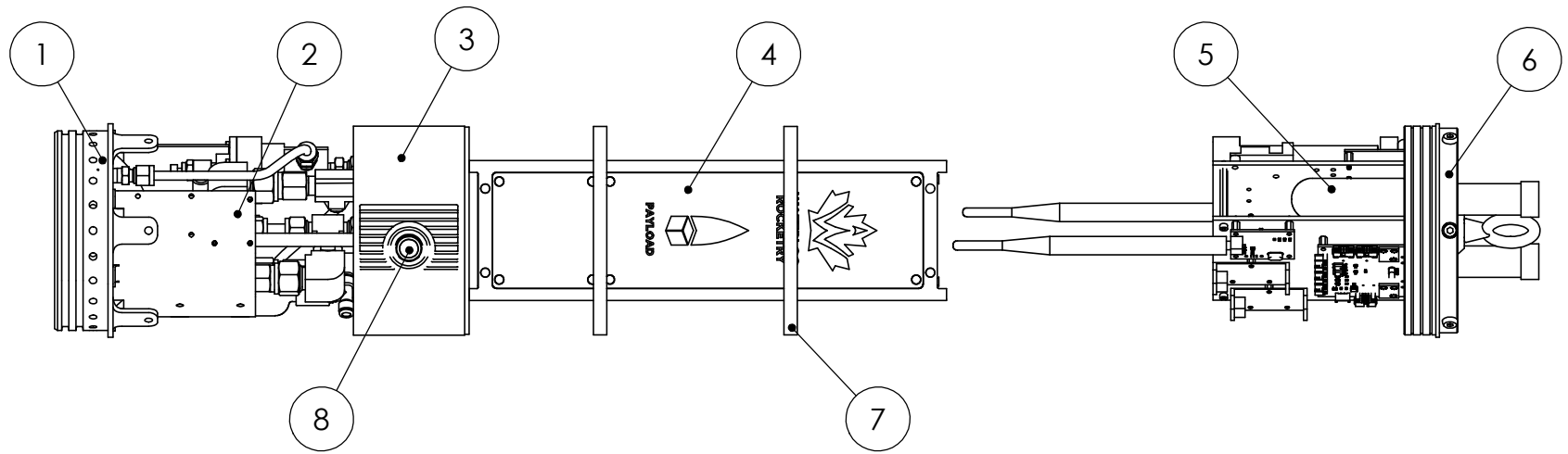


UNLESS OTHERWISE SPECIFIED:
 DIMENSIONS ARE IN INCHES
 REMOVE BURRS AND SHARP EDGES
 TOLERANCES:
 LINEAR: 2 DECIMALS: $\pm 0.010''$
 3 DECIMALS: $\pm 0.005''$
 ANGULAR: $\pm 1^\circ$



NAME	DATE	DESCRIPTION:	
S. A-C	2021-12-22	L-BRACKET	
MATERIAL:		SIZE	DRAWING NUMBER:
6061 Alloy		A	21-RC-015
FINISH:		REVISION	
AS MACHINED			01
WEIGHT:	0.00 LBS	SCALE: 2:1	DO NOT SCALE DRAWING
		SHEET 1 OF 1	

REVISION HISTORY			
REV	DESCRIPTION	DATE	AUTHOR
00	INITIAL RELEASE	2022-05-09	A.L



NOTE: UPPER BODYTUBE NOT SHOWN

ITEM NO.	DESCRIPTION	QTY.
1	VENT BULKHEAD	1
2	VENT SECTION	1
3	PAYLOAD BAY SHEAR RING	1
4	CUBESAT	1
5	RECOVERY ELECTORNICS	1
6	RECOVERY ELECTRONICS TOP COUPLER	1
7	PAYBAY CENTERING PLATE	2
8	PICAM	2

UNLESS OTHERWISE SPECIFIED: DIMENSIONS ARE IN INCHES REMOVE BURRS AND SHARP EDGES TOLERANCES: LINEAR: 2 DECIMALS: ±0.010" 3 DECIMALS: ±0.005" ANGULAR: ±1°		
DRAWN	NAME	DATE
	A.LEW	2022-05-09
MATERIAL:		
FINISH:		
WEIGHT:	103.61	LBS



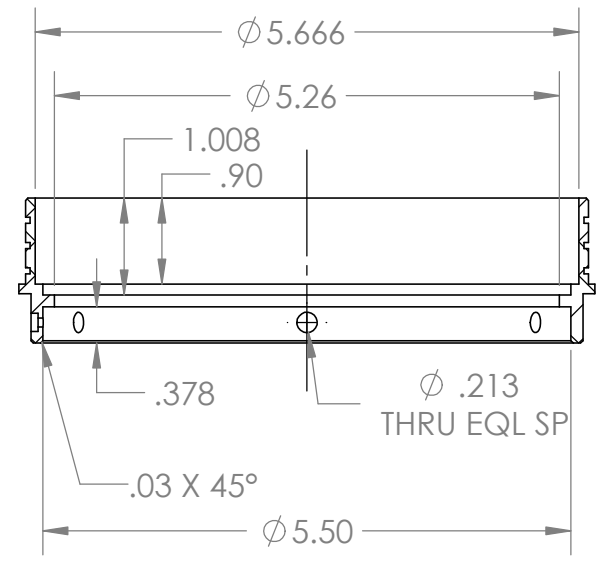
WATERLOO ROCKETRY

DESCRIPTION: UPPER BODYTUBE SECTION		
SIZE A	DRAWING NUMBER: 22-AF-013	REVISION 00
SCALE: 1:12	DO NOT SCALE DRAWING	SHEET 1 OF 1

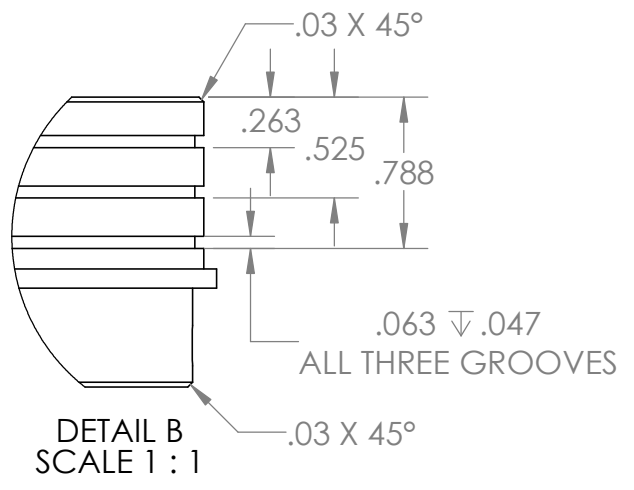
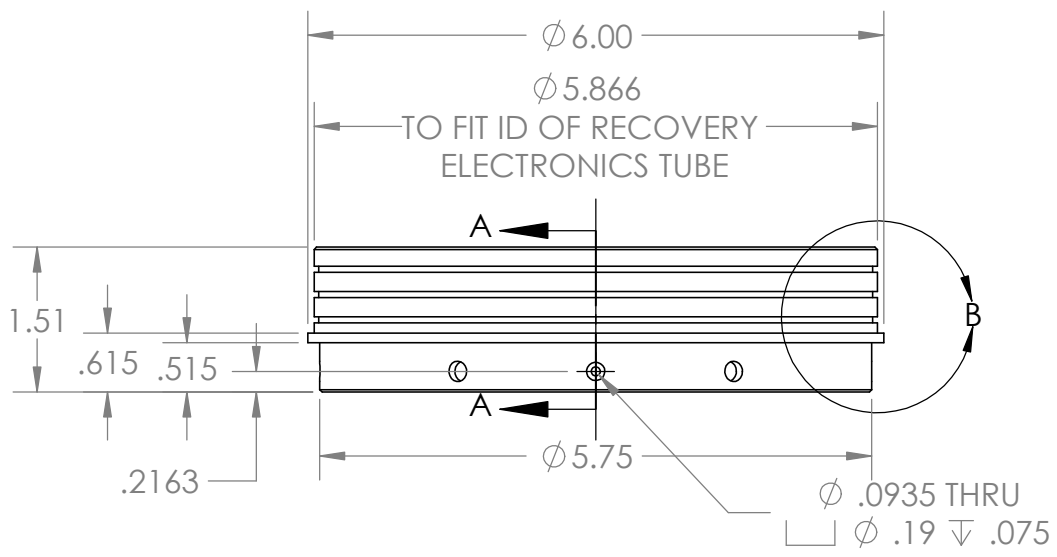
REVISION HISTORY			
REV	DESCRIPTION	DATE	AUTHOR
00	INITIAL RELEASE	2021-11-13	A.LEW
01	REDUCED THICKNESS OF EPOXIED SIDE TO .1IN	2021-12-22	A.LEW



SCALE 1:5



SECTION A-A



DETAIL B
SCALE 1 : 1

UNLESS OTHERWISE SPECIFIED:
DIMENSIONS ARE IN INCHES
REMOVE BURRS AND SHARP EDGES
TOLERANCES:
LINEAR: 2 DECIMALS: ±0.010"
3 DECIMALS: ±0.005"
ANGULAR: ±1°

DRAWN	NAME	DATE
A.LEW		2021-11-13
MATERIAL: 6061-T6		
FINISH: AS MACHINED		
WEIGHT:	0.36	LBS

**WATERLOO
ROCKETRY**

DESCRIPTION: RECOVERY ELECTRONICS TOP COUPLER		
SIZE A	DRAWING NUMBER: 22-AF-005	REVISION 01
SCALE: 1:2	DO NOT SCALE DRAWING	SHEET 1 OF 1

6

5

4

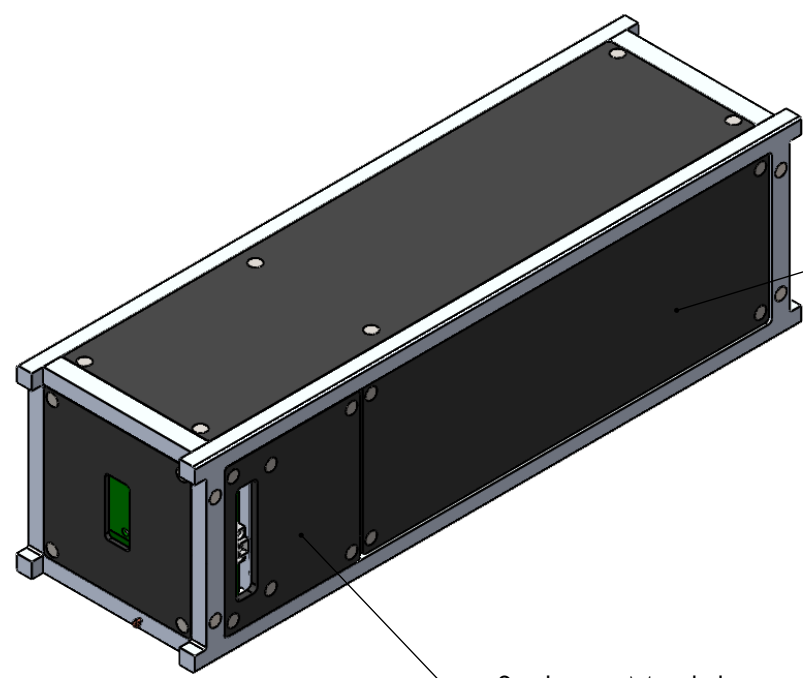
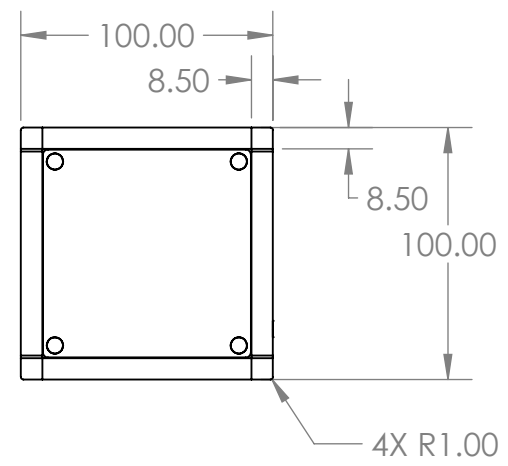
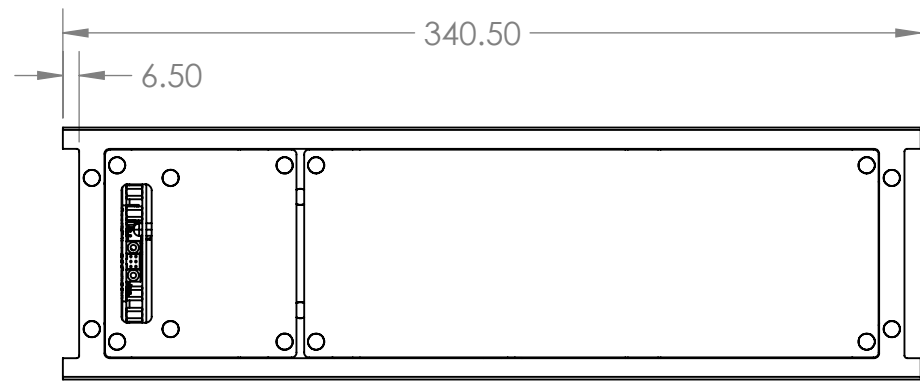
3

2

1

REVISION HISTORY

REV	DESCRIPTION	DATE	AUTHOR
0	INITIAL RELEASE	2021-05-16	K.T.



Scintillator Module

Systems Module

UNLESS OTHERWISE SPECIFIED:
 DIMENSIONS ARE IN MILLIMETERS
 REMOVE BURRS AND SHARP EDGES

TOLERANCES:
 LINEAR: ±0.15 mm
 ANGULAR: ±1°



NAME	DATE	DESCRIPTION:
K. TAM	2021-05-16	PAYLOAD 2021 ASSEMBLY
MATERIAL: Various		SIZE
FINISH: Finely Sanded		DRAWING NUMBER: A 21-PA-000
WEIGHT: ~4000	GRAMS	REVISION: 0

SCALE: 1:3	DO NOT SCALE DRAWING	SHEET 1 OF 1
------------	----------------------	--------------

6

5

4

3

2

1

D

D

C

C

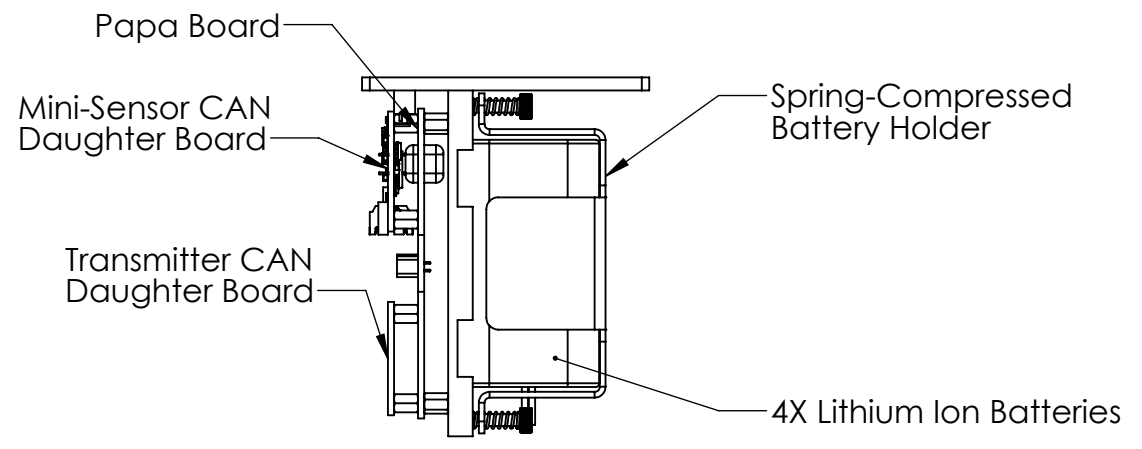
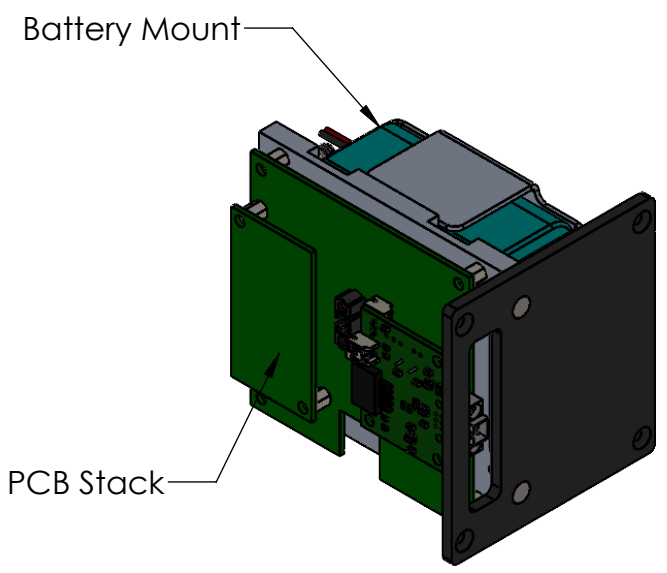
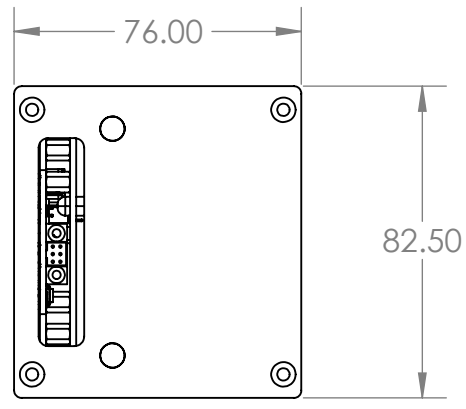
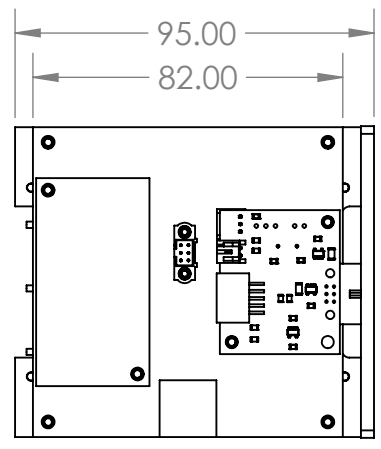
B

B

A

A

REVISION HISTORY			
REV	DESCRIPTION	DATE	AUTHOR
00	INITIAL RELEASE	2021-05-16	K.T.



UNLESS OTHERWISE SPECIFIED:
DIMENSIONS ARE IN MILLIMETERS
REMOVE BURRS AND SHARP EDGES

TOLERANCES:
LINEAR: ± 0.15 mm
ANGULAR: $\pm 1^\circ$

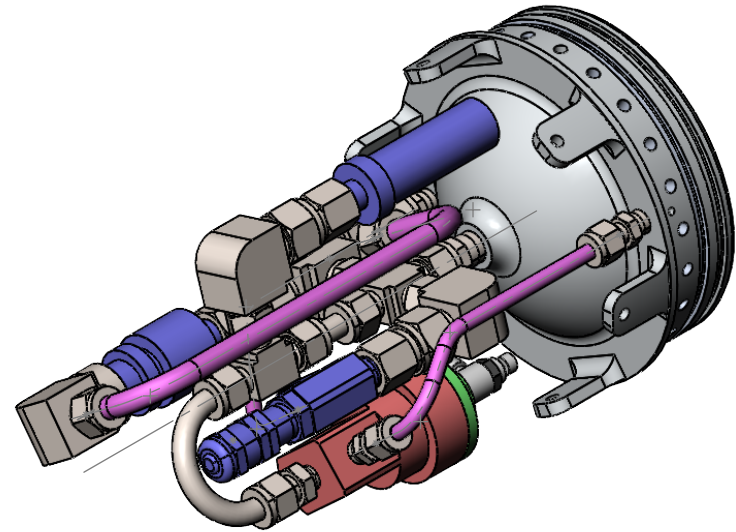
NAME	DATE
DRAWN	
MATERIAL:	VARIOUS
FINISH:	FINELY SANDED
WEIGHT:	645.55 GRAMS

WATERLOO ROCKETRY

DESCRIPTION: SYSTEMS MODULE ASSEMBLY		
SIZE: A	DRAWING NUMBER: 21-PA-016	REVISION: 0
SCALE: 1:2	DO NOT SCALE DRAWING	SHEET 1 OF 1

ITEM NO.	PART NUMBER	QTY.
1	Vent Valve Assembly	1
2	Burst Disk Model	1
3	straight tubing	1
4	SS-600-4	1
5	SS-6-TA-1-4	1
6	SS-6-TA-7-4	3
7	SS-12M0-2R-12M	3
8	U-bend tube	1
9	SS-600-1-2	1
10	SS-600-3	1
11	Pressure Transducer Model	1
12	22-N01-06-J	1
13	SOTS- Vent Bulkhead w vent ports	1
14	SS-6-TA-1-2	1
15	SS-4R3A1	1
16	SS-600-8-8	1
17	SS-600-3-4-6	1
18	Tube_1-Vent Section	1
19	Tube_2-Vent Section	1
20	SS-400-1-2	2
21	Tube_3-Vent Section	1

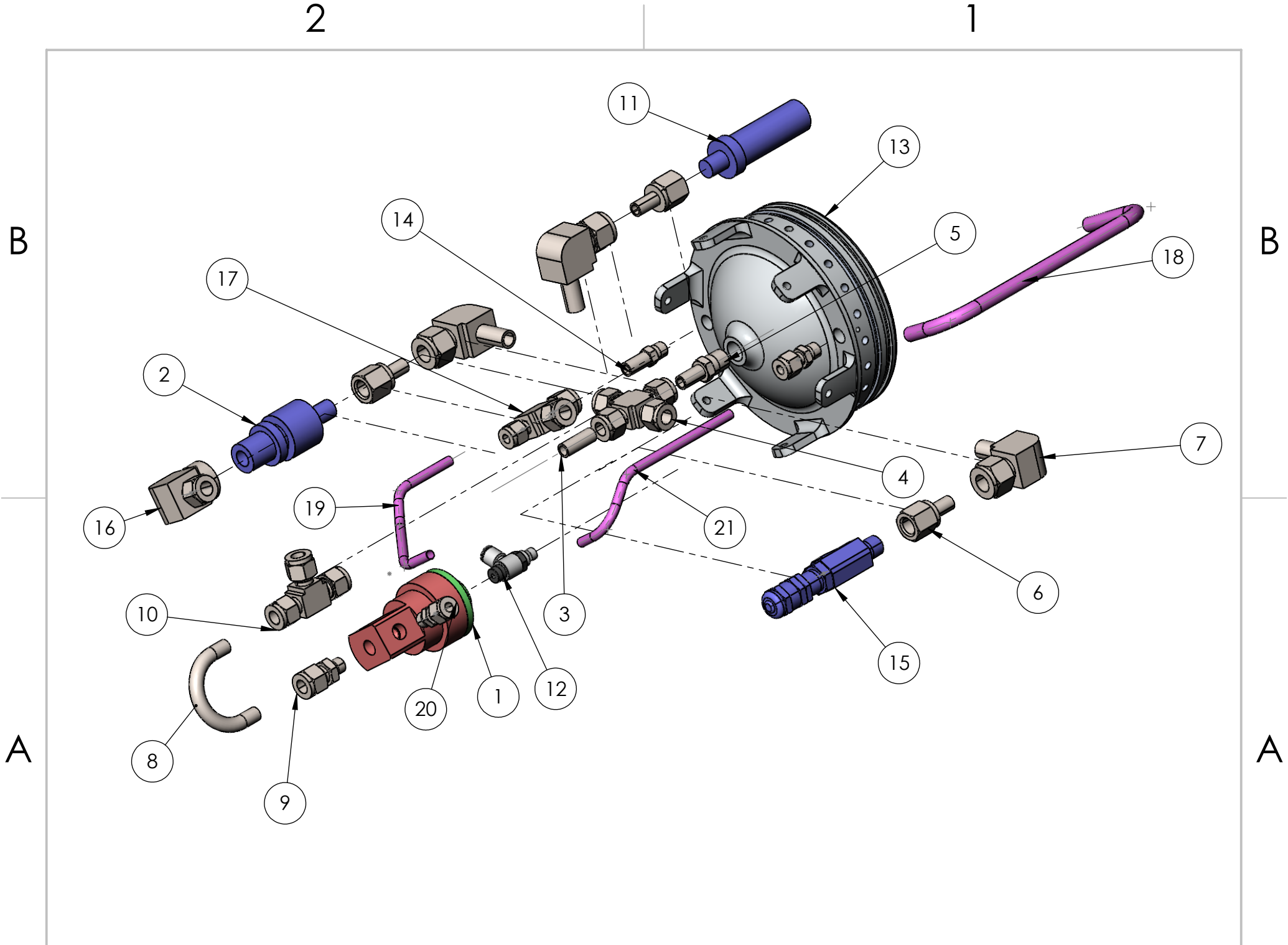
REVISION HISTORY			
REV	DESCRIPTION	DATE	AUTHOR
01	XXXXXXXXXXXXXX	XXX XX/XXXX	J.L



UNLESS OTHERWISE SPECIFIED:
 DIMENSIONS ARE IN INCHES
 REMOVE BURRS AND SHARP EDGES
 TOLERANCES:
 LINEAR: 2 DECIMALS: ±0.010"
 3 DECIMALS: ±0.005"
 ANGULAR: ±1°



DRAWN		NAME		DATE		DESCRIPTION: Vent Section HPP	
MATERIAL: Material <not specified>		SIZE A		DRAWING NUMBER:		REVISION	
FINISH:		WEIGHT: 6.78		LBS		SCALE: 1:4	
				DO NOT SCALE DRAWING		SHEET 1 OF 7	

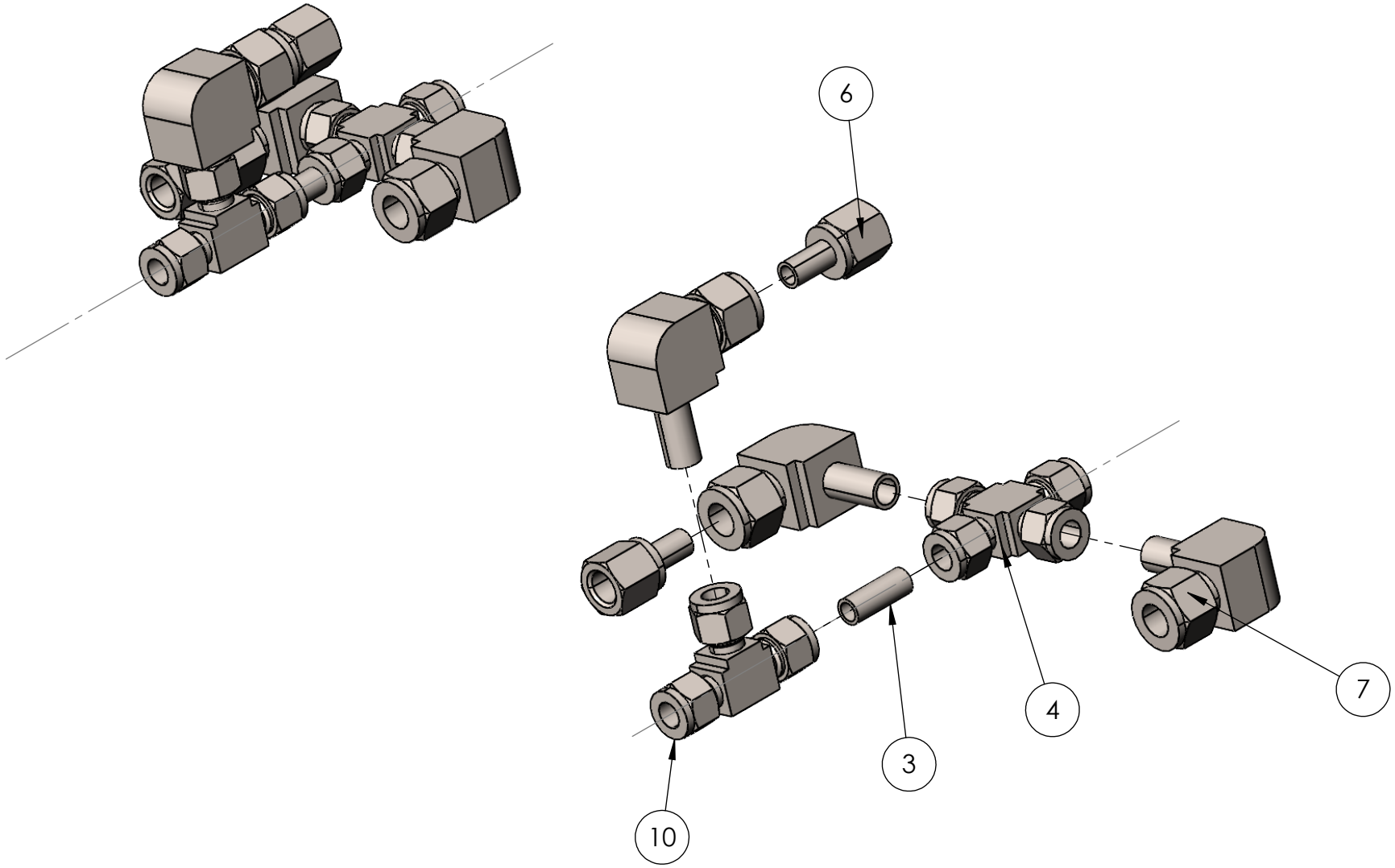


2

1

B

B



A

A

2

1

2

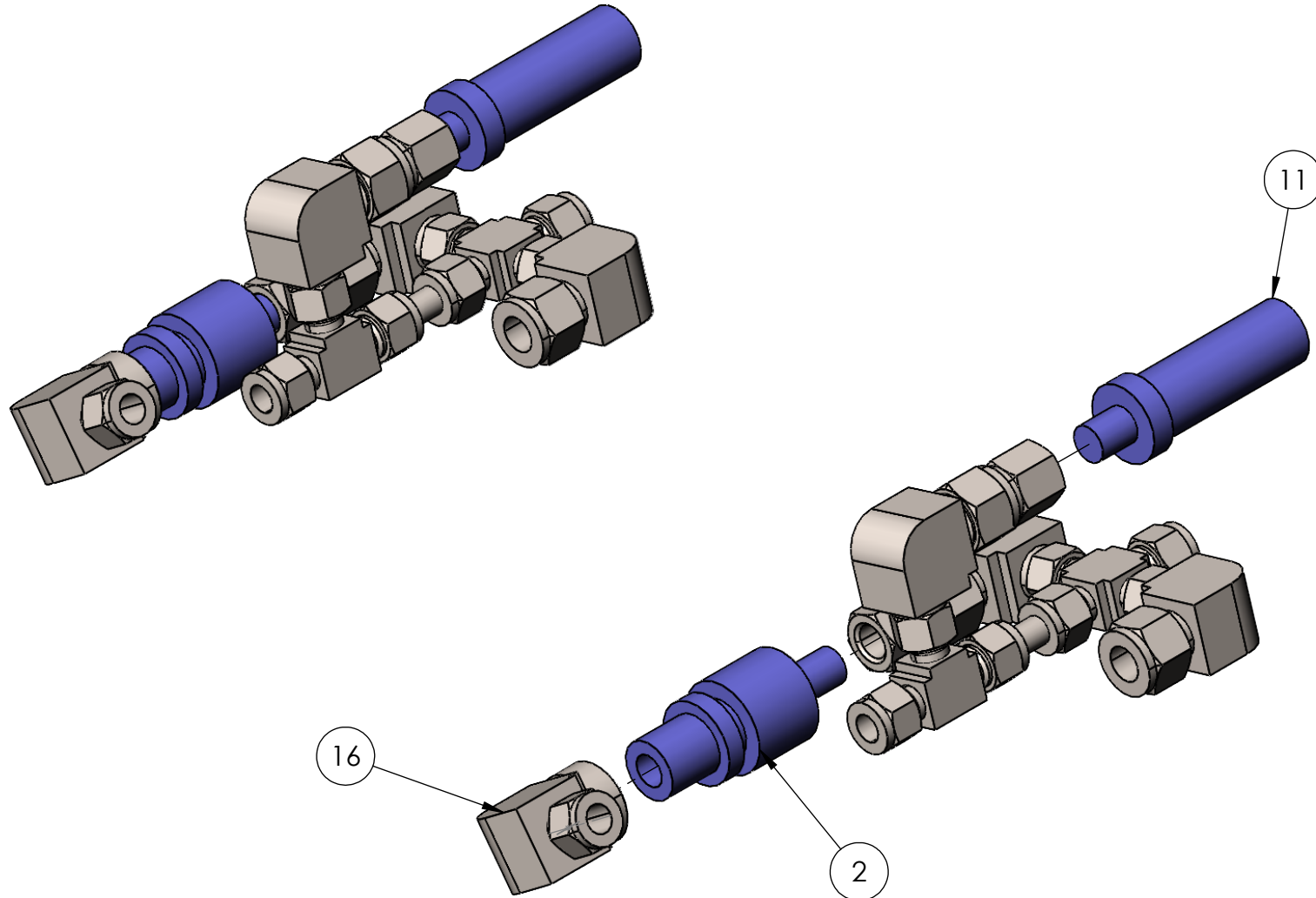
1

B

B

A

A



2

1

2

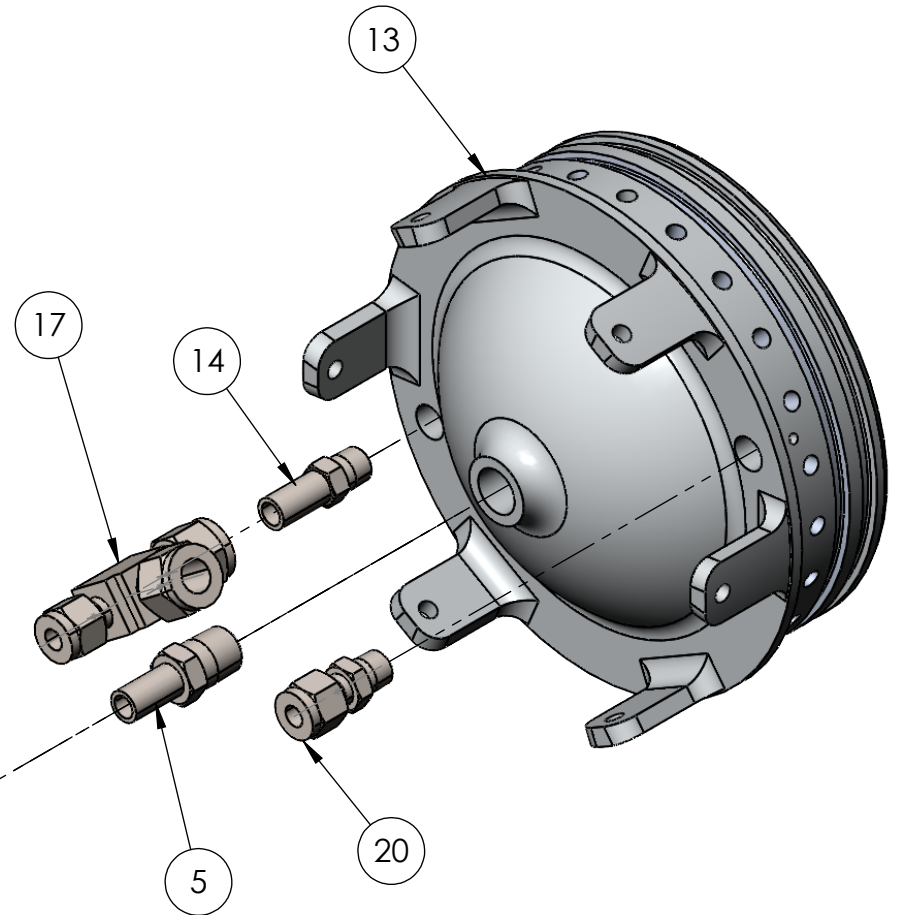
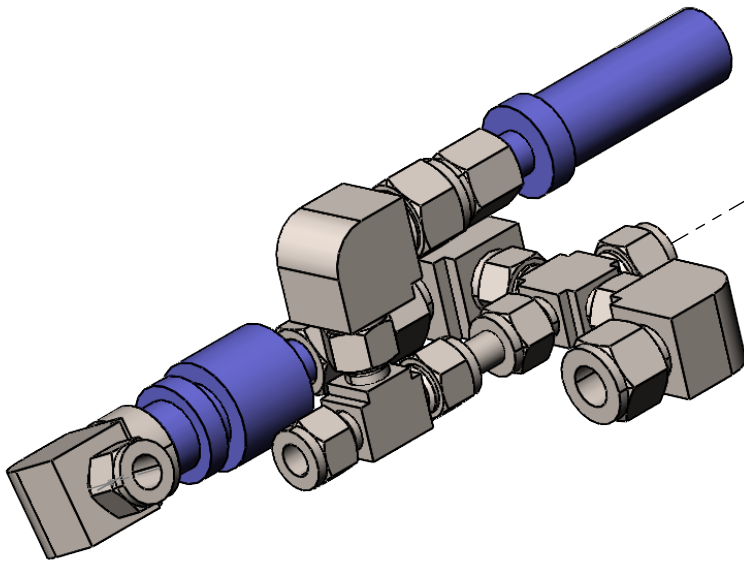
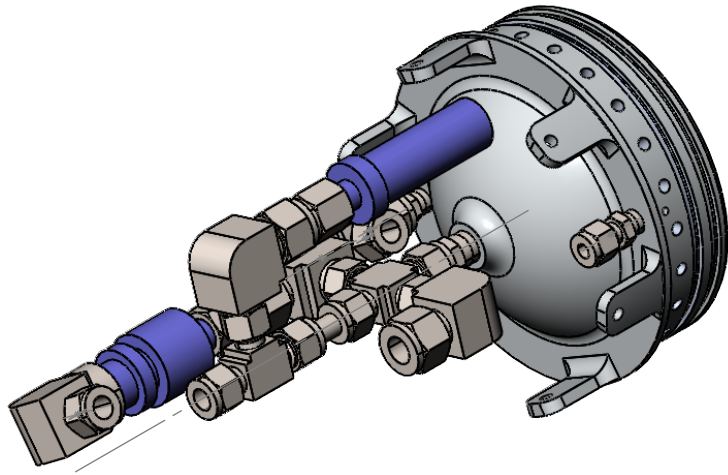
1

B

B

A

A



2

1

2

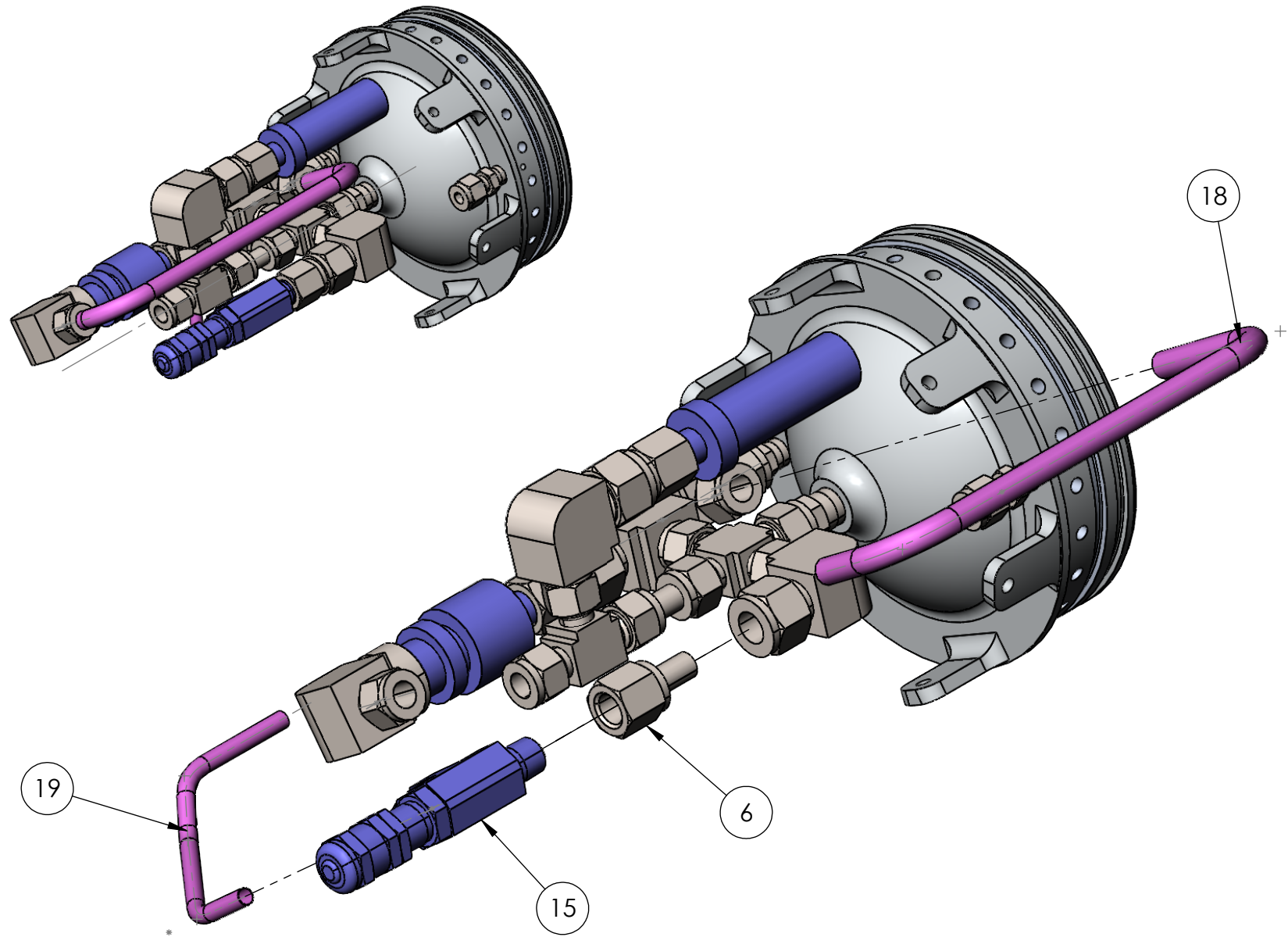
1

B

B

A

A



2

1

2

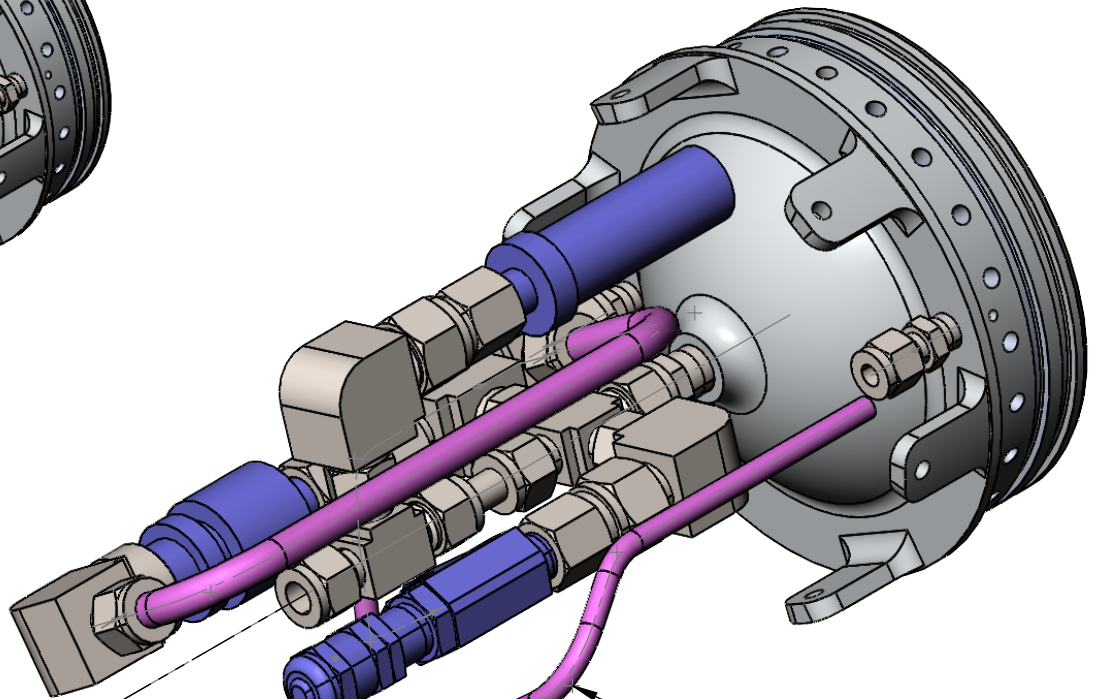
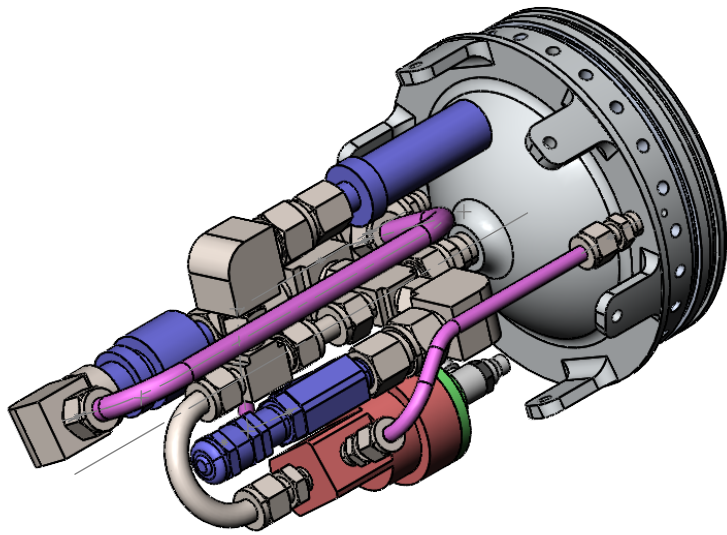
1

B

B

A

A



8

21

12

20

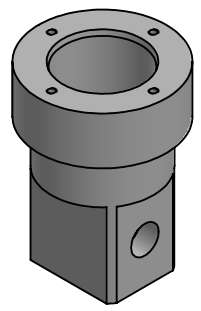
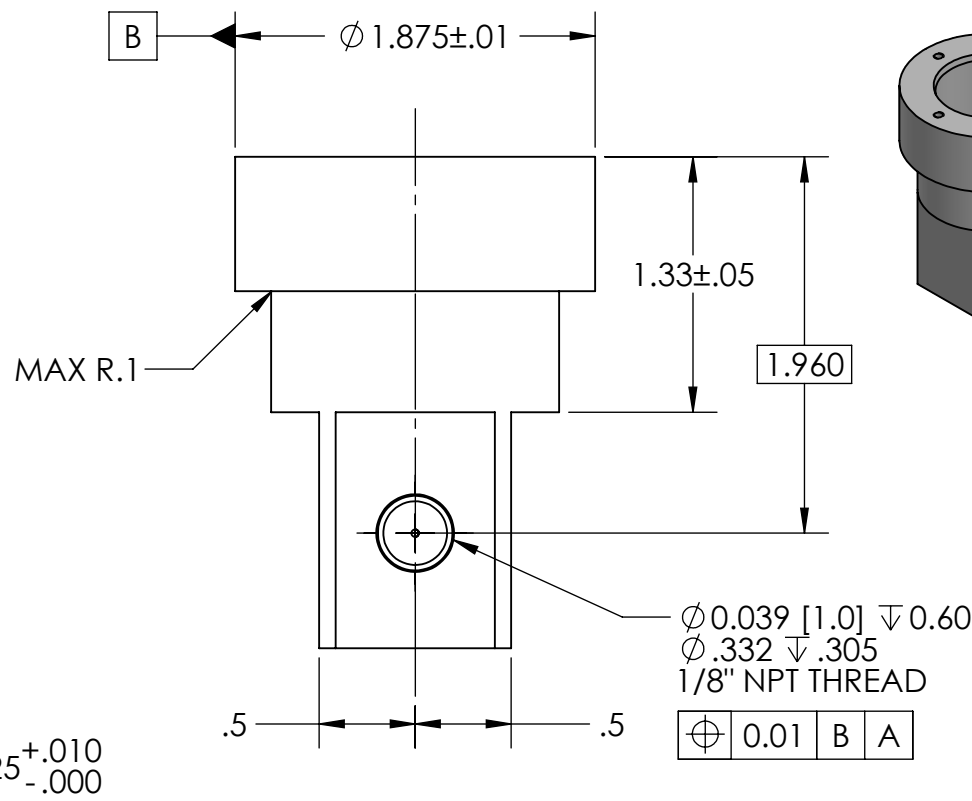
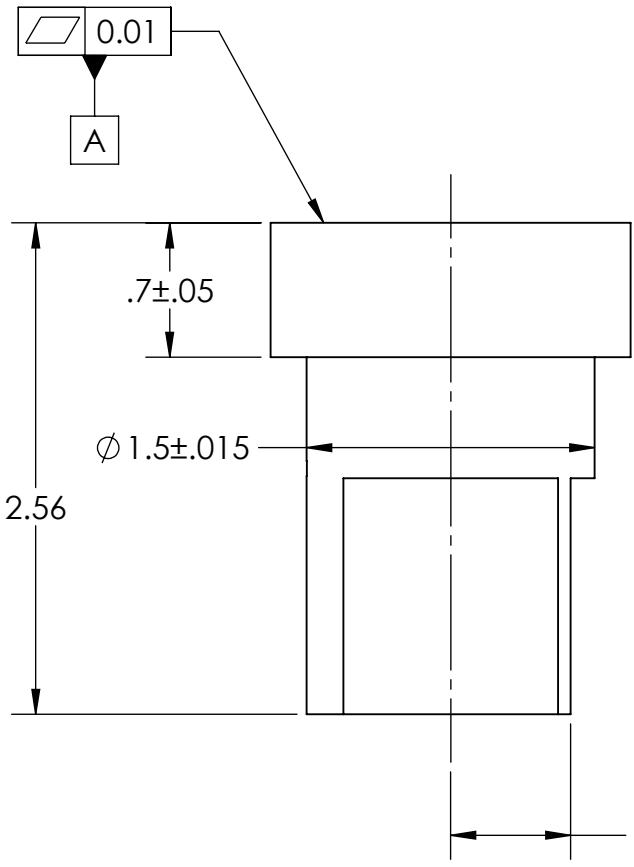
1

9

2

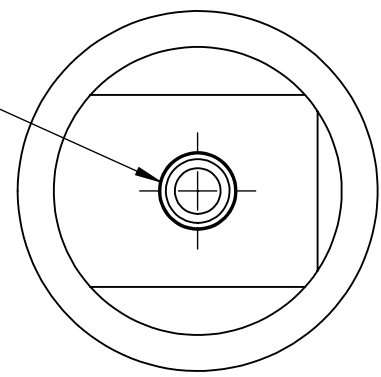
1

REVISION HISTORY			
REV	DESCRIPTION	DATE	AUTHOR
00	INITIAL RELEASE	2020-02-18	M. ZHOU



Ø.332 ∇.305
1/8" NPT THREAD

⊕	0.01	A	B
---	------	---	---



UNLESS OTHERWISE SPECIFIED:
DIMENSIONS ARE IN INCHES
REMOVE BURRS AND SHARP EDGES
TOLERANCES:
LINEAR: 2 DECIMALS: ±0.010"
3 DECIMALS: ±0.005"
ANGULAR: ±1°



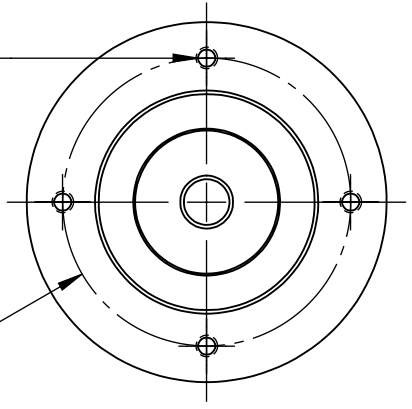
**WATERLOO
ROCKETRY**

NAME	M. ZHOU	DATE	2020-02-18
MATERIAL:	6061-T6 (SS)		
FINISH:	N/A		
WEIGHT:	0.32	LBS	

DESCRIPTION: VENT VALVE BODY		
SIZE A	DRAWING NUMBER: 21-PR-007	REVISION 00
SCALE: 1:1		DO NOT SCALE DRAWING
		SHEET 1 OF 2

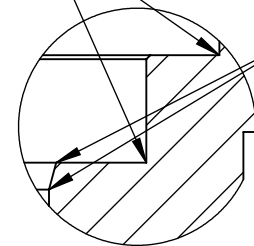
REVISION HISTORY			
REV	DESCRIPTION	DATE	AUTHOR
00	INITIAL RELEASE	2020-02-18	M. ZHOU

4X #4-40 ∇ 0.4
EQUAL SPACING
 \oplus 0.02 A B



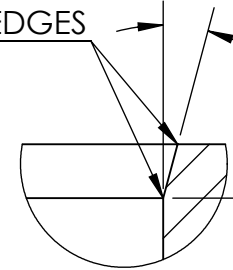
ϕ 1.500
BOLT CIRCLE

MAX R.02



DETAIL A
SCALE 2 : 1

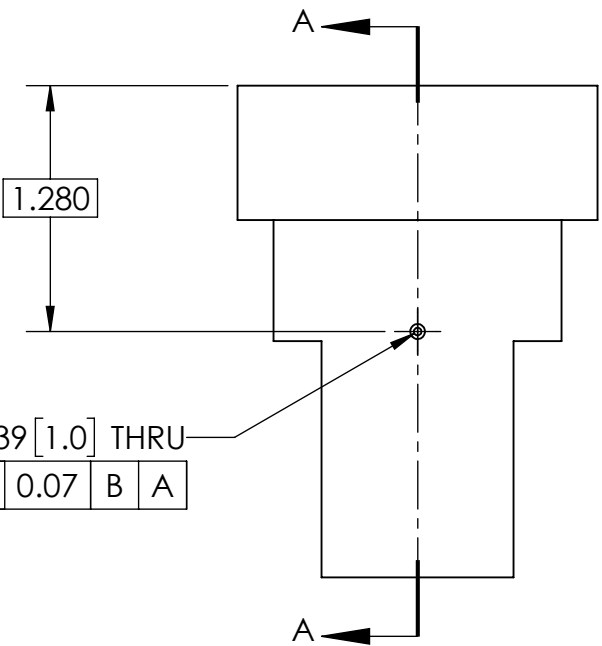
BREAK EDGES



DETAIL B
SCALE 4 : 1

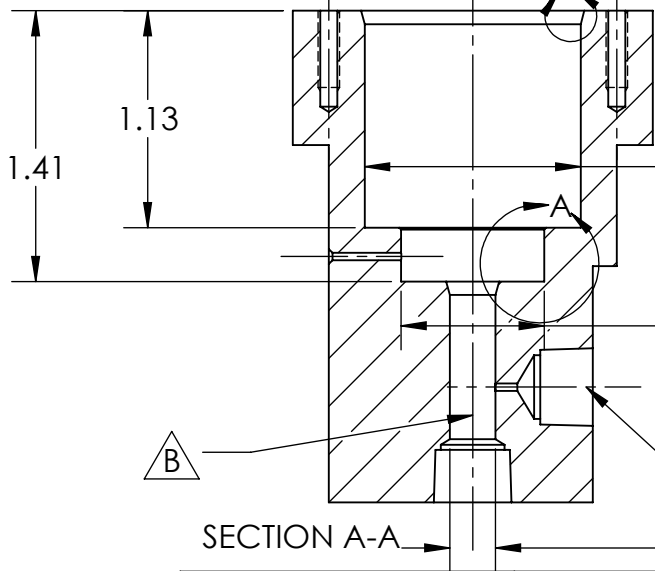
2X 15°±5°

2X .07^{+0.02}_{-.00}



1.280

ϕ .039 [1.0] THRU
 \oplus 0.07 B A



1.41

1.13

ϕ 1.125^{+0.002}_{-.000}
 \oplus 0.000 (M) A B

ϕ .745^{+0.015}_{-.005}

SECTION A-A

ϕ .238 THRU

NOTES:

1. DRILL OXIDIZER VENT PORT ∇ BEFORE DRILLING CENTER BORE ∇
2. ENSURE INTERIOR EDGE OF OXIDIZER VENT PORT IS DEBURRED

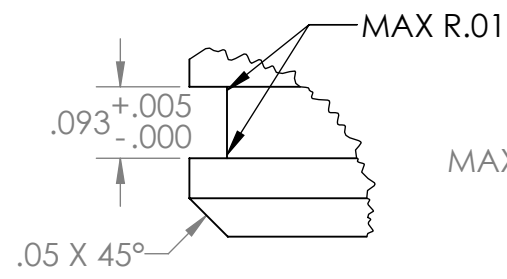
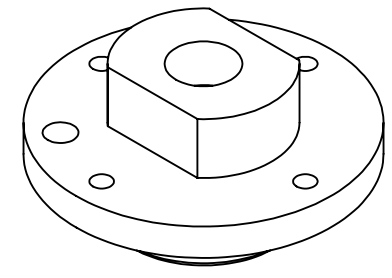
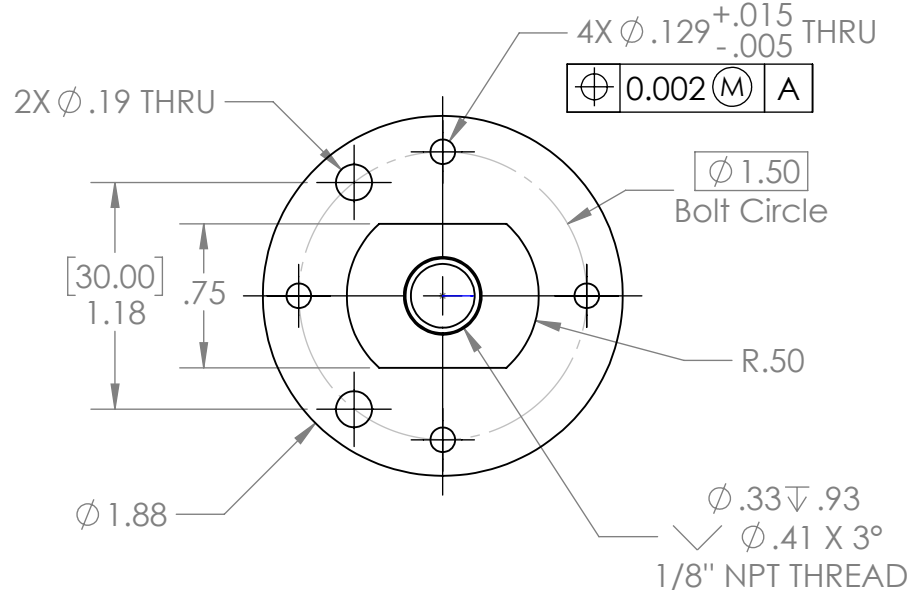
UNLESS OTHERWISE SPECIFIED: DIMENSIONS ARE IN INCHES REMOVE BURRS AND SHARP EDGES TOLERANCES: LINEAR: 2 DECIMALS: ± 0.010 " 3 DECIMALS: ± 0.005 " ANGULAR: $\pm 1^\circ$		
NAME	DATE	
M. ZHOU	2020-02-18	
MATERIAL:	6061-T6 (SS)	
FINISH:	N/A	
WEIGHT:	0.32	LBS



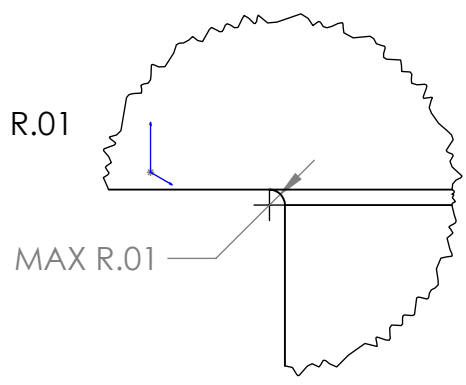
WATERLOO ROCKETRY

DESCRIPTION: VENT VALVE BODY		
SIZE A	DRAWING NUMBER: 21-PR-007	REVISION 00
SCALE: 1:1		DO NOT SCALE DRAWING
SHEET 2 OF 2		

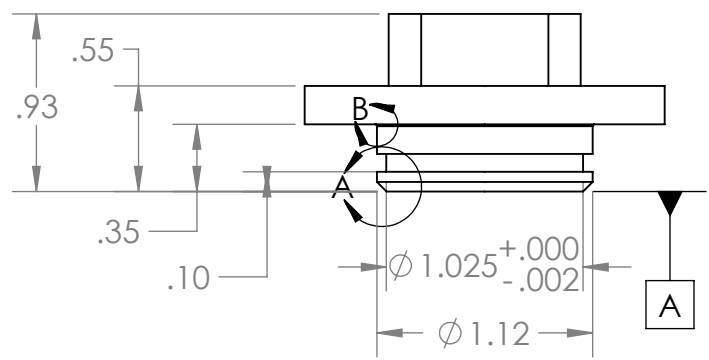
REVISION HISTORY			
REV	DESCRIPTION	DATE	AUTHOR
00	INITIAL RELEASE	FEB 16/2021	X.X



DETAIL A
SCALE 4 : 1



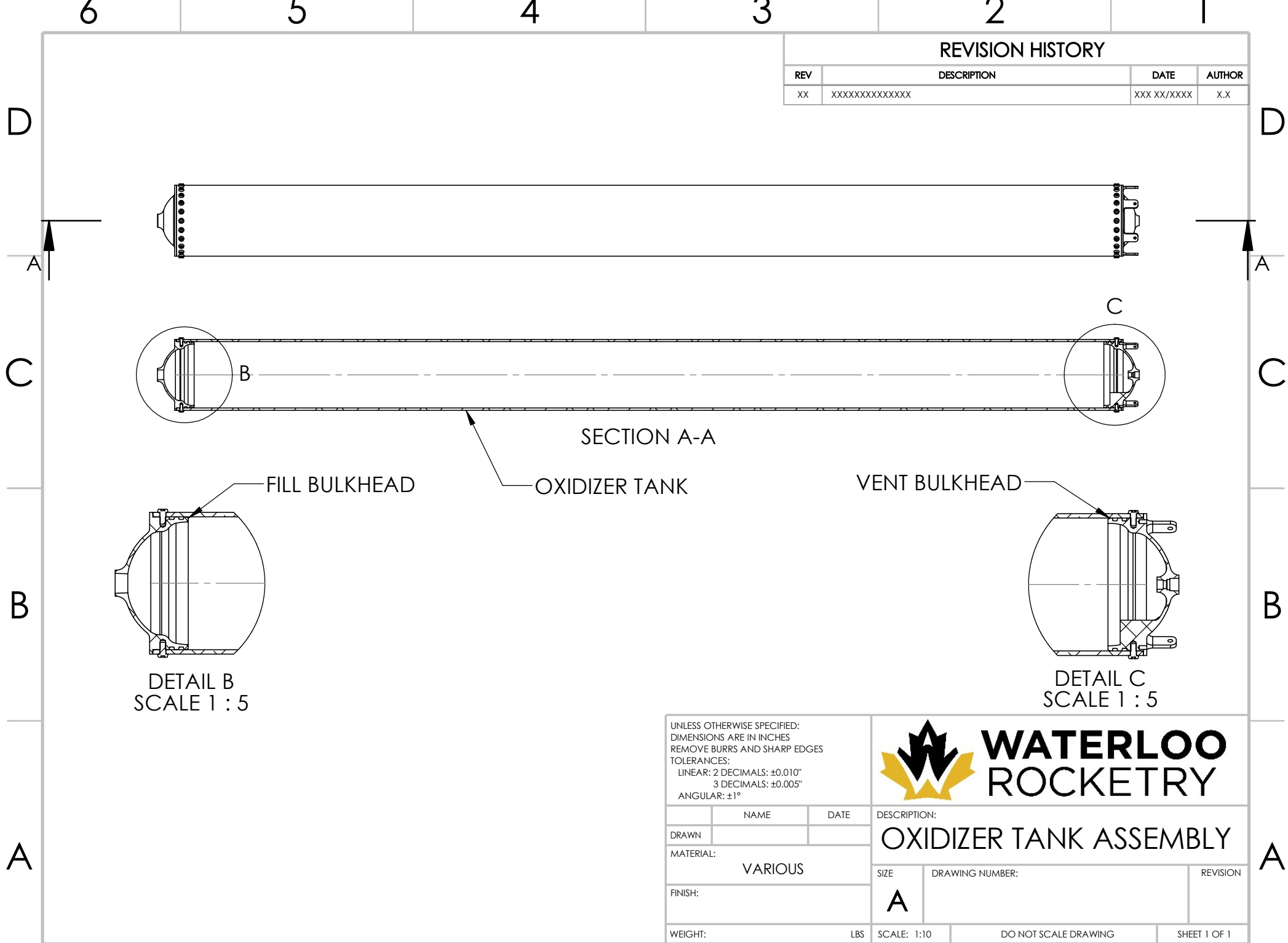
DETAIL B
SCALE 8 : 1



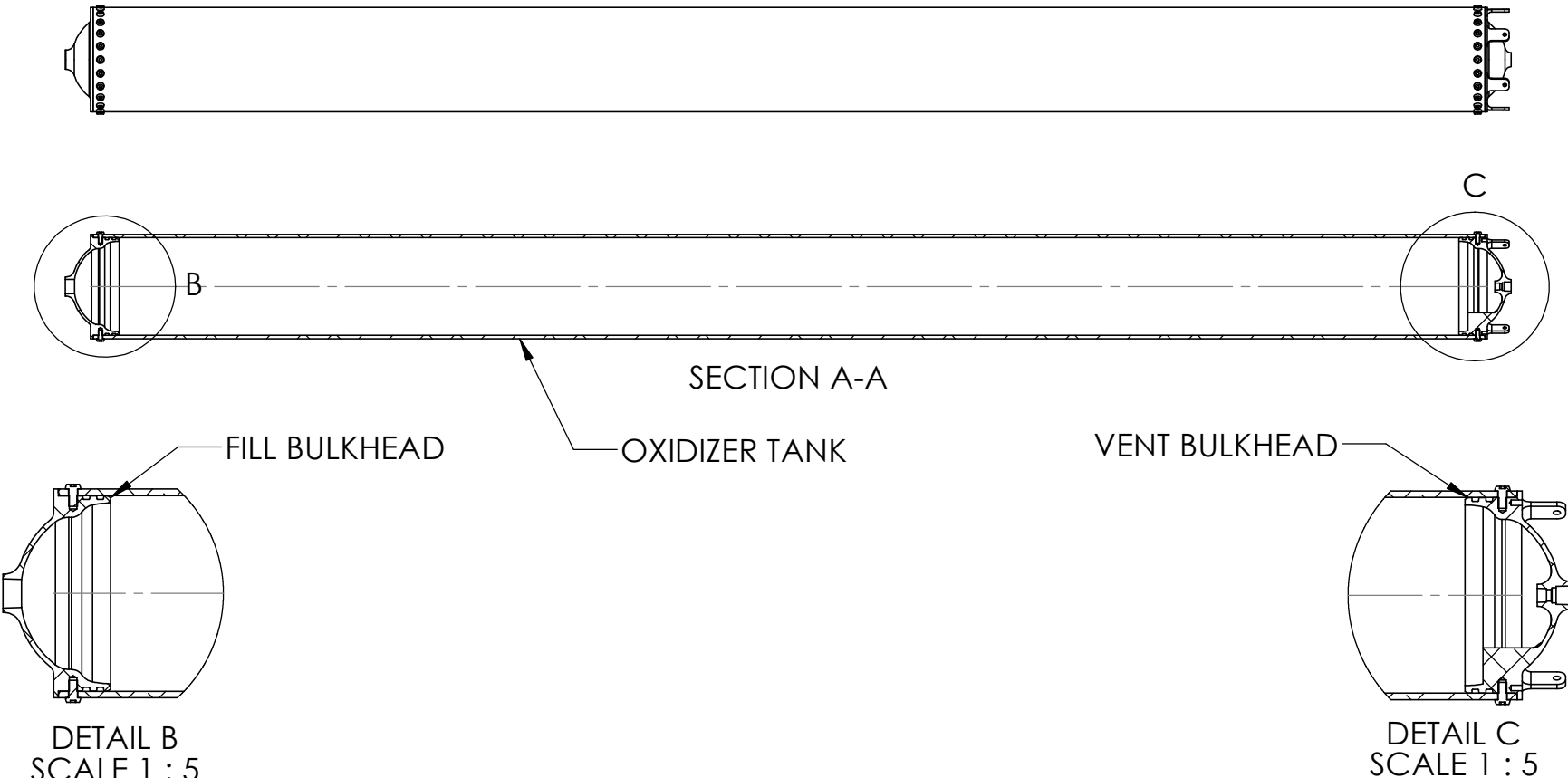
UNLESS OTHERWISE SPECIFIED:
DIMENSIONS ARE IN INCHES
REMOVE BURRS AND SHARP EDGES
TOLERANCES:
LINEAR: 2 DECIMALS: ± 0.010 "
3 DECIMALS: ± 0.005 "
ANGULAR: $\pm 1^\circ$



DRAWN: JERRY LU		DATE: FEB 16/2021	DESCRIPTION: VENT VALVE CAP	
MATERIAL: 6061-T6 (SS)			SIZE: A	DRAWING NUMBER: 21-PR-009
FINISH: N/A			REVISION:	
WEIGHT: _____ LBS		SCALE: 1:1	DO NOT SCALE DRAWING	
SHEET 1 OF 1				



REVISION HISTORY			
REV	DESCRIPTION	DATE	AUTHOR
XX	XXXXXXXXXXXXXXXX	XXX XX/XXXX	X.X

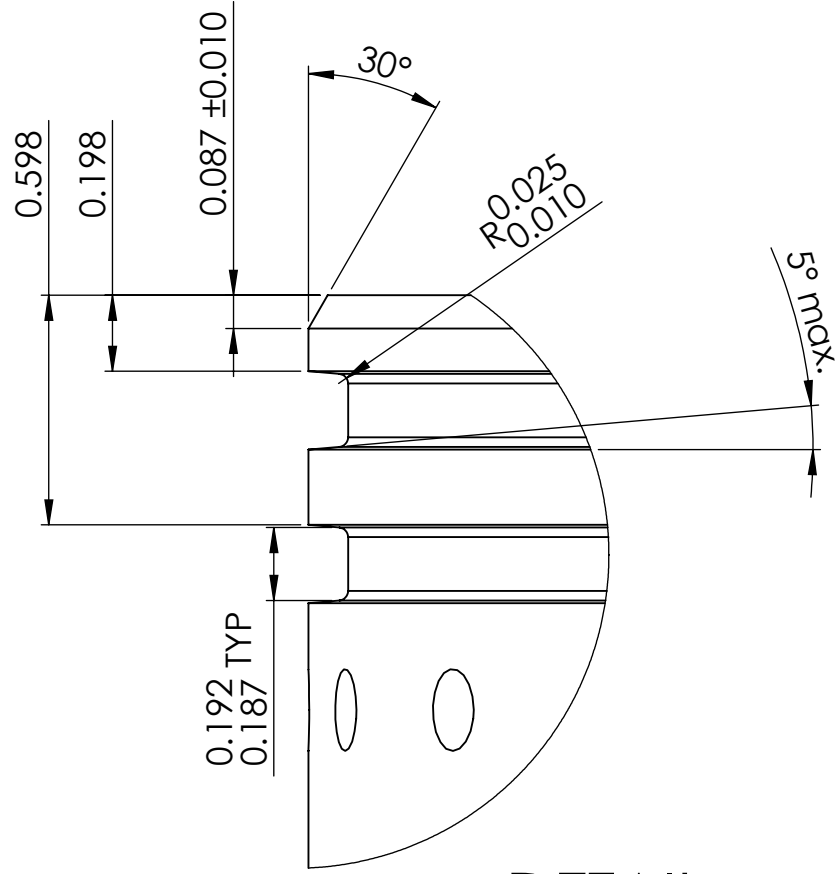


UNLESS OTHERWISE SPECIFIED:
 DIMENSIONS ARE IN INCHES
 REMOVE BURRS AND SHARP EDGES
 TOLERANCES:
 LINEAR: 2 DECIMALS: $\pm 0.010"$
 3 DECIMALS: $\pm 0.005"$
 ANGULAR: $\pm 1^\circ$

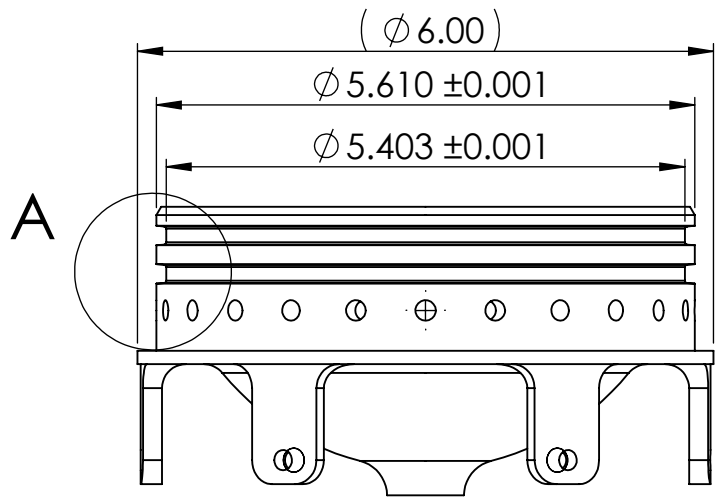


DRAWN		NAME	DATE	DESCRIPTION: OXIDIZER TANK ASSEMBLY	
MATERIAL: VARIOUS		SIZE		DRAWING NUMBER:	REVISION
FINISH:		A			
WEIGHT:		LBS	SCALE: 1:10	DO NOT SCALE DRAWING	SHEET 1 OF 1

REVISION HISTORY			
REV	DESCRIPTION	DATE	AUTHOR
00	DRAWING RELEASED	2020-11-02	H.A.
01	ADDED VENT SECTION SLED HOLES	2022-03-07	J.LU



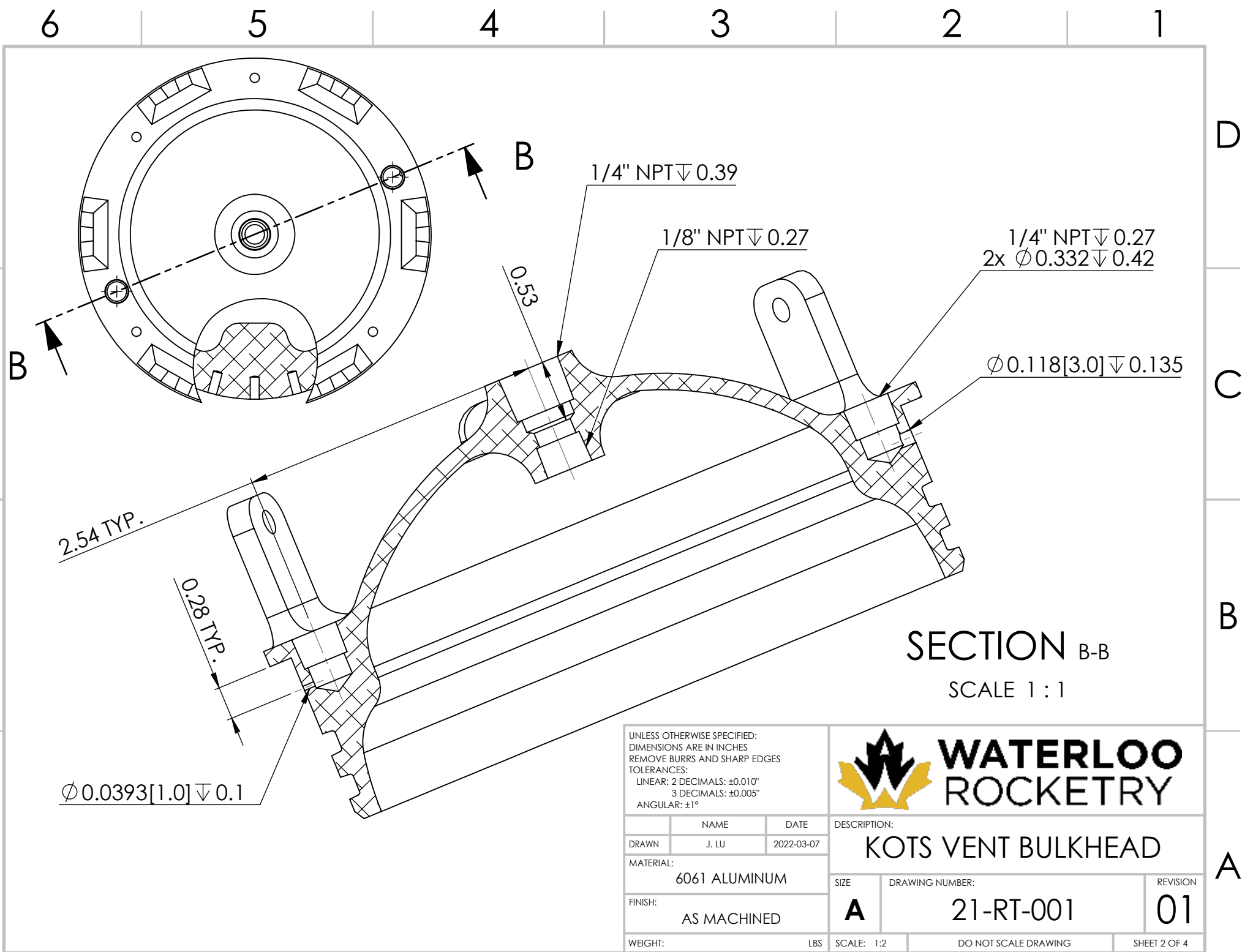
DETAIL A
SCALE 2 : 1



UNLESS OTHERWISE SPECIFIED:
DIMENSIONS ARE IN INCHES
REMOVE BURRS AND SHARP EDGES
TOLERANCES:
LINEAR: 2 DECIMALS: ±0.010"
3 DECIMALS: ±0.005"
ANGULAR: ±1°



DRAWN		NAME	DATE	DESCRIPTION:	
		J. LU	2022-03-07	KOTS VENT BULKHEAD	
MATERIAL:			SIZE	DRAWING NUMBER:	REVISION
6061 Aluminum			A	21-RT-001	01
FINISH:			SCALE: 1:2		SHEET 1 OF 4
AS MACHINED			DO NOT SCALE DRAWING		
WEIGHT:		LBS			



SECTION B-B
SCALE 1:1

UNLESS OTHERWISE SPECIFIED:
DIMENSIONS ARE IN INCHES
REMOVE BURRS AND SHARP EDGES
TOLERANCES:
LINEAR: 2 DECIMALS: $\pm 0.010''$
3 DECIMALS: $\pm 0.005''$
ANGULAR: $\pm 1^\circ$



	NAME	DATE	DESCRIPTION:	
DRAWN	J. LU	2022-03-07	KOTS VENT BULKHEAD	
MATERIAL:			SIZE	DRAWING NUMBER:
6061 ALUMINUM			A	21-RT-001
FINISH:			REVISION	
AS MACHINED				01
WEIGHT:		LBS	SCALE: 1:2	DO NOT SCALE DRAWING
				SHEET 2 OF 4

6

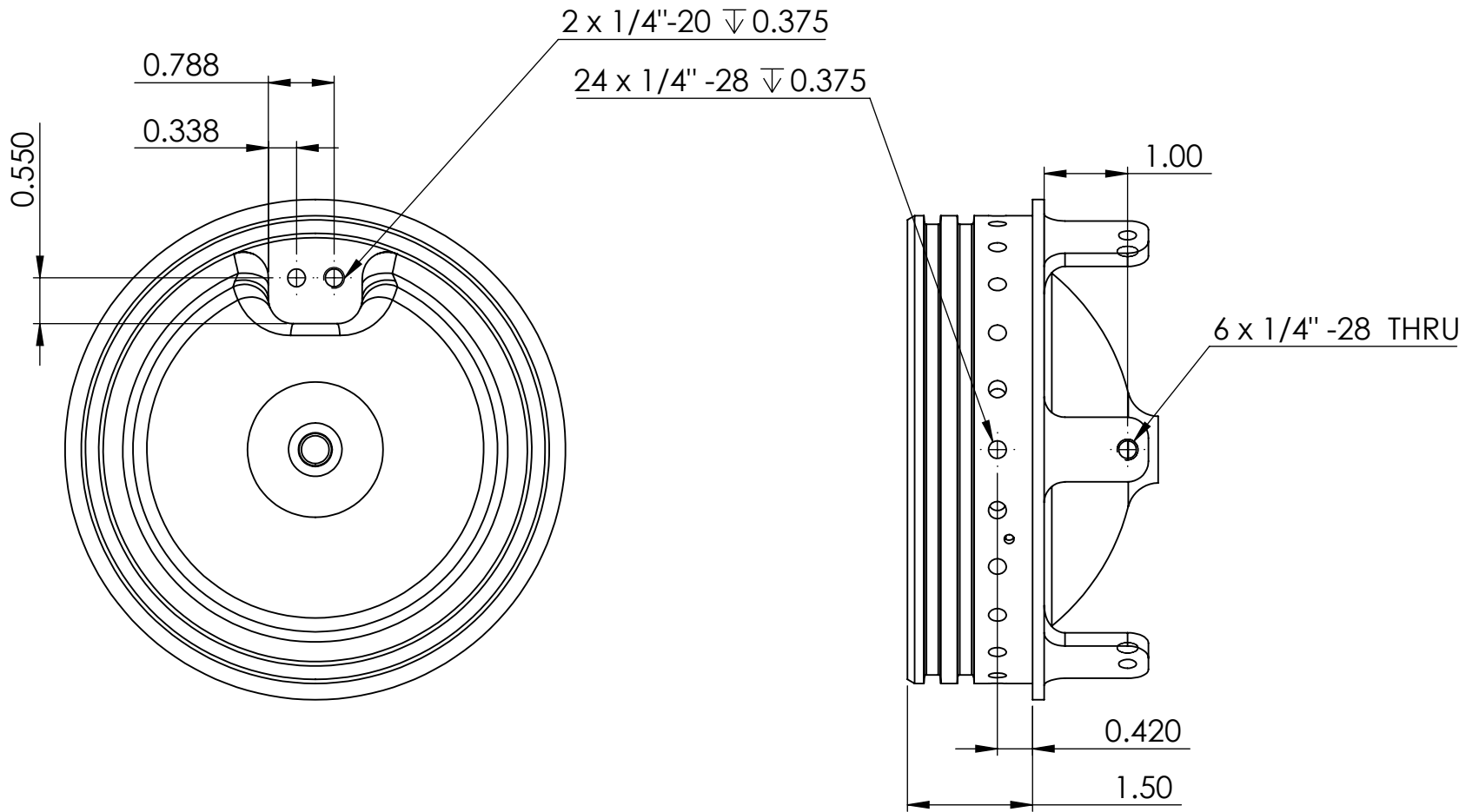
5

4

3

2

1



UNLESS OTHERWISE SPECIFIED:
 DIMENSIONS ARE IN INCHES
 REMOVE BURRS AND SHARP EDGES
 TOLERANCES:
 LINEAR: 2 DECIMALS: $\pm 0.010"$
 3 DECIMALS: $\pm 0.005"$
 ANGULAR: $\pm 1^\circ$



	NAME	DATE
DRAWN	J. LU	2022-03-07
MATERIAL: 6061 ALUMINUM		
FINISH: AS MACHINED		
WEIGHT: _____ LBS		

DESCRIPTION: KOTS VENT BULKHEAD		
SIZE A	DRAWING NUMBER: 21-RT-001	REVISION 01
SCALE: 1:2		DO NOT SCALE DRAWING
SHEET 3 OF 4		

6

5

4

3

2

1

6

5

4

3

2

1

D

D

C

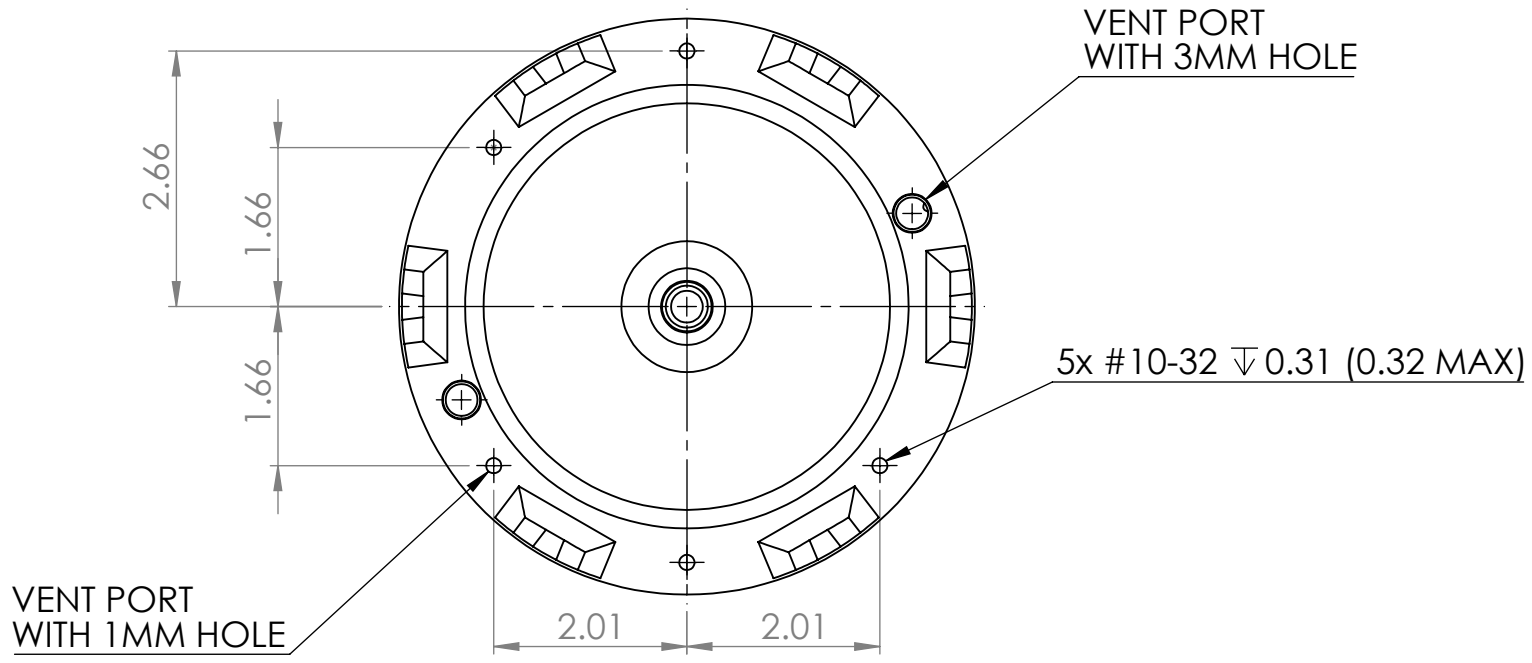
C

B

B

A

A



UNLESS OTHERWISE SPECIFIED:
 DIMENSIONS ARE IN INCHES
 REMOVE BURRS AND SHARP EDGES
 TOLERANCES:
 LINEAR: 2 DECIMALS: $\pm 0.010''$
 3 DECIMALS: $\pm 0.005''$
 ANGULAR: $\pm 1^\circ$



	NAME	DATE
DRAWN	J. LU	2022-03-07
MATERIAL: 6061 ALUMINUM		
FINISH: AS MACHINED		
WEIGHT: _____ LBS		

DESCRIPTION: KOTS VENT BULKHEAD		
SIZE A	DRAWING NUMBER: 21-RT-001	REVISION 01
SCALE: 1:2	DO NOT SCALE DRAWING	SHEET 4 OF 4

6

5

4

3

2

1

D

C

B

A

6X ϕ .21 ∇ .315
1/4-28 UNF ∇ .313

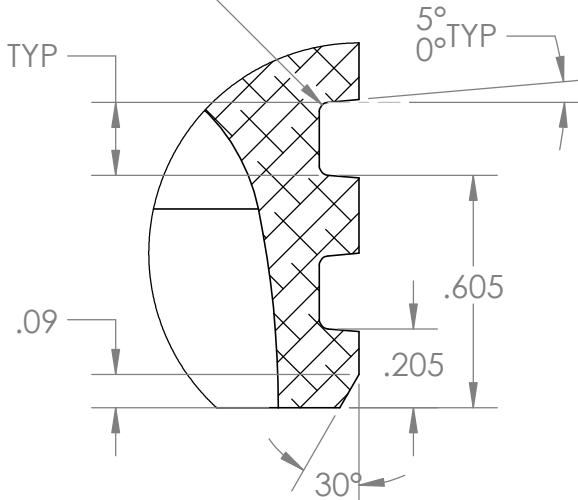
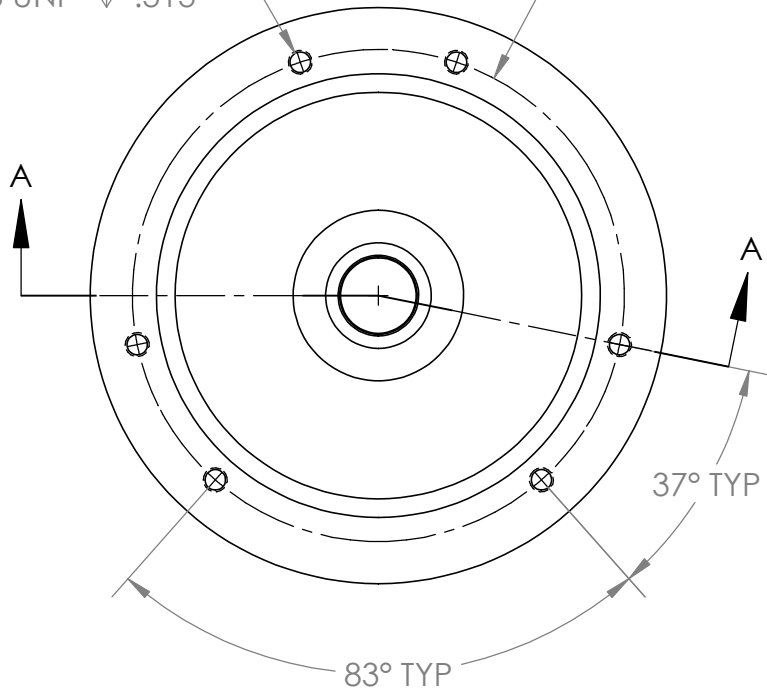
R2.563

R.025
.010 TYP

.192 TYP
.187

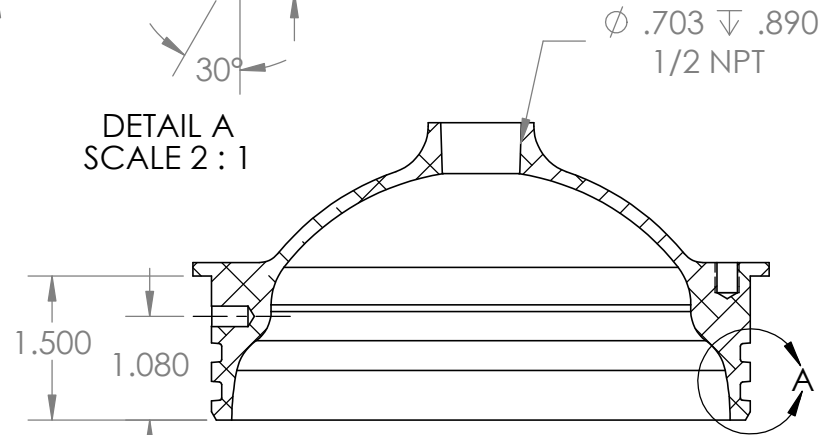
REVISION HISTORY

REV	DESCRIPTION	DATE	AUTHOR
00	TO BE MACHINED BY BRIAN/GRAEME/JEFF	OCT 26/2020	S.K

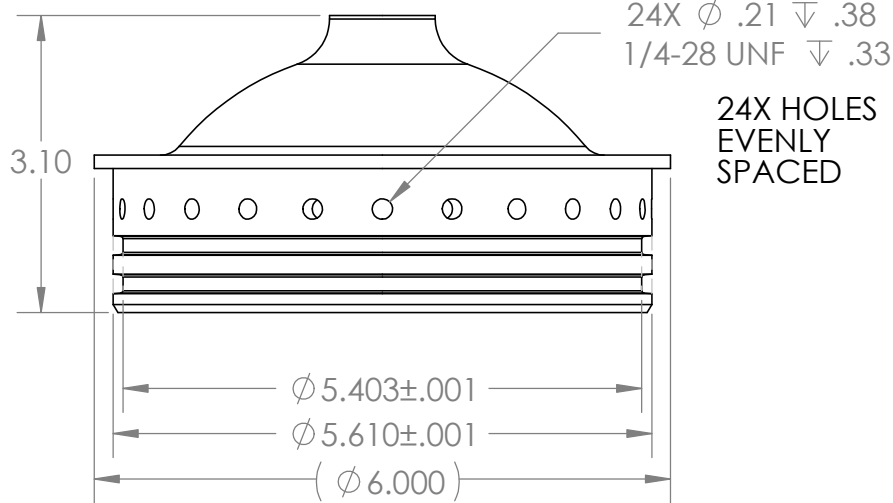


DETAIL A
SCALE 2 : 1

ϕ .703 ∇ .890
1/2 NPT



SECTION A-A



24X HOLES
EVENLY
SPACED

NOTE: ALL HOLE DEPTHS DIMENSIONED TO BOTTOM OF STRAIGHT HOLE, NOT TO DRILL POINT

UNLESS OTHERWISE SPECIFIED:
DIMENSIONS ARE IN INCHES
REMOVE BURRS AND SHARP EDGES
TOLERANCES:
LINEAR: 2 DECIMALS: ± 0.010 "
3 DECIMALS: ± 0.005 "
ANGULAR: $\pm 1^\circ$



WATERLOO ROCKETRY

	NAME	DATE
DRAWN	S.KONG	OCT 26/2020

DESCRIPTION:
KOTS FILL BULKHEAD

MATERIAL:
6061-T6 (SS)

SIZE: **A** DRAWING NUMBER: **21-RT-002** REVISION: **00**

FINISH:
AS MACHINED

WEIGHT: 1.33 LBS SCALE: 1:2 DO NOT SCALE DRAWING SHEET 1 OF 1

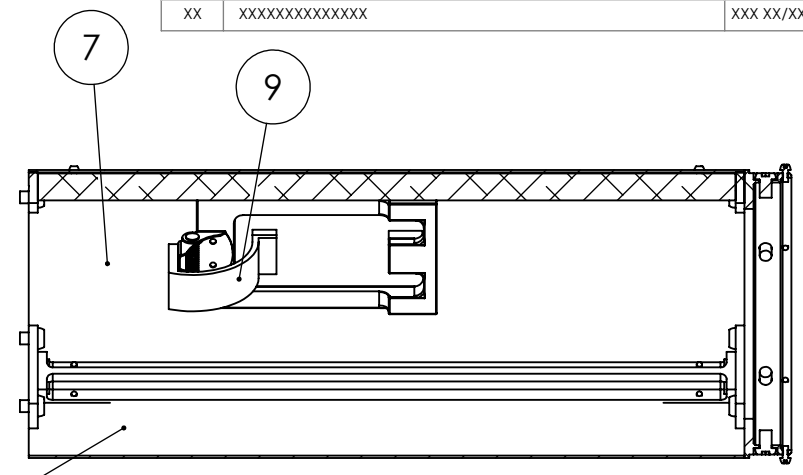
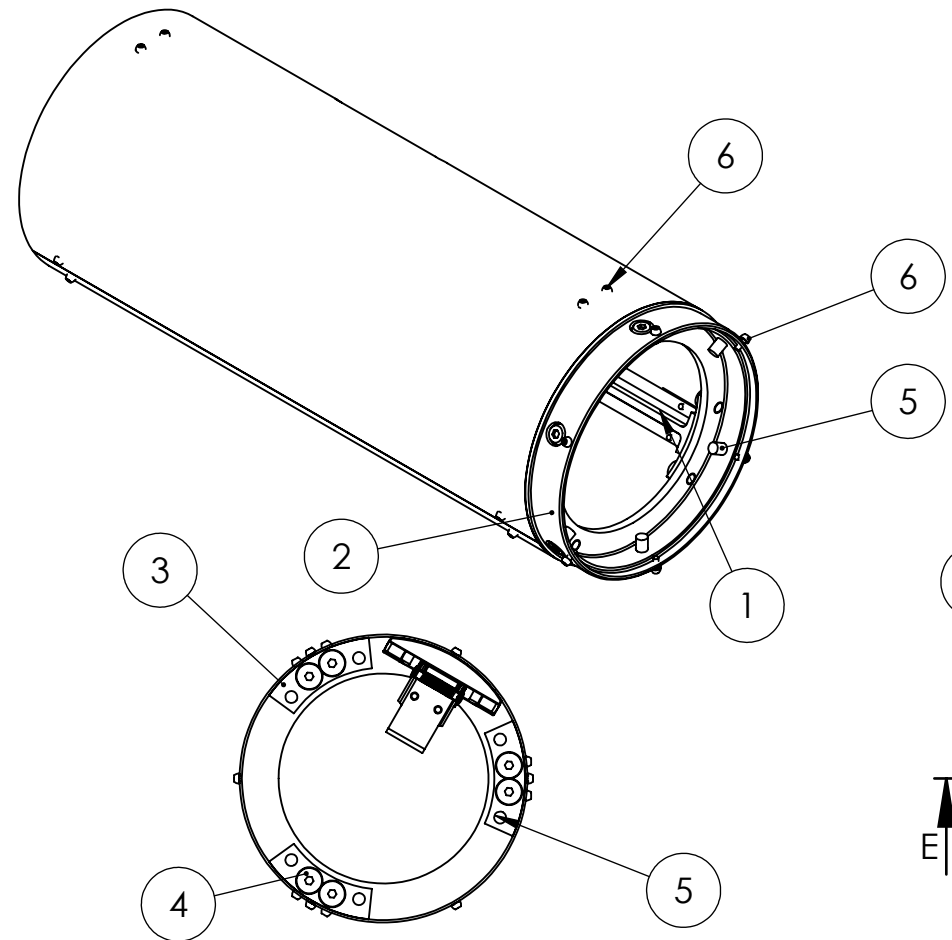
4

3

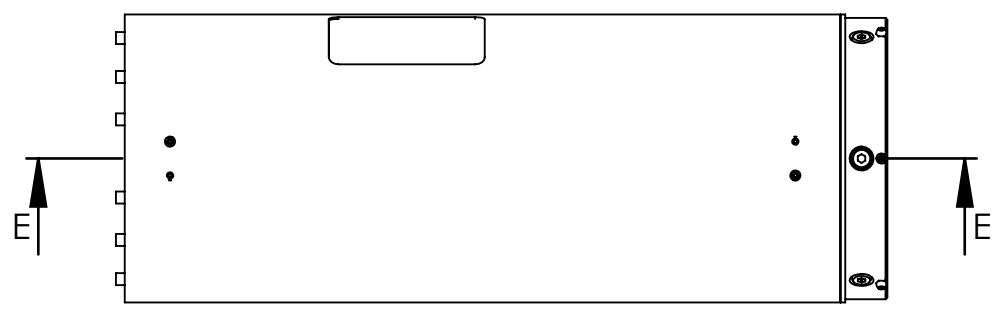
2

1

REVISION HISTORY			
REV	DESCRIPTION	DATE	AUTHOR
XX	XXXXXXXXXXXXXXXX	XXX XX/XXXX	X.X



SECTION E-E



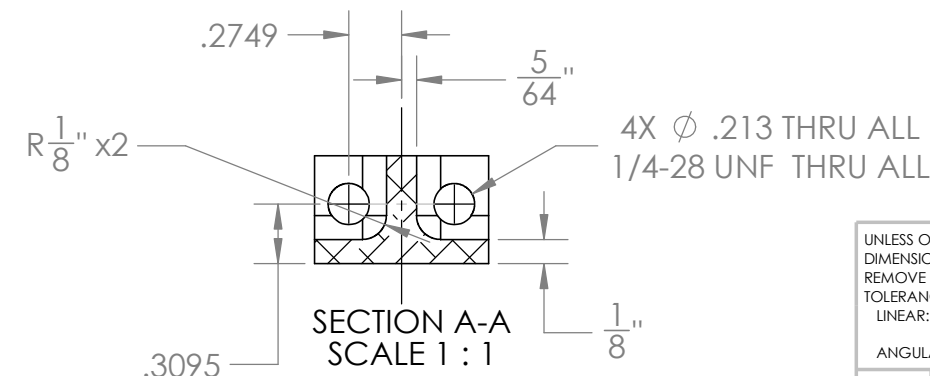
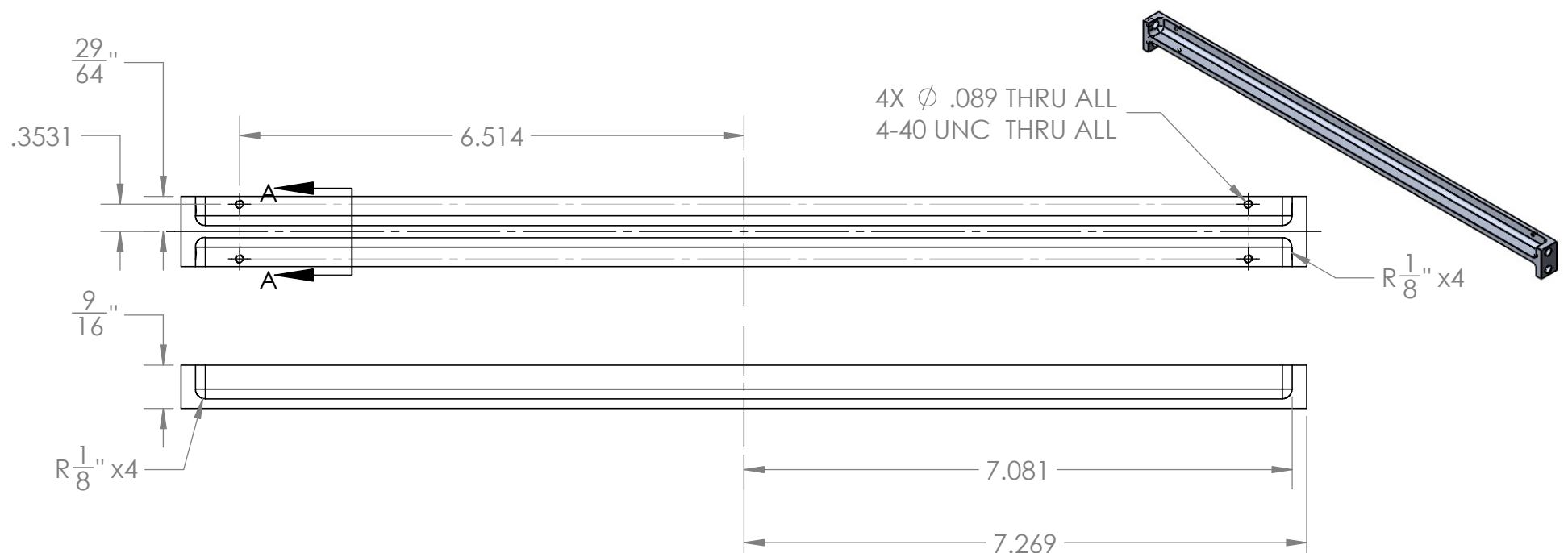
ITEM NO.	PART NUMBER	DESCRIPTION	QTY.
1	Longeron	LONGERON	3
2	Injector Bulkhead Coupler	INJECTOR BH COUPLER	1
3	Curved Tab		6
4	Flat Head Screw	0.25-28x0.25	12
5	Screw	R 0.25-28x0.375	18
6	Screw	R 4-40-0.25	18
7	Fairing-240		1
8	Fairing-120		1
9	Hinge Assembly 2		1

UNLESS OTHERWISE SPECIFIED:
 DIMENSIONS ARE IN INCHES
 REMOVE BURRS AND SHARP EDGES
 TOLERANCES:
 LINEAR: 2 DECIMALS: ±0.010"
 3 DECIMALS: ±0.005"
 ANGULAR: ±1°



DRAWN		NAME	DATE	DESCRIPTION:	
MATERIAL:		VARIOUS		OX TANK AFT SKIRT	
FINISH:		SIZE	DRAWING NUMBER:		REVISION
WEIGHT:		2.73	LBS	SCALE: 1:4	DO NOT SCALE DRAWING
				SHEET 1 OF 1	

REVISION HISTORY			
REV	DESCRIPTION	DATE	AUTHOR
00	INITIAL RELEASE	2022-MAR-16	S.K
01	UPDATED LONGERON LENGTH	2022-APR-13	S.K

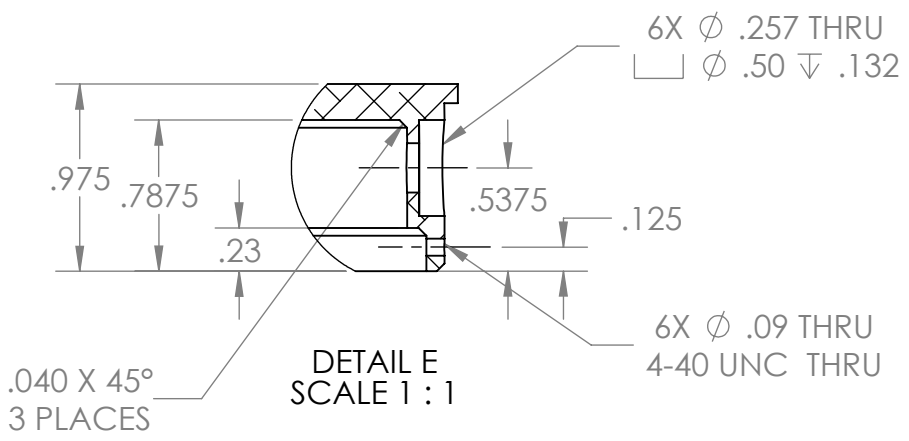
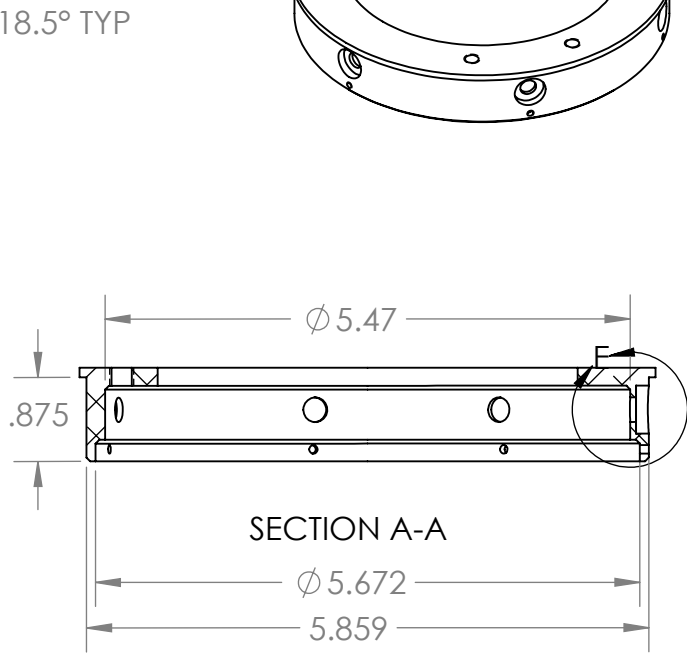
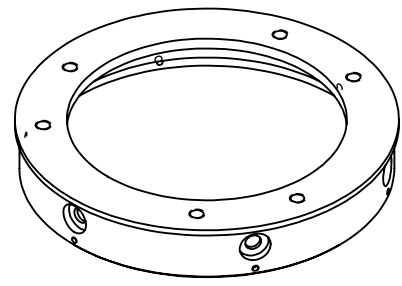
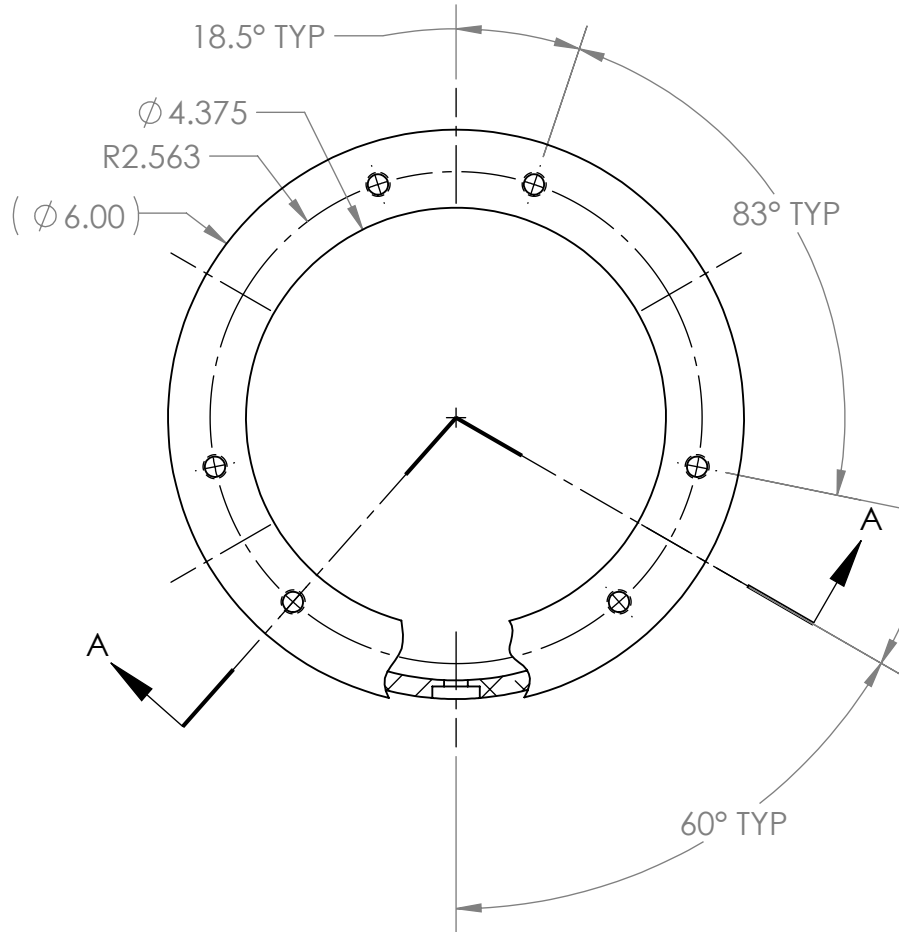


UNLESS OTHERWISE SPECIFIED:
 DIMENSIONS ARE IN INCHES
 REMOVE BURRS AND SHARP EDGES
 TOLERANCES:
 LINEAR: FRACTIONAL: $\pm 0.005''$
 3 DECIMALS: $\pm 0.005''$
 ANGULAR: $\pm 1^\circ$



DRAWN: S. KONG		DATE: 2022-MAR-16	DESCRIPTION: LONGERON	
MATERIAL: 6061-T6 (SS)			SIZE: A	DRAWING NUMBER: 22-AF-009
FINISH: AS-MACHINED			REVISION: 01	
WEIGHT: 0.2768	LBS	SCALE: 1:4	DO NOT SCALE DRAWING	SHEET 1 OF 1

REVISION HISTORY			
REV	DESCRIPTION	DATE	AUTHOR
00	INITIAL RELEASE FOR KOTS	2021-12-22	S.K
01	ELIMINATED THIN WALL	2022-01-04	S.K
02	UPDATED TO REFLECT BODYTUBE ID, CARTESIAN HOLE LOCATIONS	2022-03-13	S.K

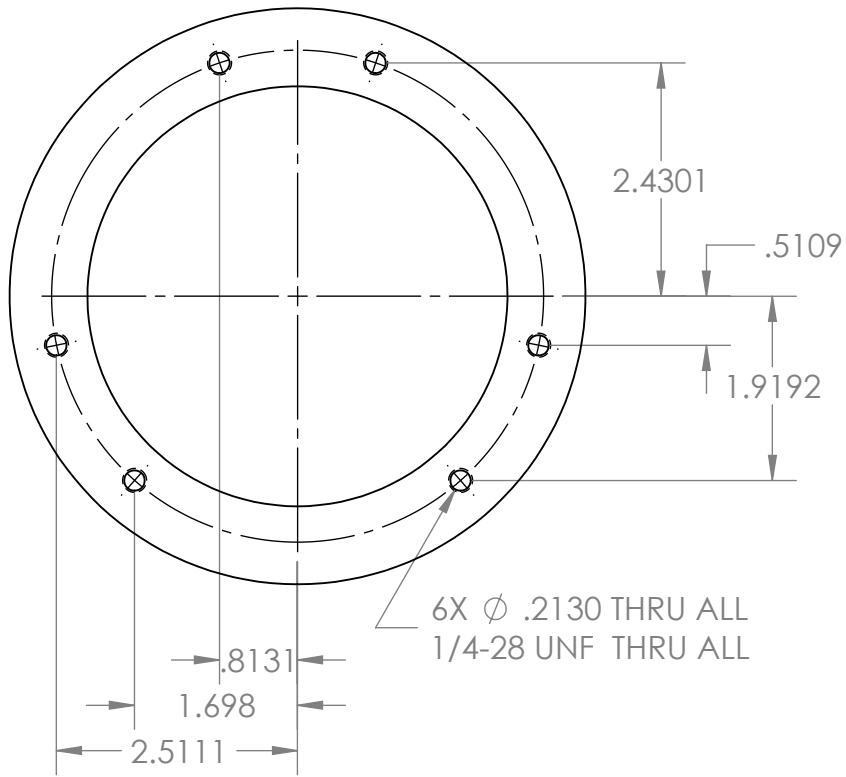


UNLESS OTHERWISE SPECIFIED:
 DIMENSIONS ARE IN INCHES
 REMOVE BURRS AND SHARP EDGES
 TOLERANCES:
 LINEAR: 2 DECIMALS: $\pm 0.010''$
 3 DECIMALS: $\pm 0.005''$
 ANGULAR: $\pm 1^\circ$



DRAWN: S.KONG		DATE: 2021-12-22	DESCRIPTION: INJECTOR BH COUPLER	
MATERIAL: 6061-T6 (SS)			SIZE: A	DRAWING NUMBER: 22-AF-007
FINISH: AS-MACHINED			REVISION: 02	
WEIGHT: 0.44	LBS	SCALE: 1:2	DO NOT SCALE DRAWING	SHEET 1 OF 2

6 5 4 3 2 1



UNLESS OTHERWISE SPECIFIED:
DIMENSIONS ARE IN INCHES
REMOVE BURRS AND SHARP EDGES
TOLERANCES:
LINEAR: 2 DECIMALS: $\pm 0.010''$
3 DECIMALS: $\pm 0.005''$
ANGULAR: $\pm 1^\circ$



	NAME	DATE
DRAWN	S.KONG	2021-12-22
MATERIAL: 6061-T6 (SS)		
FINISH: AS-MACHINED		
WEIGHT:	0.44	LBS

DESCRIPTION: INJECTOR BH COUPLER		
SIZE A	DRAWING NUMBER: 22-AF-007	REVISION 02
SCALE: 1:2	DO NOT SCALE DRAWING	SHEET 2 OF 2

D
C
B
A

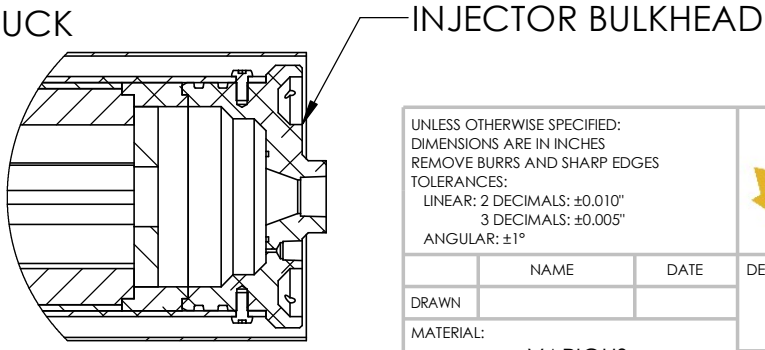
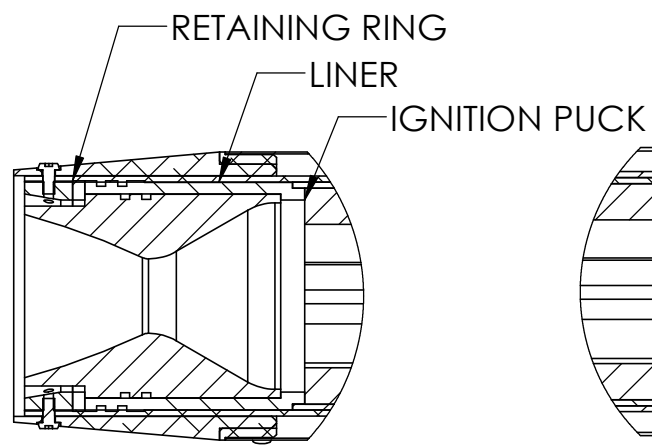
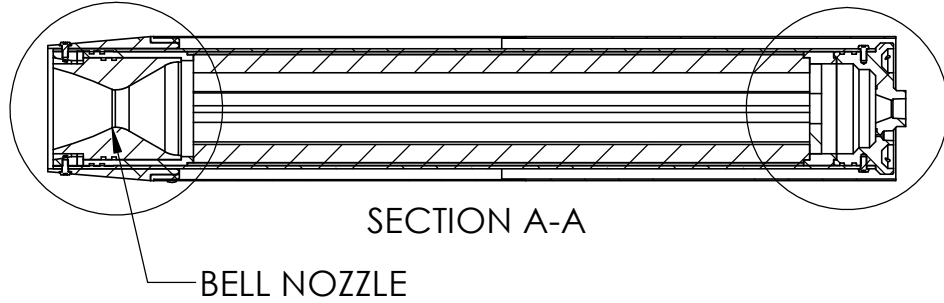
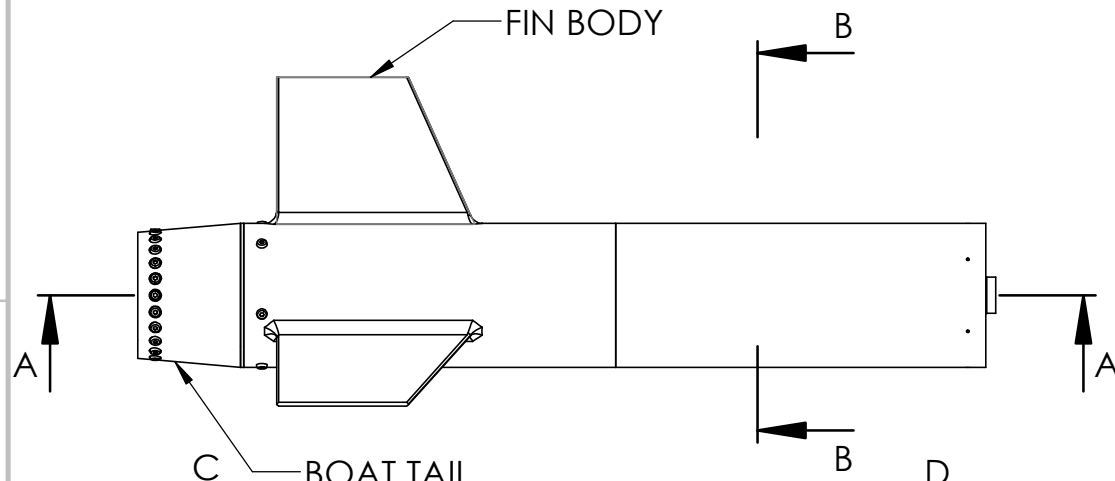
D
C
B
A

D

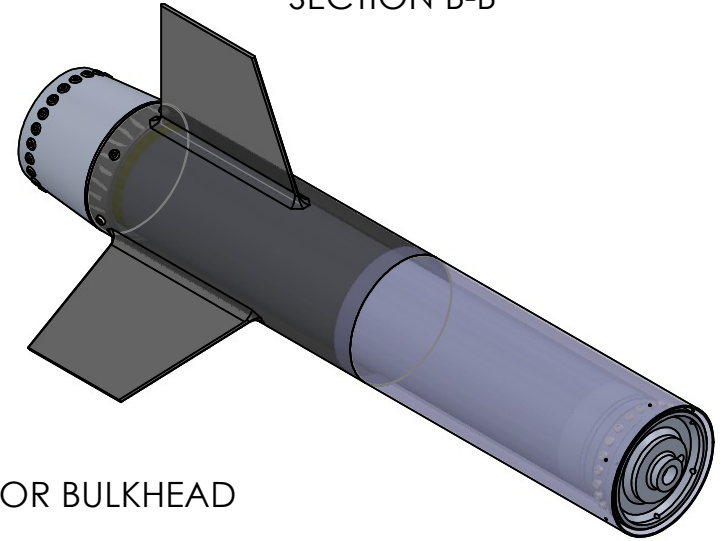
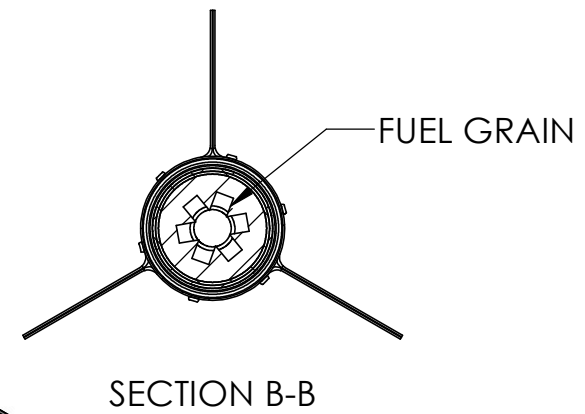
C

B

A



REVISION HISTORY			
REV	DESCRIPTION	DATE	AUTHOR
XX	XXXXXXXXXXXXXXXX	XXX XX/XXXX	X.X



UNLESS OTHERWISE SPECIFIED:
 DIMENSIONS ARE IN INCHES
 REMOVE BURRS AND SHARP EDGES
 TOLERANCES:
 LINEAR: 2 DECIMALS: ±0.010"
 3 DECIMALS: ±0.005"
 ANGULAR: ±1°



NAME	DATE	DESCRIPTION: COMBUSTION CHAMBER ASSEMBLY	
DRAWN		SIZE	DRAWING NUMBER:
MATERIAL: VARIOUS		A	REVISION
FINISH:		SCALE: 1:8	DO NOT SCALE DRAWING
WEIGHT:	LBS		SHEET 1 OF 1

4

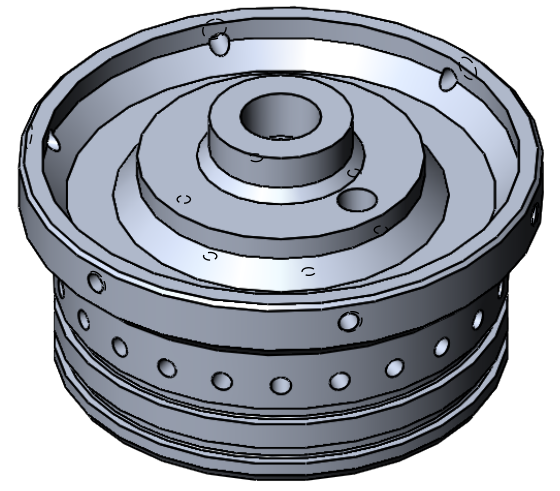
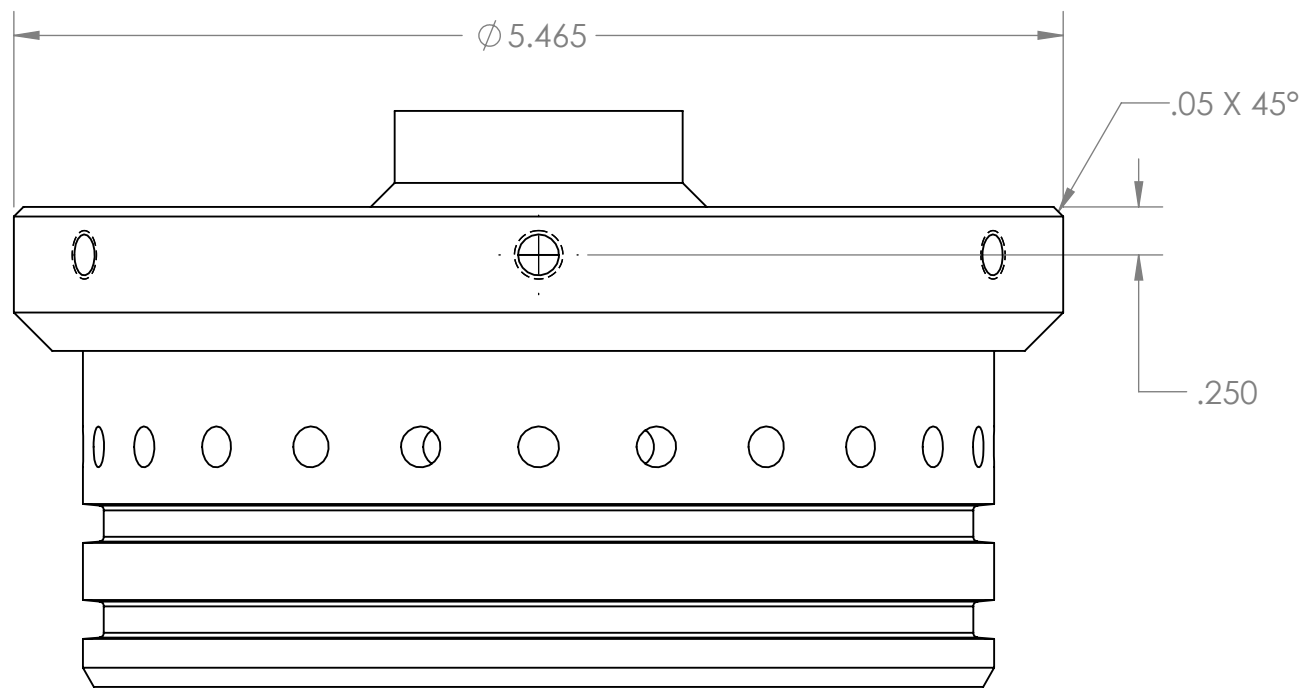
3

2

1

REVISION HISTORY			
REV	DESCRIPTION	DATE	AUTHOR
00	MODIFICATION OF UXO BULKHEAD FOR KOTS	2022-01-04	S.K

NOTE: FIT TO INJECTOR BULKHEAD COUPLER



UNLESS OTHERWISE SPECIFIED:
 DIMENSIONS ARE IN INCHES
 REMOVE BURRS AND SHARP EDGES
 TOLERANCES:
 LINEAR: 2 DECIMALS: $\pm 0.010''$
 3 DECIMALS: $\pm 0.005''$
 ANGULAR: $\pm 1^\circ$

	NAME	DATE
DRAWN	S.KONG	2022-01-04

MATERIAL:
 ALUMINUM 6061-T6

FINISH:
 AS-MACHINED

WEIGHT: 2.4 LBS



**WATERLOO
ROCKETRY**

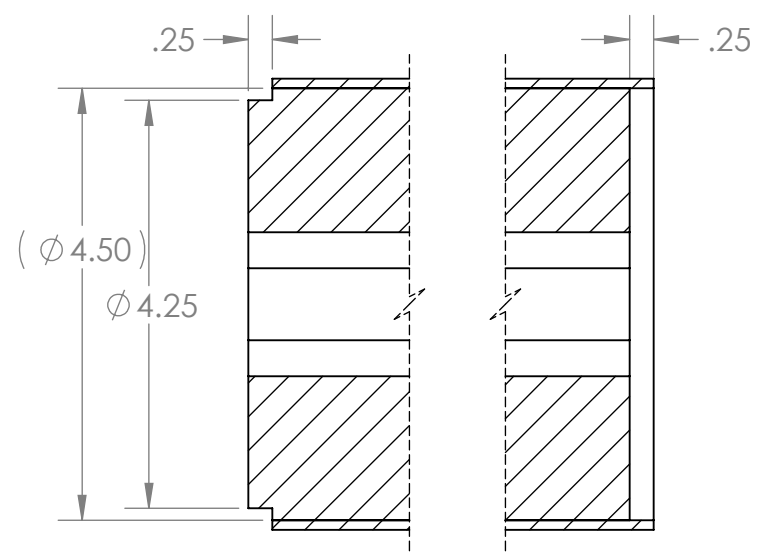
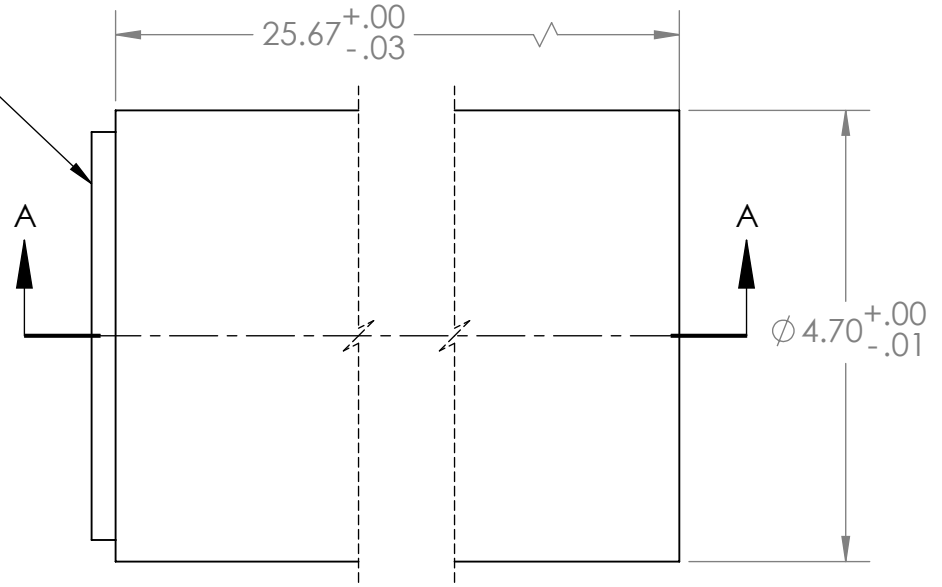
DESCRIPTION:
INJECTOR BH

SIZE	DRAWING NUMBER:	REVISION
A	22-AF-008	00

SCALE: 1:2 DO NOT SCALE DRAWING SHEET 1 OF 1

REVISION HISTORY			
REV	DESCRIPTION	DATE	AUTHOR
00	SF5 FUEL GRAIN MACHINING DRAWING	OCT 30/2020	S.K

NOTE: THIS SIDE TOWARDS SPACE



SECTION A-A
SCALE 1 : 2

UNLESS OTHERWISE SPECIFIED:
DIMENSIONS ARE IN INCHES
REMOVE BURRS AND SHARP EDGES
TOLERANCES:
LINEAR: 2 DECIMALS: $\pm 0.010''$
3 DECIMALS: $\pm 0.005''$
ANGULAR: $\pm 1^\circ$

DRAWN	NAME	DATE	DESCRIPTION:
	S. KONG	OCT 30/2020	FUEL GRAIN
MATERIAL:			SIZE
CUSTOM			DRAWING NUMBER:
FINISH:			REVISION
AS MACHINED			00
WEIGHT: 10		LBS	SCALE: 1:8
		DO NOT SCALE DRAWING	
		SHEET 1 OF 1	



D

C

B

A

6

5

4

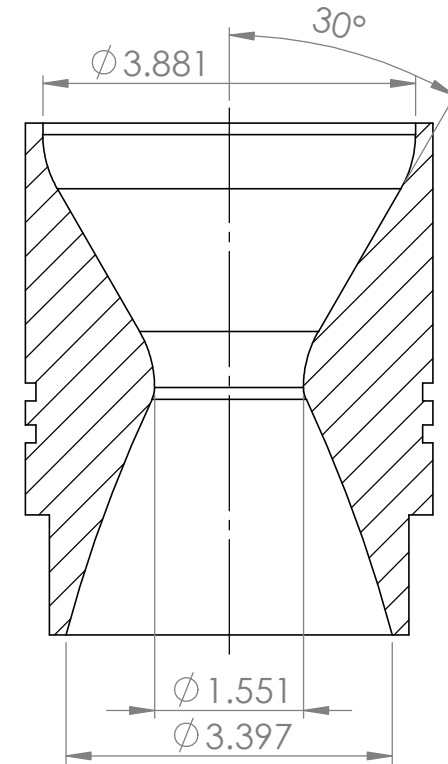
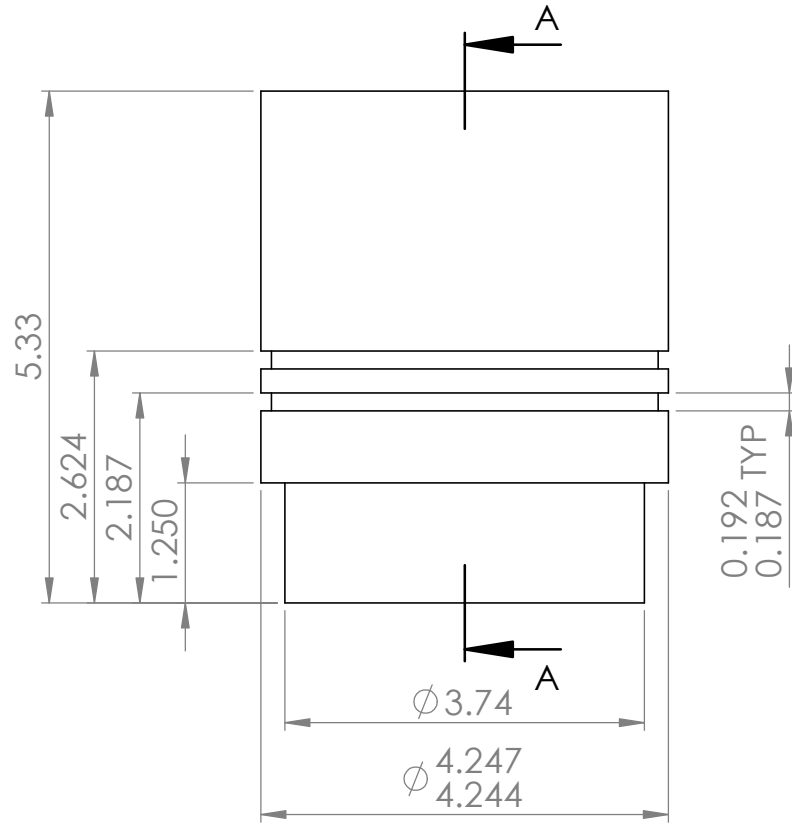
3

2

1

REVISION HISTORY

REV	DESCRIPTION	DATE	AUTHOR
XX	XXXXXXXXXXXXXXXX	XXX XX/XXXX	X.X



SECTION A-A

UNLESS OTHERWISE SPECIFIED:
DIMENSIONS ARE IN INCHES
REMOVE BURRS AND SHARP EDGES
TOLERANCES:
LINEAR: 2 DECIMALS: ±0.010"
3 DECIMALS: ±0.005"
ANGULAR: ±1°



**WATERLOO
ROCKETRY**

NAME	DATE	DESCRIPTION:
DRAWN		GRAPHITE BELL NOZZLE
MATERIAL:	GRAPHITE	SIZE
FINISH:		DRAWING NUMBER:
WEIGHT:	LBS	SCALE: 1:2

REVISION	
SIZE	DRAWING NUMBER:
A	22-PR-038
DO NOT SCALE DRAWING	SHEET 1 OF 1

4

3

2

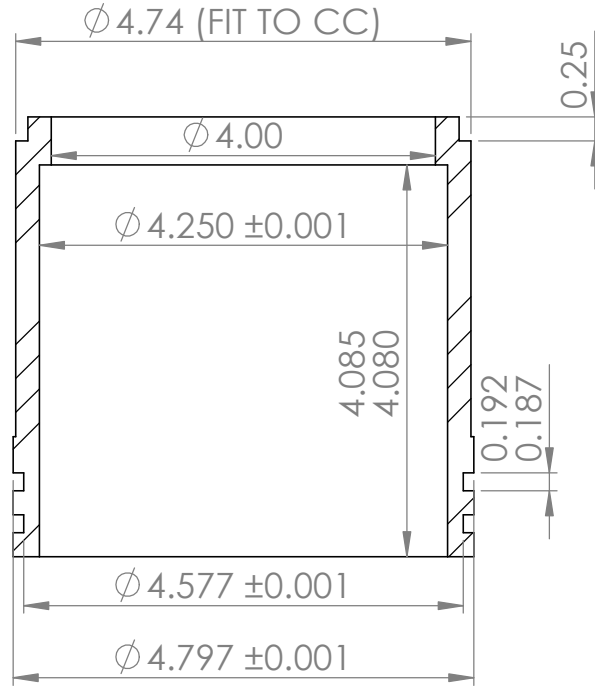
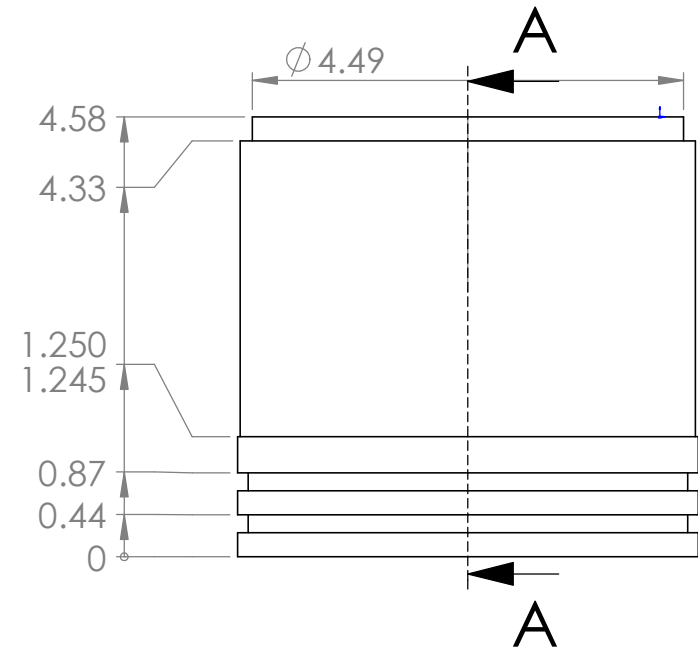
1

D

C

B

A



SECTION A-A

REVISION HISTORY

REV	DESCRIPTION	DATE	AUTHOR
XX	XXXXXXXXXXXXXX	XXX XX/XXXX	X.X

UNLESS OTHERWISE SPECIFIED:
DIMENSIONS ARE IN INCHES
REMOVE BURRS AND SHARP EDGES
TOLERANCES:
LINEAR: 2 DECIMALS: $\pm 0.010''$
3 DECIMALS: $\pm 0.005''$
ANGULAR: $\pm 1^\circ$



**WATERLOO
ROCKETRY**

DRAWN		NAME	DATE	DESCRIPTION: NOZZLE LINER	
MATERIAL: XXXXXXX		SIZE A		DRAWING NUMBER: 22-PR-039	REVISION
FINISH:		SCALE: 1:2		DO NOT SCALE DRAWING	
WEIGHT:		LBS		SHEET 1 OF 1	

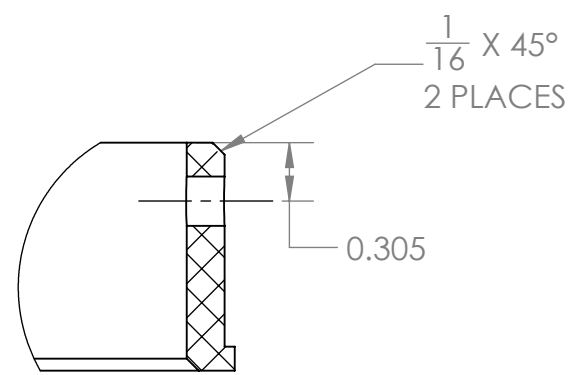
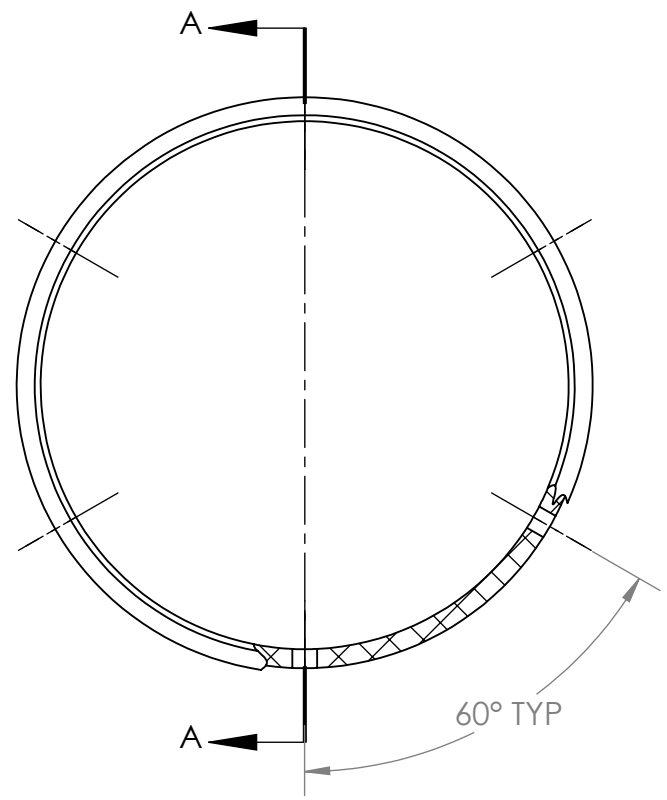
4

3

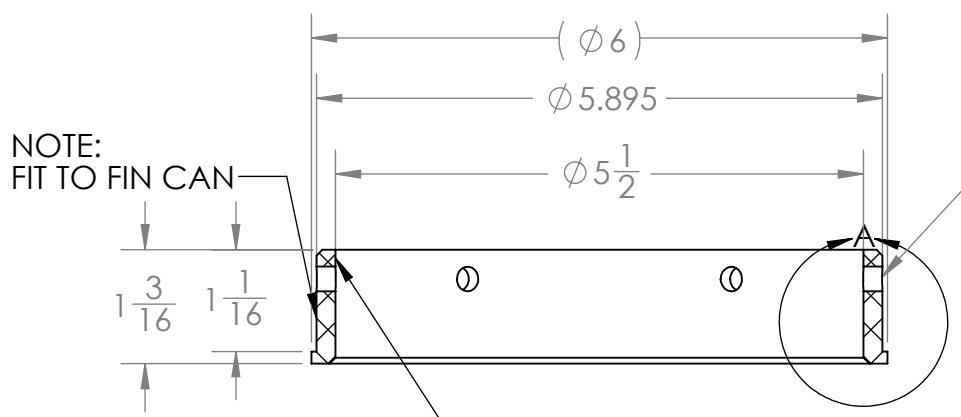
2

1

REVISION HISTORY			
REV	DESCRIPTION	DATE	AUTHOR
00	INITIAL RELEASE	2022-MAR-16	S.K



DETAIL A
SCALE 1 : 1



NOTE:
FIT TO FIN CAN

NOTE: FIT TO BOATTAIL

SECTION A-A

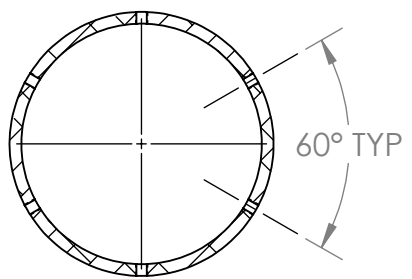
6X $\phi 0.257$ THRU

UNLESS OTHERWISE SPECIFIED:
DIMENSIONS ARE IN INCHES
REMOVE BURRS AND SHARP EDGES
TOLERANCES:
LINEAR: 2 DECIMALS: $\pm 0.010''$
3 DECIMALS: $\pm 0.005''$
FRACTIONAL: $\pm 0.005''$
ANGULAR: $\pm 0.1^\circ$

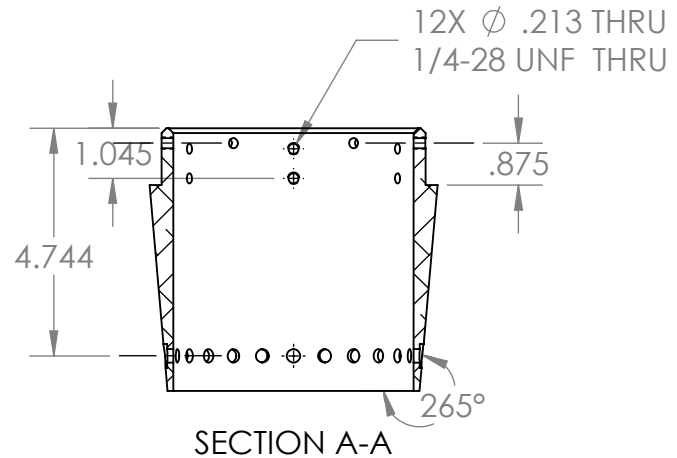
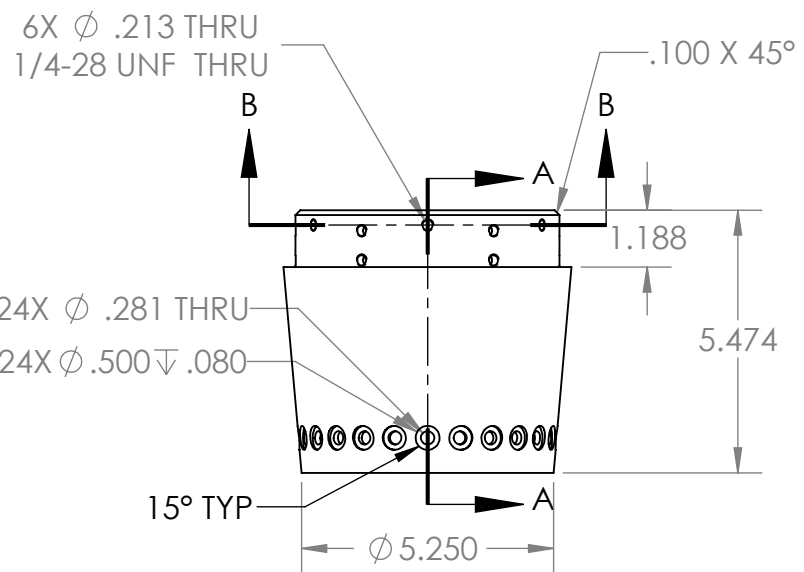
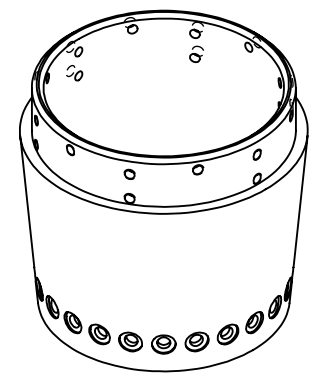


DRAWN		NAME	DATE	DESCRIPTION:	
		S. KONG	2022-MAR-16	KOTS - BOATTAIL SPACER RING	
MATERIAL:		PTFE (general)		SIZE	DRAWING NUMBER:
FINISH:		AS-MACHINED		A	22-AF-010
WEIGHT:		0.3511	LBS	SCALE: 1:2	DO NOT SCALE DRAWING
				REVISION	00
				SHEET 1 OF 1	

REVISION HISTORY			
REV	DESCRIPTION	DATE	AUTHOR
00	INITIAL RELEASE	2018	N.C
01	Added new upper hole pattern	20/04/2022	F.Y



SECTION B-B



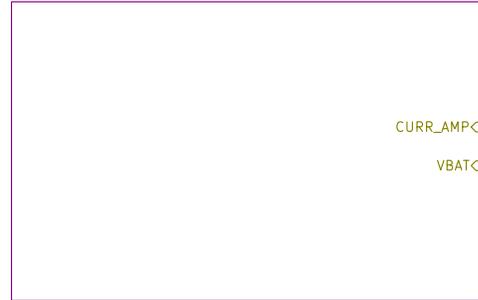
SECTION A-A

UNLESS OTHERWISE SPECIFIED:
 DIMENSIONS ARE IN INCHES
 REMOVE BURRS AND SHARP EDGES
 TOLERANCES:
 LINEAR: 2 DECIMALS: ±0.010"
 3 DECIMALS: ±0.005"
 ANGULAR: ±1°



DRAWN: FRANCIS YAO		DATE: 19/04/2022	DESCRIPTION: BOATTAIL	
MATERIAL: AL 6061 T6		SIZE: A	DRAWING NUMBER: 22-AF-011	REVISION: 01
FINISH: BRUSHED		SCALE: 1:4		DO NOT SCALE DRAWING
WEIGHT: _____ LBS		SHEET 1 OF 1		

Power



File: power.sch

MCU



File: mcu.sch

Valve Control



File: valvctrl.sch

Sheet: /

File: actuator.sch

Title: RocketCAN – Actuator Board

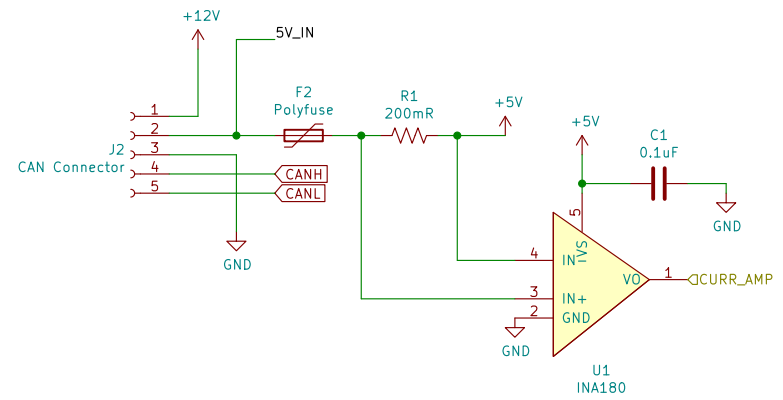
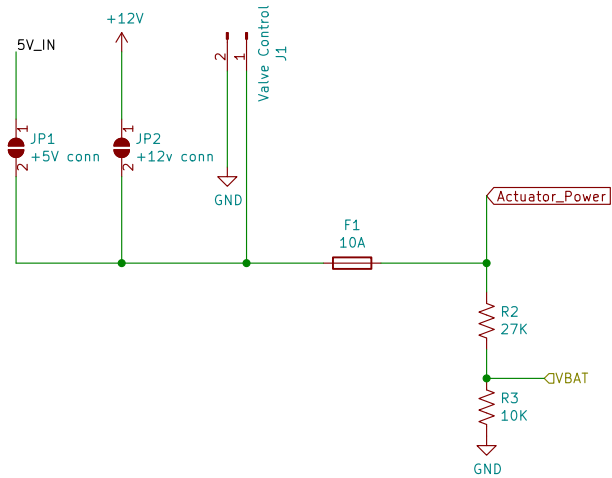
Size: A4

Date:

Rev:

KiCad E.D.A. eeschema (6.0.1)

Id: 1/4



Sheet: /Power/
File: power.sch

Title:

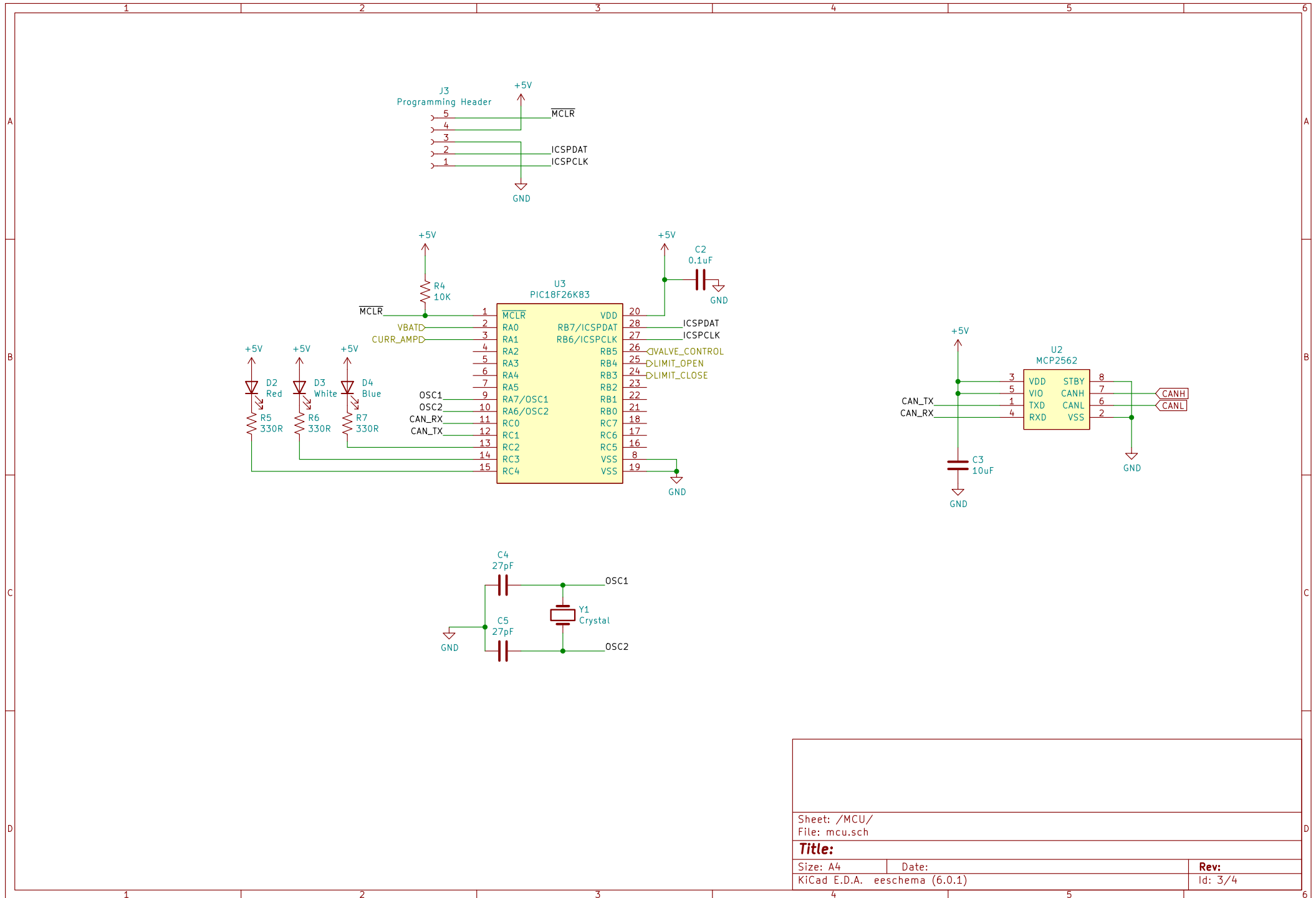
Size: A4

Date:

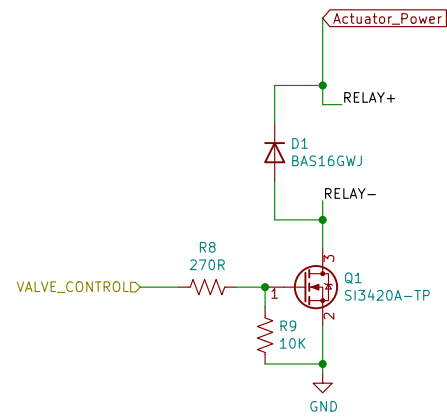
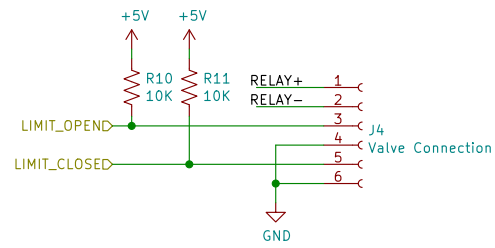
KiCad E.D.A. eeschema (6.0.1)

Rev:

Id: 2/4



Sheet: /MCU/		File: mcu.sch	
Title:			
Size: A4	Date:	Rev:	
KiCad E.D.A. eeschema (6.0.1)			Id: 3/4



Sheet: /Valve Control/
 File: valvectrl.sch

Title:

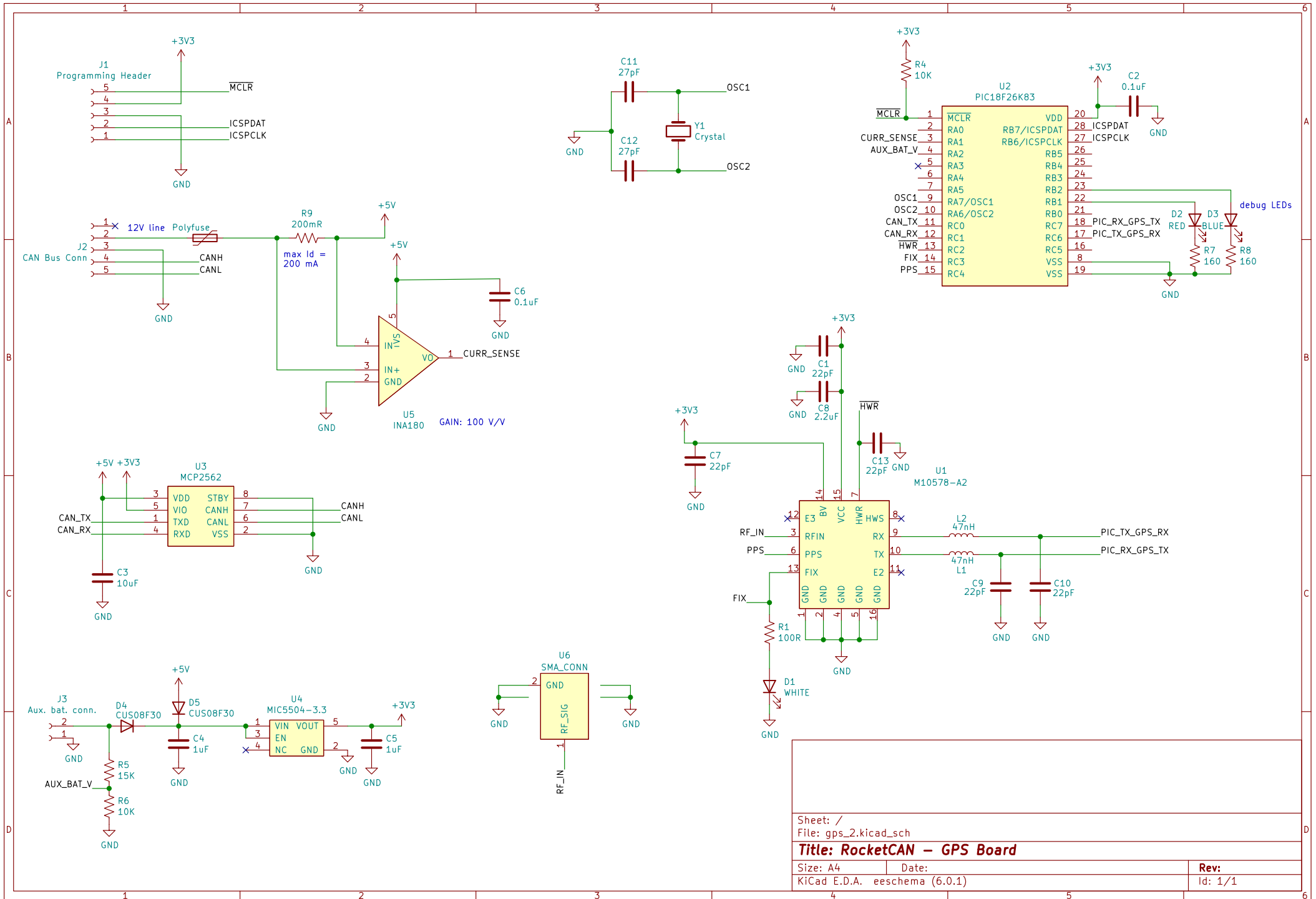
Size: A4

Date:

KiCad E.D.A. eeschema (6.0.1)

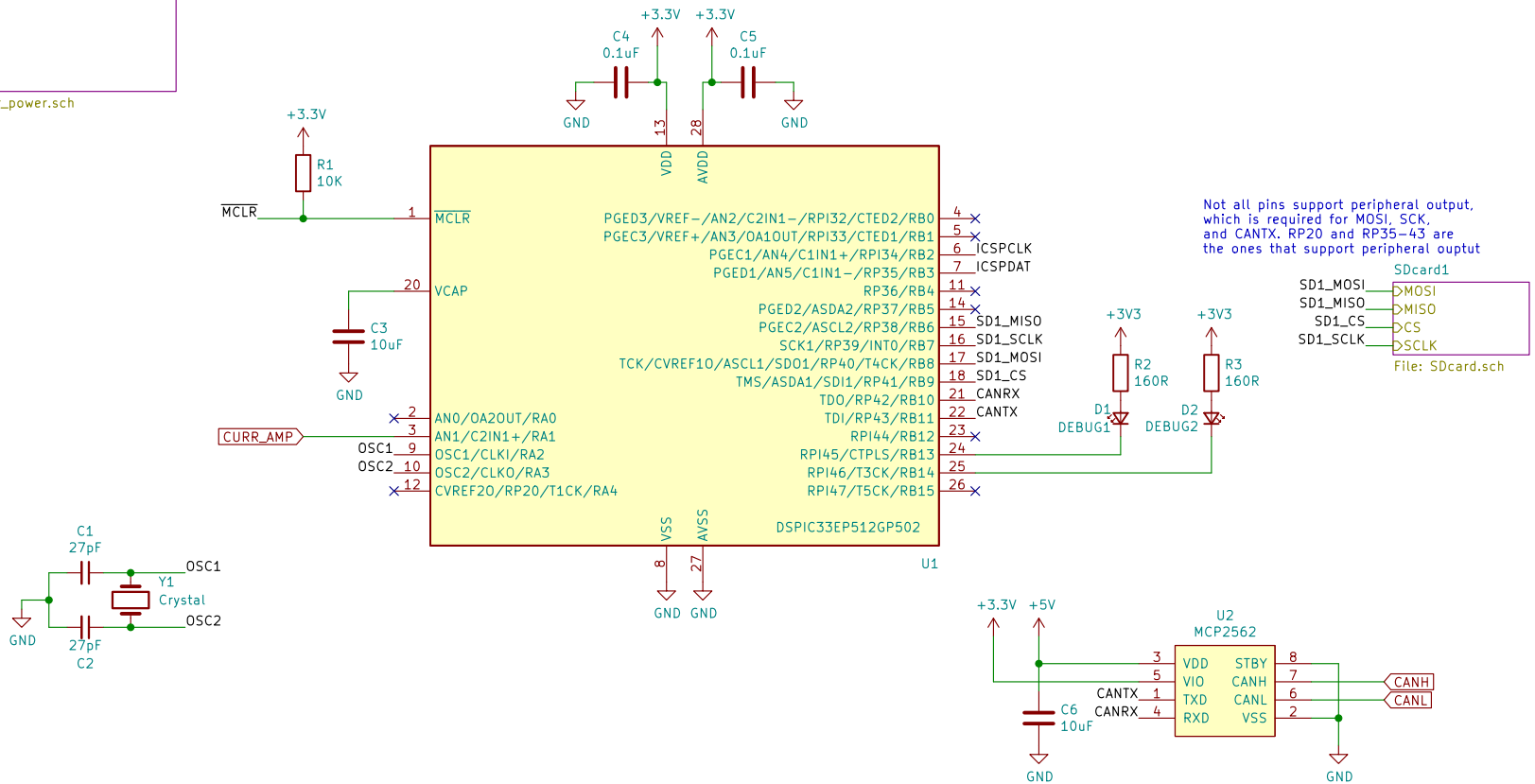
Rev:

Id: 4/4



Power

File: logger_power.sch



Waterloo Rocketry

Sheet: /
File: logger.sch

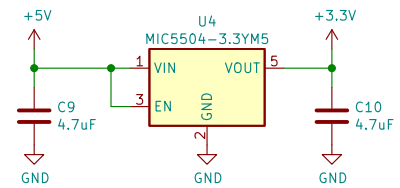
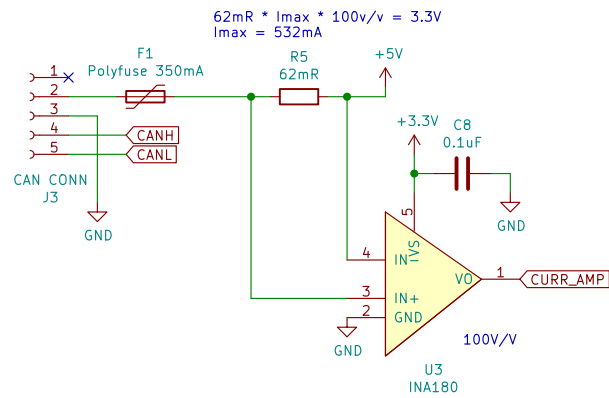
Title: RocketCAN - Logger Board

Size: A4 Date: 2022-01-04

KiCad E.D.A. eeschema (6.0.1)

Rev:

Id: 1/3



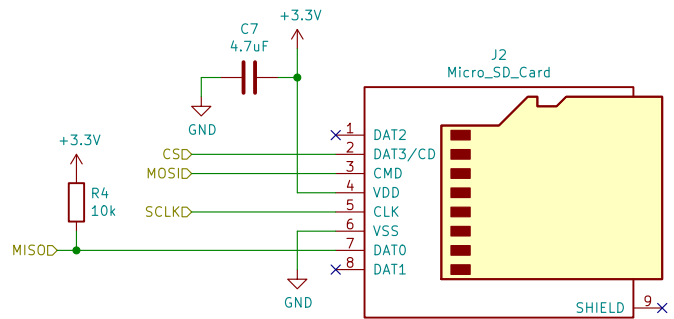
Waterloo Rocketry

Sheet: /Power/
 File: logger_power.sch

Title: Power

Size: A4 Date: 2022-01-04
 KiCad E.D.A. eeschema (6.0.1)

Rev:
 Id: 2/3



Waterloo Rocketry

Sheet: /SDcard1/

File: SDcard.sch

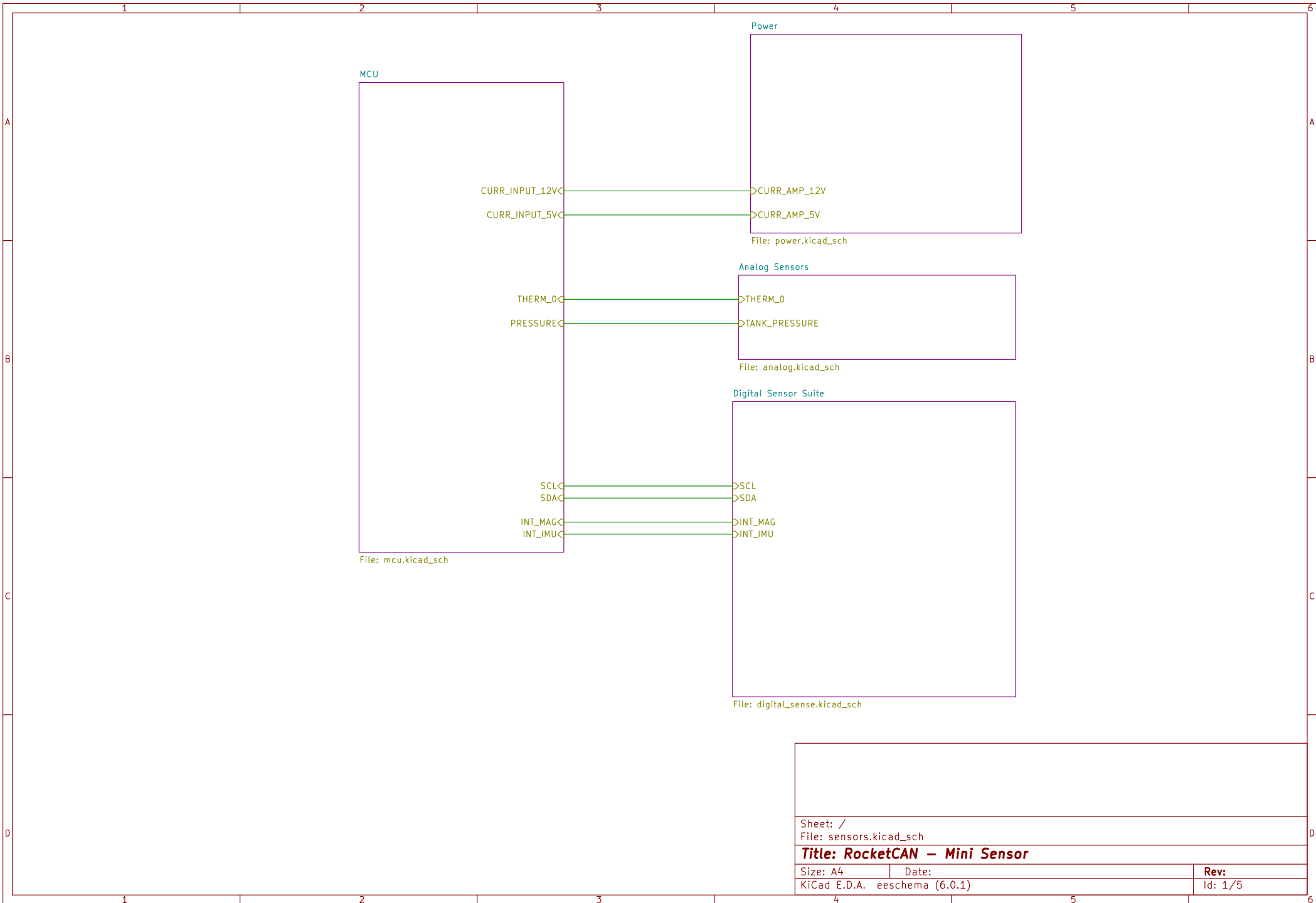
Title: SD Card Breakout

Size: A4 Date: 2022-01-04

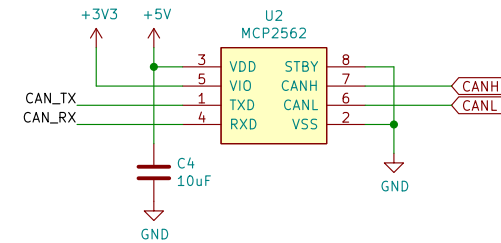
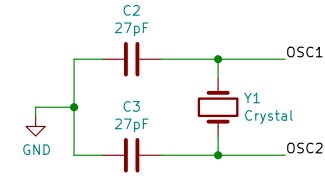
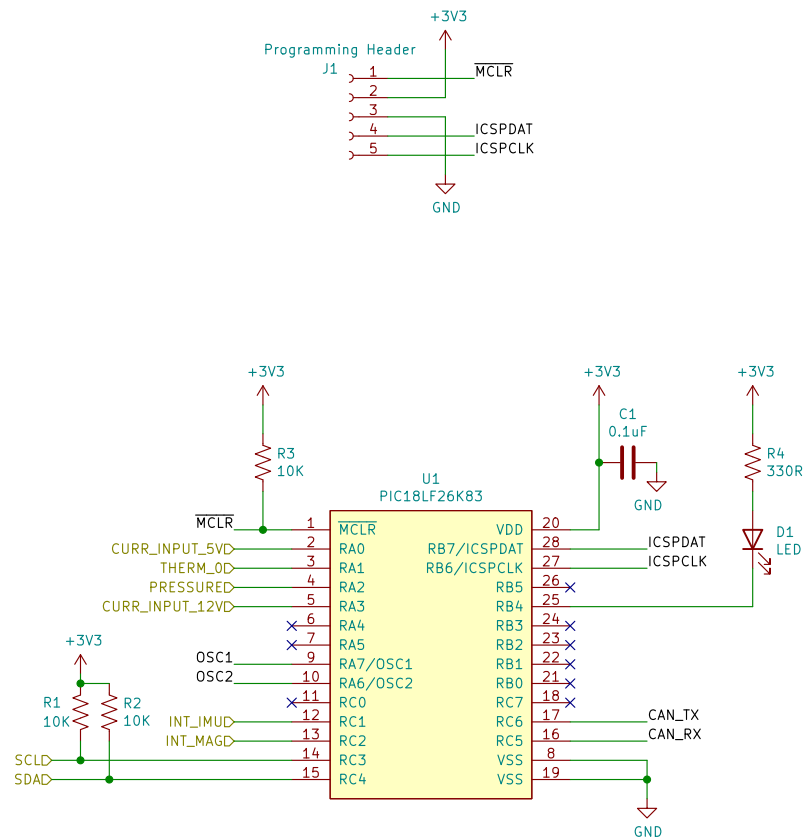
KiCad E.D.A. eeschema (6.0.1)

Rev:

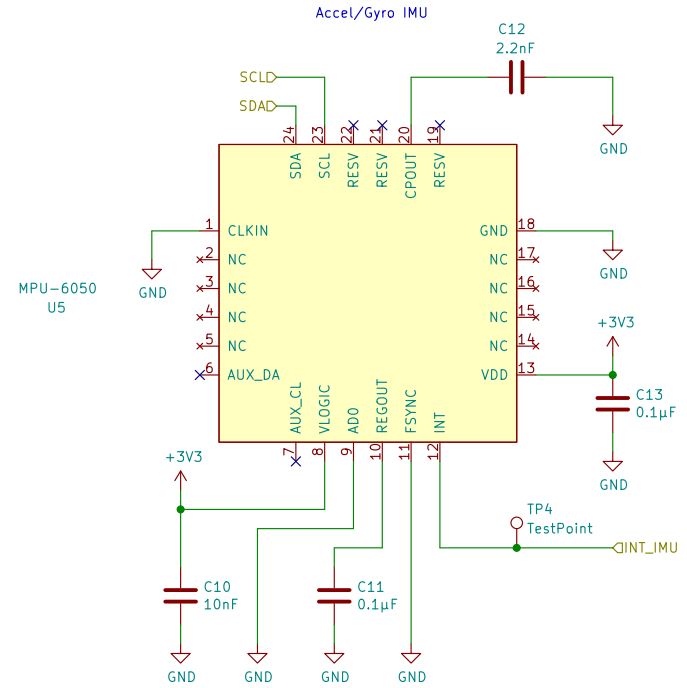
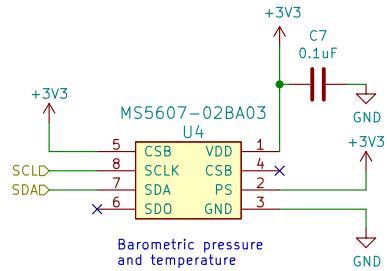
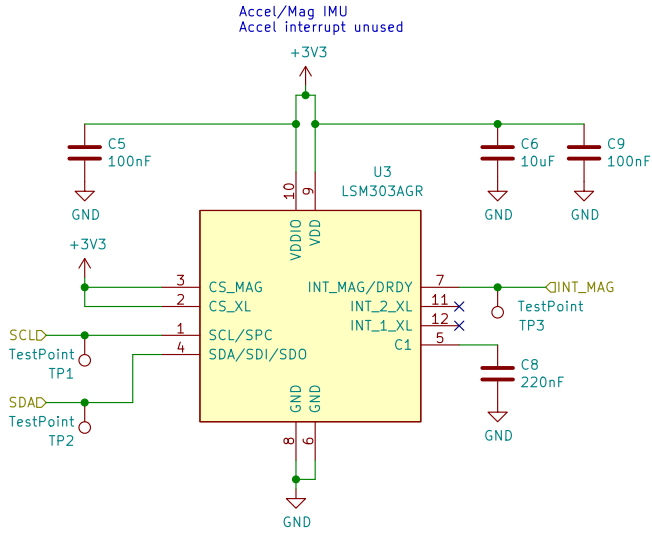
Id: 3/3



Sheet: /		File: sensors.kicad_sch	
Title: RocketCAN – Mini Sensor			
Size: A4	Date:	Rev:	
KiCad E.D.A. eeschema (6.0.1)			Id: 1/5



Sheet: /MCU/		File: mcu.kicad_sch	
Title:			
Size: A4	Date:	Rev:	
KiCad E.D.A. eeschema (6.0.1)			Id: 2/5



Sheet: /Digital Sensor Suite/
File: digital_sense.kicad_sch

Title:

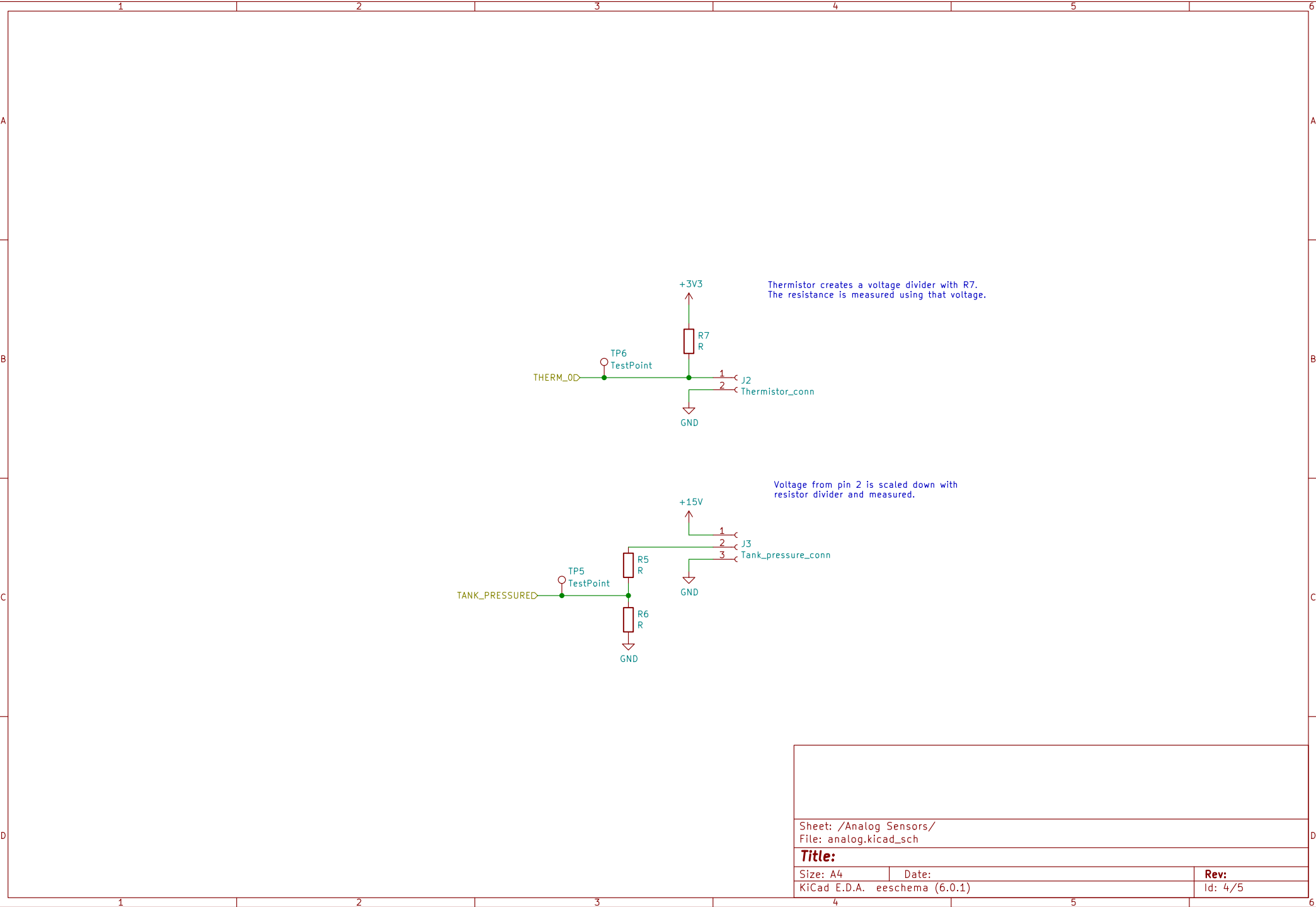
Size: A4

Date:

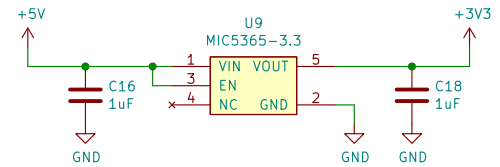
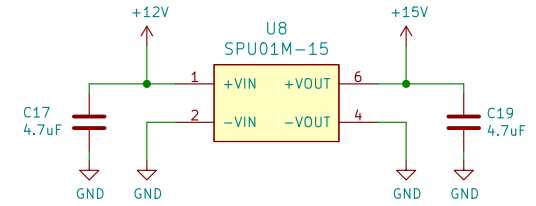
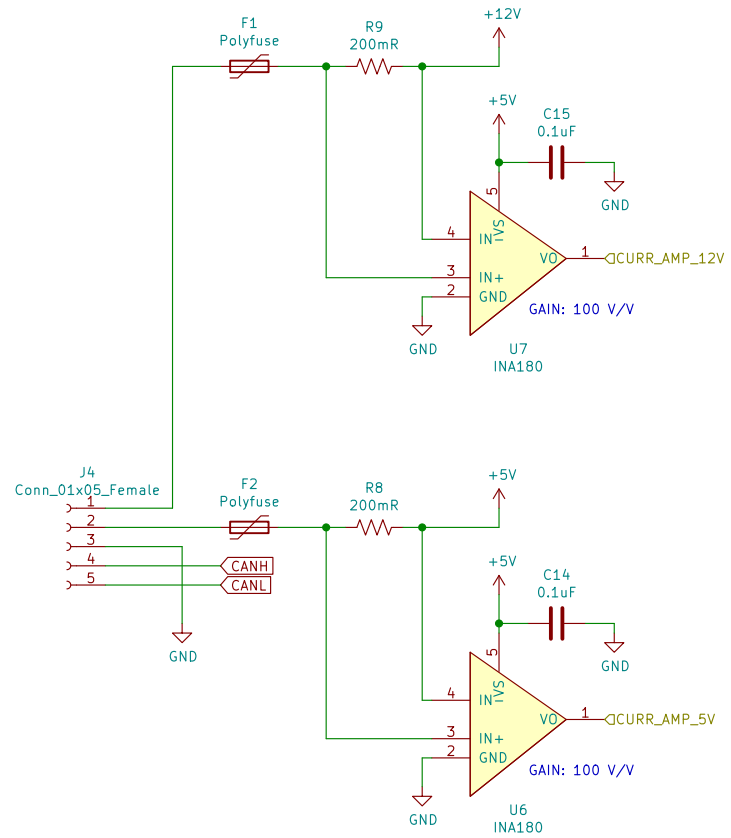
KiCad E.D.A. eeschema (6.0.1)

Rev:

Id: 3/5



Sheet: /Analog Sensors/		
File: analog.kicad_sch		
Title:		
Size: A4	Date:	Rev:
KiCad E.D.A. eeschema (6.0.1)		Id: 4/5



Sheet: /Power/
File: power.kicad_sch

Title:

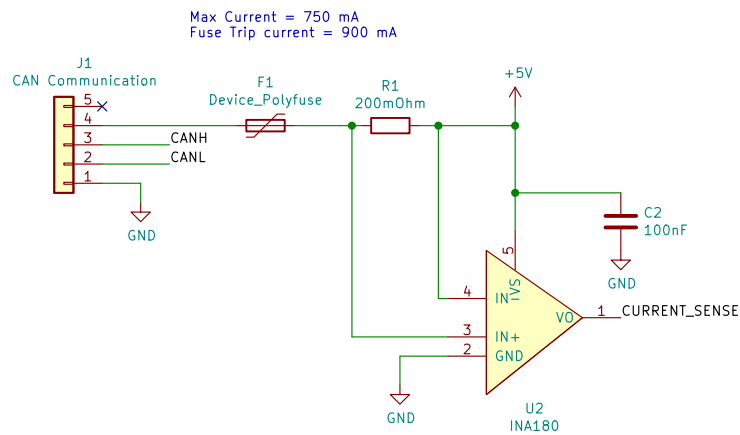
Size: A4 Date:

KiCad E.D.A. eeschema (6.0.1)

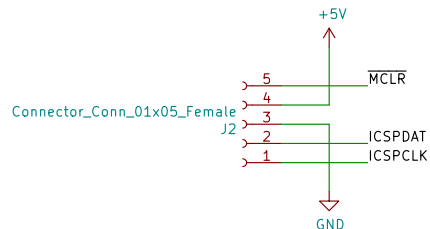
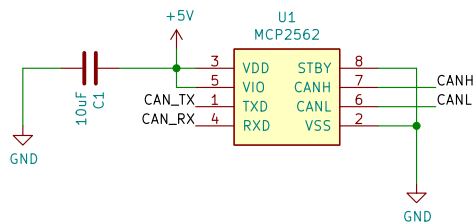
Rev:

Id: 5/5

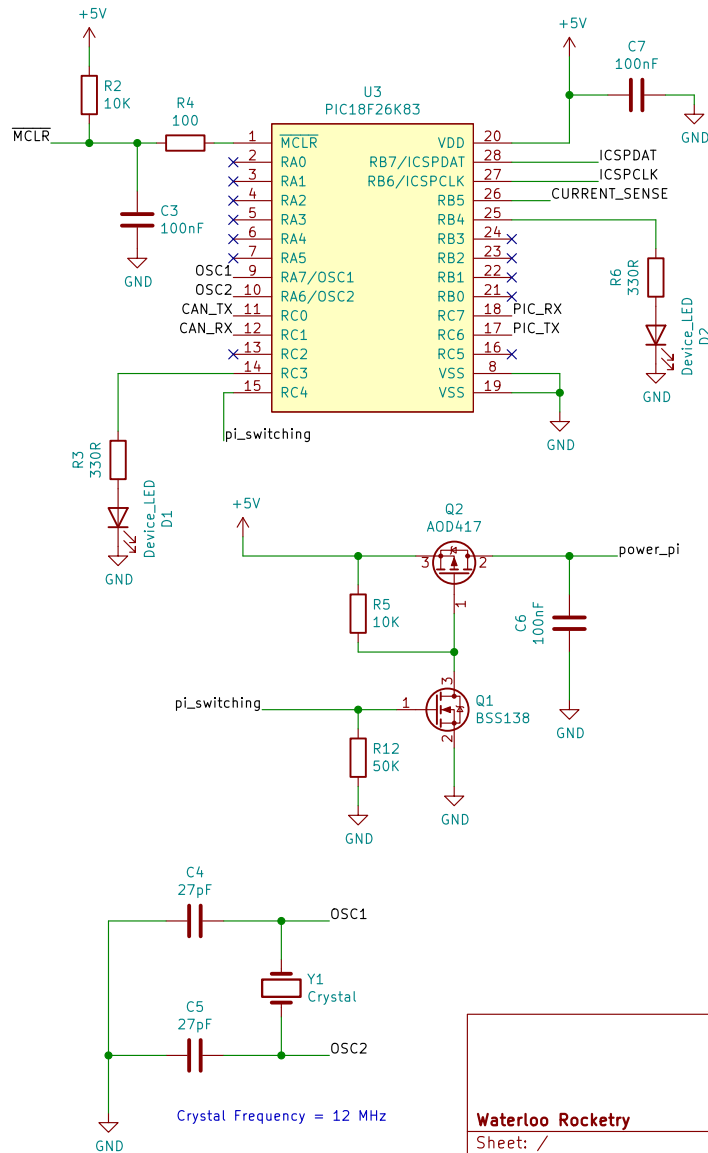
EXTERNAL CONNECTORS



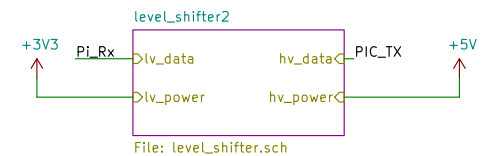
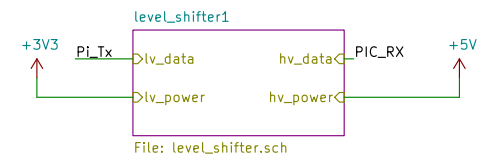
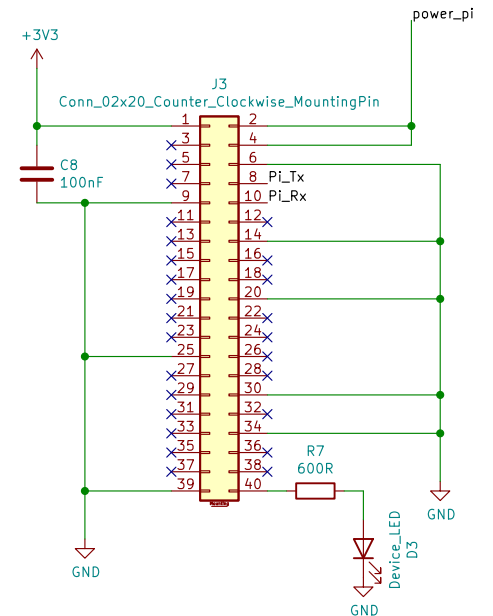
HIGHSPEED CAN TRANSCEIVER



MICROCONTROLLER



MISC PERIPHERALS



Waterloo Rocketry

Sheet: /
File: RocketPi.sch

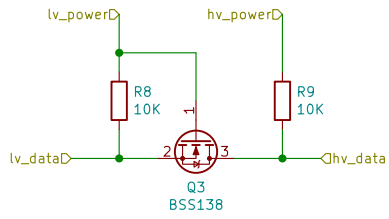
Title: RocketCAN - PiCam

Size: A4 Date: 2020-12-31

KiCad E.D.A. eeschema (6.0.1)

Rev: v0

Id: 1/3



Sheet: /level_shifter1/
File: level_shifter.sch

Title:

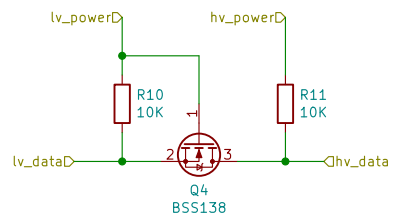
Size: A4

Date:

Rev:

KiCad E.D.A. eeschema (6.0.1)

Id: 2/3



Sheet: /level_shifter2/
File: level_shifter.sch

Title:

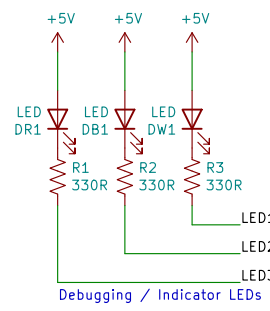
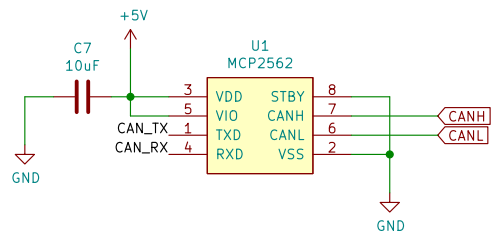
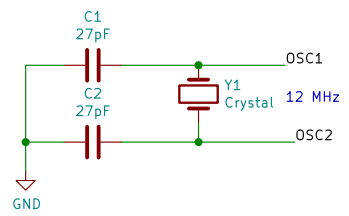
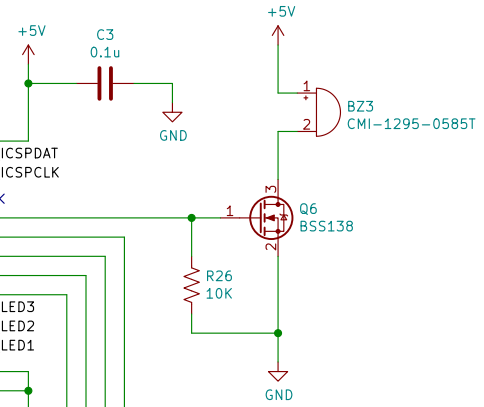
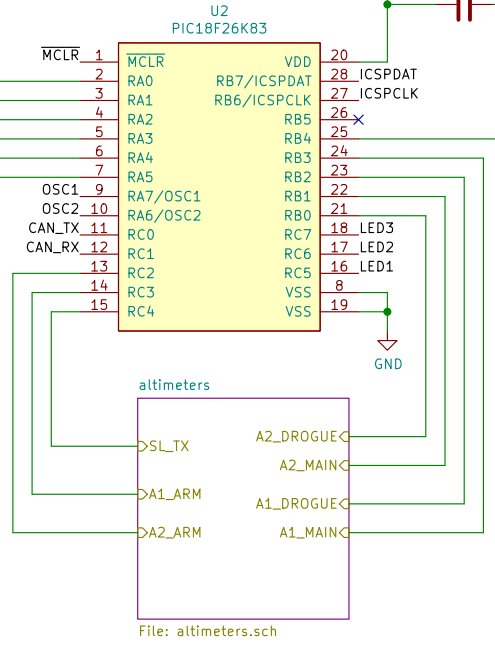
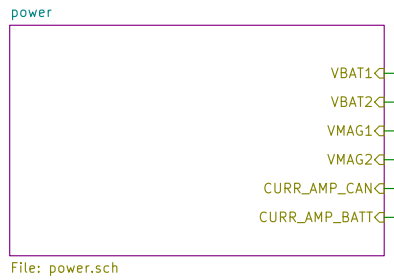
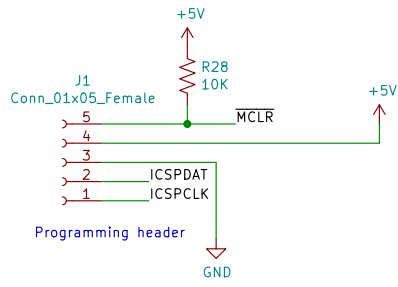
Size: A4

Date:

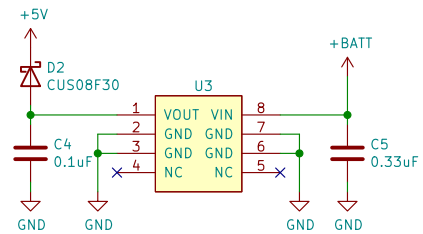
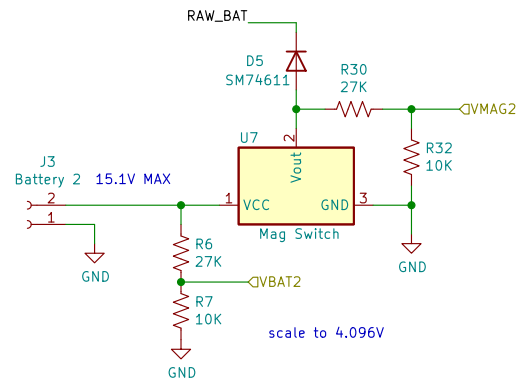
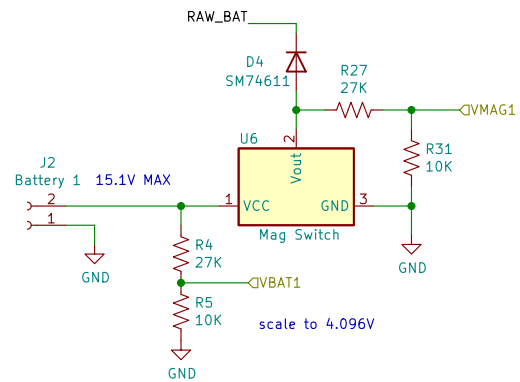
Rev:

KiCad E.D.A. eeschema (6.0.1)

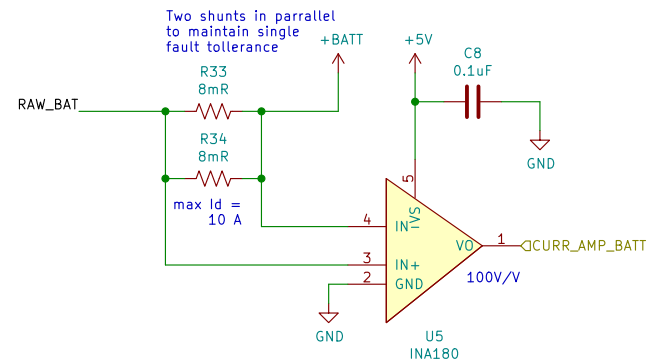
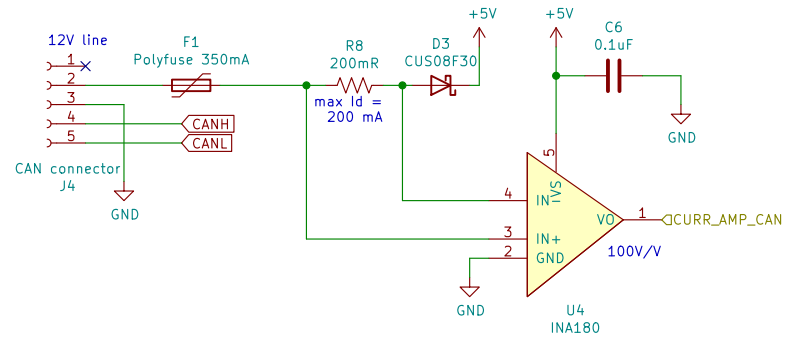
Id: 3/3



Waterloo Rocketry	
Sheet: /	
File: remote_arming.sch	
Title: RocketCAN – Remote Arming	
Size: A4	Date:
KiCad E.D.A. eeschema (6.0.1)	Rev: Id: 1/3



TL750L05CD or LM2931AMX-5.0/NO PB



Sheet: /power/
File: power.sch

Title:

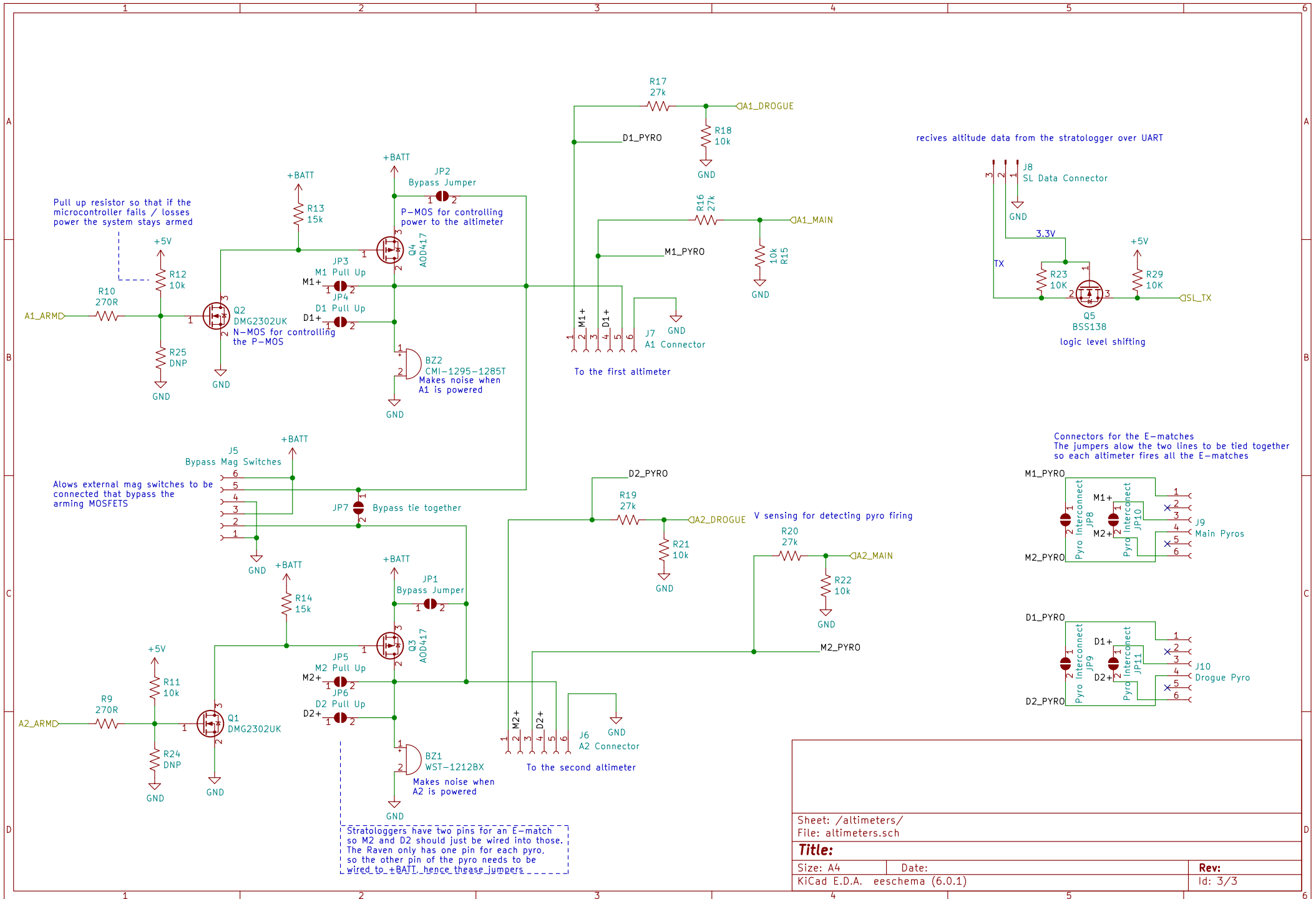
Size: A4

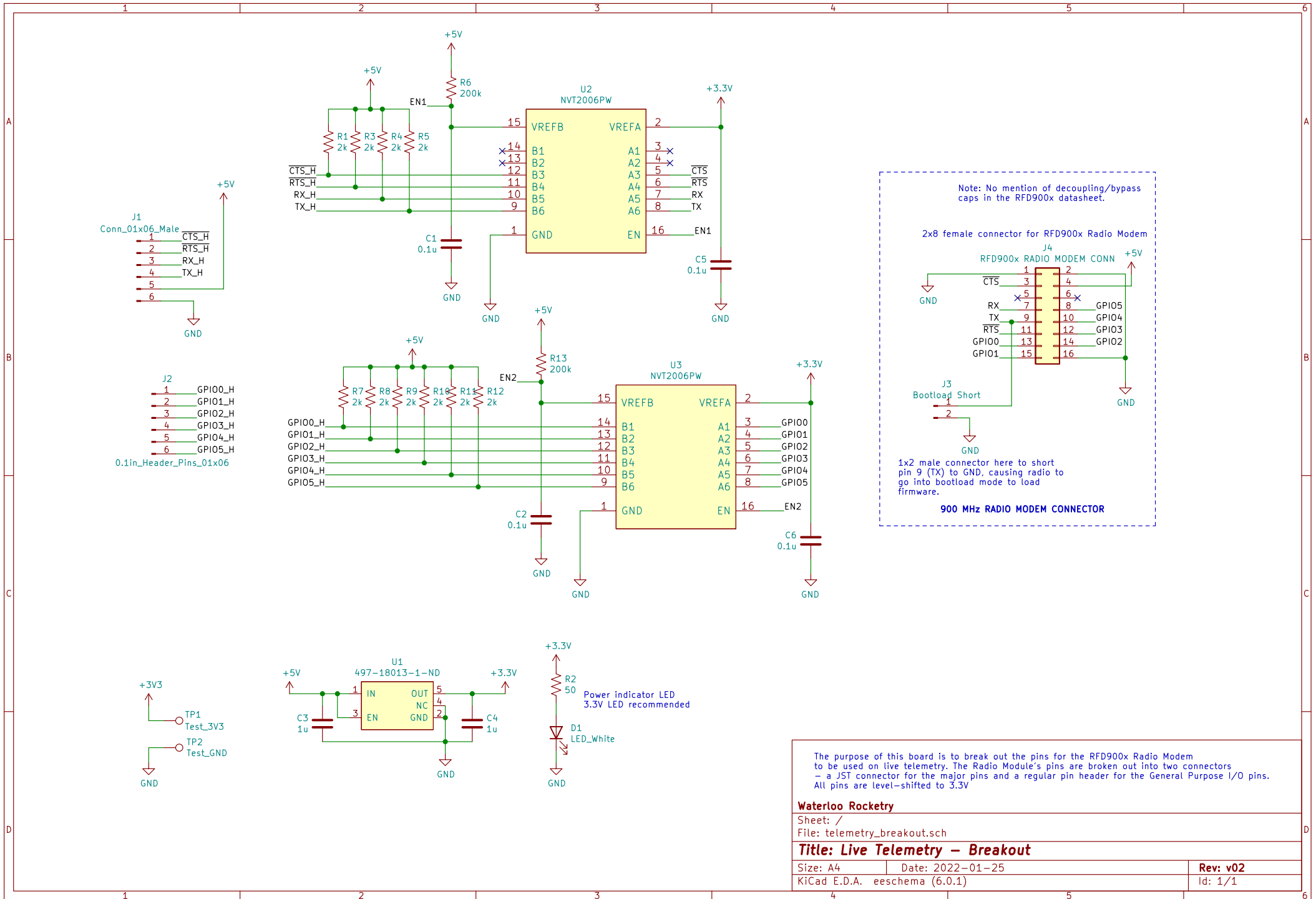
Date:

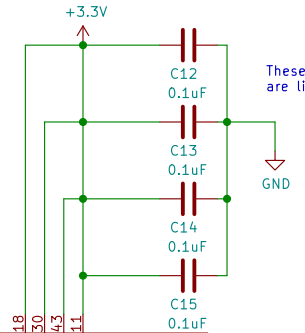
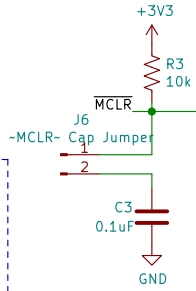
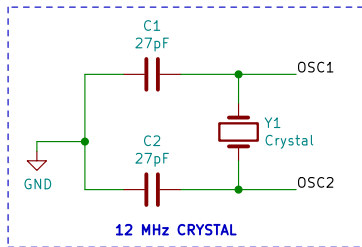
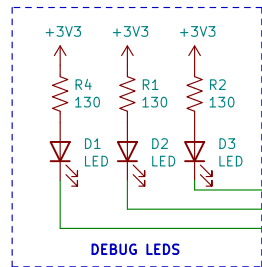
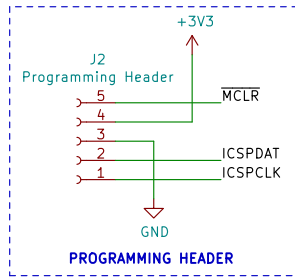
KiCad E.D.A. eeschema (6.0.1)

Rev:

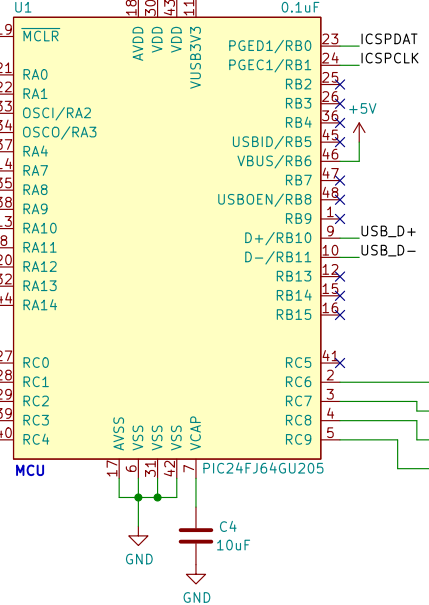
Id: 2/3

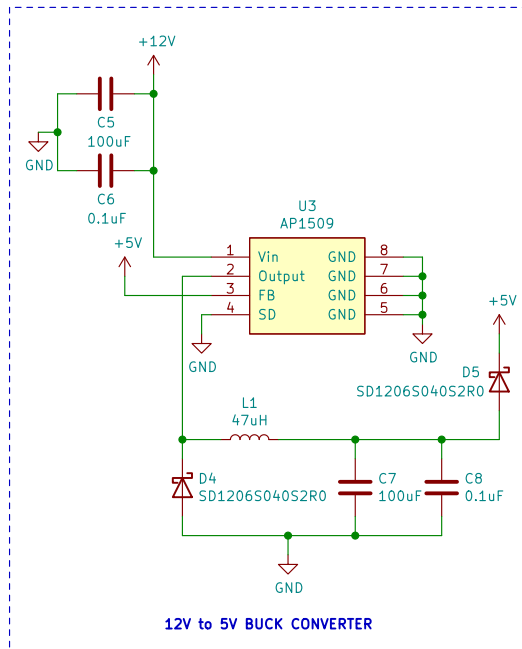
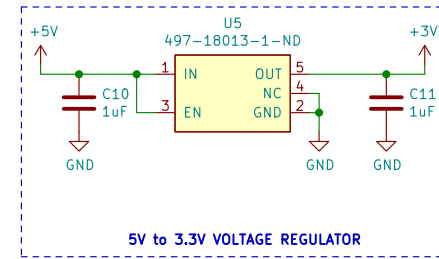
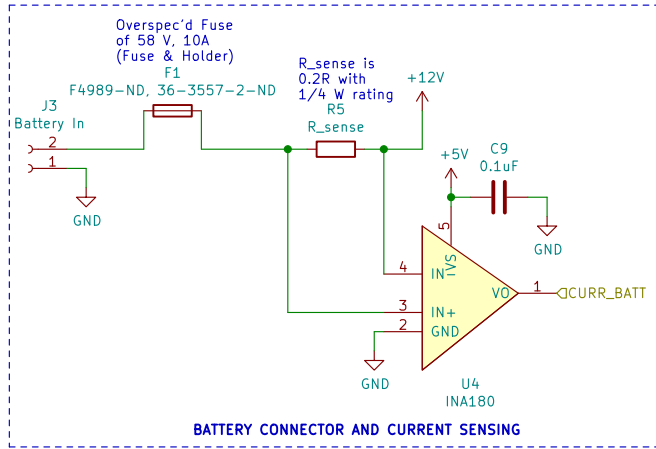






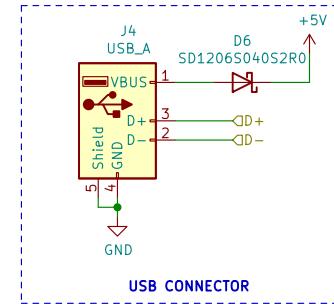
Note: This PIC has lots of unused pins, but not many PICs had USB support. This PIC also has CAN support for potential future CAN debugging on LTR.





Schottky diode is used here to protect line from other power sources.

Schottky diode is used here to protect line from other power sources.

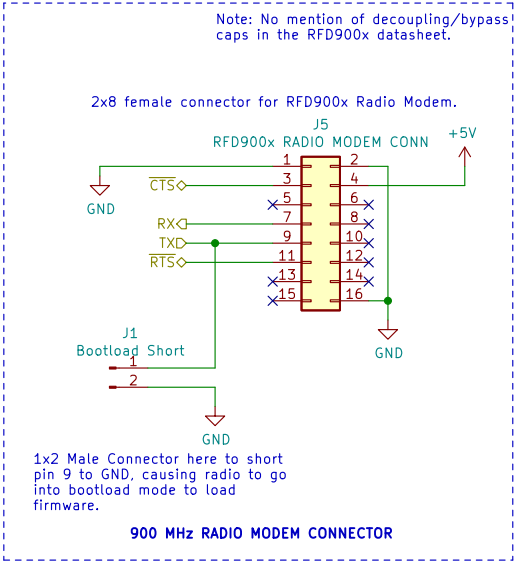


Sheet: /power/
File: power.sch

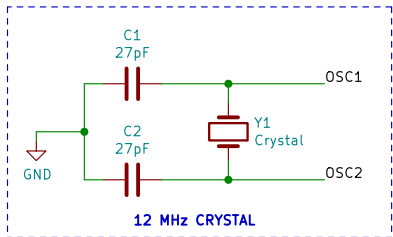
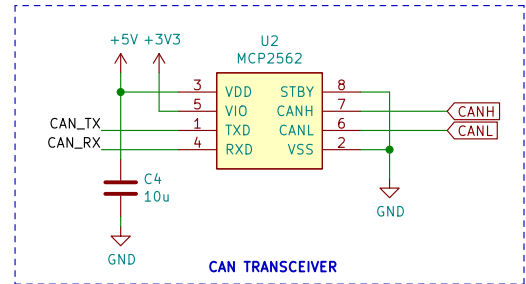
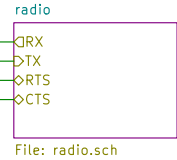
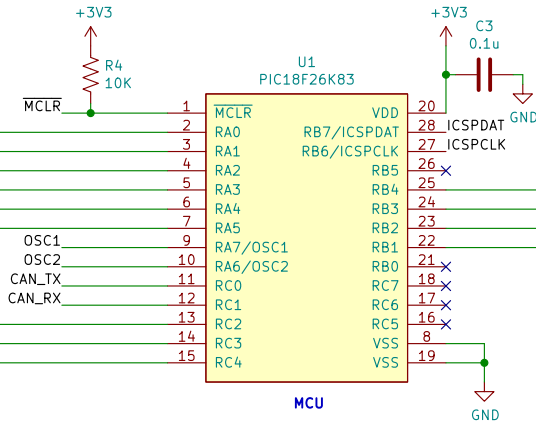
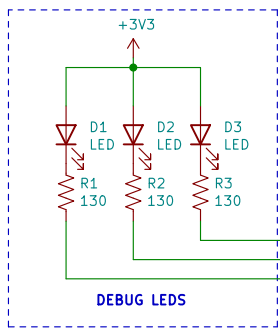
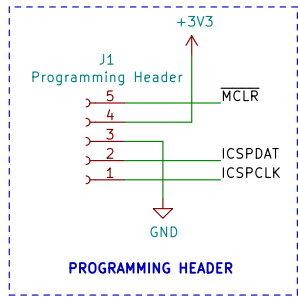
Title:

Size: A4 Date: 2021-11-04
KiCad E.D.A. eeschema (6.0.1)

Rev: 2.2
Id: 2/3



Sheet: /radio.sch/		Date: 2021-11-04	
File: radio.sch		Rev: 2.2	
Size: A4	KiCad E.D.A. eeschema (6.0.1)		Id: 3/3

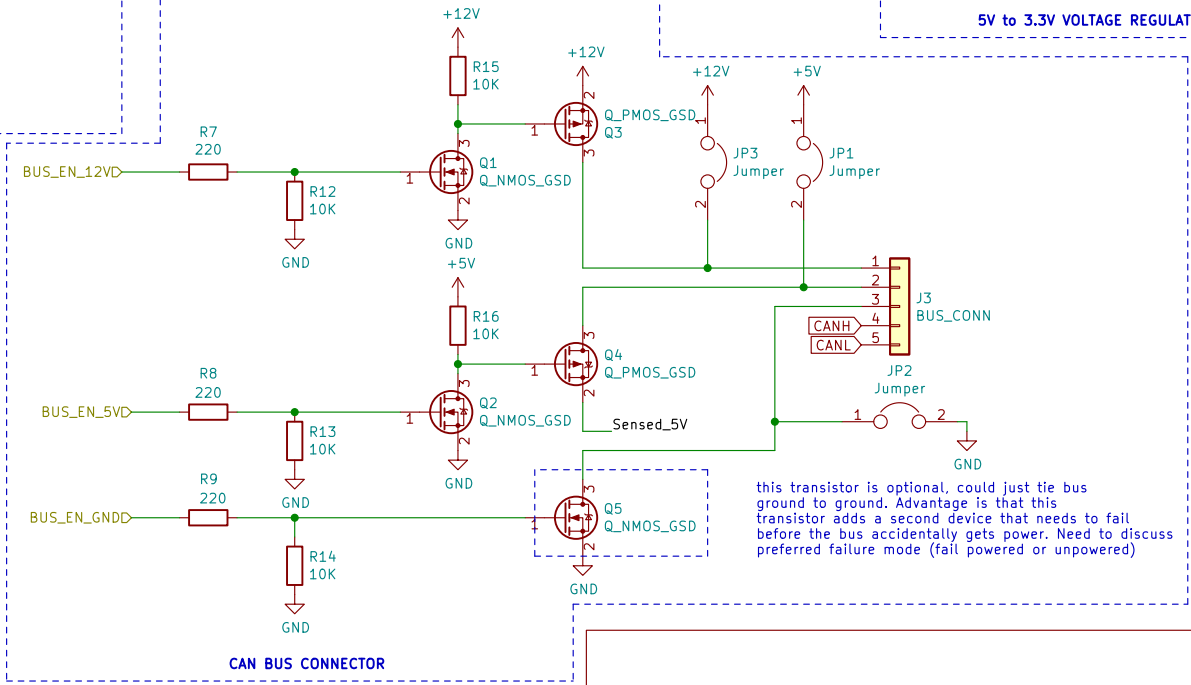
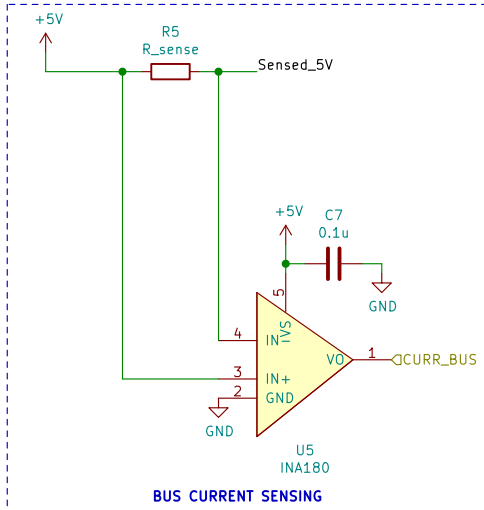
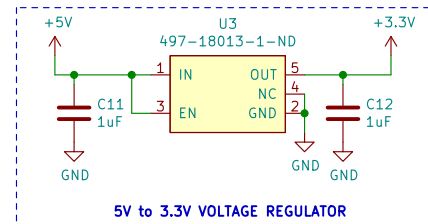
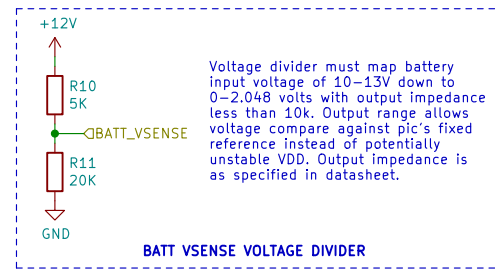
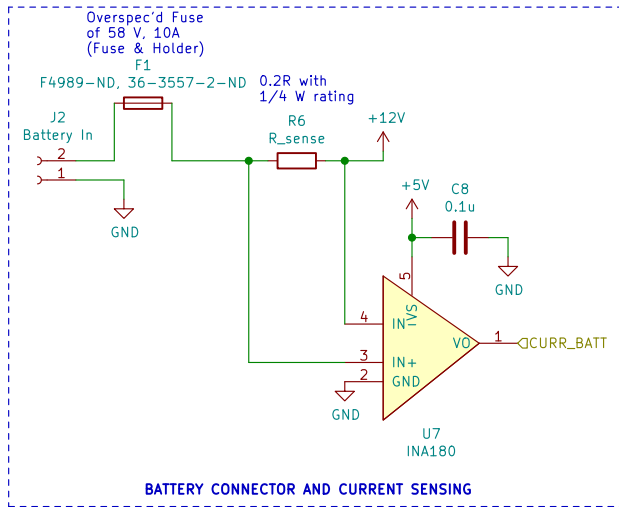
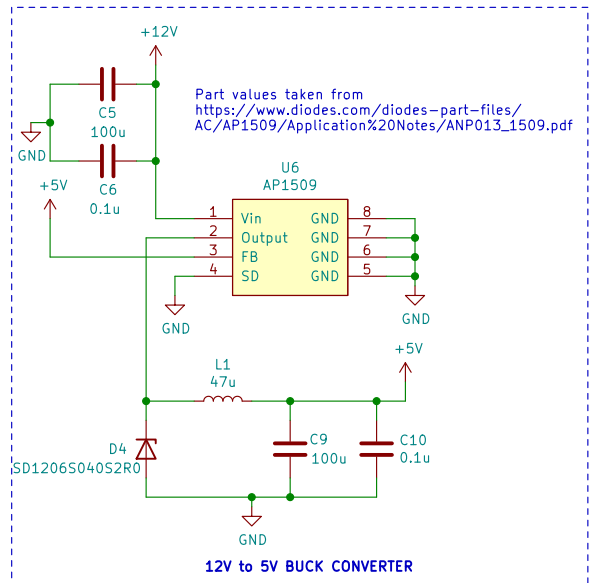


The purpose of the telemetry transmitter board before flight is to communicate and provide power to other boards on the CAN bus to initiate rocket launch. The purpose of the telemetry transmitter board during flight is to supply power and take in data from the CAN bus and transmit this data to the telemetry receiver board. The telemetry transmitter board will transmit this data via a RF module.

Sheet: /
File: telemetry_transmitter.sch

Title: Live Telemetry – Transmitter

Size: A4	Date: 2021-10-01	Rev: 2.1
KiCad E.D.A. eeschema (6.0.1)		Id: 1/3



Note: This is the power sheet from what used to be radio board.

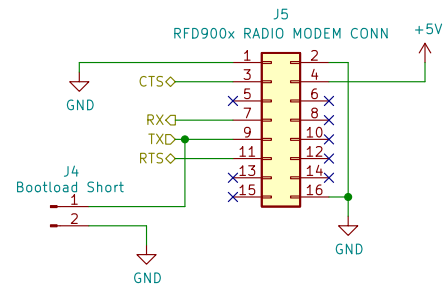
Sheet: /power/
File: power.sch

Title: Live Telemetry Transmitter

Size: A4	Date: 2021-11-03	Rev: 2.1
KiCad E.D.A. eeschema (6.0.1)		Id: 2/3

Note: No mention of decoupling/bypass caps in the RFD900x datasheet.

2x8 female connector for RFD900x Radio Modem.



1x2 Male Connector here to short pin 9 to GND, causing radio to go into bootload mode to load firmware.

900 MHz RADIO MODEM CONNECTOR

Sheet: /radio/
File: radio.sch

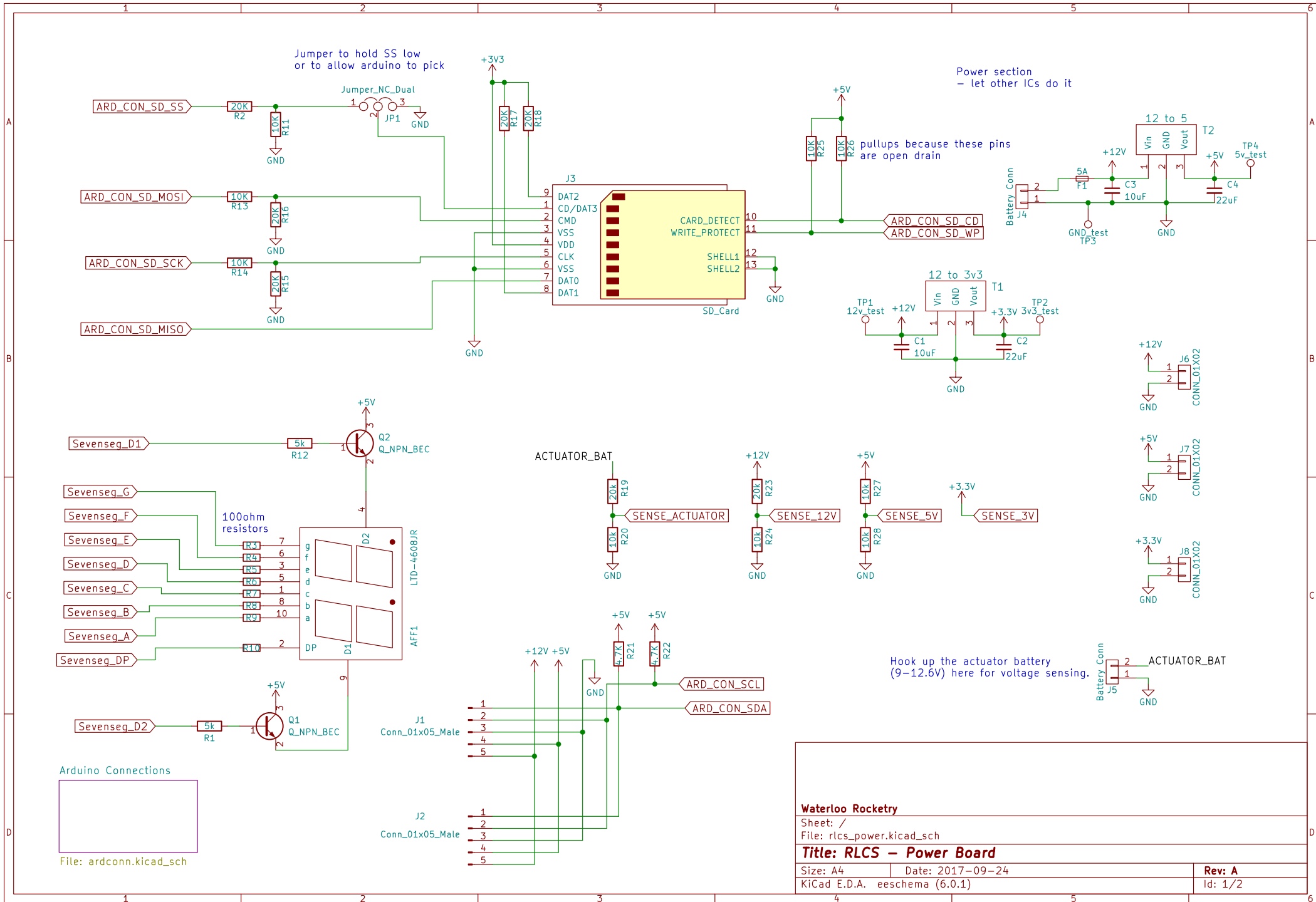
Title: Live Telemetry Transmitter

Size: A4 Date: 2021-10-01

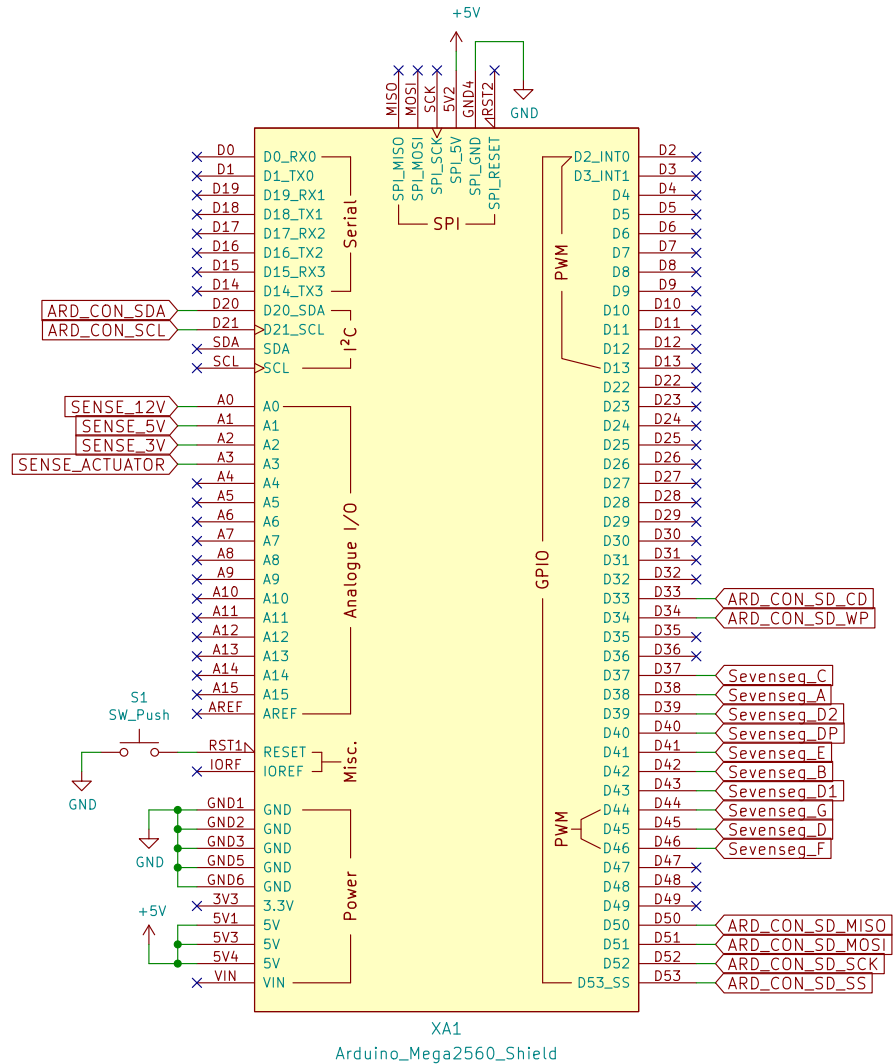
Rev: 2.1

KiCad E.D.A. eeschema (6.0.1)

Id: 3/3

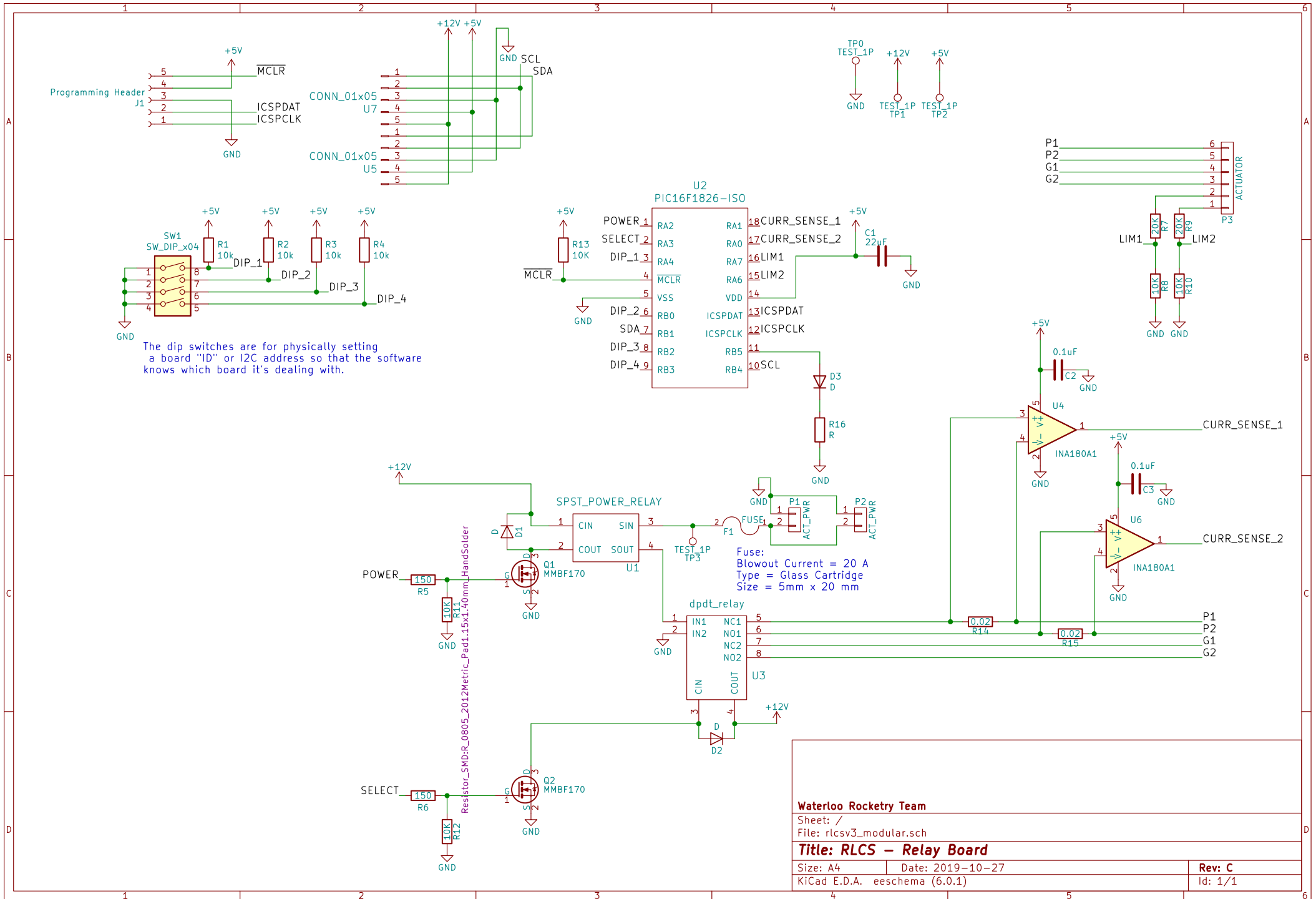


Waterloo Rocketry	
Sheet: /	
File: rlcs_power.kicad_sch	
Title: RLCS - Power Board	
Size: A4	Date: 2017-09-24
KiCad E.D.A. eschema (6.0.1)	Rev: A
	Id: 1/2



All Arduino connections put on this sheet so they can be reordered without screwing up the main sheet
 (this doesn't include power out)

Waterloo Rocketry	
Sheet: /Arduino Connections/	
File: ardconn.kicad_sch	
Title: RLCS power board	
Size: A4	Date: 2017-09-24
KiCad E.D.A. eeschema (6.0.1)	Rev: A
	Id: 2/2



Waterloo Rocketry Team

Sheet: /
File: rlcsv3_modular.sch

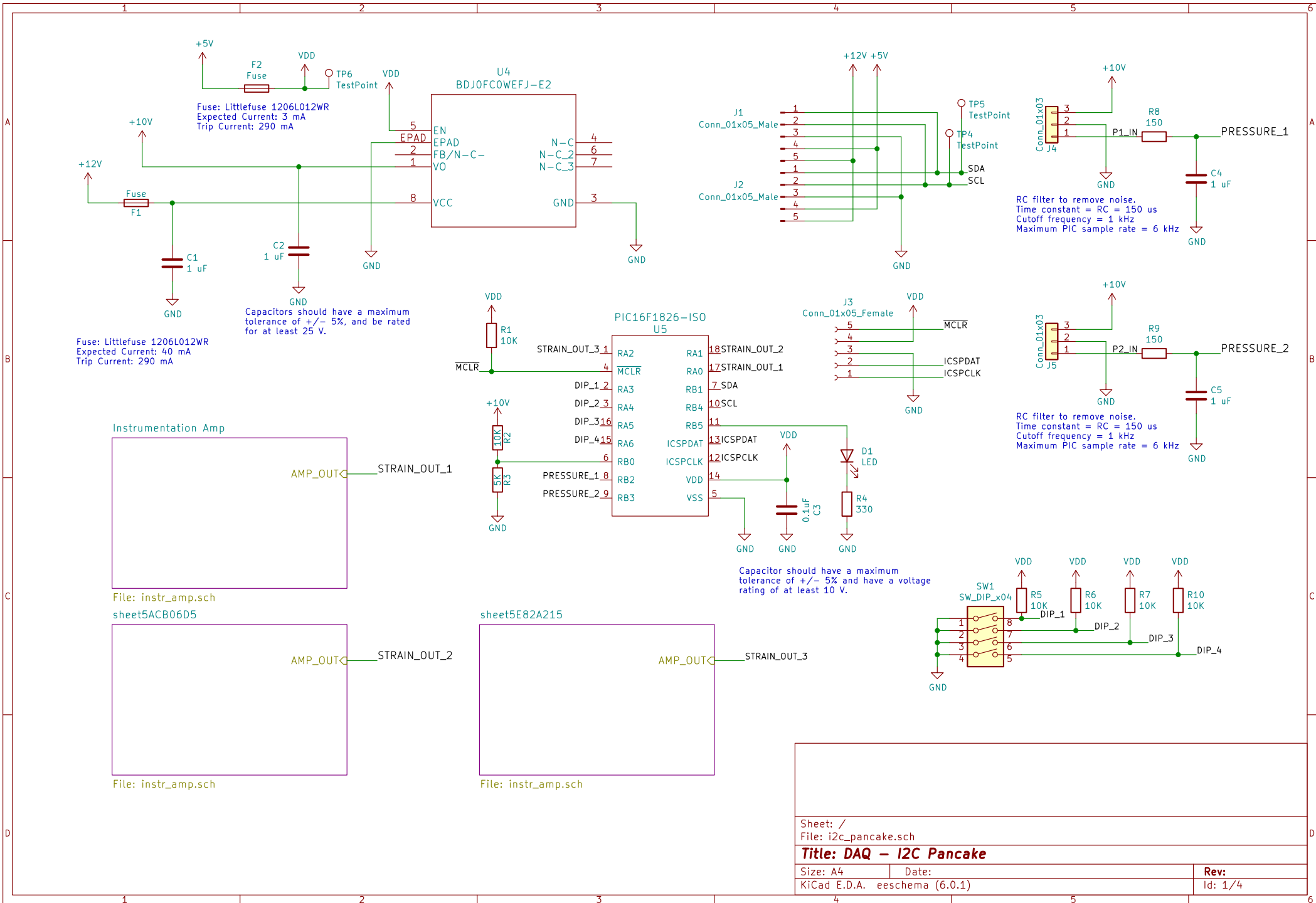
Title: RLCS - Relay Board

Size: A4 Date: 2019-10-27

KiCad E.D.A. eeschema (6.0.1)

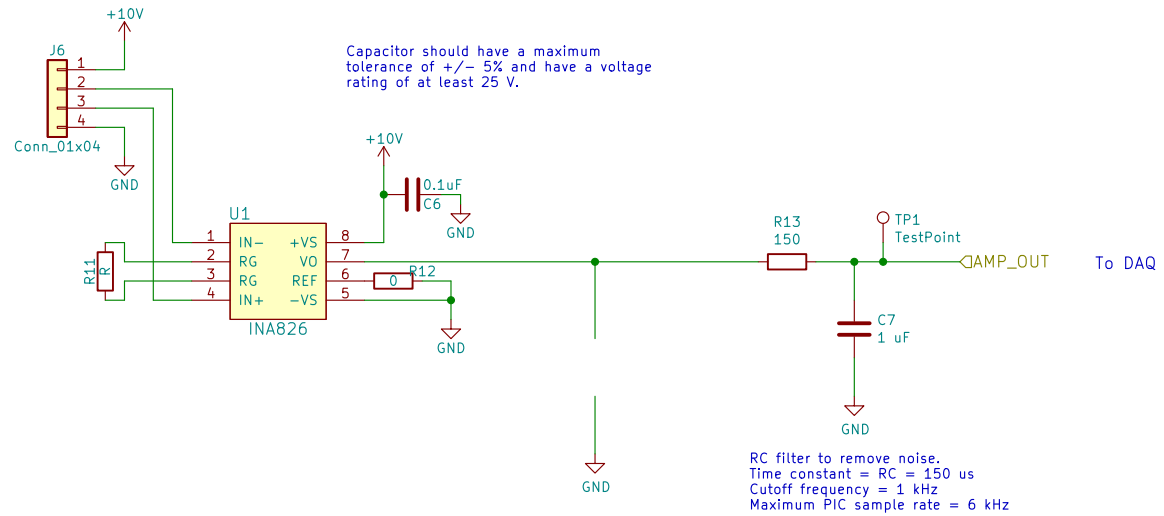
Rev: C

Id: 1/1



Power to sensor & signal from sensor

$$G = 1 + 49.4K/RG$$



Sheet: /Instrumentation Amp/
File: instr_amp.sch

Title:

Size: A4

Date:

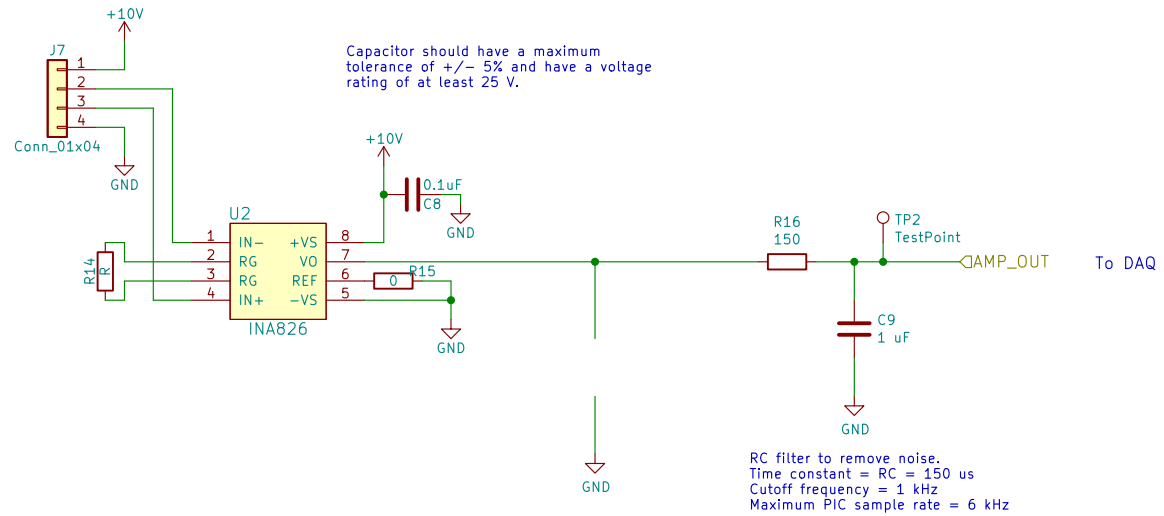
KiCad E.D.A. eeschema (6.0.1)

Rev:

Id: 2/4

Power to sensor & signal from sensor

$$G = 1 + 49.4K/RG$$



Sheet: /sheet5ACB06D5/
File: instr_amp.sch

Title:

Size: A4

Date:

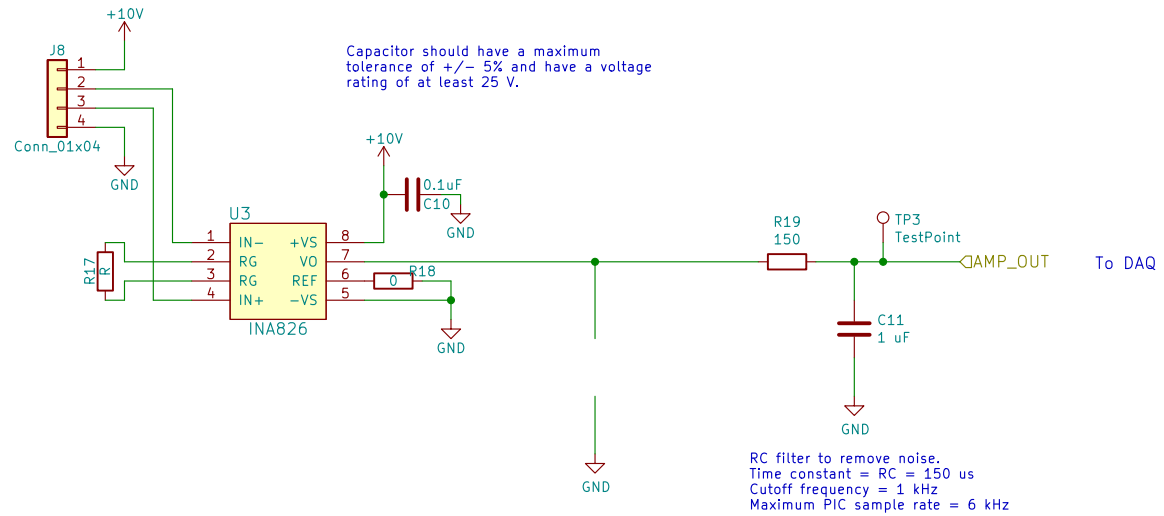
KiCad E.D.A. eeschema (6.0.1)

Rev:

Id: 3/4

Power to sensor &
signal from sensor

$$G = 1 + 49.4K/RG$$



Sheet: /sheet5E82A215/
File: instr_amp.sch

Title:

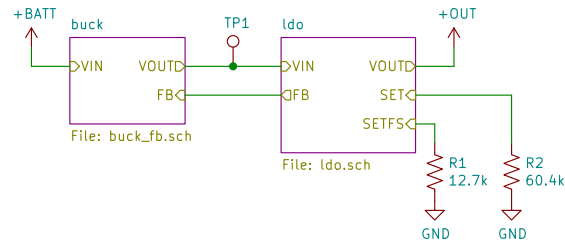
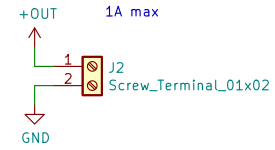
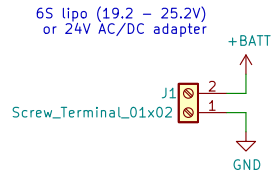
Size: A4

Date:

KiCad E.D.A. eeschema (6.0.1)

Rev:

Id: 4/4



Resistor values:
SET sets the voltage output, SETFS sets the threshold voltage it uses to initially charge up the capacitors.

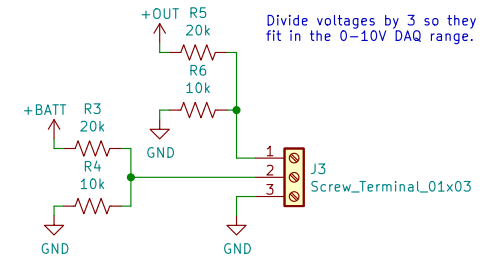
for 12V:
 $SETFS(k\Omega) = 442 / (12 \cdot 3 - 1) = 12.63k$
 $SET(k\Omega) = 5 \cdot 12 = 60k$

for 10V:
 $SETFS(k\Omega) = 442 / (10 \cdot 3 - 1) = 15.24k$
 $SET(k\Omega) = 5 \cdot 10 = 50k$

for 5V:
 $SETFS(k\Omega) = 442 / (5 \cdot 3 - 1) = 31.57k$
 $SET(k\Omega) = 5 \cdot 5 = 25k$

Both 1%

DAQ Voltage Monitoring



All resistors/capacitors are 0805/5% unless otherwise specified.

Sheet: /
File: power_board.sch

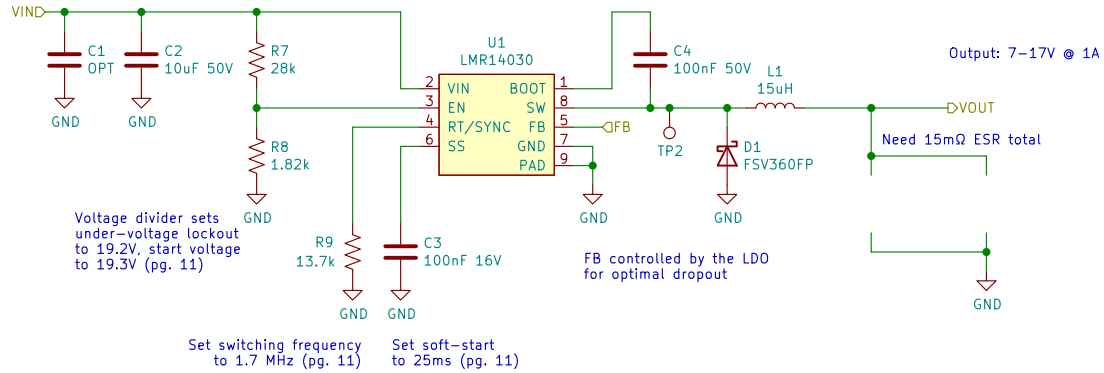
Title: DAQ - Power Board

Size: A4 Date:
KiCad E.D.A. eeschema (6.0.1)

Rev:
Id: 1/3

Variable buck regulator. Most values taken from webench.ti.com for 17V 1A out.
<https://www.ti.com/lit/ds/symlink/lmr14050.pdf>

Input: 19.2–25.2V or 24V from wall



Sheet: /buck/
 File: buck_fb.sch

Title:

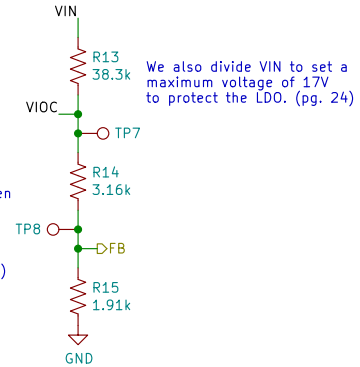
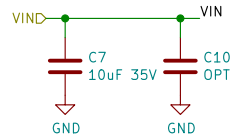
Size: A4

Date:

KiCad E.D.A. eeschema (6.0.1)

Rev:

Id: 2/3



VIOC is driven to the difference between the set voltage and VOUT. We want VIOC=2V so we divide such that $2V \rightarrow 0.75V$, the switching threshold for the buck converter, and use it as the buck converter's feedback. (pg. 23)

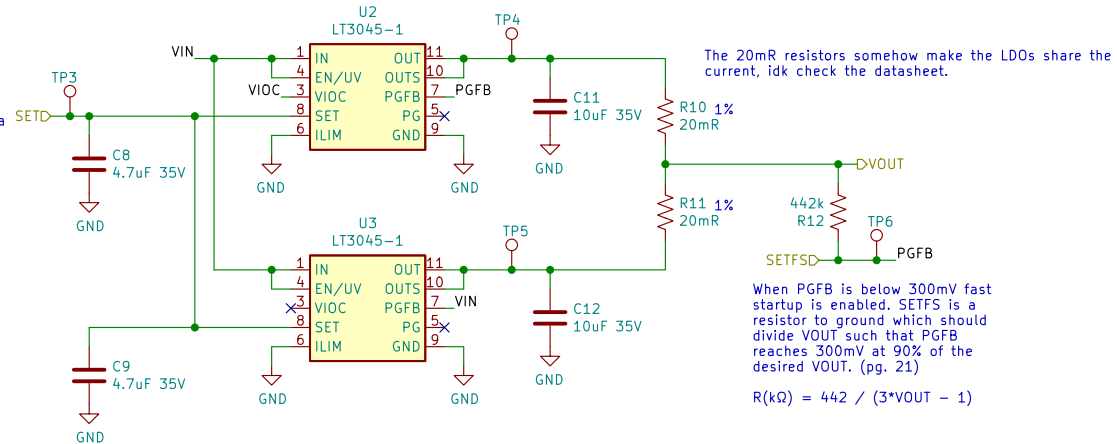
We also divide VIN to set a maximum voltage of 17V to protect the LDO. (pg. 24)

Parallel two LDOs for 1A output. (pg. 22)

<https://www.analog.com/media/en/technical-documentation/data-sheets/30451fa.pdf>

A resistor between SET and GND sets the output voltage based on a 200uA current source (two LDOs).

$$R(k\Omega) = 5 * VOUT$$



The 20mR resistors somehow make the LDOs share the current, idk check the datasheet.



When PGFB is below 300mV fast startup is enabled. SETFS is a resistor to ground which should divide VOUT such that PGFB reaches 300mV at 90% of the desired VOUT. (pg. 21)

$$R(k\Omega) = 442 / (3 * VOUT - 1)$$

Sheet: /ldo/
File: ldo.sch

Title:

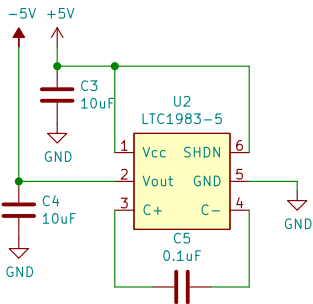
Size: A4

Date:

KiCad E.D.A. eeschema (6.0.1)

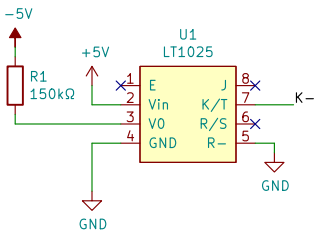
Rev:

Id: 3/3

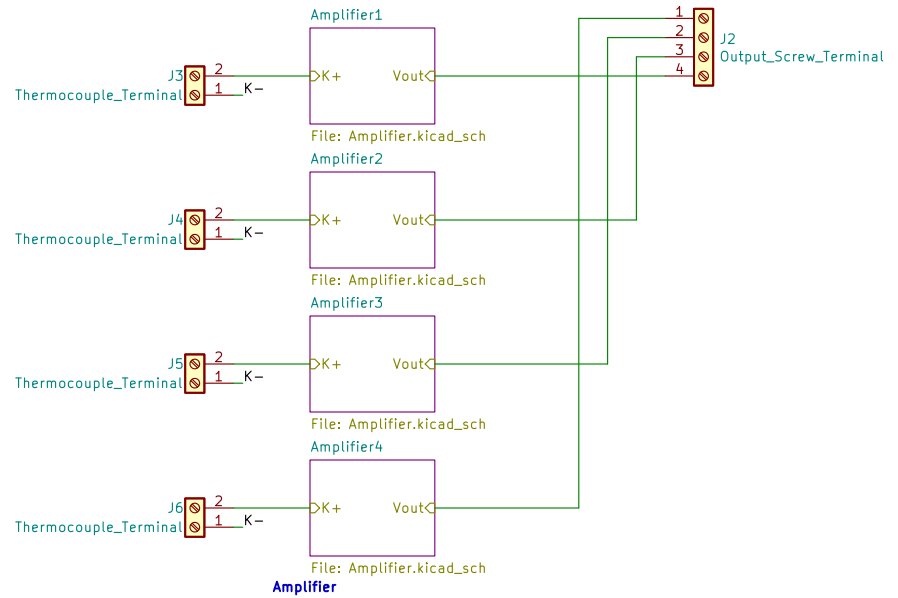
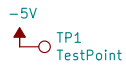


DC/DC Switching Voltage Regulator

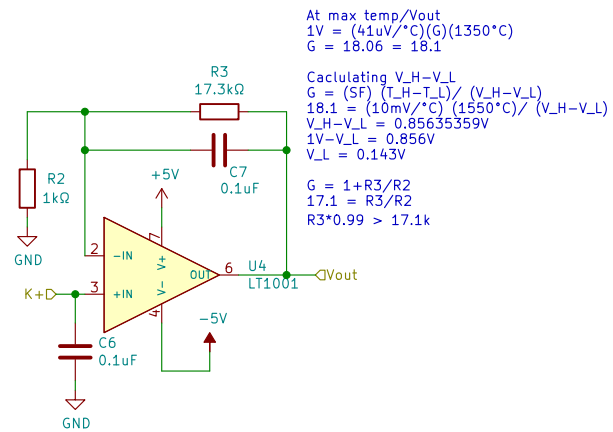
LT1025 Datasheet
<https://www.analog.com/media/en/technical-documentation/data-sheets/1025fb.pdf>



Thermocouple Cold Junction Compensator



Sheet: /	
File: spidey_sense.kicad_sch	
Title: DAQ – Spidey Sense	
Size: A	Date: Jan. 27, 2022
KiCad E.D.A. eeschema (6.0.1)	Rev: 1
	Id: 1/5



Sheet: /Amplifier1/
 File: Amplifier.kicad_sch

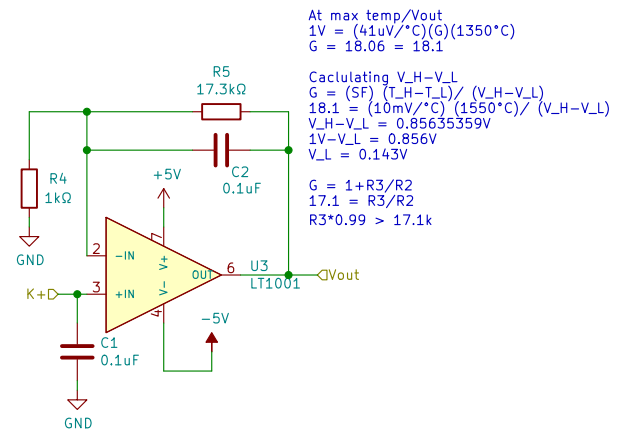
Title: Thermocouple Amplifier

Size: A4 Date: Jan. 27, 2022

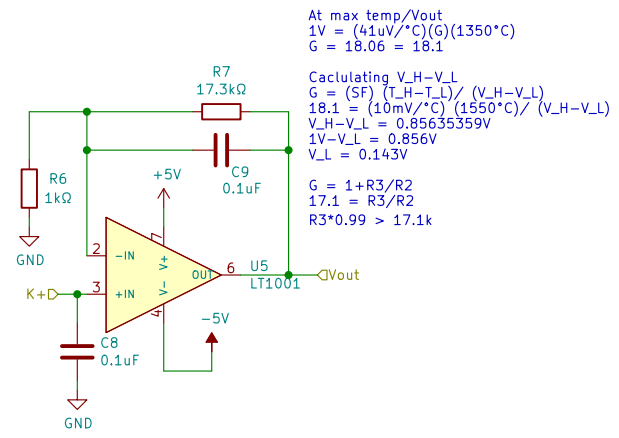
KiCad E.D.A. eeschema (6.0.1)

Rev: 1

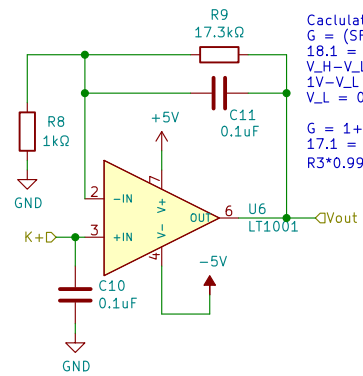
Id: 2/5



Sheet: /Amplifier2/		Date: Jan. 27, 2022	
File: Amplifier.kicad_sch		Rev: 1	
Size: A4	KiCad E.D.A. eeschema (6.0.1)		Id: 3/5



Sheet: /Amplifier3/	
File: Amplifier.kicad_sch	
Title: Thermocouple Amplifier	
Size: A4	Date: Jan. 27, 2022
KiCad E.D.A. eeschema (6.0.1)	Rev: 1 Id: 4/5



At max temp/Vout
 $1V = (41\mu V/^{\circ}C)(G)(1350^{\circ}C)$
 $G = 18.06 = 18.1$

Calculating $V_H - V_L$
 $G = (SF) (T_H - T_L) / (V_H - V_L)$
 $18.1 = (10mV/^{\circ}C) (1550^{\circ}C) / (V_H - V_L)$
 $V_H - V_L = 0.85635359V$
 $1V - V_L = 0.856V$
 $V_L = 0.143V$

$G = 1 + R3/R2$
 $17.1 = R3/R2$
 $R3 * 0.99 > 17.1k$

Sheet: /Amplifier4/
 File: Amplifier.kicad_sch

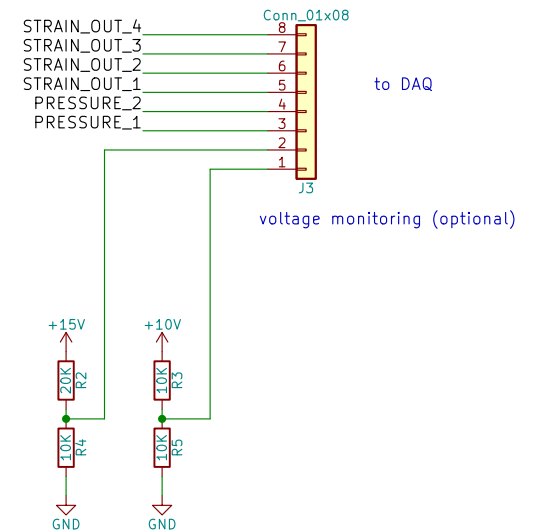
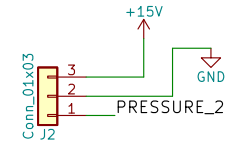
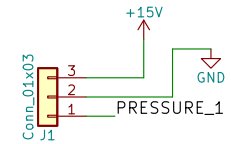
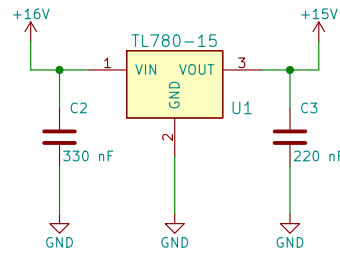
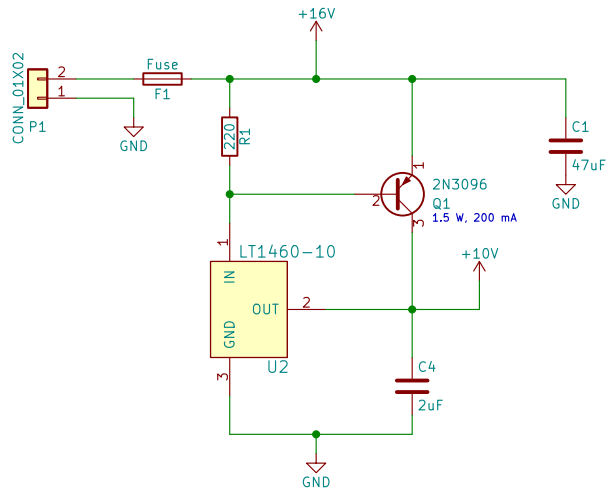
Title: Thermocouple Amplifier

Size: A4 Date: Jan. 27, 2022

KiCad E.D.A. eeschema (6.0.1)

Rev: 1

Id: 5/5



Instrumentation Amp



File: instr_amp.sch

sheet5ACB07B5



File: instr_amp.sch

sheet5ACB06D5



File: instr_amp.sch

sheet5ACB0847

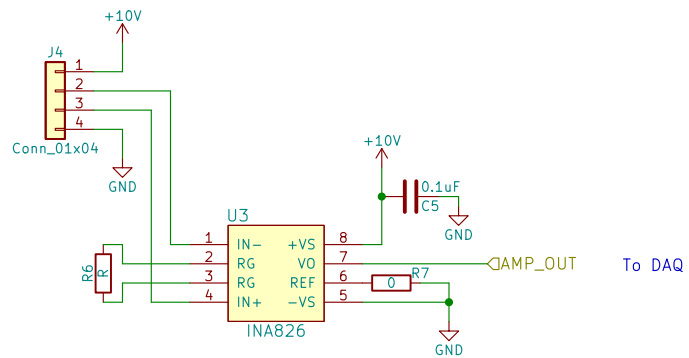


File: instr_amp.sch

Sheet: /		File: strain_gauges_rtr.sch	
Title: DAQ - Strain Gauges			
Size: A4	Date:	Rev:	
KiCad E.D.A. eeschema (6.0.1)			Id: 1/5

Power to sensor &
signal from sensor

$$G = 1 + 49.4K/RG$$



Sheet: /Instrumentation Amp/
File: instr_amp.sch

Title:

Size: A4

Date:

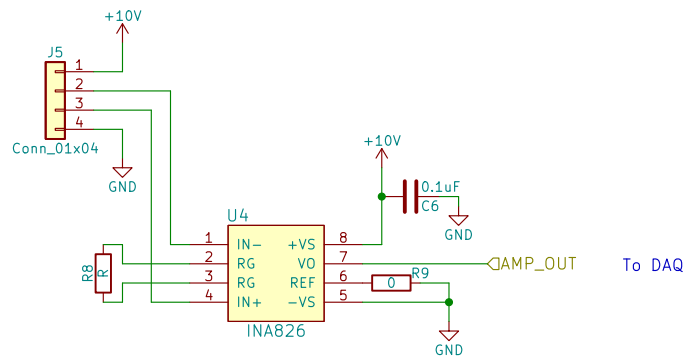
KiCad E.D.A. eeschema (6.0.1)

Rev:

Id: 2/5

Power to sensor &
signal from sensor

$$G = 1 + 49.4K/RG$$



Sheet: /sheet5ACB06D5/
File: instr_amp.sch

Title:

Size: A4

Date:

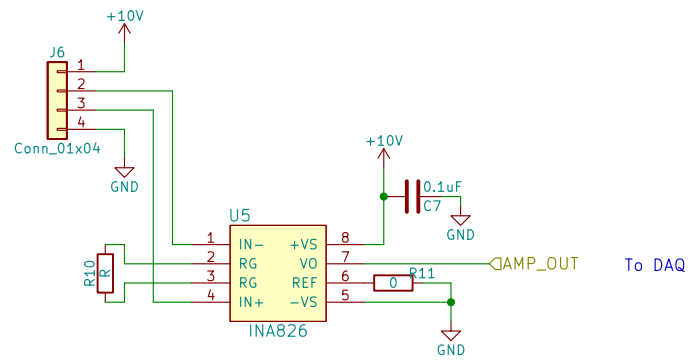
Rev:

KiCad E.D.A. eeschema (6.0.1)

Id: 3/5

Power to sensor &
signal from sensor

$$G = 1 + 49.4K/RG$$



Sheet: /sheet5ACB07B5/
File: instr_amp.sch

Title:

Size: A4

Date:

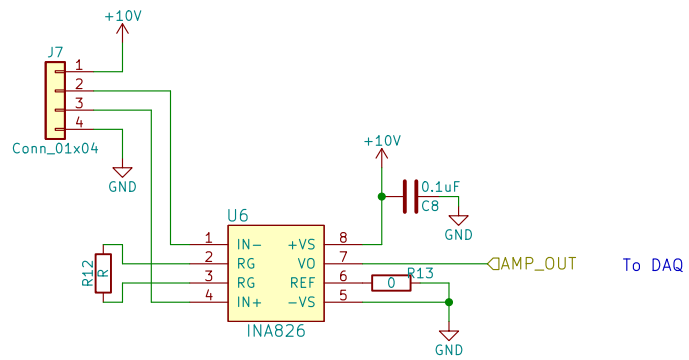
Rev:

KiCad E.D.A. eeschema (6.0.1)

Id: 4/5

Power to sensor &
signal from sensor

$$G = 1 + 49.4K/RG$$



Sheet: /sheet5ACB0847/
File: instr_amp.sch

Title:

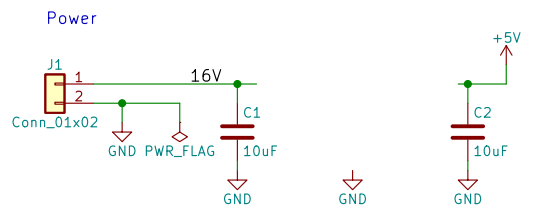
Size: A4

Date:

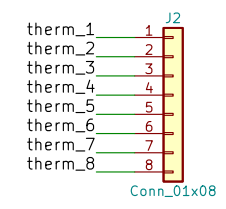
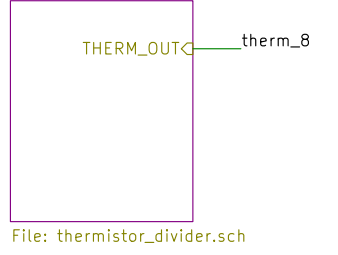
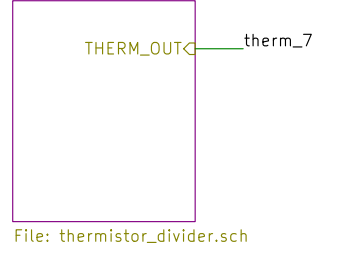
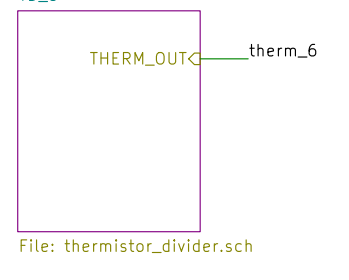
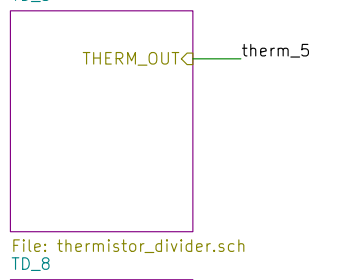
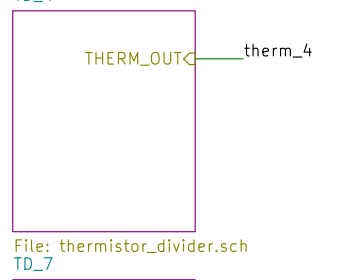
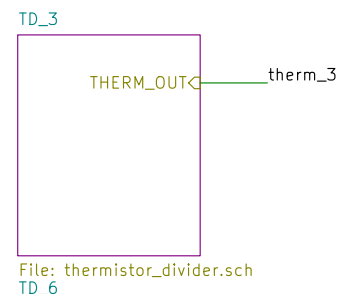
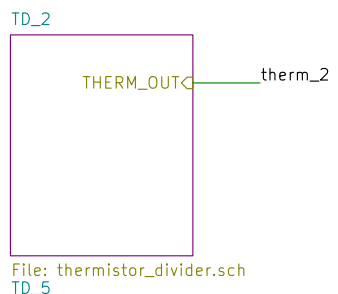
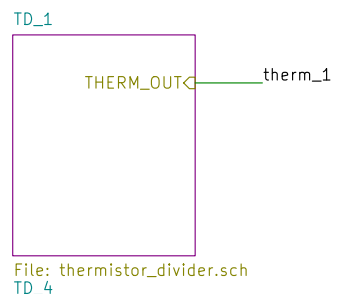
Rev:

KiCad E.D.A. eeschema (6.0.1)

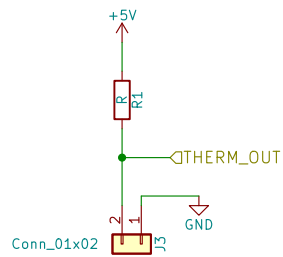
Id: 5/5



DAQ Thermistor Board.
 Supports up to 8 thermistors in a low side divider configuration. Powered off a 5V switching converter.
 TODO: add conversion formula.



Sheet: /		File: thermistors.sch	
Title: DAQ - Thermistors			
Size: A4	Date:	Rev:	
KiCad E.D.A. eeschema (6.0.1)			Id: 1/9



Sheet: /TD_1/
File: thermistor_divider.sch

Title:

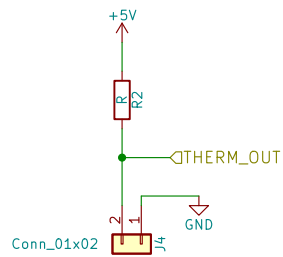
Size: A4

Date:

KiCad E.D.A. eeschema (6.0.1)

Rev:

Id: 2/9



Sheet: /TD_4/
File: thermistor_divider.sch

Title:

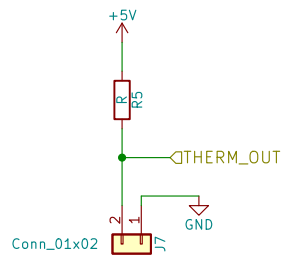
Size: A4

Date:

KiCad E.D.A. eeschema (6.0.1)

Rev:

Id: 3/9



Sheet: /TD_7/
File: thermistor_divider.sch

Title:

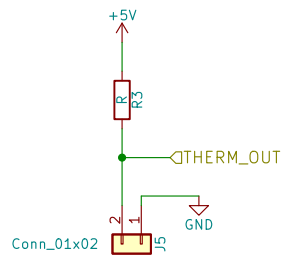
Size: A4

Date:

KiCad E.D.A. eeschema (6.0.1)

Rev:

Id: 4/9

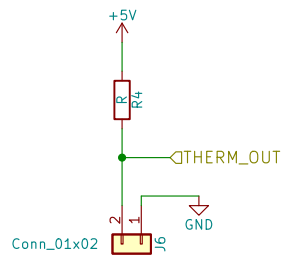


Sheet: /TD_2/
File: thermistor_divider.sch

Title:

Size: A4 Date:
KiCad E.D.A. eeschema (6.0.1)

Rev:
Id: 5/9



Sheet: /TD_5/
File: thermistor_divider.sch

Title:

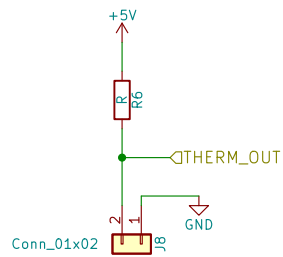
Size: A4

Date:

KiCad E.D.A. eeschema (6.0.1)

Rev:

Id: 6/9



Sheet: /TD_8/
File: thermistor_divider.sch

Title:

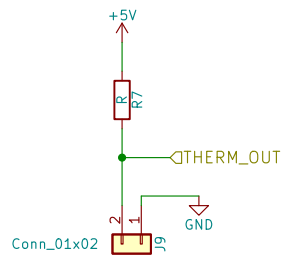
Size: A4

Date:

KiCad E.D.A. eeschema (6.0.1)

Rev:

Id: 7/9



Sheet: /TD_3/
File: thermistor_divider.sch

Title:

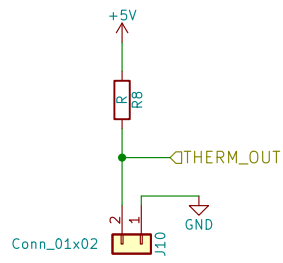
Size: A4

Date:

KiCad E.D.A. eeschema (6.0.1)

Rev:

Id: 8/9



Sheet: /TD_6/
File: thermistor_divider.sch

Title:

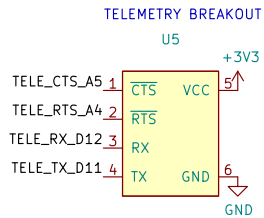
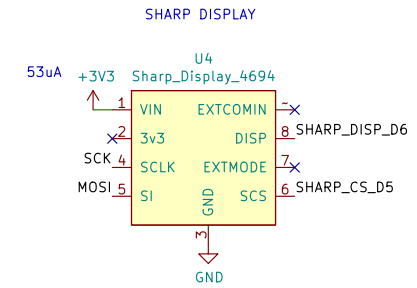
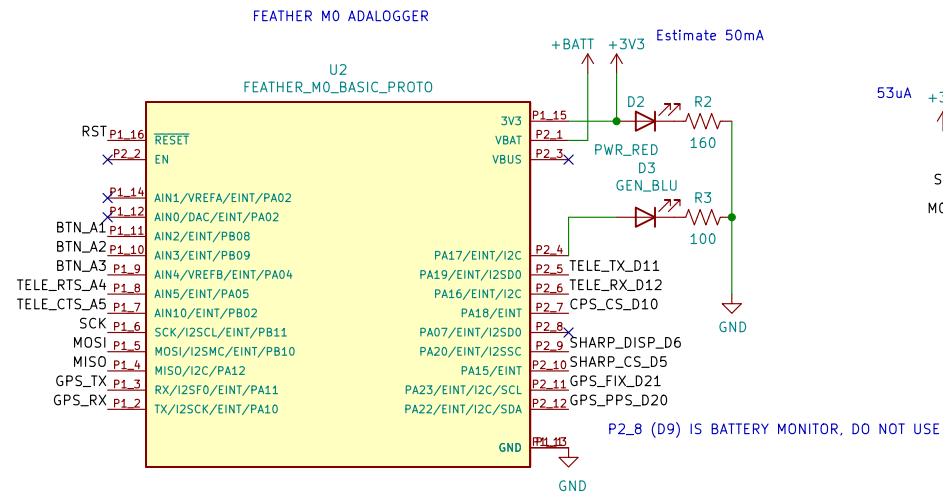
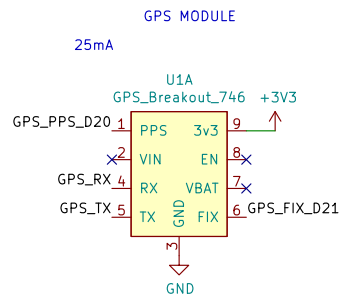
Size: A4

Date:

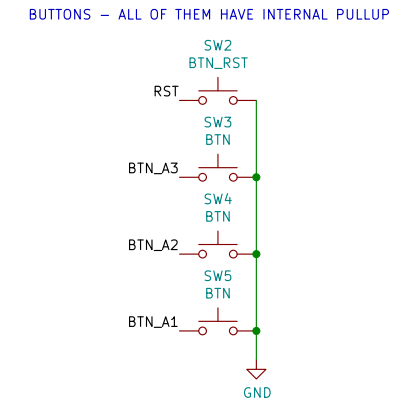
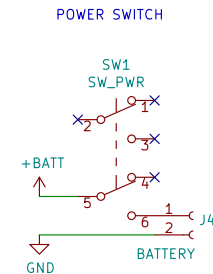
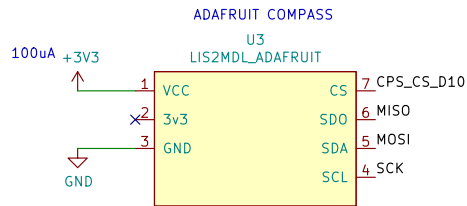
KiCad E.D.A. eeschema (6.0.1)

Rev:

Id: 9/9



COTS_GPS_RECEIVER



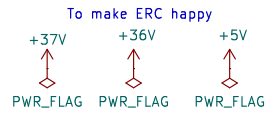
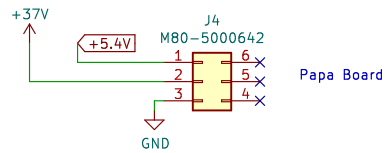
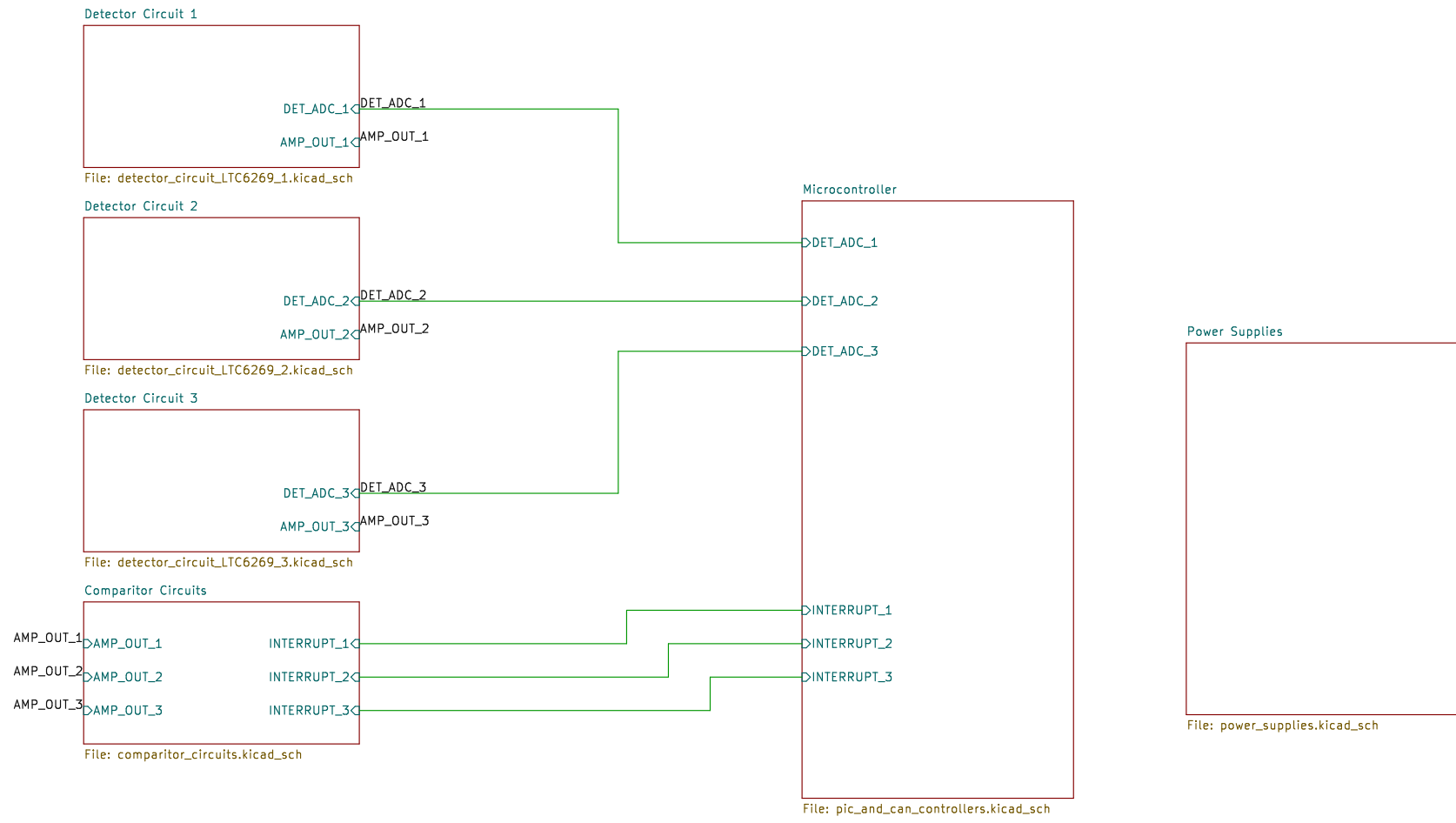
RIO LIU

Sheet: /
File: st_pat.kicad_sch

Title: ST PATS

Size: A4 Date: 2021-02-05
KiCad E.D.A. eeschema (6.0.1)

Rev:
Id: 1/1



Filter frequency cutoff equation: $1/(2 \cdot \pi \cdot R \cdot C)$
 Transimpedance Amplifier:
 Gain = 150, output peak approx. 1V
 Low-pass cutoff = 1Mhz

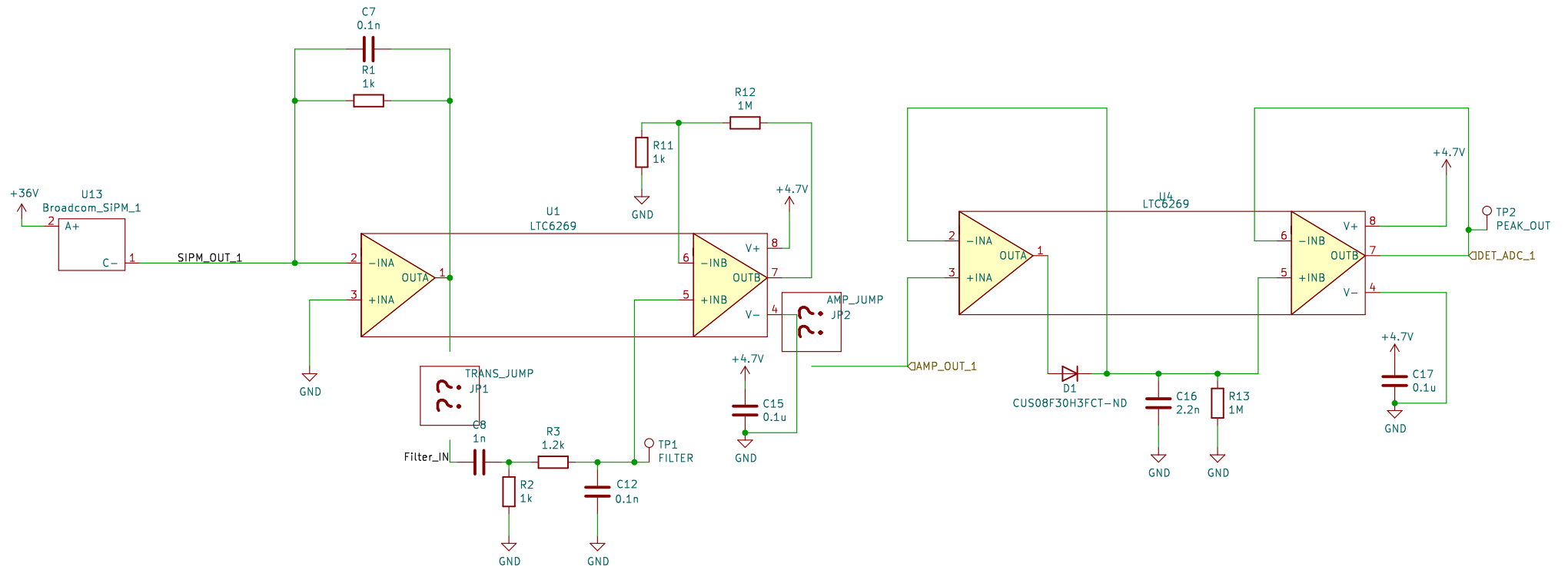
Band-pass filter
 High-pass cutoff: 200kHz
 Low pass cut-off: 1Mhz
 Est. voltage drop: 300mV

Amplifier

Op-amp removes diode drop
 for peak detector

2.2ms peak detector
 $T_{delay} = RC$

Voltage follower
 Ensures that measurements on ADC_OUT
 do not affect value



Filter frequency cutoff equation: $1/(2 \cdot \pi \cdot R \cdot C)$
 Transimpedance Amplifier:
 Gain = 150, output peak approx. 1V
 Low-pass cutoff = 1Mhz

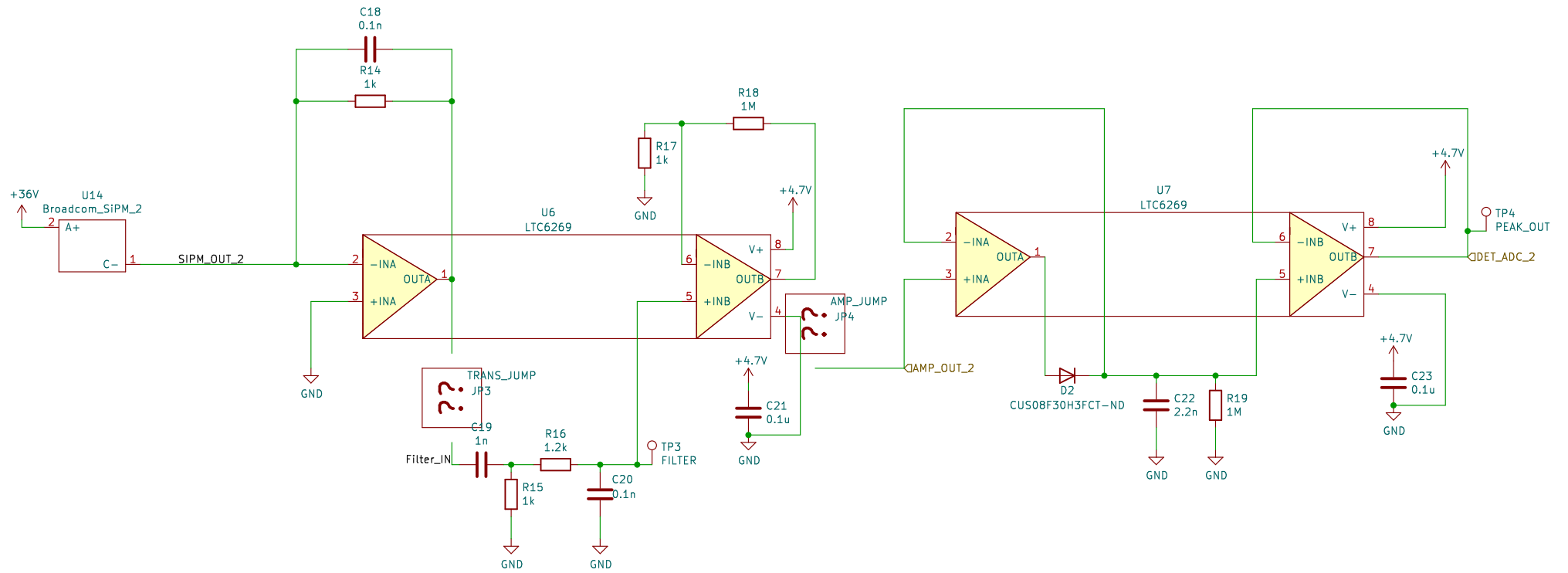
Band-pass filter
 High-pass cutoff: 200kHz
 Low pass cut-off: 1Mhz
 Est. voltage drop: 300mV

Amplifier

Op-amp removes diode drop
 for peak detector

2.2ms peak detector
 Tdelay = RC

Voltage follower
 Ensures that measurements on ADC_OUT
 do not affect value



Filter frequency cutoff equation: $1/(2 \cdot \pi \cdot R \cdot C)$
 Transimpedance Amplifier:
 Gain = 150, output peak approx. 1V
 Low-pass cutoff = 1Mhz

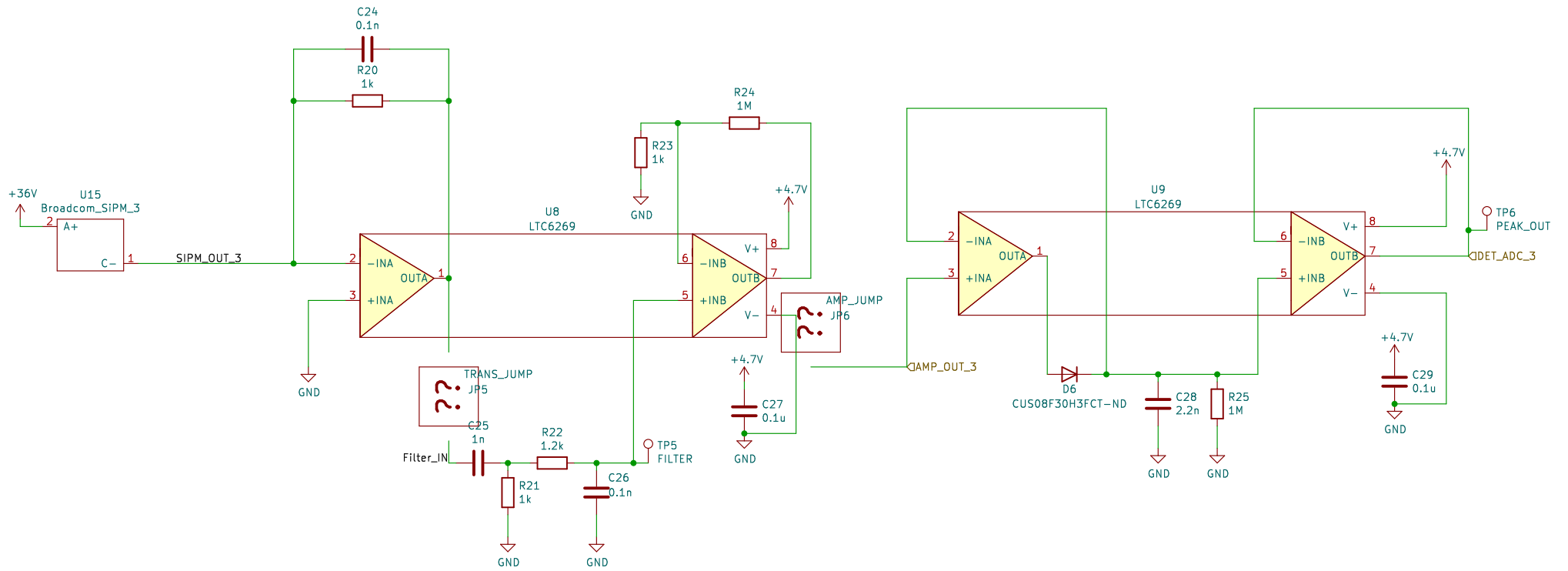
Band-pass filter
 High-pass cutoff: 200kHz
 Low pass cut-off: 1Mhz
 Est. voltage drop: 300mV

Amplifier

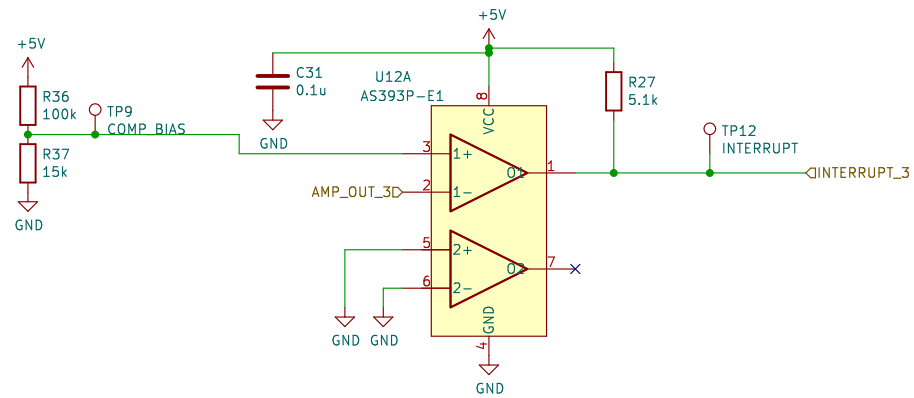
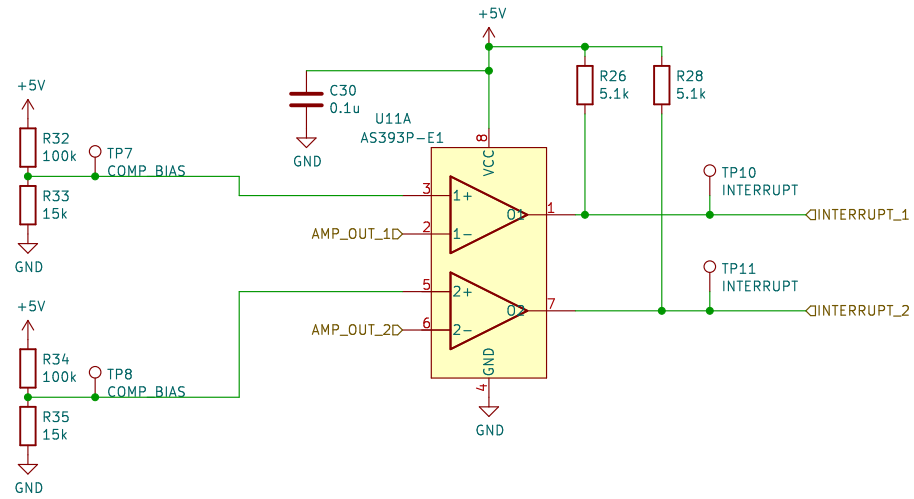
Op-amp removes diode drop
 for peak detector

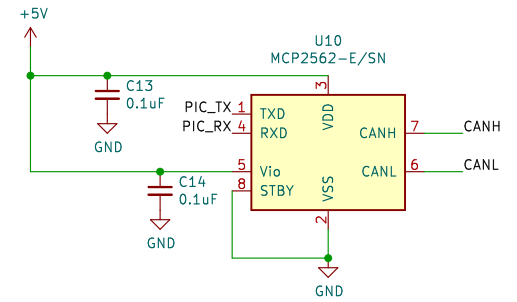
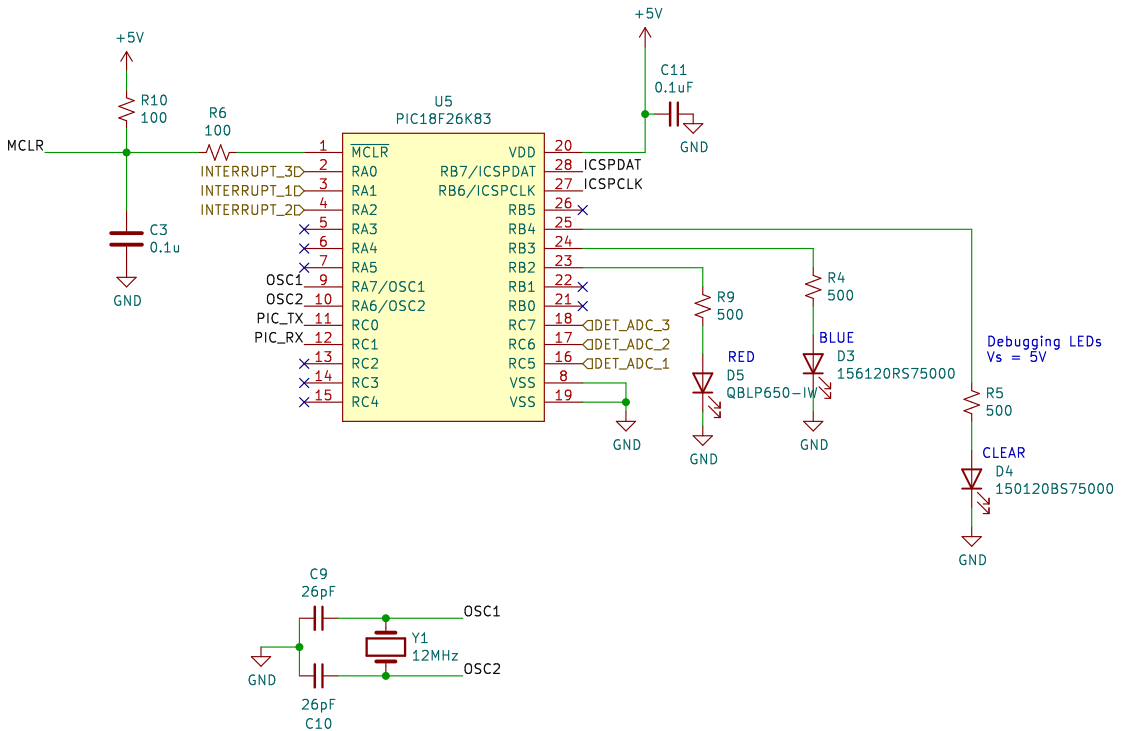
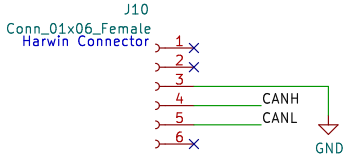
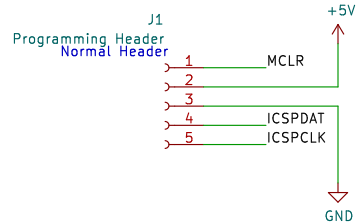
2.2ms peak detector
 $T_{delay} = RC$

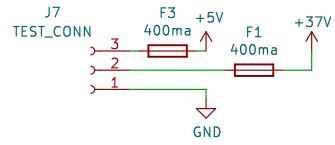
Voltage follower
 Ensures that measurements on ADC_OUT
 do not affect value



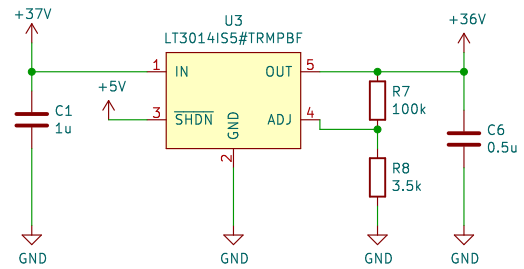
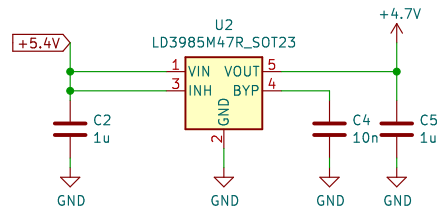
Comparator triggers interrupt, which informs PIC to measure analog signal

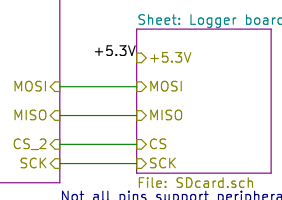
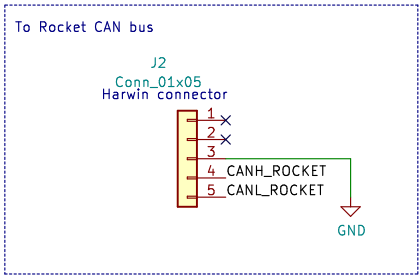
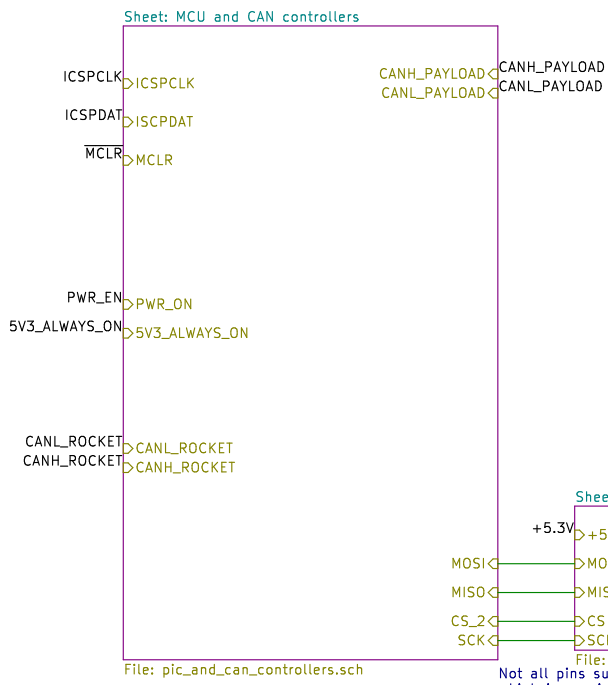
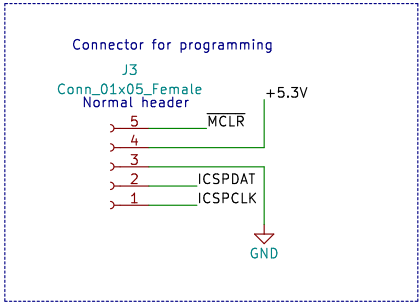
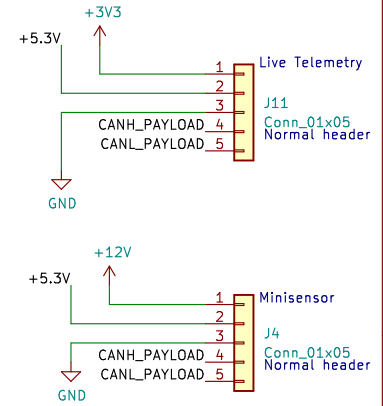
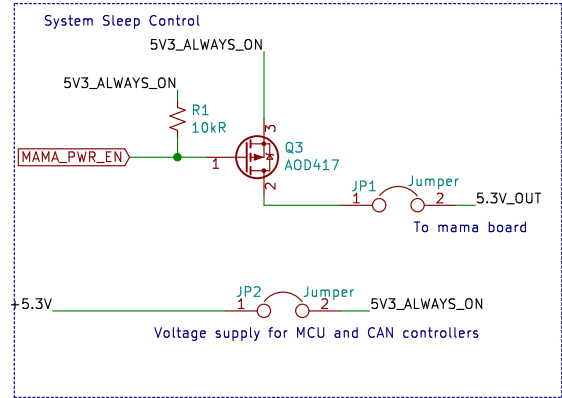
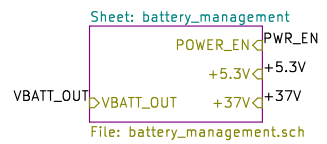
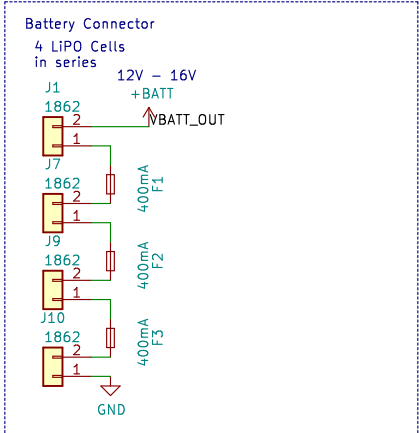




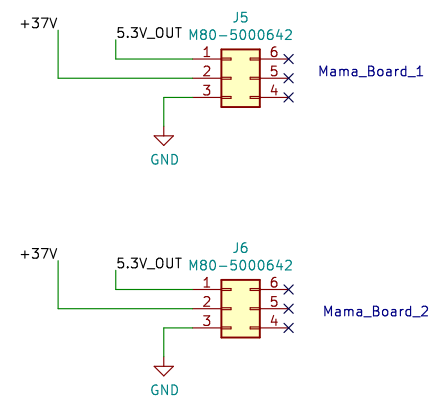


LDOs for noise reduction



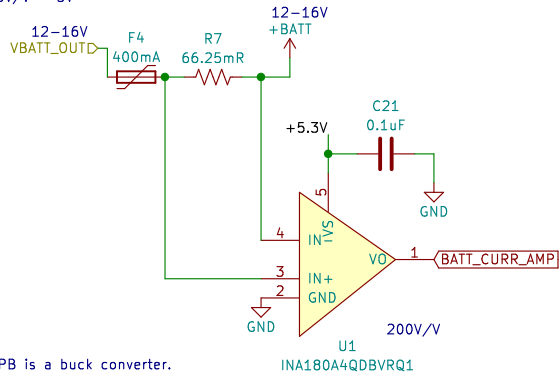


Not all pins support peripheral output, which is required for MOSI, SCK, and CANTX. RP20 and RP35-43 are the ones that support peripheral output



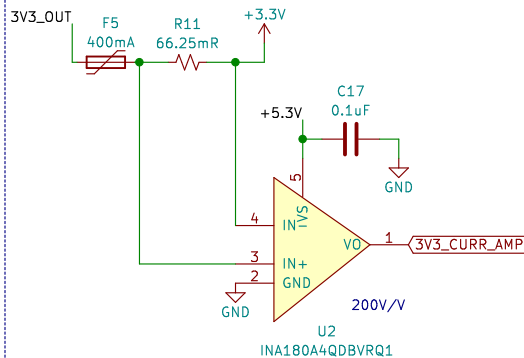
Waterloo Rocketry	
Sheet: /	
File: payload2020_base_board.sch	
Title: Papa Board	
Size: A4	Date:
KiCad E.D.A. kicad (5.1.9)-1	Rev: Id: 1/4

Main Power Supplies
 $66.25\text{mR} * I * 200\text{v/v} = 5\text{V}$
 $I_{\text{max}} = 400\text{mA}$

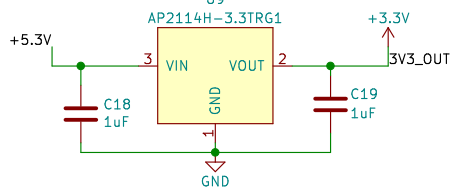


LM22678TJ-5.0/NOPB is a buck converter.
 Iout: 1.5A
 Values are taken from WEBENCH power designer
<https://webench.ti.com/appinfo/webench/scripts/SDP.cgi?ID=68E5BFACDBC533EB>
 PDF version:
<https://drive.google.com/file/d/13pYM-p7NzNzNQYZXknj9P6BV4uZ4R9wv/view?usp=sharing>

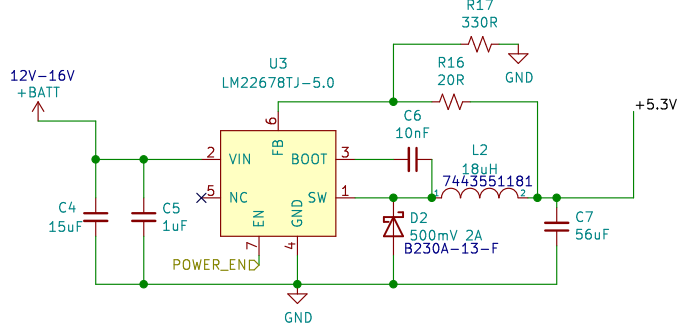
Logger Board Power Supplies
 $66.25\text{mR} * I * 200\text{v/v} = 5.3\text{V}$
 $I_{\text{max}} = 400\text{mA}$



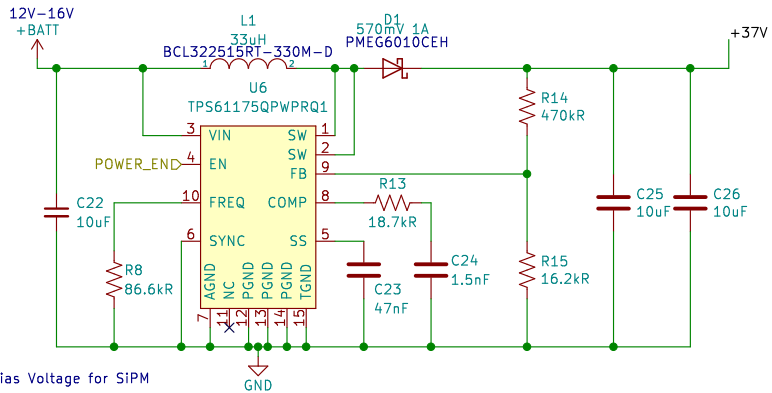
AP2114H-3.3TRG1 is a 3.3V LDO
 Iout = 600mA
 U9



+5.3V
 +3.3V



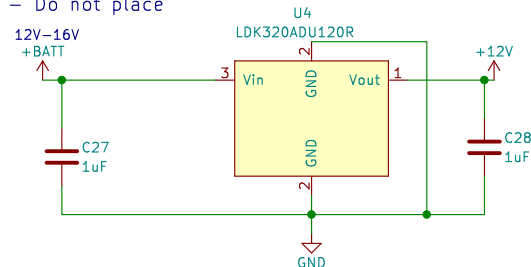
TPS61175 is a boost converter.
 Max Iout rating: 3A
 Values are taken from WEBENCH power designer
<https://webench.ti.com/appinfo/webench/scripts/SDP.cgi?ID=72ECE7EF0AA4EE07>
 PDF version:
<https://drive.google.com/file/d/1ktwurgh3BjmDxpc3J00zTu8lIix18m34/view?usp=sharing>



Bias Voltage for SIPM

1uF capacitors as per datasheet directly (no calculations)
 LDK320ADU120R is a 12V fixed-voltage regulator.
 Max Iout rating: 0.2A

DNP - Do not place



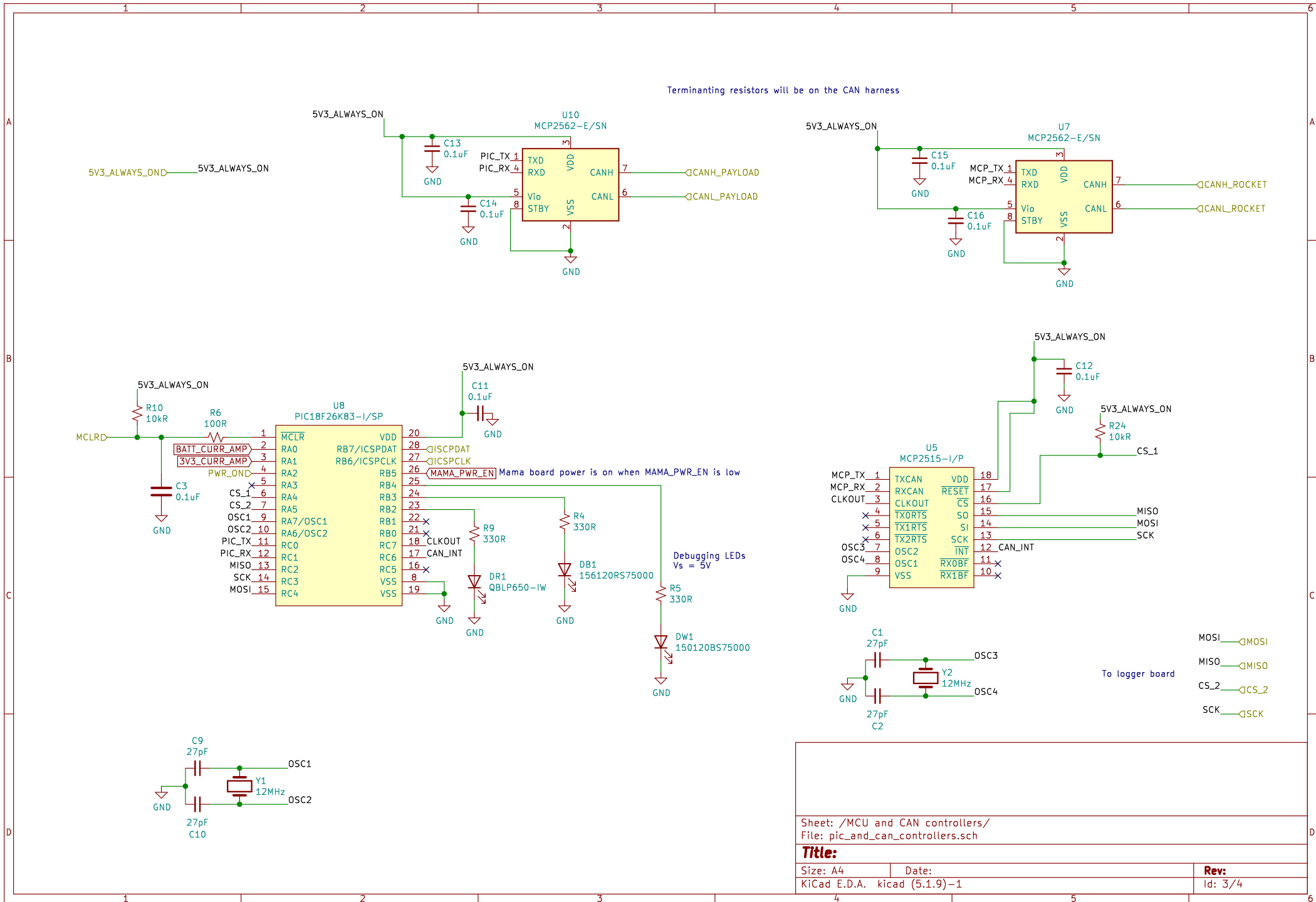
Sheet: /battery_management/
 File: battery_management.sch

Title:

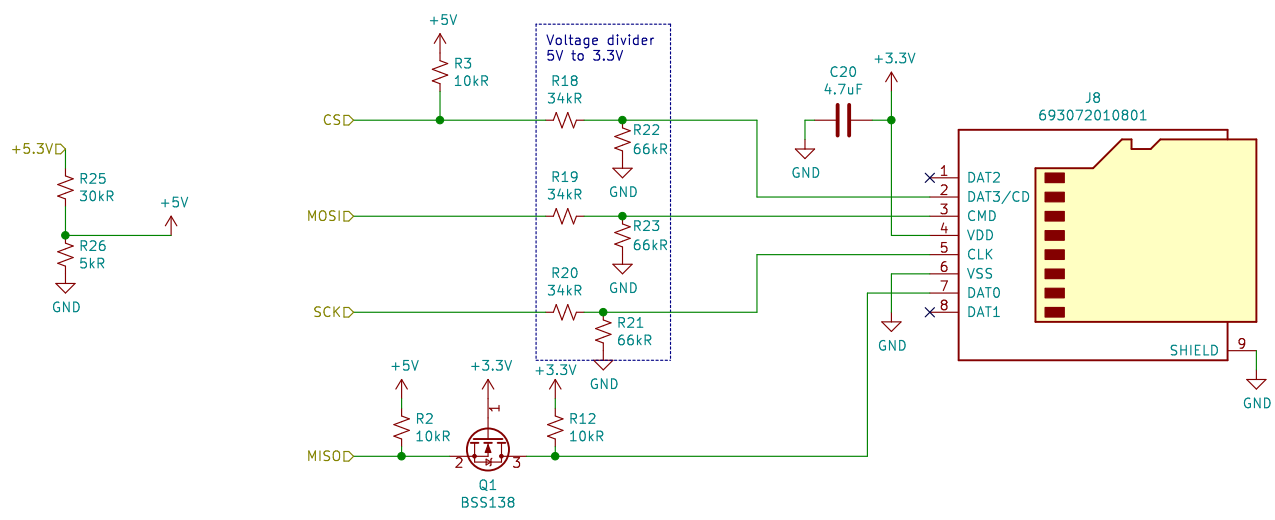
Size: A4
 KiCad E.D.A. kicad (5.1.9)-1

Date:

Rev:
 Id: 2/4



Sheet: /MCU and CAN controllers/ File: pic_and_can_controllers.sch	
Title:	
Size: A4	Date:
KiCad E.D.A. kicad (5.1.9)-1	Rev: Id: 3/4



Sheet: /Logger board/
 File: SDcard.sch

Title:

Size: A4	Date:	Rev:
KiCad E.D.A. kicad (5.1.9)-1		Id: 4/4

Acknowledgments

There are a great number of people without whom this rocket, and this team, would not be where they are today. We offer sincere thanks to our advisors, who have offered sound advice and support over the past design cycle and for many years prior. Specifically, we would like to thank Dr. Andrew Milne, Dr. Jean-Pierre Hickey, Andy Phillips, and Dan Steinhaur for their significant contributions to our team. We would also like to acknowledge the contributions of all our sponsors. Without their support, we would not be able to continue providing valuable learning opportunities for our team members and community. In particular, Stein Industries has made and continues to make significant investments in our team's success. Stein Industries and Dan Steinhaur deserve special acknowledgement for the many years of support that they have provided to our team. In addition, we thank the Sedra Student Design Center for their continued support. To the management, the machine shop staff, and the building operations and cleaning staff, thank you for the many hours of work that go into creating a space for our students to learn and work safely and comfortably. To our alumni, thank you for the time and effort you put in that paved the way for the current generation of Waterloo Rocketry. We would not be where we are without your dedication and advice, and we thank you for everything that you have taught us. Finally, to our team members: you are the heart and soul of this team, and we hope that your efforts in building this rocket have given you something valuable. We are proud of you, and we thank you for the late nights, early mornings, and seemingly endless dedication that you have given to get us to this point. You have made this team something special.

References

- [1] Christopher, N., Cojocar, T., Deery, J., Jiang, R., Kletke, D., Kobets, R., Kong, S., Martin, S., Mears, Z., Mihaila, A., Morrison, A., Rajkumar, V., Robinson, J., Tam, K., Tang, T., and Yang, E. *Shark of the Sky Hybrid Rocket*. 2019.
- [2] Abuabah, H., Bian, Z., Deery, J., Dymont, D., Hussien, A., Kletke, D., Kobets, R., Kong, S., Leszkowiat, A., Mears, Z., Sankey, C., Sotnikov, A., Tam, K., Tang, T., Tomlin, L., and Yu, W. *Design Proposal Report for Kraken of the Sky Competing Team 6*. Waterloo, 2021.
- [3] Praxair Technologies. Praxair - Specialty Gases Reference Guide. <http://read.dmtmag.com/i/25778-specialty-gases-reference-guide/0?> Accessed May 12, 2021.
- [4] Air Liquide. Nitrous Oxide. *Gas Encyclopedia*. <https://encyclopedia.airliquide.com/nitrous-oxide>. Accessed Apr. 29, 2021.
- [5] Newlands, R. Hybrid Safety. *Aspire Space*. http://www.aspirespace.org.uk/downloads/Hybrid_safety.pdf. Accessed May 13, 2021.
- [6] Waxman, B. S. *AN INVESTIGATION OF INJECTORS FOR USE WITH HIGH VAPOR PRESSURE PROPELLANTS WITH APPLICATIONS TO HYBRID ROCKETS*. Stanford University, 2014.
- [7] Martin, S., and McCourt, T. *ME739: Topological Optimization in Additive Manufacturing of Rocket Engines*. Waterloo, 2020.
- [8] Christopher, N., Wong, N. H., and Dalglish, S. *ME481 Design Project Report Design of a Hybrid Rocket Engine*. Waterloo, 2017.
- [9] Newlands, R. The Thrust Optimised Parabolic Nozzle. *Aspire Space*. http://www.aspirespace.org.uk/downloads/Thrust_optimised_parabolic_nozzle.pdf.
- [10] Sutton, G. P., and Biblarz, O. *Rocket Propulsion Elements*. John Wiley & Sons, New York, 2001.
- [11] Parker Hannifin Corporation. Parker O-Ring Handbook. https://www.parker.com/Literature/O-Ring_Division_Literature/ORD_5700.pdf.
- [12] Nakka, R. Richard Nakka's Experimental Rocketry Web Site. <http://www.nakka-rocketry.net/>. Accessed May 12, 2022.
- [13] Knacke, T. W. *Parachute Recovery Systems: Design Manual*. Para Pub., Santa Barbara, 1992.
- [14] Fields, T. "Evaluation of Control Line Reefing Systems for Circular Parachutes." *Journal of Aircraft*, Vol. 53, 2016, pp. 1–5.
- [15] Sadeck, J. E., and Lee, C. K. "Continuous Disreefing Method for Parachute Opening." *Journal of Aircraft*, Vol. 46, 2009, pp. 501–504.
- [16] Mentzer, A. P. What Is the Range of Barometric Pressure? *Sciencing*. <https://sciencing.com/range-barometric-pressure-5505227.html>. Accessed Jan. 8, 2020.
- [17] Windyty. Windy. <https://www.windy.com/>.
- [18] Perez, J. Why Space Radiation Matters. *NASA*. <https://www.nasa.gov/analogs/nsrl/why-space-radiation-matters>. Accessed May 12, 2021.
- [19] Kim, J., Pham, T., Hwang, J., Kim, C., and Kim, M. "Boron Nitride Nanotubes: Synthesis and Applications."

- Nano Convergence*, Vol. 5, No. 1, 2018.
- [20] Harrison, C., Weaver, S., Bertelsen, C., Burgett, E., Hertel, N., and Grulke, E. “Polyethylene/Boron Nitride Composites for Space Radiation Shielding.” *Journal of Applied Polymer Science*, Vol. 109, No. 4, 2008.
 - [21] DeVanzo, M., and Hayes, R. B. “Ionizing Radiation Shielding Properties of Metal Oxide Impregnated Conformal Coatings.” *Radiation Physics and Chemistry*, Vol. 171, 2020.
 - [22] Axini, S. N., Frankiewicz, K., and Conrad, J. M. *CosmicWatch: The Desktop Muon Detector*. Boston, 2018.
 - [23] California Polytechnic State University. *CubeSat Design Specification Rev. 14*. 2020.
 - [24] Thomas Publishing Company. Materials Used in Radiation Shielding. *Insights*. <https://www.thomasnet.com/articles/plant-facility-equipment/radiation-shielding-materials/>.
 - [25] Allison, J., Amako, K., Apostolakis, J., Araujo, H., Arce Dubois, P., Asai, M., Barrand, G., Capra, R., Chauvie, S., Chytracsek, R., Cirrone, G. A. P., Cooperman, G., Cosmo, G., Cuttone, G., Daquino, G. G., Donszelmann, M., Dressel, M., and Folger, G. “Geant4 Developments and Applications.” *IEEE Transactions on Nuclear Science*, Vol. 53, No. 1, 2006, pp. 270–278. <https://doi.org/10.1109/TNS.2006.869826>.
 - [26] IBM Cloud Education. What Is Monte Carlo Simulation? <https://www.ibm.com/cloud/learn/monte-carlo-simulation>.
 - [27] Goldhagen, P., Reginatto, M., Van Steveninck, W., Singleterry Jr., R. C., Wilson, J. W., Tai, H., Jones, I. W., and Shinn, J. L. The Atmospheric Ionizing Radiation (AIR) Project – Preliminary Results for Neutron Spectra and Ionization Rate. https://www.nasa.gov/centers/johnson/pdf/516250main_AIR_project.pdf.